Wind and Seismic Effects
Proceedings of the 38th Joint Panel Meeting

NIST Special Publication 1057

Stephen A. Cauffman, Editor

NIST National Institute of Standards and Technology • Technology Administration • U.S. Department of Commerce

The National Institute of Standards and Technology was established in 1988 by Congress to "assist industry in the development of technology ... needed to improve product quality, to modernize manufacturing processes, to ensure product reliability ... and to facilitate rapid commercialization ... of products based on new scientific discoveries."

NIST, originally founded as the National Bureau of Standards in 1901, works to strengthen U.S. industry's competitiveness; advance science and engineering; and improve public health, safety, and the environment. One of the agency's basic functions is to develop, maintain, and retain custody of the national standards of measurement, and provide the means and methods for comparing standards used in science, engineering, manufacturing, commerce, industry, and education with the standards adopted or recognized by the Federal Government.

As an agency of the U.S. Commerce Department's Technology Administration, NIST conducts basic and applied research in the physical sciences and engineering, and develops measurement techniques, test methods, standards, and related services. The Institute does generic and precompetitive work on new and advanced technologies. NIST's research facilities are located at Gaithersburg, MD 20899, and at Boulder, CO 80303. Major technical operating units and their principal activities are listed below. For more information visit the NIST Website at http://www.nist.gov, or contact the Public Inquiries Desk, 301-975-NIST.

Office of the Director
- National Quality Program
- International and Academic Affairs

Technology Services
- Standards Services
- Technology Partnerships
- Measurement Services
- Information Services
- Weights and Measures

Advanced Technology Program
- Economic Assessment
- Information Technology and Applications
- Chemistry and Life Sciences
- Electronics and Photonics Technology

Manufacturing Extension Partnership Program
- Regional Programs
- National Programs
- Program Development

Electronics and Electrical Engineering Laboratory
- Microelectronics
- Law Enforcement Standards
- Electricity
- Semiconductor Electronics
- Radio-Frequency Technology[1]
- Electromagnetic Technology[1]
- Optoelectronics[1]
- Magnetic Technology[1]

Materials Science and Engineering Laboratory
- Intelligent Processing of Materials
- Ceramics
- Materials Reliability[1]
- Polymers
- Metallurgy
- NIST Center for Neutron Research

Chemical Science and Technology Laboratory
- Biotechnology
- Process Measurements
- Surface and Microanalysis Science
- Physical and Chemical Properties[2]
- Analytical Chemistry

Physics Laboratory
- Electron and Optical Physics
- Atomic Physics
- Optical Technology
- Ionizing Radiation
- Time and Frequency[1]
- Quantum Physics[1]

Manufacturing Engineering Laboratory
- Precision Engineering
- Manufacturing Metrology
- Intelligent Systems
- Fabrication Technology
- Manufacturing Systems Integration

Building and Fire Research Laboratory
- Applied Economics
- Materials and Construction Research
- Building Environment
- Fire Research

Information Technology Laboratory
- Mathematical and Computational Sciences[2]
- Advanced Network Technologies
- Computer Security
- Information Access
- Convergent Information Systems
- Information Services and Computing
- Software Diagnostics and Conformance Testing
- Statistical Engineering

---

[1] At Boulder, CO 80303

[2] Some elements at Boulder, CO

NIST Special Publication 1057

Wind and Seismic Effects

Proceedings of the 38th Joint Panel Meeting

Stephen A. Cauffman, Editor
Materials and Construction Research Division
Building and Fire Research Laboratory
National Institute of Standards and Technology
Gaithersburg, MD 20899-8611

September 2006

U.S. Department of Commerce
Carlos M. Gutierrez, Secretary

Technology Administration
Robert C. Cresanti, Under Secretary of Commerce for Technology

National Institute of Standards and Technology
William A. Jeffrey, Jr., Director

Certain commercial entities, equipment, or materials may be identified in this document in order to describe an experimental procedure or concept adequately. Such identification is not intended to imply recommendation or endorsement by the National Institute of Standards and Technology, nor is it intended to imply that the entities, materials, or equipment are necessarily the best available for the purpose.

National Institute of Standards and Technology Special Publication 1057
Natl. Inst. Stand. Technol. Spec. Publ. 1057, 402 pages (September 2006)
CODEN: NSPUE2

U.S. GOVERNMENT PRINTING OFFICE
WASHINGTON: 2006

624.175
Un32w
v.38
2006

Engineering

CONTENTS

PREFACE vii

ABSTRACT xv

AGENDA OF JOINT MEETING xvii

LIST OF PANEL MEMBERS xxiii
  Japan-Side Panel Members xxv
  U.S.-Side Panel Members xxxiii

RESOLUTIONS & STRATEGIC PLAN xxxvii

MANUSCRIPTS 1

Technical Session 1 – GEOTECHNICAL ENGINEERING AND GROUND MOTION 3

Fundamental Study on Health Monitoring and Evaluation System for Port/Airport Facilities 5
Takahiro Sugano, Tomohiro Tanaka, and Eiji Kohama

Response of an Integrated Building and Free-Field Surface Downhole Network 11
Mehmet Celebi

Technical Session 2 -- NEXT-GENERATION BUILDING AND INFRASTRUCTURE SYSTEMS 21

Reparability Limit of Steel Structural Buildings Based on the Actual Data of the Hyogoken-Nanbu Earthquake 23
Yoshihiro Iwata, Hirokazu Sugimoto, and Hitoshi Kuwamura

Recent Developments on the Design and Evaluation of Steel Structures for Seismic Loads: An NSF Perspective 33
Douglas Foutch

Wood Building Collapse Test Using E-Defense 37
Isao Sakamoto, Naohito Kawai, Takahiro Tsuchimoto, and Chikahiro Minowa

Civil and Mechanical Systems (CMS) Program at the National Science and Foundation 45
Shi Chi Liu

Crack Detection Methods Using Radio Frequency Identification and Electrically Conductive Materials 59
Koichi Morita and Kazuya Noguchi

Technical Session 3 – WIND ENGINEERING 67

Design and Testing of Iowa State University's AABL Wind and Gust Tunnel 69
Partha Sarkar and Fred Haan

High Wind Damage to Buildings Caused by Typhoon in 2004 87
Yasuo Okuda, Yukio Tamura, Hiroaki Nishimura, Hitomitsu Kikitsu, and Hisashi Okada

Meteorological Aspects of the Gulf of Mexico Hurricanes. 93
John Gaynor

Technical Session 4 – STORM SURGE AND TSUNAMIS 107

Application of Storm Surge and Tsunami Simulator in Oceans and Coastal Areas (STOC) to Tsunami Analysis 109
Takashi Tomita, Kazuhiko Honda, and Taro Kakinuma

Experimental and Numerical Modeling of Storm Surge and Tsunami Effects on Structures 117
Solomon Yim and Kwok Fai Cheung

Development of Estimation Method on Drift and Collision Behaviors of Debris Caused by Tsunamis 127
Katsuya Oda, Osamu Okamoto, and Kentaro Kumagai

Technical Session 5 – RECENT NATURAL DISASTERS AND NATURAL DISASTER MANAGEMENT PLAN 135

Toward the Establishment of a Regional Society that is Safe and Secure Against Disasters 137
Tsuneyoshi Mochizuki, Kiyoshi Minami, Koichi Yamashita, Keiichi Tamura,
Koh-ichi Fujita, and Katsuya Oda

Recovery and Monitoring Challenges with Water Quality Issues in New Orleans During Hurricane Katrina Recovery Operations 147
William Roper, Kevin Weiss, and James Wheeler

PWRI's New Organizations and Research Projects on Natural Disasters 165
Tadahiko Sakamoto and Hiroshi Sato

Reconnaissance of Damage to Physical Structures in the Gulf States from Hurricanes Katrina and Rita 175
William Fritz

Establishing a Disaster Information System to Practically Support Disaster Countermeasures: Conducting and Reviewing Demonstration Experiment 185
Akihiro Sanada, Takaaki Kusakabe, and Keiichi Tamura

Health Concerns Associated with Mold in Water-Damaged Homes After Hurricanes Katrina and Rita --- New Orleans Area, Louisiana, October 2005 199
Clive Brown, Margaret Riggs, Carol Rao, and Kristin Cummings

Technical Session 6 – DAMS 209

Investigation into Crack Phenomena of Unreinforced Concrete Structures for Aseismic Evaluation of Concrete Dams 211
Tadahiko Sakamoto, Yoshikazu Yamaguchi, Takashi Sasaki, Kei Takafuji, and Ken-ichi Kanenawa

Federal Initiatives for Security and Protection of Dams 221
Enrique Matheu

Establishment of Input Large-scale Earthquake Motions for Earthquake Proof Evaluation of Existing Dams 245
Nario Yasuda, Kazujito Shimamoto, Takayuki Sano, and Koji Sujino

Technical Session 7 – TRANSPORTATION SYSTEMS 259

The FHWA Long-Term Bridge Performance Program 261
Hamid Ghasemi, Ian Friedland, Steven Chase, and Joey Hartmann

Damage Investigation and the Preliminary Analyses of Bridge Damage Caused by the 2004 Indian Ocean Tsunami 267
Shigeki Unjoh and Kazuo Endoh

Multi-Hazards Design Criteria of Highway Bridge 279
George Lee, Mai Tong, and Phillip Yen

Technical Session 8 – FIRE PERFORMANCE OF STRUCTURES 285

Outline of the Fire Resistance Verification Method in the Building Standard Law of Japan 287
Mamoru Kohno

Fire Endurance Testing of Floor Systems - Effects of Scale and Restraint 295
John Gross

A Study on the Collapse Control Design Method for High-rise Steel Buildings 303
Akira Wada, Kenichi Ohi, Hiroyuki Suzuki, Mamoru Kohno, and Yoshifumi Sakumoto

The Need for International Collaboration on Structural Fire Endurance Research 315
William Grosshandler and Kuldeep Prasad

MANUSCRIPT AUTHORED BUT NOT PRSENTED ORALLY 327

Interpretation of Slope Failure Distribution Triggered by the Northern Pakistan Earthquake on 8 October 2005 using SPOT 5 Stereo-imageries 329
Hiroshi Sato, Mamoru Koarai, Hiroshi Une, Hiroyuki Hasegawa, Junko Iwahashi, and Izumi Kamiya

APPENDIX 335
Task Committee Reports 337

PREFACE

This publication contains the Proceedings of the 38th Joint Meeting of the U.S.-Japan Panel on Wind and Seismic Effects. The technical meetings were held at the National Institute of Standards and Technology in Gaithersburg, Maryland during 15-17 May 2006 followed by three-day technical site visits to discuss New Orleans Hurricane damages. The Panel Meeting centered on eight Sessions: 1) Geotechnical Engineering and Ground Motion; 2) Next-Generation Building and Infrastructure Systems; 3) Wind Engineering; 4) Storm Surge and Tsunamis; 5) Recent Natural Disasters and Natural Disaster Management Plan; 6) Dams; 7) Transportation Systems; and 8) Fire Performance of Structures. Twenty-nine papers were presented during this meeting (15 from Japan and 14 from the US). These papers comprise the majority of this report.

Delegation members, 38th US-Japan Joint Panel Meeting in front of NIST

BACKGROUND

Responding to the need for improved engineering and scientific practices through exchange of technical data and information, research personnel, and research equipment, the United States and Japan in 1961 created the U.S.-Japan Cooperative Science Program. Three collateral programs comprise the Cooperative Science Program. The U.S.-Japan Cooperative Program in Natural Resources (UJNR), one of the three, was created in January 1964. The objective of UJNR is to exchange information on research results and exchange scientists and engineers in the area of natural resources for the benefit of both countries. UJNR is composed of 16 Panels each responsible for specific technical subjects.

The Panel on Wind and Seismic Effects was established in 1969. Eighteen U.S. and 14 Japanese organizations participated with representatives of private sector organizations to develop and exchange technologies aimed at reducing damages from high winds, earthquakes, storm surge, and tsunamis. This work is produced through collaboration between U.S. and Japanese member researchers working in seven Task Committees. Each committee focuses on specific technical issues, e.g., earthquake strong motion data, wind engineering, storm surge and tsunamis, fire performance of structures. The Panel provides the forum to exchange technical data and information on design and construction of civil engineering lifelines, buildings, and water front structures, and to exchange high wind and seismic measurement records. Annual meetings alternate between Japan and the United States (odd numbered years in Japan; even numbered years in the United States). These one-week technical meetings that include technical site visits, that follow the meetings, facilitate discussions of ongoing research and research results. The National Institute of Standards and Technology (NIST) provides the U.S.-side chair and secretariat. The Public Works Research Institute (PWRI), Japan, provides the Japan-side chair and secretariat.

Task Committee meetings, exchanges of data and information through technical presentations at annual Panel meetings, exchanges of guest researchers, visits to respective research laboratories and informal interactions between Panel meetings, joint workshops and seminars, and joint cooperative research programs all contribute to the development and effective delivery of knowledge that has influenced design and construction practices in both countries. Guest research exchanges have contributed to advancing the state of technology in areas of steel, concrete, and masonry structures under seismic forces; developing techniques to analyze risks from liquefaction; modeling water seepage in dam foundations; and performing comparative analyses of seismic design of U.S. and Japanese bridges.

Direct communication between counterpart country organizations is the cornerstone of the Panel. Effective information exchanges and exchanges of personnel and equipment have strengthened domestic research programs in both countries. There are opportunities for experts in various technical fields to get to know their foreign counterparts, conduct informal exchanges, bring their respective views to the frontiers of knowledge, and advance knowledge of their specialties.

The data produced by the Panel influence on-going structural engineering research and contribute to the revision of existing provisions and creation of new provisions in U.S. building codes and standards. Examples include:

1. Created and exchanged digitized earthquake records used as the basis of design and research in both Japan and the United States.
2. Produced full-scale test data that advanced seismic design standards for buildings.
3. Translated into English a Port and Harbour Research Institute Handbook on *Liquefied Remediation of Reclaimed Land*, A. A. Balkema, The Netherlands, publisher that provided general guidance for the U.S. design profession on remediation of liquefiable soils.
4. In collaboration with Japan's Geotechnical Society translated into English a report from the Port and Harbour Research Institute, *Remedial Measures Against Soil Liquefaction: From Investigation and Design to Implementation*, A. A. Balkema, The Netherlands, 1998, publisher that served as background and guidance for the U.S. Army Corps of Engineers (USACE) in performing dam remediation at Clemson University.
5. Developed a protocol for testing bridge columns subjected to earthquake loads that facilitated the exchange of experimental data between both countries. The protocol serves as a basis for the Federal Highway Administration's development of new seismic design criteria for bridge columns.
6. Facilitated a USACE team to Kobe within days after the Kobe Earthquake to access to data and information through post disaster investigations. This would not have been possible without the Panel's endorsement.
7. Performed joint post disaster investigations whose findings influenced revisions to and development of new U.S. seismic design and rehabilitation criteria.
8. Accessed a large U.S. and Japan database that helped develop a USACE Guidance Criteria in Geotechnical Engineering.

9. Provided access to data that helped characterize gravelly soils in determining the seismic instability of gravelly soils for dams which were used to improve USACE construction criteria.
10. Through a Japan Guest Researcher from the Port and Harbour Research Institute working at USACE geotechnical research findings were transferred into USACE documents.
11. Created a database comparing Japanese and U.S. standard penetration tests to improve prediction of soil liquefaction.
12. Influenced the creation of a NIST research program in Seismic Base Isolation using data from translated Japan reports into English on base isolation systems.
13. Increased awareness of wind engineering practice, problems, and breakthroughs in Japan and the United States.
14. Improved cross-discipline research among wind engineers/meteorologists/sociologists in each country.
15. Increased the dissemination of latest research findings in wind engineering, especially post-storm events (typhoons/hurricanes) to each country.
16. Developed field test data for use in aerodynamic retrofit of bridge structures.
17. Produced data that advanced retrofit techniques for bridge structures.
18. Advanced technology for repairing and strengthening reinforced concrete, steel, and masonry structures.
19. Improved in-situ measurement methods for soil liquefaction and stability under seismic loads.
20. Created database on storm surge and tsunamis and verified mathematical models of tsunami and storm surge warning systems.
21. Established a library resource of current research on wind and earthquake engineering and on storm surge and tsunamis.
22. Exchanged more than 200 guest researchers between Japan and the United States that has resulted in advancing their respective organizations mission research, advanced the state-of-technology, and provided career growth opportunities for these guest researchers.
23. Performed joint research in more than 10 collaborative research projects that resulted in new U.S. seismic design criteria for buildings and bridges.
24. Gained better knowledge of both countries research, design and construction capabilities from in-depth visits to host country's laboratories and building and public works projects. Results of such visits contribute to creation of new Task Committees, agendas for Joint Panel meetings and task committee workshops, special visits of U.S.-Japan researchers, and joint collaborative research.

HIGHLIGHTS OF THE TECHNICAL SITE VISITS

During 18-20 May, the delegation visited New Orleans to meet with officials from the Louisiana Department of Transportation and Development, The Army Corps of Engineers, the New Orleans Planning Commission and the Louisiana State University's Hurricane Research Center. Discussions centered on the extent of flooding and damages to the infrastructure resulting from Hurricanes Katrina and Rita. These hurricanes caused a large number of deaths, displaced hundreds of thousands of persons, and greatly impacted the local economies. Approximately eighty percent of the city was flooded. At the time of our visit, we were told that approximately 50 percent of the population had returned. New Orleans' French Quarter and Garden Districts that are situated on higher ground were not flooded, but other neighborhoods such as the 9th Ward were flooded.

Flood destroyed residences in New Orleans' Lower 9th Ward

The delegation visited several New Orleans neighborhoods including the Lower 9th Ward, originally a cypress swamp, adjacent to the Industrial Canal and also neighborhoods adjacent to the 17th Street Canal. Detailed information about these sites, performance of local structures, key findings, and recommendations are available from NIST's report, *Performance of Physical Structures in Hurricane Katrina and Hurricane Rita: A Reconnaissance Report*, NIST Technical Note 1476, June 2006. The report is available online at: http://www.nist.gov/public_affairs/releases/hurricane_report060906.htm.

Highlights of each visit follow.

1. LOUSIANA DEPARTMENT OF TRANSPORTATION AND DEVELOPMENT (LADOTD) http://www.dotd.state.la.us.

Officials from the Louisiana Department of Transportation and Development (LADOTD) provided the delegation with an overview of their response and recovery following the two disastrous hurricanes. LADOTD staff presented examples of infrastructural damage such as the Lake Pontchartrain I-10 Twin Span; flooding of Parishes in New Orleans near the Inner Harbor Navigation Canal; scouring that undermined bridge approach slabs and bridge piers; wind damages to structures such as electrical gear systems on vertical lift bridges and paint blasted from bridge structures such as the Huey P. Long Bridge; 52 movable bridges were damaged; some swing span bridges experienced flood debris lodged in their gear and motor systems. Some highlights from LADOTD discussions follow.

Lake Pontchartrain I-10 Twin Span Bridge Repair. This 8.6 km (5.4 mi) monolithic twin-span prestressed girder bridge experienced multiple span displacements on the north end of the east and west bound roadways. LADOTD representatives described and showed photographs of spans that had been uplifted and displaced into the water, and others where the alignment of spans was shifted. Repairs were performed using a LADOTD design-build bid contract working with many organizations. One repair method involved the use of a self propelled jacking system on a barge to repair and reposition tens of bridge spans and hundreds of 300 ton concrete panels. The panels were transported to site using the barges that were floated under the deck sections and lifted by hydraulic jacks. The realignment and repair of damaged spans on the east bound roadway were completed in 34 days, 11 days quicker than the original estimation and at a cost of $1.1 million. About 1.6 km (1 mi) of the westbound roadway was replaced with Acrow 700[1] Series bridging (modular spans replacing the former military Bailey Bridge System) that were prefabricated and assembled at the site. Repairs of the eastbound lanes were completed in October 2005 and the westbound lanes in January 2006. The Acrow bridge spans will be maintained for 3 years. During this time period, plans will be developed for a six lane bridge at a higher elevation (currently the bridges are about 4.3 m (14 ft) above mean sea level) with enhanced vessel collision resistance, and a planned service-life of 100 years. The new bridge is planned to be 17.8 km (11.1 mi) long.

Huey P. Long Bridge

The delegation was briefed about and visited LADOTD's bridge truss widening project of the 70-year old Huey P. Long Bridge to improve traffic flow. Work includes widening the existing 2.9 m (9 ft) travel lanes to three 3.4 m (11 ft) travel lanes in each direction, adding a 2.4 m (8 ft) outside shoulder and 0.6 m (2 ft) offset inside shoulders. The project is estimated to cost $600 to $800 million.

John James Audubon Bridge, http://www.timedla.com/bridge/audubon.

The delegation was briefed on the design of the John James Audubon[2] Bridge, a design-build project that will be the longest cable-stayed bridge in North America. Its center span will be 482 m (1 583 ft) long with end spans of 197 m (647 ft). Its design life is 100 years. The bridge will cross the Mississippi river between Natchez, Mississippi and Baton Rouge, Louisiana. It is constructed by Audubon Bridge Constructors, a joint venture comprised of Flatiron Constructors, Granite Construction, and Parsons Transportation Group. The $334 million project will include a 3.9 km (2.4 mi) long, four 3.7 m (12 ft) lanes, 3 m (10 ft) shoulder, and approximately 19.2 km (12 mi) of approaches. The bridge is scheduled to be complete by summer 2010. The cable stays are semi-fan arranged parallel strand system with corrosion protection. Wind tunnel testing included wind induced flutter and rain induced vibrations.

2. US ARMY CORPS OF ENGINEERS (CORPS).

Officials from the CORPS 'Task-Force Hope', New Orleans hosted the delegation to the 17th Street Canal site and the 9th Ward Inner Harbor Navigation Canal and discussed the report, *Interagency Performance Evaluation Task Force (IPET)*. 'Task Force Hope' was created by the CORPS just after Hurricane Katrina to manage the work to repair damages to levees and floodwalls and flood protection systems, debris removal, and perform emergency response efforts. The actual work was performed by the Corps and its contractors under Task Force Hope. IPET was created to determine why specific infrastructure failed and to recommend remediation methods. The American Society of Civil Engineers' External Review Panel (ERP) conducted a review of the IPET Report on 17th Street Canal Floodwall Breach that is available at http://www.asce.org/static/hurricane/erp.cfm. New Orleans is surrounded by 560 km (350 mi) of levees and floodwalls, 71 pumping stations, and 4 gated outlets.

17th Street Canal.

According to the CORPS the 17th Street Canal Floodwall was constructed of concrete I-wall and sheet steel pilings on an earthen levee. In locations of the failed floodwalls the CORPS is installing an inverted "T Wall" by driving piling down to 15.8 m (52 ft); where previous piling were driven down to 5.2 m (17 ft). The existing I-Walls are currently being strengthened.

---

[1] Reference Acrow Corporation of America http://www.acrowusa.com

[2] Named after the famous artist of American birds.

17th Street Canal levee under new construction

Inner Harbor Navigation Canal (IHNC). The delegation visited the Inner Harbor Navigation Canal and Pumping Station. New Orleans has numerous pumping stations to remove rainwater from the city. Levee and floodwall breaches occurred along the IHNC. The CORPS is replacing 1250 m (4100 ft) of levee and flood wall where two breaches occurred. Piles are driven 32 m to 36.6 m (106 ft to 120 ft) below sea level. The CORPS is constructing a new Pumping Station and 11 gates at the IHNC to prevent storm surge from entering the canal and permit existing pump stations to continue operations.

Panorama of IHNC Flood Gates and Pumping Station

The floodwalls along the IHNC were constructed with concrete I-Wall and sheet steel pilings. The CORPS is replacing failed I-Walls with inverted T-Walls. They are designed for heights of 4.9 m (16 ft) up from the previous 3.4 m (11 ft). Sheet piling is drilled to 7 m (23 ft) below sea level to prevent water underseepage. A concrete pad base is constructed where H-Piles are welded to the sheet piles for each of the steel reinforced monolith sections. Additionally, some levees will be raised and their backsides armored with stone and concrete.

3. NEW ORLEANS REGIONAL PLANNING COMMISSION (RPC) http://www.norpc.org. The Planning Commission serves metro New Orleans including its five Parishes and 1.3 million residents. The Commission is managed by an elected 26 member Board of Governors from such industries as trucking, transit, airports, railroads, highways and from citizen members. The Commission addresses economic development planning, coordinates highway and transport projects such as air quality, traffic counting and monitoring, and urban area planning. The RPC performs forecasts of business growth 25-years out to promote the competitiveness of the region by working with Federal, State, parish, and municipal governments. Discussions centered on recovery following Hurricanes Katrina and Rita to bring citizens back to New Orleans. RPC's emphasis is on closely working with the Federal Government for repairing and restoring New Orleans and on providing incentives for citizens to return to New Orleans, improving communications with the community, working to restore medical technologies at closed hospitals and reopening Tulane University's Engineering Program. The Commission is:

a. obtaining high resolutions images of the greater New Orleans region for performing detailed analysis of land and transportation use in planning future growth, infrastructure maintenance, and economic development,
b. working to clean-up and develop Brownfield sites into useful land for living and agriculture,
c. encouraging the restoration of the wetlands that play an important role in protecting New Orleans from flooding,
d. organizing commercial neighborhood revitalization programs,
e. partnering with public and private organizations to make New Orleans become a green city by greater conservation of energy and enhanced air quality, and
f. developing a database of traffic patterns and signals to facilitate traffic flow and identifying equipment needs for remote site monitoring.

4. LOUSIANA STATE UNIVERSITY HURRICANE RESEARCH CENTER (LSU/HRC)

http://www.hurricane.lsu.edu.

The delegation was welcomed at the Hurricane Research Center where they discussed a series of presentations and visited HRC's aerodynamic and boundary layer wind tunnel with capabilities for flow visualization, flow measurement, and force and pressure measurement. Presentations included:

a. *Overview of Hurricane Research and Katrina-Specific Research and Operations* by Marc Levitan, Director, LSU Hurricane Research Center. Discussions included HRC's activities in hurricane frequency and intensity modeling, hurricane impacts, preparedness, use of Geographic Information System (GIS) for planning and response activities, response (real-time data analysis for land fall hurricanes), mitigation, education in disaster science and management. Hong Kong has used information and data from the Hurricanes Katrina and Rita as case studies in wind, flood, and evacuation modeling.
b. *Katrina Storm Surge Modeling, Levee Failure Analysis and the Way Forward* by Ivor van Heerden, Director, Hurricane Public Health Center and Deputy Director LSU HRC. van Heerden recently published, The Storm: What Went Wrong and Why During Hurricane Katrina--the Inside Story from One Louisiana Scientist. Dr. van Heerden noted that many of the earth levees consisted of cypress wood and organic matter like peat and clays that swell when saturated.
c. *Development and Application of a Method for Hurricane Shelter Assessment/Operations Planning for a New Orleans Hospital* by James P. Gregg, Structural Engineer, HNTB Corporation. Gregg described a project in which they developed a shelter assessment and mitigation method by incorporating the Saffir-Simpson Hurricane Scale; ASCE-7; and a flood, wind, structural, and cladding analyses to assess the performance of a 60-year old hospital.
d. *Flood Fatality Modeling and Hurricane Katrina* by Ezra Boyd, Graduate Research Assistant. Boyd discussed research to estimate the number of expected fatalities for different flood scenarios using three models: 1) disaster mitigation (optimal configuration of levees to reduce loss of life); 2) disaster planning (2004 hurricane Pam simulation); and 3) disaster response (real time support for search and rescue).
e. *Storm Surge Damage to Bridges* by Ayman Okeil, Assistant Professor of Civil and Engineering. Okeil assessed short- and medium-span bridges in the New Orleans area and concluded there is great need to identify improved methods to absorb energy from storm surge and wave actions.
f. *Hurricane Effects on Long-span Bridges* by Xianzhi Liu, Graduate Research Assistant, LSU.

Reviewed advanced bridge aerodynamics analysis that incorporates the results from past research evaluation of the performance of bridges under similar conditions experienced from Hurricanes Katrina and Rita.

g. *Information Management for Hurricane Katrina Recovery* by John Pine, Chair, Geography and Anthropology and Director, LSU Disaster Science and Management Academic Programs. Pine reviewed work in creating a management information system containing data, photographs including satellite, reports, reference information for use by researchers, community planners, and others.

h. *Hurricane Katrina Environmental Impacts and Contamination* by John Pardue, Director, Louisiana Water Resources Research Institute. Pardue reviewed his analysis on levels of contaminates from chemicals and bacteria in floodwaters following Katrina. He noted that no agency has the responsibility for regulatory control of indoor contamination including mold, a major problem in restoring damaged buildings. Landfills created to accommodate debris from damaged and destroyed residences and other buildings and structures may present environmental problems. These landfills are not lined and are being filled with a wide range of hazardous materials including aerosols, paints, oils, and other chemicals that can leach into the ground.

i. *Hurricane Evacuations and Contraflow* by Brian Wolshon, Associate Professor of Civil and Environmental Engineering. Prior to Hurricane George in 1998, New Orleans did not have coordinated evacuation plans. Studies were performed following Hurricanes Katrina and Rita to maximize traffic flows by improved scheduling and reducing traffic congestion at contraflow nodes (loading points).

ABSTRACT

This publication is the Proceedings of the 38th Joint Meeting of the U.S.-Japan Panel on Wind and Seismic Effects. The meeting was held at the National Institute of Standards and Technology, Gaithersburg, Maryland during 15-17 May 2006. The Proceedings include the technical program, list of members, Panel Resolutions, Task Committee Reports, and 29 technical papers.

The manuscripts were presented in eight sessions: Geotechnical Engineering and Ground Motion, Next-Generation Building and Infrastructure Systems, Wind Engineering, Storm Surge and Tsunamis, Recent Natural Disasters and Natural Disaster Management Plan, Dams, Transportation Systems, and Fire Performance of Structures.

KEYWORDS: bridges; building performance; disaster information systems; disaster reduction; earthquakes; geospatial engineering; geotechnical engineering; ground motion; infrastructure; liquefaction; NEES; progressive collapse; public health; risk assessment; seismic; standards; structural engineering; tsunami; and wind loads.

AGENDA

38th TECHNICAL MEETING on PANEL ON WIND AND SEISMIC EFFECTS

15-20 May 2006

MONDAY 15 MAY

1000 OPENING CEREMONIES
(Lecture Room B, Administration Building)

Call to order by Mr. Stephen CAUFFMAN, Secretary-General US--side Panel

Opening remarks by Dr. Hratch SEMERJIAN, Deputy Director, National Institute of Standards and Technology

Remarks by Mr. Hiroshi IKUKAWA, Counsellor for Science and Technology, Embassy of Japan

Remarks by Mr. James ST. PIERRE, Chairman US-Side, Panel on Wind and Seismic Effects, Chief, Materials and Construction Research Division, Building and Fire Research Laboratory

Remarks by Dr. Tadahiko SAKAMOTO, Chairman Japan-Side, Panel on Wind and Seismic Effects, Chief Executive, Public Works Research Institute

Introduction of U.S. Members by U.S. Panel Chairman

Introduction of Japan Members by Japan Panel Chairman

Elect Joint Meeting Chairman

Adopt Agenda

Adjourn

1115 Group Photograph

TECHNICAL SESSION 1

1130-1235 Technical Session 1 – GEOTECHNICAL ENGINEERING AND GROUND MOTION

Chairman: Dr. Tadahiko SAKAMOTO

1130 *Fundamental Study on Health Monitoring and Evaluation System for Port/Airport Facilities*, Takahiro Sugano, Tomohiro Tanaka, Eiji Kohama*, PARI

1145 *Response of an Integrated Building and Free-Field Surface Downhole Network*, Mehmet Celebi, USGS.

1200 Discussion

1220 Lunch (Employees Lounge)

TASK COMMITTEE MEETINGS

1330-1645 Task Committee Meetings

T/C A: **Geotechnical Engineering and Ground Motion**. Dr. Keiichi TAMURA, NILIM (Japan-side Co-Chair) and Dr. Eiji KOHAMA, PARI (Acting Japan-side Co-Chair) and Dr. Mehmet CELEBI, USGS (U.S.-side Co-Chair)
Administration Building, Conference Room-111

T/C B: **Next-Generation Building and Infrastructure Systems**. Dr. Taiki SAITO, BRI (Acting Japan-side Co-Chair), Dr. Chikahiro MINOWA, NIED (Acting Japan-side Co-Chair), Dr. Yoshihiro IWATA, BRI, Dr. Koichi MORITA, BRI, and Dr. George LEE, MCEER and Dr. Douglas FOUTCH, NSF (U.S.-side Co-Chairs)
Administration Building, Conference Room-113

T/C C: **Dams**. Dr. Yoshikazu YAMAGUCHI, PWRI (Japan-side Chair) and Dr. Robert HALL and Dr. Enrique MATHEU, Corps of Engineers (U.S.-side Chairs)
Administration Building, Dining Room A

T/C D: **Wind Engineering**. Dr. Hiroshi SATO, PWRI (Acting Japan-side Co-Chair) and Dr. Nicholas JONES, Johns Hopkins University and Mr. John GAYNOR, NOAA (U.S.-side Chairs)
Administration Building, Employees Lounge

T/C G: **Transportation Systems**. Dr. Shigeki UNJOH, PWRI (Acting Japan-side Chair) and Dr. Phillip YEN, FHWA (U.S.-side Chair)
Administration Building Lecture Room B

T/C H: **Storm Surge and Tsunami**. Dr. Takashi TOMITA, PARI (Japan-side Chair) and Mr. Katsuya ODA, NILIM, and Dr. Solomon YIM, OSU, (US-side Co-Chair)
Administration Building, Dining Room C

T/C I: **Fire Performance of Structures**. Dr. Mamoru KOHNO, NILIM (Japan-side Chair) and Dr. William GROSSHANDLER, NIST and Dr. John GROSS, NIST (US-side Co-Chairs)
Administration Building, Lecture Room F

1645 Conclusion of Day 1

TUESDAY 16 MAY

TECHNICAL SESSION 2

0800-0935 Technical Session 2 – NEXT-GENERATION BUILDING AND INFRASTRUCTURE SYSTEMS

Chairman: Mr. James ST. PIERRE

0800 *Reparability Limit of Steel Structural Buildings Based on the Actual Data of Hyogoken-Nanbu Earthquake*, Yoshihiro Iwata*, BRI; Hirokazu Sugimoto, Schokbeton-Japan Co., Ltd.; and Hitoshi Kuwamura, University of Tokyo
0815 *Recent Development on the Design and Evaluation of Steel Structures for Seismic Loads: An NSF Perspective*, Douglas Foutch, NSF
0830 *Wood Building Collapse Test Using E-Defense*, Isao Sakamoto, Keio University; Naohito Kawai, BRI; Takahiro Tsuchimoto, MLIT; and Chikahiro Minowa*, NIED
0845 *Multi-hazard Protection of Structures: A New Frontier on Smart Structures Technology for Earthquake Engineers*, Shi Chi Liu, NSF
0900 *Crack Detection Methods Using Radio Frequency Identification and Electrically Conductive Materials*, Koichi Morita*, BRI and Kazuya Noguchi, NILIM
0915 Discussion

0935 Break

TECHNICAL SESSION 3

0955-1100 Technical Session 3 – WIND ENGINEERING

Chairman: Mr. James ST. PIERRE

0955 *Design and Testing of Iowa State University's AABL Wind and Gust Tunnel*, Partha Sarkar* and Fred Haan, ISU
1010 *High Wind Damage to Buildings Caused by Typhoon in 2004*, Yasuo Okuda, Hitomitsu Kikitsu and Hisashi Okada, BRI (presented by Taiki SAITO, BRI)
1025 *Meteorological Aspects of the Gulf of Mexico Hurricanes*, John Gaynor, NOAA
1040 Discussion

TECHNICAL SESSION 4

1100-1220 Technical Session 4 – STORM SURGE AND TSUNAMIS

Chairman: Mr. James St. PIERRE

1100 *Application of Storm Surge and Tsunami Simulator in Oceans and Coastal Areas (STOC) to Tsunami Analysis*, Takashi Tomita*, Kazuhiko Honda and Taro Kakinuma, PARI
1115 *Experimental and Numerical Modeling of Storm Surge and Tsunami Effects on Structures*, Solomon Yim*, Oregon State University and Kwok Fai Cheung, University of Hawaii
1130 *Development of Estimation Method on Drift and Collision Behaviors of Debris Caused by Tsunamis*, Katsuya Oda*, Osamu Okamoto and Kentaro Kumagai, NILIM
1145 Discussion

1210 Lunch: NIST Employees Lounge

TECHNICAL SESSION 5

1330-1530 Technical Session 5 – RECENT NATURAL DISASTERS AND NATURAL DISASTER MANAGEMENT PLAN

Chairman: Mr. James St. PIERRE

1330 *Toward the Establishment of a Regional Society that is Safe and Secure Against Disasters*, Tsuneyoshi Mochizuki, Kiyoshi Minami, Koichi Yamashita, Keiichi Tamura*, Koh-ichi Fujita and Katsuya Oda, NILIM
1345 *Recovery and Monitoring Challenges with Water Quality Issues in New Orleans during Hurricane Katrina Recovery Operations*, William Roper*, George Mason University and Kevin Weiss and James Wheeler, EPA
1400 *PWRI's New Organizations and Research Projects on Natural Disasters*, Tadahiko Sakamoto and Hiroshi Sato*, PWRI
1415 *Reconnaissance of Damage to Physical Structures in the Gulf States from Hurricanes Katrina and Rita*, William Fritz, NIST
1430 *Establishing a Disaster Information System to practically Support Disaster Countermeasures: Conducting and Reviewing Demonstration Experiment*, Akihiro Sanada; Takaaki Kusakabe; and Keiichi Tamura*, NILIM
1445 Hea*lth Concerns Associated with Mold in Water-Damaged Homes After Hurricanes Katrina and Rita --- New Orleans Area, Louisiana, October 2005*, Clive Brown, CDC.
1500 Discussion
1530 Break

STRATEGIC PLANNING SESSION

1545 – 1730 Strategic Planning Session

1730 Conclusion of Day 2

WEDNESDAY 17 MAY

TECHNICAL SESSION 6

0900 – 1005 Technical Session 6 – DAMS

Chairman: Dr. Tadahiko SAKAMOTO

0900 *Investigation into Crack Phenomena of Unreinforced Concrete Structure for Aseismic Evaluation of Concrete Dams*, Tadahiko Sakamoto, PWRI; Yoshikazu Yamaguchi*, PWRI; Takashi Sasaki, PWRI; Kei Takafuji, PWRI; and Ken-ichi Kanenawa, MLIT

0915 *Federal Initiatives for Security and Protection of Dams*, Enrique Matheu, DHS on loan from ERDC/Corps

0930 *Establishment of Input Large-scale Earthquake Motions for Earthquake Proof Evaluation of Existing Dams*, Nario Yasuda, NILIM; Koji Sujino, METI; and Takayuki Sano, NILIM (presented by Yoshikazu YAMAGUCHI, PWRI)

0945 Discussion

TECHNICAL SESSION 7

1005-1110 Technical Session 7 – TRANSPORTATION SYSTEMS

Chairman: Dr. Tadahiko SAKAMOTO

1005 *FHWA Long-Term Bridge Performance Program*, Hamid Ghasemi*, Ian Friedland, Steven Chase, and Joey Hartmann, FHWA

1020 *Damage Investigation and the Preliminary Analyses of Bridge Damage Caused by the 2004 Indian Ocean Tsunami*, Shigeki Unjoh* and Kazuo Endoh, PWRI

1035 *Multi-Hazard Design Criteria of Highway Bridges*, George Lee and Mai Tong, University at Buffalo and Phil Yen, FHWA

1050 Discussion

1110 **Break**

TECHNICAL SESSION 8

1125 – 1245 Technical Session 8 – FIRE PERFORMANCE OF STRUCTURES

Chairman: Dr. Tadahiko SAKAMOTO

1125 *Outline of the Fire Resistance Verification Method in the Building Standard Law of Japan*, Mamoru Kohno*, NILIM
1140 Fire *Endurance Testing of Floor Systems - Effects of Scale and Restraint*, John Gross, NIST
1155 *A Study on the Collapse Control Design Method for High-rise Steel Buildings*, Akira Wada, Tokyo Institute of Technology; Ken-ichi Ohi, Kobe University; Hiroyuki Suzuki, Tsukuba University; Mamoru Kohno*, NILIM; and Yoshifumi Sakumoto, Nippon Steel Corp.
1210 *The Need for International Collaboration on Structural Fire Endurance Research*, William Grosshandler and Anthony Hamins*, NIST
1225 Discussions

1245 Lunch: NIST Lunch Club

TASK COMMITTEE REPORTS AND RESOLUTIONS

1345-1500 REPORT OF TASK COMMITTEES

Chairman: Mr. James ST. PIERRE

T/C A: Geotechnical Engineering and Ground Motion
T/C B: Next-Generation Building and Infrastructure Systems
T/C C: Dams
T/C D. Wind Engineering
T/C G: Transportation
T/C H: Storm Surge and Tsunamis
T/C I: Fire Performance of Structures
1500 **Break**

1515-1600 ADOPTION OF FINAL RESOLUTIONS

1600 **Break**

CLOSING CEREMONIES

1610 Call to Order by Mr. Stephen CAUFFMAN, Secretary-General, U.S.-Side Panel
Closing Remarks by Dr. Tadahiko SAKAMOTO, Chairman Japan-Side Panel
Closing Remarks by Mr. James St. PIERRE, Chairman U.S.-Side Panel

1630 **Conclusion of 38th Joint Panel Technical Session**

LIST OF PANEL MEMBERS

JAPAN-SIDE PANEL ON WIND AND SEISMIC EFFECTS
MEMBERSHIP LIST

STEERING COMMITTEE MEMBERS

Dr. Tadahiko Sakamoto
Chairman, Japan-side Panel on Wind and Seismic Effects
Chief Executive, Public Works Research Institute
1-6 Minamihara, Tsukuba-shi, Ibaraki-ken 305-8516
Tel: 029-879-6700
Fax: 029-879-6741
E-mail: sakamoto@pwri.go.jp

Mr. Osamu Matsuo
Secretary-General, Japan-side Panel on Wind and Seismic Effects
Director, Earthquake Disaster Prevention Research Group
Public Works Research Institute
1-6 Minamihara, Tsukuba-shi, Ibaraki-ken 305-8516
Tel: 029-879-6721
Fax: 029-879-6736
E-mail: matsuo@pwri.go.jp

Mr. Jiro Fukui
Director, Structures Research Group
Public Works Research Institute
1-6 Minamihara, Tsukuba-shi, Ibaraki-ken 305-8516
Tel: 029-879-6726
Fax: 029-879-6739
E-mail: fukui@pwri.go.jp

Dr. Hiroshi Fukuyama
Chief Research Engineer and Research Coordinator
Department of Structural Engineering
Building Research Institute
1 Tachihara, Tsukuba-shi, Ibaraki-ken 305-0802
Tel: 029-864-6647
Fax: 029-864-6773
E-mail: fukuyama@kenken.go.jp

Dr. Hiromichi Higashihara
Director, Earthquake Mitigation Research Center (EDM),
National Research Institute for Earth Science and Disaster Prevention
1-5-2 Wakinohama Kaigandori, Chuo-ku, Kobe, Hyogo 651-0073
Tel: 078-262-5520
Fax: 078-262-5526
E-mail: higashi@edm.bosai.go.jp

Dr. Masanori Iiba
Research Coordinator for Disaster Mitigation of Buildings
Research Center for Disaster Risk Management
National Institute for Land and Infrastructure Management
Ministry of Land, Infrastructure and Transport
1 Asahi, Tsukuba-shi, Ibaraki-ken 305-0804
Tel: 029-864-4963
Fax: 029-864-0598
E-mail: iiba-m92hx@nilim.go.jp

Dr. Takashi Iijima
President, Civil Engineering Research Laboratory
1-18 Kanda Suda-cho Chiyoda-ku, Tokyo 101-0041
Tel: 03-3254-9481
Fax: 03-3254-9448
E-mail: iijima@crl.or.jp

Mr. Jun Inomata
Director, Planning and Research Administration Department
National Institute for Land and Infrastructure Management
Ministry of Land, Infrastructure and Transport
1 Asahi, Tsukuba-shi, Ibaraki-ken 305-0804 Japan
Tel: 029-864-2826
Fax: 029-864-1527
E-mail: inomata-j92ta@nilim.go.jp

Mr. Hidemi Ito
Director, Seismological and Volcanological Research Department
Meteorological Research Institute
Japan Meteorological Agency
1 Nagamine, Tsukuba-shi, Ibaraki-ken 305-0052
Tel: 029-853-8675
Fax: 029-853-3730
E-mail: hideito@mri-jma.go.jp

Dr. Naohito Kawai
Chief Research Engineer, Department of Structural Engineering
Building Research Institute
1 Tachihara, Tsukuba-shi, Ibaraki-ken 305-0802
Tel: 029-864-6753
Fax: 029-864-6773
E-mail: kawai@kenken.go.jp

Prof. Kazuhiko Kawashima
Professor, Department of Civil Engineering
Tokyo Institute of Technology
2-12-1 O-okayama, Meguro-ku, Tokyo 152-0033
Tel: 03-5734-2922
Fax: 03-3729-0728
E-mail: kawasima@cv.titech.ac.jp

Mr. Syuhei Kazusa
Director, Volcanic and Earthquake Disaster Management
Disaster Prevention Bureau
Cabinet Office
1-2-2 Kasumigaseki, Chiyoda-ku, Tokyo 100-8918
Tel: 03-3501-5693
Fax: 03-3501-5199
E-mail: shuhei.kazusa@cao.go.jp

Dr. Mamoru Kohno
Head, Fire Standards Division
Building Department
National Institute for Land and Infrastructure Management
Ministry of Land, Infrastructure and Transport
1 Tachihara, Tsukuba-shi, Ibaraki-ken 305-0802
Tel: 029-864-4348
Fax: 029-864-6774

E-mail: kouno-m92ta@nilim.go.jp

Mr. Hiromichi Maruyama
Director, Geographic Department
Geographical Survey Institute
Ministry of Land, Infrastructure and Transport
1 Kitasato, Tsukuba-shi, Ibaraki-ken 305-0811
Tel: 029-864-1111
Fax: 029-864-1804
E-mail: maruyama@gsi.go.jp

Dr. Chikahiro Minowa
Scientific Research Advisor
National Research Institute for Earth Science and Disaster Prevention
3-1 Tennodai, Tsukuba-shi, Ibaraki-ken 305-0006
Tel: 029-851-1611
Fax: 029-851-1674
E-mail: minowa@bosai.go.jp

Mr. Tsuneyoshi Mochizuki
Director-General, National Institute for Land and Infrastructure Management
Ministry of Land, Infrastructure and Transport
1 Asahi, Tsukuba-shi, Ibaraki-ken 305-0804
Tel: 029-864-2211
Fax: 029-864-2148
E-mail: mochizuki-t28j@nilim.go.jp

Mr. Tomokazu Morii
International Cooperation Coordinator
International Science and Technology Affairs Division
Science and Technology Policy Bureau
Ministry of Education, Culture, Sports, Science and Technology
2-5-1 Marunouchi, Chiyoda-ku, Tokyo 100-8959
Tel: 03-6734-3989
Fax: 03-6734-4058
E-mail: tmorii@mext.go.jp

Mr. Jun Murakoshi
Team Leader, Bridge Structure Research Team
Structures Research Group
Public Works Research Institute
1-6 Minamihara, Tsukuba-shi, Ibaraki-ken 305-8516
Tel: 029-879-6792
Fax: 029-879-6739
E-mail: murakosi@pwri.go.jp

Dr. Tatsuro Murota
Director, Research & Testing Laboratory, The Japan Housing and Wood Technology Center Foundation
1-6 Minamihara, Tsukuba-shi, Ibaraki-ken 305-8516
Tel: 03-3647-3930
Fax: 03-3647-3840
E-mail: t-murota@howtec.or.jp

Prof. Shinsuke Nakata
Professor, Infrastructure System Engineering Course
Kochi University of Technology
185 Miyanokuchi, Tosa-Yamada-cho, Kochi-ken 782-8502
Tel: 0887-53-1040
Fax: 0887-57-2420
E-mail: nakata.shinsuke@kochi-tech.ac.jp

Dr. Masayoshi Nakashima
Director, Hyogo Earthquake Engineering Center
National Research Institute for Earth Science and Disaster Prevention
1501-21, Mituta, Nishikameya, Shijimi-cho, Miki-shi, Hyogo 673-0515
Tel: 0794-85-8211
Fax: 0794-85-7994
E-mail: naka@bosai.go.jp

Dr. Junichi Nishikawa
Director
Cold Region Construction Engineering Research Group
Public Works Research Institute
1-3 Hiragishi, Toyohira-ku, Sapporo-shi Hokkaido 062-8602
Tel: 011-841-5175
Fax: 011-820-2714
E-mail: nishikaw@ceri.go.jp

Dr. Isao Nishiyama
Director, Housing Department,
National Institute for Land and Infrastructure Management
1 Tachihara, Tsukuba-shi, Ibaraki-ken 305-0802
Tel: 029-864-3942
Fax: 029-864-6772
E-mail: nishiyama-i92ta@nilim.go.jp

Dr. Setsuo Noda
Advisor, Mitsubishi Heavy Industries, Ltd.
2-5-1 Marunouchi, Chiyoda-ku, Tokyo 102-0092
Tel: 03-3212-9378
Fax: 03-3212-9833
E-mail: setsuo_noda@mhi.co.jp

Dr. Hisashi Okada
Director, Department of Structural Engineering
Building Research Institute
1 Tachihara, Tsukuba-shi, Ibaraki-ken 305-0802
Tel: 029-864-6633
Fax: 029-864-6773
E-mail: okada@kenken.go.jp

Mr. Atsuo Okazaki
Director, International Codes and Standards
Building Guidance Division
Housing Bureau
Ministry of Land, Infrastructure and Transport
2-1-3 Kasumigaseki, Chiyoda-ku, Tokyo 100-8918
Tel: 03-5253-8514
Fax: 03-5253-1630
E-mail: okazaki-a263@mlit.go.jp

Dr. Izuru Okawa
Senior Research Fellow
Department of Structural Engineering
Building Research Institute
1 Tachihara, Tsukuba-shi, Ibaraki-ken 305-0802
Tel: 029-864-6627
Fax: 029-864-6773
E-mail: okawa@kenken.go.jp

Dr. Yasuo Okuda
Chief Research Engineer
Department of Structural Engineering
Building Research Institute
1 Tachihara, Tsukuba-shi, Ibaraki-ken 305-0802

Tel: 029-864-6618
Fax: 029-864-6773
E-mail: y_okuda@kenken.go.jp

Dr. Hiroshi Sato
Executive Research Coordinator
Public Works Research Institute
1-6 Minamihara, Tsukuba-shi, Ibaraki-ken 305-8516
Tel: 029-879-6715
Fax: 029-879-6702
E-mail: hsato@pwri.go.jp

Mr. Seiji Sato
Director, Disaster Risk Management Division
River Bureau
Ministry of Land, Infrastructure and Transport
2-1-3 Kasumigaseki, Chiyoda-ku, Tokyo 100-8918
Tel: 03-3580-8111
Fax: 03-5253-1608
E-mail: satou-s2yc@mlit.go.jp

Mr. Yasuhiro Shoji
Head, Earthquake Disaster Prevention Division
Research Center for Disaster Risk Management
National Institute for Land and Infrastructure Management
Ministry of Land, Infrastructure and Transport
1 Asahi, Tsukuba-shi, Ibaraki-ken 305-0804
Tel: 029-864-2211
Fax: 029-864-0598
E-mail: shoji-y92pc@nilim.go.jp

Dr. Hideki Sugita
Team Leader, Ground Vibration Research Team
Earthquake Disaster Prevention Research Group
Public Works Research Institute
1-6 Minamihara, Tsukuba-shi, Ibaraki-ken 305-8516
Tel: 029-879-6770
Fax: 029-879-6735
E-mail: sugita@pwri.go.jp

Dr. Kei-ichi Tamura
Research Coordinator for Earthquake Disaster Prevention
Research Center for Disaster Risk Management
National Institute for Land and Infrastructure Management
Ministry of Land, Infrastructure and Transport
1 Asahi, Tsukuba-shi, Ibaraki-ken 305-0804
Tel: 029-864-2926
Fax: 029-864-0598
E-mail: tamura-k92ta@nilim.go.jp

Mr. Masaaki Togashi
Director, Typhoon Research Division
Meteorological Research Institute
Japan Meteorological Agency
1 Nagamine, Tsukuba-shi, Ibaraki-ken 305-0052
Tel: 029-853-8663
Fax: 029-853-8735
E-mail: mtogashi@mri-jma.go.jp

Dr. Takashi Tomita
Tsunami Research Director
Tsunami Research Center
Port and Airport Research Institute
3-1-1 Nagase, Yokosuka-shi, Kanagawa-ken 239-0826
Tel: 0468-44-5052
Fax: 0468-44-1274
E-mail: tomita@pari.go.jp

Mr. Yuichi Toya
Director, Disaster Prevention Office
Coast Administration and Disaster Prevention Division
Ports and Harbors Bureau
Ministry of Land, Infrastructure and Transport
2-1-3 Kasumigaseki, Chiyoda-ku, Tokyo 100-8918
Tel: 03-5253-8689
Fax: 03-5253-1654
E-mail: toya-y2nz@mlit.go.jp

Mr. Kazushige Umeyama
Director, Road Emergency Management Office
Road Bureau
Ministry of Land, Infrastructure and Transport
2-1-3 Kasumigaseki, Chiyoda-ku, Tokyo 100-8918
Tel: 03-5253-8111
Fax: 03-5253-1620
E-mail: umeyama-k2gw@mlit.go.jp

Dr. Shigeki Unjoh
Team Leader, Earthquake Engineering Research Team
Earthquake Disaster Prevention Research Group
Public Works Research Institute
1-6 Minamihara, Tsukuba-shi, Ibaraki-ken 305-8516
Tel: 029-879-6773
Fax: 029-879-6736
E-mail: unjoh@pwri.go.jp

Mr. Atsushi Watanabe
Director, Office of Disaster Reduction Research
Research and Development Bureau
Ministry of Education, Culture, Sports, Science and Technology
2-5-1 Marunouchi, Chiyoda-ku, Tokyo 100-8959
Tel: 03-6734-4134
Fax: 03-6734-4139
E-mail: watanabe@mext.go.jp

Dr. Yoshikazu Yamaguchi
Team Leader, Dam Structure Research Team
Hydraulic Engineering Research Group
Public Works Research Institute
1-6 Minamihara, Tsukuba-shi, Ibaraki-ken 305-8516
Tel: 029-879-6780
Fax: 029-879-6737
E-mail: yamaguti@pwri.go.jp

Mr. Naoyuki Yamane
Director, International Division for Infrastructure
Policy Bureau
Ministry of Land, Infrastructure and Transport
2-1-3 Kasumigaseki, Chiyoda-ku, Tokyo 100-8918
Tel: 03-5253-8111
Fax: 03-5253-1562
E-mail: Yamane-n8310@mlit.go.jp

Dr. Hiroyuki Yamanouchi
Chief Executive, Building Research Institute
1 Tachihara, Tsukuba-shi, Ibaraki-ken 305-0802
Tel: 029-864-2151
Fax: 029-864-2989
E-mail: yamanoch@kenken.go.jp

Prof. Koichi Yokoyama

Professor, Department of Urban and Civil Engineering
Ibaraki University
4-12-1 Nakanarusawa, Hitachi-shi, Ibaraki-ken 316-0033
Tel: 0294-38-5161
Fax: 0294-38-5268
E-mail: yokoyama@mx.ibaraki.ac.jp

Dr. Tatsuo Yokoyama
Senior Assistant for Disaster Prevention, Planning Division
Administration Department
Japan Meteorological Agency
1-3-4 Ohte-machi, Chiyoda-ku, Tokyo 100-8918
Tel: 03-3212-8341
Fax: 03-3211-2032
E-mail: yokoyama-t@met.kishou.go.jp

Mr. Hitoshi Yoshida
Director, Hydraulic Engineering Research Group
Public Works Research Institute
1-6 Minamihara, Tsukuba-shi, Ibaraki-ken 305-0804
Tel: 029-879-6723
Fax: 029-879-6737
E-mail: h-yshida@pwri.go.jp

SECRETARIES COMMITTEE MEMBERS

Mr. Osamu Matsuo
Secretary-General, Japan-side Panel on Wind and Seismic Effects
Director, Earthquake Disaster Prevention Research Group
Public Works Research Institute
1-6 Minamihara, Tsukuba-shi, Ibaraki-ken 305-8516
Tel: 029-879-6721
Fax: 029-879-6736
E-mail: matsuo@pwri.go.jp

Mr. Jiro Fukui
Director, Structures Research Group
Public Works Research Institute
1-6 Minamihara, Tsukuba-shi, Ibaraki-ken 305-8516
Tel: 029-879-6726
Fax: 029-879-6739
E-mail: fukui@pwri.go.jp

Dr. Hiroshi Fukuyama
Chief Research Engineer and Research Coordinator
Department of Structural Engineering
Building Research Institute
1 Tachihara, Tsukuba-shi, Ibaraki-ken 305-0802
Tel: 029-864-6647
Fax: 029-864-6773
E-mail: fukuyama@kenken.go.jp

Mr. Hiroyuki Ishikawa
Team Leader, Structures Research Team
Cold Region Construction Engineering Research Group
Public Works Research Institute
1-3 Hiragishi, Toyohira-ku, Sapporo-shi Hokkaido 062-8602
Tel: 011-841-1698
Fax: 011-820-2714
E-mail: hi-iskw@ceri.go.jp

Dr. Mamoru Kohno
Head, Fire Standards Division
Building Department
National Institute for Land and Infrastructure Management
Ministry of Land, Infrastructure and Transport
1 Tachihara, Tsukuba-shi, Ibaraki-ken 305-0802
Tel: 029-864-4348
Fax: 029-864-6774
E-mail: kouno-m92ta@nilim.go.jp

Dr. Shin Koyama
Chief Research Engineer
Department of Structural Engineering
Building Research Institute
1 Tachihara, Tsukuba-shi, Ibaraki-ken 305-0802
Tel: 029-864-6642
Fax: 029-864-6773
E-mail: skoyama@kenken.go.jp

Mr. Yasuhiro Shoji
Head, Earthquake Disaster Prevention Division
Research Center for Disaster Risk Management
National Institute for Land and Infrastructure Management
Ministry of Land, Infrastructure and Transport
1 Asahi, Tsukuba-shi, Ibaraki-ken 305-0804
Tel: 029-864-2211
Fax: 029-864-0598
E-mail: shoji-y92pc@nilim.go.jp

Dr. Chikahiro Minowa
Scientific Research Advisor
National Research Institute for Earth Science and Disaster Prevention
3-1 Tennodai, Tsukuba-shi, Ibaraki-ken 305-0006
Tel: 029-851-1611
Fax: 029-851-1674
E-mail: minowa@bosai.go.jp

Mr. Akiyoshi Mukai
Head, Structural Standard Division
Building Department
National Institute for Land and Infrastructure Management
Ministry of Land, Infrastructure and Transport
1 Tachihara, Tsukuba-shi, Ibaraki-ken 305-0802
Tel: 029-864-4299
Fax: 029-864-6774
E-mail: mukai-a92ta@nilim.go.jp

Mr. Jun Murakoshi
Team Leader, Bridge Structure Research Team
Structures Research Group
Public Works Research Institute
1-6 Minamihara, Tsukuba-shi, Ibaraki-ken 305-8516
Tel: 029-879-6792
Fax: 029-879-6739
E-mail: murakosi@pwri.go.jp

Mr. Shoichi Nakatani
Team Leader, Foundation Engineering Team
Structures Research Group
Public Works Research Institute
1-6 Minamihara, Tsukuba-shi, Ibaraki-ken 305-8516
Tel: 029-879-6794
Fax: 029-879-6739
E-mail: nakatani@pwri.go.jp

Dr. Tetsuo Nakazawa
Head, The Second Research Laboratory
Typhoon Research Department
Meteorological Research Institute
Japan Meteorological Agency
Ministry of Land, Infrastructure and Transport
1-1 Nagamine, Tsukuba-shi, Ibaraki-ken 305-0052
Tel: 029-853-8671
Fax: 029-853-8735
E-mail: nakazawa@mri-jra.go.jp

Dr. Yasuo Okuda
Chief Research Engineer
Department of Structural Engineering
Building Research Institute
1 Tachihara, Tsukuba-shi, Ibaraki-ken 305-0802
Tel: 029-864-6618
Fax: 029-864-6773
E-mail: y_okuda@kenken.go.jp

Dr. Hideki Sugita
Team Leader, Ground Vibration Research Team
Earthquake Disaster Prevention Research Group

Public Works Research Institute
1-6 Minamihara, Tsukuba-shi, Ibaraki-ken 305-8516
Tel: 029-879-6770
Fax: 029-879-6735
E-mail: sugita@pwri.go.jp

Mr. Shinji Takazawa
Head, Planning Division, Geographic Department
Geographical Survey Institute
Ministry of Land, Infrastructure and Transport
1 Kitasato, Tsukuba-shi, Ibaraki-ken 305-0811
Tel: 029-864-5917
Fax: 029-864-1804
E-mail: tnemoto@gsi.go.jp

Dr. Kei-ichi Tamura
Research Coordinator for Earthquake Disaster Prevention
Research Center for Disaster Risk Management
National Institute for Land and Infrastructure Management
Ministry of Land, Infrastructure and Transport
1 Asahi, Tsukuba-shi, Ibaraki-ken 305-0804
Tel: 029-864-2926
Fax: 029-864-0598
E-mail: tamura-k92ta@nilim.go.jp

Dr. Takashi Tomita
Tsunami Research Director
Tsunami Research Center
Port and Airport Research Institute
3-1-1 Nagase, Yokosuka-shi, Kanagawa-ken 239-0826
Tel: 0468-44-5052
Fax: 0468-44-1274
E-mail: tomita@pari.go.jp

Dr. Shigeki Unjoh
Team Leader, Earthquake Engineering Research Team
Earthquake Disaster Prevention Research Group
Public Works Research Institute
1-6 Minamihara, Tsukuba-shi, Ibaraki-ken 305-8516
Tel: 029-879-6773
Fax: 029-879-6736
E-mail: unjoh@pwri.go.jp

Dr. Yoshikazu Yamaguchi
Team Leader, Dam Structure Research Team
Hydraulic Engineering Research Group
Public Works Research Institute
1-6 Minamihara, Tsukuba-shi, Ibaraki-ken 305-8516
Tel: 029-879-6780
Fax: 029-879-6737
E-mail: yamaguti@pwri.go.jp

ASSOCIATE MEMBERS

Mr. Tomomitsu Fujii	Foundation of River Basin Integrated Communications
Dr. Minoru Fujiwara	Strait Crossing Highway Research Association
Dr. Masami Fukuoka	Manegement System Assessment Center
Prof. Masaya Hirosawa	Kogakuin University
Prof. Shiro Ibukiyama	Kogyokusha College of Technology
Dr. Kaoru Ichihara	Central Consultant Inc.
Dr. Ryuichi Iida	Japan Dam Engineering Center
Dr. Takashi Iijima	Civil Engineering Research Laboratory
Mr. Yasutake Inoue	Fukuda Corporation
Dr. Toshio Iwasaki	Public Works Research Center
Mr. Shunichiro Kamijo	Mitsui Sumitomo Construction Corporation
Mr. Kenji Kawakami	Kubota Corporation
Prof. Eiichi Kuribayashi	Professor Emeritus, Toyohashi University of Technology
Dr. Tatsuro Murota	Japan Housing and Wood Technology Center
Mr. Mitsuru Nagao	Japan Construction Mechanization Association
Prof. Kiyoshi Nakano	Nakano Architectural and Engineering Associate
Prof. Shinsuke Nakata	Kochi University of Technology
Dr. Kazuto Nakazawa	Formerly, Public Works Research Center
Dr. Nobuyuki Narita	Public Works Research Center
Dr. Setsuo Noda	Mitsubishi Heavy Industries, Ltd.
Dr. Michio Okahara	Advanced Construction Technology Center
Dr. Shin Okamoto	P. S. Mitsubishi Construction Co. Ltd.
Mr. Kei-ichi Ohtani	Formerly, National Research Institute for Earth Science and Disaster Prevention
Mr. Yoshijiro Sakagami	Japan Development Construction Corporation
Dr. Yasushi Sasaki	Japan Institute of Construction Engineering
Dr. Yukihiko Sumiyoshi	Central Consultant Inc.
Mr. Jiro Taguchi	Sakurada Co. Ltd.
Dr. Masateru Tominaga	Public Works Research Center
Dr. Hajime Tsuchida	Echo Corporation
Mr. Seizo Tsuji	Japan Utility Subway Company Inc.
Prof. Koichi Yokoyama	Ibaraki University

US-SIDE PANEL ON WIND AND SEISMIC EFFECTS
MEMBERSHIP LIST

1 May 2006

Mr. James St. Pierre
Chairman, U.S.-side Panel
Chief, Materials and Construction Research Division
Building and Fire Research Laboratory
National Institute of Standards and Technology
100 Bureau Drive, Stop 8611
Gaithersburg, MD 20899-8611
301-975-4124 (F) 301-975-6122
james.st.pierre@nist.gov

Mr. Stephen A. Cauffman
Secretary-General, U.S.-side Panel
Leader, Structures Group
Materials and Construction Research Division
Building and Fire Research Laboratory
National Institute of Standards and Technology
100 Bureau Drive, Stop 8611
Gaithersburg, MD 20899-8611
301-975-6051 (F) 301-869-6275
stephen.cauffman@nist.gov

Dr. Kharaiti L. Abrol
Principal Structural Engineering Consultant
Room 475
Department of Veterans Affairs
810 Vermont Avenue, NW
Washington, DC 20420
202-565-5579 (F) 202-565-5478
abrkha@hq.med.va.gov

Dr. Jon Ake
Geophysicist
Seismotectonics and Geophysics Section
Code D-8330
P.O. Box 25007
Bureau of Reclamation
U.S. Department of the Interior
Denver, CO 80225
303-445-3169 (F) 303-236-9127
303-445-3170
jake@do.usbr.gov

Mr. John Baals
Seismic Safety Coordinator

P.O. Box 25007 (D-8110)
Bureau of Reclamation
U.S. Department of the Interior
Denver, CO 80225
303-236-9129 x304 (F) 303-236-9099
jbaals@do.usbr.gov

Dr. Eddie N. Bernard
Director, Pacific Marine Environmental Laboratory
National Oceanic and Atmospheric Administration
U.S. Department of Commerce
7600 Sand Point Way, NE
BIN C15700/Building 3
Seattle, WA 98115-0070
206-526-6800 (F) 206-526-4576
Eddie.N.Bernard@noaa.gov

Dr. David M. Boore
U.S. Geological Survey
345 Middlefield Road MS 977
Menlo Park, CA 94025
650-329-5616 (F) 650-329-5163
boore@usgs.gov

Dr. Roger D. Borcherdt
U.S. Geological Survey
U.S. Department of the Interior
345 Middlefield Road, MS 977
Menlo Park, CA 94025
650-329-5619 (F) 650-329-5163
borcherdt@usgs.gov

Dr. Mehmet K. Celebi
Research Civil Engineer
U.S. Geological Survey
U.S. Department of the Interior
345 Middlefield Road, MS 977
Menlo Park, CA 94025
650-329-5623 (F) 650-329-5163
celebi@usgs.gov

Dr. Harish Chander
U.S. Dept. of Energy (EH-53),
Room 3097,
270 Corporate Center
19901 Germantown Road
Germantown, MD 20874
301-903-6681 (F) 301-903-6172
harish.chander@hq.doe.gov

Dr. C.Y. Chen
Senior Civil/Geotechnical Engineer
Office of Foreign Buildings
Department of State
Code SA-6, Rm. 347
Washington, DC 20520
703-875-6207 (F) 703-875-6204
chency@state.gov

Dr. Ken Chong
Program Director
Mechanics and Materials
Engineering Directorate
National Science Foundation
4201 Wilson Boulevard - Room 545
Arlington, VA 22230
703-292-7008 (F) 703-292-9053
kchong@nsf.gov

Dr. Anjana Chudgar
U.S. Army Corps of Engineers
Headquarters, 441 G Street NW
ATTN: CECW-EWS
Washington, DC 20314
202-761-7750 (F) 202-761-0633
anjana.k.chudgar@hq02.usace.army.mil

Ronald T. Eguchi, President
ImageCat, Inc.
Union Bank of California Building
400 Oceangate, Suite 1050
Long Beach, CA 90802
562-628-1675 (F) 562-628-1676
rte@imagecatinc.com
http://imagecatinc.com

Dr. Amr Elnashai
Director, Mid-America Earthquake Center
Professor of Civil Engineering
University of Illinois
1245 Newmark Laboratory
205 North Mathews Avenue
Urbana, IL 61801
217-265-5497 217-333-3821
aelnash@uiuc.edu

Dr. Douglas Foutch
Program Director
Structural Systems and Hazard Mitigation of Structures (SSHM)
Room 545 S
National Science Foundation
4201 Wilson Boulevard
Arlington, VA 22230
703-292-7003
dfoutch@nsf.gov

Mr. John Gaynor
Program Office Director
US Weather Research Program
Mail Code R/WA
National Oceanic and Atmospheric Administration
Silver Spring, MD 20910
301-713-0460 x117 (F) 301-713-3515
john.gaynor@noaa.gov

Dr. Hamid Ghasemi
Bridge Safety, Reliability and Security
Office of Infrastructure and Security
Office of Infrastructure R&D
Federal Highway Administration
6300 Georgetown Pike
McLean VA 22101
202-493-3042 (F) 202-493-3443
hamid.ghasemi@fhwa.dot.gov

Dr. John Gross
Research Structural Engineer
Materials and Construction Research Division
Building and Fire Research Laboratory
National Institute of Standards and Technology
100 Bureau Drive, Stop 8611
Gaithersburg, MD 20899-8611
301-975-6068 (F) 301-869-6275
john.gross@nist.gov

Dr. William Grosshandler
Chief, Fire Research Division
Building and Fire Research Laboratory
National Institute of Standards and Technology
100 Bureau Drive, Stop 8660
Gaithersburg, MD 20899-8660
301-975-2310
William.grosshandler@nist.gov

Dr. Robert L. Hall
Chief, Structural Analysis Group
US Army Engineer Research and Development Center
CEERD-GS
3909 Halls Ferry Road
Vicksburg, MS 39180-6199
601-634-2567 (F) 601-634-3412
(C) 601-618-0644
Robert.L.Hall@erdc.usace.army.mil

Dr. Mary Ellen Hynes
Chief, Earthquake Engineering and Geophysics Branch
Geotechnical Laboratory
US Army Engineer Research and Development Center
CEERD-GS-R
3909 Halls Ferry Road
Vicksburg, MS 39180
601-634-2280 (F) 601-634-3453
202-254-5809 (DHS on detail)
mary.e.hynes@erdc.usace.army.mil

Dr. Nicholas P. Jones
Dean, Whiting School of Engineering
Johns Hopkins University
Baltimore MD 21218 USA
410-516-4050 (Jeannie Pugh)
npjones@jhu.edu

Mr. Michael Keever
Chief, Earthquake Engineering Office
California Department of Transportation Division of Engineering Services, MS9-2/7J
P.O. Box 168041
Sacramento, CA 95816
916-227-8806 (F) 916-227-8242
mike_keever@dot.ca.gov

Dr. George C. Lee
Special Task Director, Multidisciplinary Center for Earthquake Engineering Research (MCEER)
University at Buffalo

122 Red Jacket Quad
Buffalo, NY 14261
716-645-3391 x111 (F) 716-645-3399
716-645-2039
gclee@mceermail.buffalo.edu

Dr. H.S. Lew
Materials and Construction Research Division
Building and Fire Research Laboratory
National Institute of Standards and Technology
100 Bureau Drive Stop 8611
Gaithersburg, MD 20899-861
301-975-6060 (F) 301-869-6275
hai.lew@nist.gov

Mr. Michael Mahoney
Physical Scientist
Federal Emergency Management Agency
500 C Street, SW
Washington, DC 20472
202-646-2794 (F) 202-646-4387
mike.mahoney@dhs.gov

Dr. Josephine Malilay, MPH
Team Leader, Disaster Epidemiology and Assessment
Centers for Disease Control and Prevention
National Center for Environmental Health
1600 Clifton Rd. NE (Mail stop E-23)
Atlanta, GA 30333
770-488-3465 (F) 404-498-1355
JMalilay@cdc.gov

Dr. Enrique E. Matheu
Research Structural Engineer
U.S. Army Engineer Research and Development Center
ATTN: CEERD-GS-E
3909 Halls Ferry Road,
Vicksburg, MS 39181
Tel: 601-634-3235 / Fax: 601-634-4656 (202-282-8757)
Enrique.E.Matheu@erdc.usace.army.mil

Dr. Vilas Mujumdar
Director, Engineering Research Centers Program
Division of Engineering Education and Centers (EEC)
Room 585 N
National Science Foundation
4201 Wilson Blvd
Arlington, VA, 22230
703-292-7262 (F) 703-292-9052
vmujumda@nsf.gov

Noel Raufaste
NIST Guest Researcher
Building and Fire Research Laboratory
National Institute of Standards and Technology
Gaithersburg, MD 20899-8611
301-975-6062
noel.raufaste@nist.gov

Dr. William E. Roper
School of Computational Sciences
Center for Earth Observing and Space Research
George Mason University
4400 University Drive, MS 5C3
Fairfax, VA 22030
703 993-1648 (F) 703-993-1521
(C) 703-967-9694
wroper@gmu.edu

Dr. Michael Sharp
Director, Centrifuge Research Center
Geotechnical and Structures Laboratory
US Army Engineer Research and Development Center
3909 Halls Ferry Road
Vicksburg, MS 39180-6199
601-634-4127 (F) 601-634-4894
michael.k.sharp@erdc.usace.army.mil

Dr. Charles E. Smith
Senior Technical Advisor
Engineering and Research Branch
U. S. Minerals Management Service
381 Elden Street, MS 4021
Herndon, VA 20170-4817
703-787-1561 (F) 703-787-1549
smithc@mms.gov or Charles.E.Smith@mms.gov

Mr. Steven Sweeney
Seismic and Structural Engineering Group
US Army Engineer Research and Development Center
CEERD-CF-M
Construction Engineering Research Laboratory
2902 Newmark Drive
Champaign, IL 61822-1076
Steven.C.Sweeney@erdc.usace.army.mil

Dr. Maria I. Todorovska
Research Professor
University of Southern California
Department of Civil & Environmental Engineering
Kaprielian Hall 216A
Los Angeles, CA 90089-2531
(T) 213-740-0616; (F) 213-744-1426
mtodorov@usc.edu

Dr. David Wald
Supervisory Research Geophysicist
Central Geologic Hazards Team
U.S. Geological Survey
Denver Federal Center
PO Box 25046, MS966
Lakewood, CO 80225
303-273-8441 (F)303-273-8600
wald@usgs.gov

Dr. W. Phillip Yen
Seismic Hazard Mitigation
Office of Infrastructure, R&D
Federal Highway Administration
6300 Georgetown Pike
McLean, VA 22101
202-493-3056 (F) 202-493-3442

Wen-huei.Yen@fhwa.dot.gov

Dr. Solomon C. Yim
Professor
Structural and Ocean Engineering

Oregon State University
202 Apperson Hall
Corvallis, OR 97331-2302
541-737-6894 (F) 541-737-3052
solomon.yim@oregonstate.edu
http://www.ccee.orst.edu/~yim

RESOLUTIONS

RESOLUTIONS OF THE THIRTY-EIGHTH JOINT MEETING U.S.-JAPAN PANEL ON WIND AND SEISMIC EFFECTS (UJNR)

National Institute of Standards and Technology, Gaithersburg, Maryland, USA
May 15-17, 2006

The following resolutions are hereby adopted:

1. The Thirty-eighth Joint Panel Meeting provided the forum to exchange valuable technical information that is beneficial to both countries. In view of the importance of cooperative programs on the subject of wind and seismic effects, the continuation of Joint Panel Meetings is considered essential. Both sides agreed to explore new ideas and areas to strengthen cooperative activities in support of the Panel's mission.

2. The following activities have been conducted since the Thirty-seventh Joint Meeting:
   a. Technology Exchanges. Technical experts and technical documents have been exchanged. These exchanges have contributed to the development of new research and enhanced ongoing research programs in both countries.
   b. Task Committee Workshops. The Panel held two workshops:
      i. Task Committee (G), 21st U.S.-Japan Bridge Engineering Workshop, 3-5 October 2005, Tsukuba, Japan.
      ii. Task Committee (H), 2nd International Workshop on Coastal Disaster Prevention, 18-20 January 2006, Tokyo.
   c. Major Products. The Panel members produced or made significant contributions to the following major products:
      i. Development of the US national plan, *Wind Storm Impact Prediction Implementation Plan* (WindHRP) for the Office of Science and Technology Policy (OSTP).
      ii. Two Task Committees (T/Cs A and G) have created web sites to share their activities.
      iii. Task Committees have performed collaborative research in topics such as wind tunnel estimates of wind effect on low-rise buildings and non-linear analysis of concrete dams.

3. The Panel accepted the Task Committee reports presented during the Thirty-eighth Joint Panel Meeting. Each report included objectives, scope of work, accomplishments and future plans.

4. The Panel continues to work toward streamlining its structure and encouraging the collaboration of researchers in both countries.

5. The Panel conducted its annual Strategic Planning Session. During this meeting the Panel discussed and adopted its 2nd Five-Year Strategic Plan (see below). The Plan's emphasis is on emerging technologies to address hazards including environmental health hazards; evaluating Task Committees accomplishments; increasing partnering opportunities with other Panel Task Committees; identifying opportunities for joint research; and more broadly disseminating Panel results and activities.

6. The Panel endorses the following six proposed Task Committee Workshops during the coming year:
    a. Task Committee B, Workshop on Multi-Hazard Risk Reduction for Building Systems, January or February 2007, Hawaii
    b. Task Committee C, 4th US – Japan Workshop on Advanced Research for Dams, fall 2006, Tsukuba
    c. Task Committee D, 4th Workshop, New Challenges for Reduction of High-Wind Disasters, 20-22 July 2006, Tsukuba
    d. Task Committee G, 22nd US-Japan Bridge Engineering Workshop, fall 2006, U.S.A
    e. Task Committee H, 3rd Tsunami Workshop, July 2006, U.S.A
    f. Task Committee I, Workshop on Fire Performance of Structures, November 2006, Japan.

    In the event that T/C co-chairs consider it essential to conduct a joint meeting or workshop prior to the next annual meeting, that is not included in this resolution, the T/C co-chairs will make such a request through their respective Secretary-General for approval by the Joint Panel Chairmen.

7. The Panel encourages continued cooperative research interactions between the National Science Foundation's Network for Earthquake Engineering Simulation (NSF/NEES) and Ministry of Education, Culture, Sports, Science and Technology/National Research Institute for Earth Science and Disaster Prevention's E-Defense (MEXT/NIED).

8. The U.S. and Japan sides will plan and conduct, as appropriate, joint investigations following earthquake, wind, and fire disasters in the U.S. and Japan.

9. The results of the Panel's work should be widely disseminated to improve the quality of life globally. The Panel will make use of the internet to the extent possible to disseminate its accumulated and timely information.

10. The Thirty-ninth Joint Panel Meeting of the UJNR Panel on Wind and Seismic Effects will be organized by the Japan-side Panel, to be held in Japan in May 2007. The Japan-side secretariat will propose dates, program, location, and itinerary with the concurrence of the U.S.-side Panel.

ADDENDUM 1
Panel Expectations During 2006-2010

STRATEGIC PLAN
U.S.-JAPAN JOINT PANEL ON WIND AND SEISMIC EFFECTS

1.0 Introduction

This document is Addendum 1 of the Strategic Plan for the US-Japan Panel on Wind and Seismic Effects 2001-2005 (attachment). The Panel's 2001 Strategic Plan serves as the base of the Panel's operations and structure. This Addendum 1 provides a roadmap of outlined technical approaches for the Panel's operations during the next five-year period 2006-2010. As background, the Panel's Charter, developed in 1987 at the 19th Joint Panel Meeting, is to:

a. Encourage, develop, and implement the exchange of wind and seismic technology between appropriate US and Japanese organizations to share scientific and technological knowledge.
b. Develop strong technical links of scientific and engineering researchers between the two countries and encourage exchanges of guest researchers.
c. Conduct joint research in areas of winds and seismic technology including exchange of available research equipment and facilities in both countries. Publish findings from joint research efforts.
d. Conduct cooperative programs to improve engineering design and construction practices and other wind and earthquake hazard mitigation practices. Publish results from cooperative programs.

2.0 Panel Approaches During 2006-2010

The Panel's operational procedure is defined in the attached Strategic Plan (2001-2005). Annually the Panel performs a self-evaluation during a Strategic Planning session held during its May Joint Panel Meeting. Based on the Panel's evaluation, incremental modifications are carried out to enhance the Panel's operations and to bring 'value-added' to its users.

2.1 Panel Mission and Vision for 2006-2010

1. Continue performing post disaster investigations and reconnaissance and sharing findings with Panel members and others as was carried out for:
   a) Earthquakes: (2004 Niigata, 2004 Indonesia, 2005 Pakistan, and others)
   b) Typhoons and Hurricanes: (2005 Katrina and Rita, 2004 Typhoon)
2. Share US and Japan National Disaster Mitigation Plan among the Panel members such as:
   a) USA. NSTC/SDR: *Grand Challenge for Disaster Prevention- a 10-year strategy for disaster reduction through science and technology*; *Windstorm Impact Reduction Implementation Plan*; the NEHRP Annual Plan.
   b) Japan. *Central Disaster Prevention Council: Reduction by half of human damage and economic damage in coming 10 years*, Technology Development Plan at "Council for Science and Technology"
3. Identify methods that support each countries efforts in disaster mitigation through cooperation between the US and Japan and explore opportunities for joint research projects.
4. During 2006-2010 the Panel will focus on topics such as:

a) Understand disaster mechanism and accumulation of data
b) Evaluate and estimate methods of risk of natural disasters
c) Improve/develop disaster mitigation technology and dissemination of disaster response technology into practical applications
d) Promote attention to increase research that considers societal implications of natural disasters
e) Integrate technology development and the viewpoint of social/civil engineering by increasing the importance of the cooperative works between related UJNR Panels, the Panel's Task Committees, and the private sector and academia
f) Create methods to better integrate comprehensive technology information as a base for transmitting information throughout the Panel member's organizations
g) Contribute to dissemination of cooperative products that will facilitate global standardization of related civil engineering technologies.

2.2. Evaluate Task Committees. The Panel operates under seven Task Committees; an optimum number for Panel management and productivity. The Task Committees serve as the heart of the Panel's operations:

Task Committee A. Geotechnical Engineering and Ground Motion
Task Committee B. Next Generation Building and Infrastructure Systems
Task Committee C. Dams
Task Committee D. Wind Engineering
Task Committee G. Transportation Systems
Task Committee H. Storm Surge and Tsunami
Task Committee I. Fire Performance of Structures

Findings from Task Committees' evaluations will help the Task Committees 1) measure achievements, productivity, and impact on contributions to improving design and construction practices, 2) identify opportunities for making contributions and addressing emerging technical challenges, and 3) assess when they completed their mission and are ready for retirement. Task Committee Evaluation Criteria includes: 1) workshops conducted at least every three-years, 2) implementing recommendations from workshops, 3) publications and other outreach, 4) and collaborations beyond their Task Committee.

The Panel will encourage its respective Task Committees to identify thematic focuses requiring technology sharing and joint collaborations. These Themes will be discussed at annual Panel Meetings. The Panel will consider the merits of creating new Task Committees that meet special needs and eliminating Task Committees that have completed their mission or can be strengthened through consolidation with an other Task Committee(s).

2.3. Partnering Opportunities. Identify partnering opportunities through clustering appropriate Panel's Task Committees, collaborating with other UJNR Panels, and working together with the private sector and academia. Clustering provides Task Committee optimization of resources (human and financial). Partnering and clustering will be discussed at annual Panel Meetings including increasing participation from the private sector and academia.

2.4. Joint Research. Perform joint research initiated by the Panel and its Task Committees. The Task Committees are encouraged to identify key joint-research opportunities to improve the state-of-knowledge or to consider engaging in a significant long-term research funded from one or more sponsoring organizations. For the latter, below are 11 Panel Cooperative Research Projects performed during the past 27-years that improved design and construction practices for both countries.

1. Reinforced Concrete Structures (1979-1987), accomplishments include testing six-story full scale buildings which led to improve seismic design methods of reinforced concrete buildings.
2. Seismic Performance of Lifeline Facilities (1982-1989); accomplishments included development of improved seismic design methods of bridge columns.
3. *In-situ* Testing Methods for Soil Liquefaction (1983-1986); accomplishments include development of rationale for Standard Penetration Test (SPT) data based on energy ratio.
4. Masonry Structures (1984-1988); accomplishments include development of strength-based design guidelines for reinforced masonry buildings.
5. Steel-Frame Structures (1985-1987); accomplishments include testing of a full-scale five-story building to confirm prediction of performance based on components and subassemblages.
6. Bridge Hybrid Control Systems (1990-1994); accomplishments include development of hybrid control algorithms that require less energy for controlling bridge response.
7. Precast Seismic Structural Systems (1991-1992); accomplishments include development of strength-based design guidelines.
8. Seismic Performance of Composite and Hybrid Structures.
9. Countermeasures for Soil Liquefaction.
10. Development of Smart Structural Systems.
11. Develop Comparative Analysis of Seismic Performance Testing Guidelines for Bridge Piers (1999-2006); accomplishments included a joint publication on the comparative analysis of US and Japan bridge piers.

The respective Task Committees will identify candidate joint research for discussion at annual Panel meetings.

2.5. Panel Communications. More broadly disseminate Panel's activities, accomplishments, and impacts including findings from post-disaster investigations using the Panel's eNewsletter, a more active Web Site, Task Committee publications, and identify Panel accomplishments and impacts. The Panel will increase information sharing among its member organizations and include links to related organizations in both countries. Task Committees will serve as a knowledge base of information on their respective themes and share their information to users following Panel communication protocols.

3.0. Conclusion

This Addendum represents the Panel's focus to address Panel's technology needs of the next five-years. The Panel is annually evaluated during its annual May Meetings.

U.S.-Japan Joint Panel on Wind and Seismic Effects
Strategic Plan
(May 2001)

1.0 Introduction

1.1 Context
The U.S. and Japan must maintain an awareness of international developments in earthquake and wind mitigation technology. The international exchange of information is achieved through a combination of formal and informal mechanisms, including: attendance at conferences and workshops; cooperative research projects and programs; and exchange of scientists and engineers. There is a long-established tradition of joint research activities between Japan and the United States. The U.S.-Japan Cooperative Program in Natural Resources (UJNR) Panel on Wind and Seismic Effects (WSE Panel) provides a formal government-to-government mechanism for cooperation between the two countries in the area of earthquake and wind mitigation technology.

At the 32nd Joint Panel Meeting, a resolution was passed to establish a joint Ad-Hoc Committee for the purpose of developing a strategic plan for the WSE Panel. The catalyst for this effort was the need to address immediate issues related to cost and participation. While the Panel recognized the importance of addressing these immediate issues, it also realized that an opportunity existed to strengthen the WSE Panel's focus on its core mission and foster greater collaboration between researchers in the U.S. and Japan while streamlining the overall operation of the Panel. It was with this goal in mind that the ad-hoc committee developed the strategic plan contained in this document.

1.2 Approach
Before meeting to develop the strategic plan, each side held domestic panel meetings and conducted one-on-one meetings with participating agencies to identify issues that needed to be addressed by the strategic plan and to understand which features of the Panel and its operation should be retained and which needed to be changed or adapted to meet current and future needs. Each side developed a concept paper to capture these ideas. The concept papers, however, tended to focus on addressing the immediate issues rather than positioning the Panel to address the needs and challenges of the future. Through the exchange of the concept papers and subsequent discussion, the two sides moved close to agreement on near-term changes to the Panel's operation. Thus, the strategic plan emphasizes longer-term goals for the operation and growth of the Panel and a time-phased approach to implementation of steps to achieve these goals.

The strategic plan is intended to establish a course for the WSE Panel over the next 5-10 years. It recognizes that there are many ways in which the Panel may work to achieve the goals identified, and so while some steps in the implementation process are clear, others are left open to be determined through experimentation. However, the Panel believes working toward the goals identified will strengthen its role in engineering and scientific communities of the U.S. and Japan and will allow our countries to make more efficient use of resources to conduct research and disseminate results to the benefit of both countries.

2.0 Role of the Panel

2.1 Guide Research Agendas
As a government-to-government mechanism for collaboration, the WSE Panel is in a unique position to guide the development and execution of each country's research agenda. Currently, each country defines its own research priorities, projects are

formulated in a fragmented manner, and results are reported through vehicles such as the Annual Joint Panel Meeting. By strengthening its ties to industry and academia, the Panel will be able to identify specific research needs and align those with government priorities. The Panel shall work toward a coordinated research agenda that permits the efficient use of human resources, funding, and research facilities to achieve mutual research objectives.

The new Task Committees formed through implementation of this strategic plan shall work to identify areas where joint research projects can be established and conducted as a part of a coordinated research agenda. Joint research projects may include participation by university or industry researchers in addition to member agency researchers.

2.2 Leverage Resources

The U.S. and Japan each possess significant expertise in the fields of earthquake and wind engineering and have a substantial investment in equipment and facilities to perform testing and measurements in support of research in these fields. Historically, the WSE Panel has facilitated the exchange of researchers between the U.S. and Japan but has not made a concerted effort to leverage the resources of the two countries. There is an opportunity for the Panel to coordinate research activities to efficiently utilize testing and measurement facilities in both countries to address mutual research needs and avoid duplication. This is an area in which the Panel can significantly strengthen its efforts and provide a tangible benefit to each country by working to establish strong partnerships for coordinated research.

2.3 Foster Cooperation

From its founding, the WSE Panel has promoted cooperation between the U.S. and Japan through annual Joint Panel Meetings, Task Committee activities, and exchange of researchers. One of the hallmarks of success for the WSE Panel through the years has been the high level of cooperation. The model these cooperative efforts have been built around, however, is one of information exchange. While the exchange of information and research results is an important facet of the WSE Panel's work, there is the opportunity to greatly expand the scope and importance of cooperative efforts to leverage resources (people, funding, facilities) through joint research projects of bilateral importance. Additionally, the Panel should look beyond the government agencies that participate to be more inclusive of universities and the private sector. At a minimum, this will include broadening participation in the Joint Panel Meetings to include industry and university participants. As industry and universities become more engaged, exchanges of researchers among government, university, and industry participants may be possible. Joint programs that include participation by government, industry, and university partners shall also be considered. These activities would broaden the reach of the Panel and provide a means for more rapid diffusion of research results into practice.

2.4 Technical Exchange

The WSE Panel has, throughout its history, been an effective mechanism for the exchange of technical information between Japan and the United States. Further, the WSE Panel has provided a means for disseminating measurements and research results to other nations affected by earthquake, wind, tsunami, and storm surge hazards. Annual Joint Panel Meetings, Task Committee Meetings and Workshops, researcher exchange programs, and personal relationships among researchers have fostered this exchange. The Panel recognizes this as one of its strengths and should seek to broaden its reach to include participation by researchers in other nations. The Panel should explore means of increasing collaboration with other countries through inclusion of representatives from other nations in Joint Panel Meetings, encouraging joint projects through the Task

Committees that include partners outside the U.S. and Japan, and through the exchange of researchers with other countries.

2.5 Engage Private Sector

The WSE Panel has engaged the private sector to a limited extent in its activities during its history, although the work of the Panel and the participating agencies can have a direct benefit to industry and ultimately the public in our respective countries. Further, some larger companies have research capabilities and programs that could enrich the Panel. More actively engaging the private sector will provide a means for obtaining input in setting priorities and for more rapidly diffusing the results of research activities into practice within Japan and the United States. The involvement of the private sector may include participation in the development of coordinated research agendas and dissemination of information perhaps through special sessions at the annual Joint Panel Meetings. The Panel should also consider involving the private sector in research projects coordinated at the Task Committee level that will have broad-based benefits to industry in both countries. Longer-term, the involvement of the private sector will facilitate dialogue between practicing engineers and builders in Japan with their counterparts in the U.S. The Joint Panel will examine ways to increase industry participation, initially by inviting key industry representatives to participate in Joint Panel Meetings and to speak about the work of their company or organization and explore possibilities for greater collaboration.

2.6 Web Page Development

The Joint Panel will explore ways to increase utilization of the Internet as a means of communication both among Panel members and with outside organizations. The Japan-side has offered to take the lead in developing an Internet presence for the Joint Panel and has begun work on an initial concept for the site. Once the site is established, the Task Committees will be relied on to provide, maintain, and update content related to their activities. The Joint Panel will also explore ways of using Internet resources as a means of facilitating communication among researchers as well as the exchange and dissemination of information and research results.

3.0 Implementation

3.1 Strategic Plan Development and Approval

This strategic plan was prepared through the efforts of the Joint Ad-Hoc Committee appointed by the Chairmen following the 32nd Joint Panel Meeting. The Joint Panel shall work toward approval of the Strategic Plan during the 33rd Joint Panel Meeting May 28-30, 2001. The approved document will reflect comments received from Panel members on the draft. Implementation of the strategic plan will begin with approval and require 12-24 months for full implementation.

3.2 Task Committee Charters and Recommended Committees

The US- and Japan-side Panels have agreed on the following seven themes around which Task Committees may be formed:

- Theme A: Geotechnical Engineering and Ground Motion
- Theme B: Buildings
- Theme C: Dams
- Theme D: Wind
- Theme E: Lifelines
- Theme F: Seismic Information and IT
- Theme G: Transportation

- Theme H: Storm Surge and Tsunami
- Theme I: Public Health

Task Committee formed to address one of these themes will be approved by the Joint Panel on annual basis, provided that the Task Committee remains active. The criteria for active Task Committees are following:

a) Conducts joint workshops or technical meetings on a regular basis for the purpose of exchanging technical information, research results, or data for the mutual benefit of both countries.
b) Engages in frequent exchange of researchers for the purpose of technical interchange and collaboration on research.
c) Conducts one or more joint research projects having clearly defined technical objectives, finite duration, and shared responsibility for producing technical results.

Task Committees will report results through papers presented during the joint panel meeting and through task committee reports. The Joint Panel will review task committee results and future plans on an annual basis and will approve task committees for the next year based on this information.

For this year, new task committees may be established by requesting approval through the Secretary-Generals at any time before the 34th Joint Panel Meeting.

3.3 Transition to New Annual Panel Meeting Format

A number of alternative formats for the annual Joint Panel Meeting were considered. Based upon the input received from Panel members, the basic format of the Joint Panel Meeting be retained. Session topics will be principally driven by the Task Committees. Each Task Committee would be given one session during which it would be able to present research results. This Task Committee-driven format should strengthen the role of the Task Committees and is intended to stimulate greater cooperation among researchers in each country. This format will foster the exchange of information that many have expressed is a desirable feature of the Joint Panel Meeting.

The Joint Panel meeting will be shortened by one day (from 4 days to 3 days). The shorter meeting, coupled with a shorter Technical Site Tour will reduce the time commitment for participants to one week. This is intended to encourage greater participation in the Panel Meetings and Site Tours, particularly by members of the visiting Panel.

Finally, the Joint Panel will explore streamlining the Joint Panel Meeting to maximize the opportunity for technical exchange.

The shortened Panel Meeting/Technical Site Tour format is implemented for the first time at the 33rd Joint Panel Meeting. The Task Committee-driven technical meeting format will be implemented at a later date when the revised Task Committee organization is in place.

4.0 Conclusion

The plan outlined above represents a strategic plan for positioning the Joint Panel to meet the challenges of the future, while retaining those aspects that have contributed to its success through it 32 year history. This plan is intended to address the current realities of the Panel, as well as increase the value and contribution of the Panel to the U.S. and Japan. Full implementation of the strategic plan will take approximately two years.

MANUSCRIPTS

Technical Session 1

GEOTECHNICAL ENGINEERING AND GROUND MOTION

Fundamental Study on Health Monitoring and Evaluation System for Port/Airport Facilities

by

Takahiro Sugano[1], Tomohiro Tanaka[2] and Eiji Kohama[3]

ABSTRACT

Port facilities, coastal facilities and man-maid island airport facilities exhibit superior performances in marine environments, however they are difficult to be maintained in good conditions while exposing to severe atmosphere. Therefore, it is important to establish a comprehensive health monitoring and evaluation system for satisfying required performances such as quick quantitative input to assess and decide on post-earthquake action. As a part of the system, this paper focuses on sensing devices to observe a steel pipe pile condition during an earthquake.

KEYWORDS: Airport Facilities, Health Monitoring, Pile, Port facilities, Post Earthquake Action, Seismic Retrofit.

1. INTRODUCTION

The occurrence of a large earthquake near a major city may be a rare event, but its societal and economic impact can be so devastating that it is a matter of national interest. Lessons learned from the 1995 Kobe earthquake disaster, from the point of view of the social port function, this experience showed us the following two important concepts for port administration and management. Those are;

a) Starting special operation for transporting living necessities for victims' daily life immediately (within one day) after an earthquake. b) Restarting commercial logistic operation within one week after an earthquake.

It is difficult to evaluate level of damage to the facilities quickly, because of major parts of facilities are located under-ground and submerged. It is also difficult to calculate stability of complex structures due to retrofit or upgrade construction work compared with simple structures.

To establish a health monitoring system, we conducted a series of fundamental experiments. In this paper, we introduce an application of optical fiber sensing technique and real time dynamic global positioning system (RTD-GPS) technique for steel pipe pile.

2. FIELD EXPERIMENTS

In case of Tokyo bay, steel pipe piles for foundation of bridge and pile supported wharf are driven into 50m-100m depth with one or two welded connections. And the design service time is 100 years.

2.1 Optical fiber sensor for steel pipe pile

To assess the applicability and reliability of optical fiber sensing system for detecting strain level of pile during construction process and during life span (100 years) of the pile, a series of full-scale experiment was conducted. As shown in Fig. 1, two pieces of 0.6m diameter, 8m long steel piles were provided and attached three types of strain sensors (i.e. FBG optical fiber, BOTDR optical fiber and conventional strain gauge). From the soil profile (Standard penetration test N value shown in red) near the driving position, we selected vibrohammer for pile driving. However, the soil profile (blue line) converted by CPT at the certain position shows more sever condition for pile driveing. Fig. 2 show that the attached sensors with protection. Figs. 3 and 4 show the driving process and special treatment at the welding position. After driving the pile, vertical load was applied using a hydraulic actuator as shown in Fig. 5

Fig. 6 show the strain distribution with depth at five loading stages. The blue line and red line indicate that the strain distribution by BOTDR

---

[1] Head, Structural Dynamics Division, Geotechnical and Structural Engineering Department, Port and Airport Institute, Nagase, Yokosuka, Kanagawa 239-0826 Japan

[2] Researcher, ditto

[3] Senior Researcher, ditto

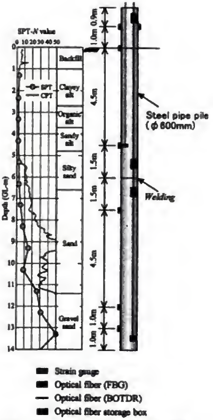

Fig. 1 Test site condition and pile

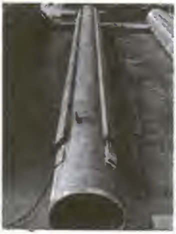

Fig.2 Test specimen pile and attached sensors

Fig.3 driving the pile with vibrohammer (Top piece of pile)

Fig.4 Welded connection between bottom and top pieces of pile and treating optical fiber

Fig.5 Setup of loading hydraulic actuator

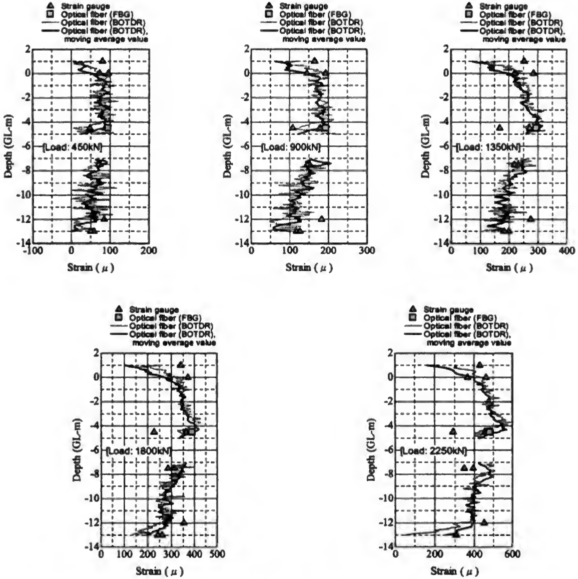

Fig.6 Strain distributions obtained by FBG, BOTDR and conventional strain gauges during loading stage.

in diagonal positions of pile cross section. The ideal neutral axis of pile is not coinciding with the actual neutral axis of the pile, and that is why probably the red and blue line are scattering. The FBG optical fiber (blue squares) and the conventional strain gauge (gray triangle) are also plotted in these figures.

From the practical point of view, the four sensing technique results show good agreement and survived during driving vibration and impact force.

We also, tried full-scale tests are ongoing as follows,

a) Tokyo-bay: 1.5m diameter, 60m length pile, steam hammer.

b) Osaka-bay: 1.2m diameter, 50m length pile, vibrohammer.

c) Exposure tests: Sensor devices expositing in seawater submerged zone, tidal level change zone and splash zone.

Left: Reference (fixed) receiver point Right: Shaking receiver point

Fig. 7 RTD-GPS test field located in Nobi, Yokosuka

2.2 Real Time Dynamics-GPS

To calculate the stress condition or bending moment distribution of the pile from the strain distribution data, we assume that the boundary condition of pile at the bottom end is fixed and the top end displacement is given. To measure the top end displacement during construction stage, during an earthquake, and after an earthquake, the RTD-GPS technique was tested. Fig. 7 shows the field test setup. During damage and failure process of a pile supported wharf, the stress condition of pile is important index to evaluate the damage level, and, it is not only residual stress condition but also maximum stress condition during an earthquake. The GPS receiver is put on a portable shaking table as shown in Fig.9.

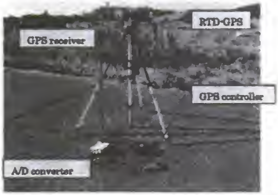

Fig. 8 RTD-GPS Reference receiver

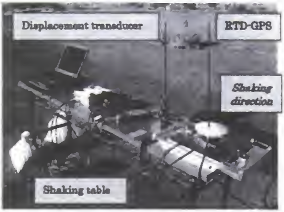

Fig. 9 RTD-GPS Moving receiver

To evaluate the dynamic property of the RTD-GPS, we compare the displacement time histories obtained by the conventional LVDT transducer and RTD-GPS with different input frequency. In the field test, sampling frequency of 100Hz in conventional LVDT, and 10Hz in RTD-GPS are used.

In Fig. 10, the displacement obtained by a conventional LVDT as shown in solid blue line and RTD-GPS data points indicate good agreement during 0.8Hz shaking. On the other hand, in case of 2.5Hz shaking condition, the RTD-GPS data points show large displacements as shown in Fig.11. Before the field test, we assumed that the sampling frequency and shaking frequency ratio leads 'under sampling' effect in case of 2.5Hz shaking.

At this stage, we can not verify it and come to a conclusion yet. Next tests are ongoing to evaluate the applicability of random shaking using strong motion records.

3. CONCLUDING REMARKS

We are just started fundamental study on a health monitoring related issues such as sensor technology, information technology, environmental impact analysis and material deterioration database etc.

The final goal is establish integrated health monitoring systems which enable real-time monitoring, automatic damage detection, assist crisis management and assist lifecycle management. Damage identification is performed based on identification of changes in salient response features of the structure, as measured by deployed sensor arrays. This proposed broad interdisciplinary research aims to develop a next-generation, versatile, efficient, and practical health monitoring strategy.

This report is a part of the join research of PARI, NTT-DATA and NTT-Infranet.

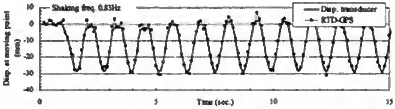

Fig. 10 Time history of horizontal displacement (shaking frequency 0.8Hz)

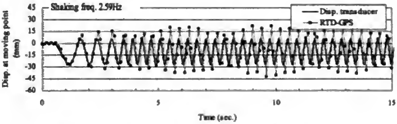

Fig. 11 Time history of horizontal displacement (shaking frequency 2.5Hz)

Response of an Integrated Building and Free-Field Surface and Downhole Network

by

M. Çelebi[1]

ABSTRACT

An integrated seismic monitoring system with a total of 55 channels of accelerometers is now operating at and in the nearby free-field site of the 20-story steel-framed Atwood Building, in highly seismic Anchorage, Alaska. The building has a single-story basement and a reinforced-concrete foundation without piles. The monitoring system comprises a 32-channel structural and a 21-channel site array. Accelerometers are deployed on 10 levels of the building to assess translational, torsional, and rocking and interstory drift (displacement) between selected pairs of adjacent and average drift between floors. The site array, located approximately a city block from the building, and comprising seven tri-axial accelerometers, one at the surface and six in boreholes ranging in depths from 15 to 200 feet (5-60 meters). The arrays have already recorded responses of the building and the site caused by numerous earthquakes both at distances ranging from tens to a couple of hundred kilometers. Analyses of the responses clearly indicate propagation of seismic waves from the lowest borehole all the way to the roof of the building. Although the response data collected to date are of low-amplitude, they reveal the complete seismic behavior and dynamic characteristics of the building and the site. Data from an earthquake that occurred 186 km away are used to identify the fundamental structural frequency as 0.58 HZ (NS) and 0.47 Hz (EW) and the fundamental site frequency as 1.5 Hz. During the low-amplitude responses recorded from this event, waves propagate in approximately 0.5 seconds from the boreholes to the roof. Mode-coupling and beating effects are identified. Soil-structure interaction effects are not observed at the low levels of recorded motion. The integrated array serves as an example for future instrumentation projects to assess their behavior and performances.

KEYWORDS: real-time monitoring, cable-stayed bridge, New Madrid Seismic Zone, seismic event, acceleration, accelerometer, downhole, internet communication, data acquisition.

1. INTRODUCTION

The Atwood Building is 20 stories tall and is located in highly seismic Anchorage, Alaska (Figure 1). The building is a steel moment-resisting framed (MRF) structure with only one level of basement, 130'x130' (39.6 m x 39.6 m) in plan with a 48'x48' (14.6 m x 14.6 m) in-plan center steel-shear walled core, and 264' (80.5 m) tall. The building foundation is without any piles and consists of a 5' (1.52 m) thick reinforced concrete mat below the core and a 4'6" (1.37 m) thick reinforced concrete perimeter mat interconnected with grade beams.

The site of the building in downtown Anchorage is underlain by an approximately 100-150-feet (30.5 – 45.7 m) thick soil layer known as the Bootlegger Cove Formation, where considerable ground failures occurred during the 1964 Great Alaska earthquake (Updike and Carpenter, 1986). Built within this geotechnical and seismic environment, Atwood Building, without piles supporting its foundation (exterior and core mats, interconnecting grade beams) and a structural system (MRF steel frame with steel core shear wall) was selected for seismic monitoring. Thus, during earthquakes of various levels of shaking, recording the response and then assessing the behavior of this building and its site can enhance seismic assessment of the behavior and performances of similar buildings during future large earthquakes.

---

[1] Earthquake Hazards Team, USGS (MS977), 345 Middlefield Rd., Menlo Park, Ca, 94025

The seismic monitoring system of the building comprises and integrates a structural (superstructure and foundation) and a site (surface and downhole) array. The superstructure and foundation array, designed by the author, consists of accelerometers deployed on the basement, at street level, and on the 2nd, 7th, 8th, 13th, 14th, 19th floors (Çelebi, 2003). This configuration, depicted in Figure 1, is designed to detect motion of the building in the E-W and N-S directions, and, in the basement, additionally, in the vertical direction to capture (a) translational, (b) torsional, (c) interstory drift (displacement between selected two consecutive floors) or average drift between any two floors, and (d) rocking of the building.

The structural array is complemented by an extensive freefield site array, located approximately one city block from the building, and consisting of seven tri-axial accelerometers, one at the surface and six in boreholes with depths ranging from 15 to 200 feet [~5-60m] (Figure 1). Removed from the vibrational effects of the building, the associated site array is designed to capture the response of varying layers of soil, and how such layering alters the characteristics of earthquake motions as they travel to the surface and shake the structure. Thus, with the integrated site and superstructure arrays, propagation of motions starting from the lowest downhole depth to the ground surface, basement and the roof of the building are recorded to facilitate structural, site response and soil-structure interaction (SSI) studies. Capturing the propagation and travel time is important as large and abrupt changes may indicate damage to structural members, components and the system.

Since the deployment of the arrays in 2003, numerous small and medium sized earthquakes from near and far sources have been recorded (Çelebi, 2006). The low-amplitude shaking of the building caused by these earthquakes did not cause any damage, but provide opportunities to identify response characteristics of the building and the site. Earlier data sets include responses from only the structure array, as the site array was not yet installed. Yang and others (2004) performed studies of only the data from the building array. This paper introduces and analyses recorded data from both structural and site arrays. However, for sake of brevity, only one set of earthquake response data is included herein.

2. ANALYSES OF STRUCTURAL AND SITE ARRAY DATA : EARTHQUAKE OF APRIL 6, 2005

Acousally-filtered accelerations and computed (double-integrated accelerations) displacements from both the site and the superstructure arrays of the Atwood Building during the April 6, 2005 Tazlina Glacier (AK) earthquake (M_L=4.9), epicenter at 183 Km from the building, are provided in Figure 2 and 3. The largest peak acceleration recorded in the building array is on the order of 0.5% g. The figures clearly show the propagation of waves from basement to the roof of the building. The height of this building is 264 ft [~81m] from ground floor and 275 ft [~85m] from basement. The travel time of waves from the basement to the roof is about 0.5 seconds and, as expected during this low-amplitude shaking event, the propagation of the waves does not indicate abrupt changes (e.g. transients or spikes) to indicate damage to structural members, components and the overall structural system.

Figure 4 shows the roof accelerations and corresponding amplitude spectra of the two parallel NS components, their difference, and the EW component. In the spectra, significant structural frequencies can be identified. Although the torsional response is not significant, the torsional frequencies computed from differential acceleration (CH30-CH31 in the figure) are similar to the predominant frequencies computed from NS and EW motions, indicating possible coupling and also possibly causing the beating effect visually most prominent in the displacement time-history plots (Figure 3).

Figure 5 presents cross-spectrum, coherence and phase angle plots of pairs of NS ([a] CH30 and CH15), EW ([b] CH32 and CH 17) and torsional (differential of NS) accelerations ([c] CH30-CH31 and CH15-CH17) at roof and 8th floor. The pairs of accelerations in each case are perfectly coherent for the modal frequencies indicated, and are 0° in phase for the lowest frequencies (indication of first mode) and 180° out of phase for the second and third lowest frequencies (indicating second and higher modes). It is noted again that the frequencies for the torsional responses are similar to the translational frequencies.

Figure 6 shows a sample system identification analysis for the NS building response. Such analyses allows computation of modal damping values in addition to the modal frequencies. The ARX (acronym – AR for autoregressive and X for extra input) model, based on the least squares method for single input-single output coded in commercially available system identification software (The MathWorks 1988), is used in system identification analyses performed herein (Ljung 1997). Typically the input is the basement or ground floor motion and the output is the roof level motion or one of the levels where the structural response is recorded. The damping ratios are extracted with the procedures outlined by Ghanem and Shinozuka (1995). The figure shows nearly perfect prediction of the roof motions. Results extracted from the analyses are summarized in Table 1 which shows that for the first mode, the modal damping values are relatively low, but this may be due to the low level of shaking. During stronger shaking, expected higher damping will affect the responses. As observed in other studies (Boroschek and Mahin, 1991, Çelebi, 1994), the low level damping and nearly identical translational and torsional frequencies could cause the coupling and beating effect observed in Figure 3 and Figure 6. Repetitively stored potential energy during the coupled translational and torsional deformations turns into repetitive vibrational energy.

Table 1. Dynamic characteristics determined by system identification (ξ=modal damping).

Mode	NS			EW		
	F(Hz)	T(s)	ξ (%)	F(Hz)	T(s)	ξ (%)
1	0.53	1.89	2.7	0.47	2.13	4.2
2	1.83	0.55	2.7	1.53	0.65	2.8
3	3.6	0.28	5.1	2.9	0.35	2.4
4	4.9	0.20	3.6	4.2	0.24	4.1

Figure 7 shows amplitude spectra of (a) NS and (b) EW accelerations in the building (roof, 8th floor and basement) and of (c) and (d) accelerations in the basement and surface and lowest downhole free-field motions. The figure illustrates, at least for the lowest frequencies below 5 Hz, that the building frequencies are different than those of the site. Simple spectral ratios, illustrated in Figure 8, of NS and EW building motions (at the roof and 8th floor with respect to basement) further corroborate and confirm the structural frequencies determined by system identification. The narrow band of the structural frequencies in the amplitude spectra or the spectral ratios reflect the low damping ratios computed by system identification.

Figures 9, 10 and 11 are presented to corroborate site frequencies as determined from records or computation of transfer functions using site borehole data. Figure 9 shows amplitude spectra of NS and EW accelerations and corresponding spectral ratios at basement and the free-field array computed with respect to the lowest borehole at -61m. Significant frequency peaks identified from the figure are approximately 1.2-1.7, 4, 7, and 9.0-9.5 Hz in the NS direction and 1.5, 4.0-4.2, 7 and 9 Hz in the EW direction. It is noted that the fundamental frequency (period) [1.2-1.7 Hz (0.58-0.83 s) NS and 1.5 Hz (0.67 s) EW] at this site are not identical and appear to be azimuthally dependent. These site frequencies are consistent with those of the transfer function computed from the shear wave velocity - depth profile (Cole, pers. comm.., 2003) at site using a software developed by Mueller (pers. comm., 2005) based on Haskell's shear wave propagation method (Haskell, 1953, 1960). In this method, the transfer function is computed using linear propagation of vertically incident SH waves and as input data related to the layered media (number of layers, depth of each layer, corresponding shear wave velocities [V_s], damping, and density), desired depth of computation of transfer function, sampling frequency, half space substratum shear wave velocity and density. Damping (ξ) in the software is provided as Q, a term used by geophysicists, and is related to damping by $\xi = 1/(2Q)$. Q values used in calculating the transfer functions are between 25-60 for shear wave velocities between 200-600 m/s – having been approximately interpolated to vary linearly within these bounds. The resulting transfer function shows significant frequency bands (Figure 10). Furthermore, in Figure 11, the computed transfer function is compared to the spectral ratio obtained from amplitude spectra of NS and EW accelerations at the surface with respect to downhole at 61 m depth. It can be concluded from this figure that the computed and observed transfer function are in reasonably good agreement. The often used simple formula, T_s=4H/V_s, requires minimal but reasonable characterization of depth to bedrock and representative average shear wave velocities of layered media (International Building Code, 2000). Computing average Vs = 300-350 m/s using the formula V_s(ave)=H/(Σ (h_i/V_{si}), and a depth H=50 m., T_s =0.57-0.67 (or f_s=1.5-1.75 Hz), similar to the computed and observed site period.

Soil-structure interaction (SSI) effects were found not to be significant during the low-amplitude shaking caused by this distant small earthquake. Even though the vertical motions at the basement are not identical for the three locations, no phase differences were observed. As a result, no rocking effects have been identified. Stronger shaking at the site and building from future earthquake may reveal such effects.

3. CONCLUSIONS

An integrated structural and site response monitoring array at the Atwood Building in downtown Anchorage, AK has recorded numerous small to medium earthquakes that occurred at near and far distances. It is expected that in the future, during stronger shaking, important data sets will be obtained. Analysis of the data from an earthquake that occurred at 186 km distance facilitates computation of significant structural frequencies [e.g. fundamental mode NS 0.58 Hz and EW 0.47 Hz]. Low damping percentages (2-4 %) are identified. Torsional motions are closely coupled with translational motions as they exhibit similar frequencies and cause beating effects. No SSI effects are observed. The Fundamental site frequency is identified to be around 1.5 Hz from the records and also from the transfer function computed with actual borehole data.

4. REFERENCES

Boroschek, R. L., and Mahin, S. A., 1991, Investigation of the seismic response of a lightly-damped torsionally-coupled building: Univ. of California, Berkeley, Earthquake Engineering Research Center Report UCB/EERC-91/18, 291pp

Çelebi, M., 2003. Seismic Instrumentation Plan for Robert B. Atwood Building, Anchorage, AK 99501., Administrative Report, United States Geological Survey.

Çelebi, M., 2005, Recorded Earthquake Responses from the Integrated Seismic Monitoring Network of the Atwood Building, Anchorage, (AK), (*in print*) Earthquake Spectra.

Çelebi, M., 2004.Responses of a 14-Story (Anchorage, Alaska) Building to Far-Distance (M_w=7.9) Denali Fault (2002) and Near Distance Earthquakes in 2002, Earthquake Spectra, Journal of EERI, *Earthquake Spectra*, vol.20, no.3, pp. 693-706, August 2004.

Ghanem, R., and Shinozuka, M., 1995,Structural System Identification. I: Theory, ASCE Journal of Engineering Mechanics, v.121, no. 2, pp. 255-264, February 1995.

Haskell, N. A., 1953. The dispersion of surface waves on multi-layered media. *Bull. Seis. Soc. Am.*, 43(1), 17-34.

Haskell, N. A., 1960, Crustal reflection of plane SH waves, *J.Geophysical Res.*,65(12), 4147-4150.

Ljung, L., 1997. System Identification – Theory for the User, Prentice-Hall, 519 p.

The MathWorks, 1998 (and 1995 editions). User Guide: System Identification Toolbox for the User with Matlab, The MathWorks Inc., South Natick, Mass., 200p.

Updike, R. G., and Carpenter, B. A., 1986. Engineering Geology of the Government Hill Area, Anchorage, Alaska. U.S. Geological Survey Bulletin No. 1588. 36p.

Yang. Z., Dutpa, U., Çelebi, M., Liu, H., Biswas, N., Kono, T, and Benz, H., 2004. Strong Motion
Instrumentation and Structural Response of Awood Building in Downtown Anchorage, Alaska, PROC. 13WCEE, Vancouver, B.C., Canada.(CD-ROM).

ACKNOWLEDGEMENTS

Thanks to J. Steidl and U. Dutta for making some of the borehole data available. USGS-NSMP Data Center, managed by C. Stephens, diligently process, store and disseminate the data.

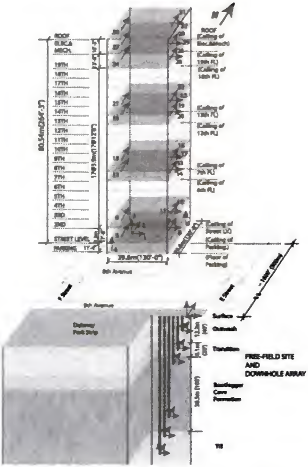

Figure 1. Three-dimensional schematic of the Atwood Building (Anchorage, AK) showing the general dimensions and locations of accelerometers deployed within the structure and at free field with tri-axial downhole accelerometers. The sub-arrays (e.g. superstructure, foundation, surface and downhole free-field sub-arrays) of this particular building monitoring scheme are designed to capture (rocking) SSI effects in addition to the traditional translational and torsional responses.

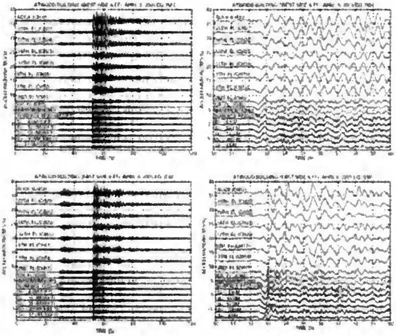

Figure 2. NS (upper panels) and EW (lower panels) accelerations from both the structure and site arrays. The 10-second records on the right are expanded views between 50-60 seconds of the longer records on the left, and show in detail the propagation of S-wave from the lowest downhole depth to the roof of the building. (Note: vertical axes are not in scale with the vertical elevations).

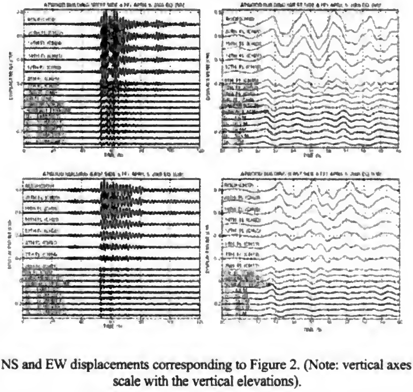

Figure 3. NS and EW displacements corresponding to Figure 2. (Note: vertical axes are not in scale with the vertical elevations).

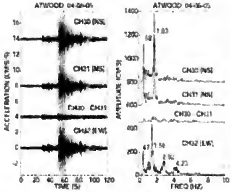

Figure 4. Roof acceleration time-histories and corresponding amplitude spectra.

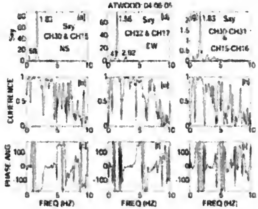

Figure 5. Cross-spectrum, coherence and phase angle plots of pairs of NS (CH30 and 15), EW (CH32 and CH 17) and differential of NS accelerations (CH30-CH31 and CH15-CH17) at roof and 8th floor identifies significant frequencies and associated modes.

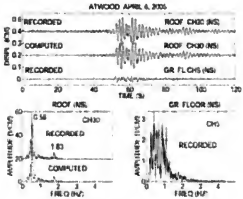

Figure 6. System identification of NS displacements (CH 5 at the ground floor is used as input and Ch 30 as the output). The recorded and computed roof displacements and their amplitude spectra are nearly perfectly matched.

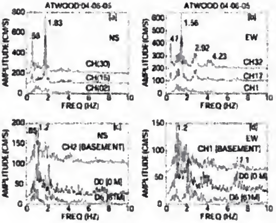

Figure 7. Amplitude spectra of (a) NS and (b) EW accelerations in the building (roof [CH30], 8th floor [CH15] and basement [CH2]) and of (c) and (d) accelerations in the basement and surface [D0] and lowest downhole [D6] free-field motions.

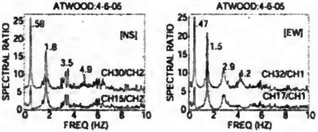

Figure 8. Spectral ratios computed from amplitude spectra of NS and EW accelerations at the roof and 8th floor with respect to those at basement.

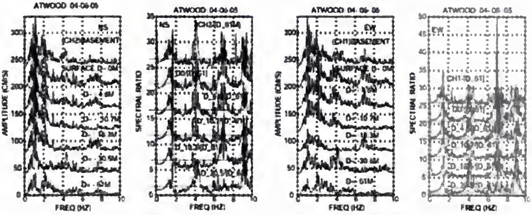

Figure 9. Amplitude spectra and corresponding spectral ratios computed from the amplitude spectra of NS and EW acceleration at basement and the free-field array computed with respect to the lowest borehole at -61m.

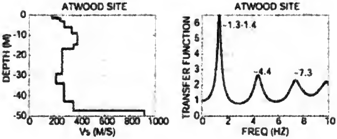

Figure 10. Shear wave velocity (V_s) - depth profile and the computed transfer function.

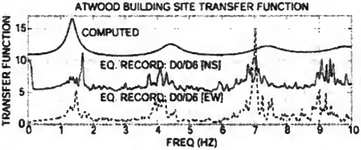

Figure 11. Comparison of computed transfer function to the spectral ratio of amplitude spectra of NS and EW accelerations at the surface with respect to downhole at 61 m depth.

Technical Session 2

NEXT-GENERATION BUILDING AND INFRASTRUCTURE SYSTEMS

Reparability Limit of Steel Structural Buildings Based on the Actual Data of the Hyogoken-Nanbu Earthquake

by

Yoshihiro Iwata[1], Hirokazu Sugimoto[2] and Hitoshi Kuwamura[3]

ABSTRACT

For the development of performance-based design taking into consideration economic losses after earthquakes, reparability limits should be clarified in order to avoid demolishing. In this paper, the reparability limits of steel structural buildings were investigated based on the actual data of repaired or demolished buildings which were damaged by Hyogoken-nanbu earthquake both from technical and economic points of view. The investigation provided the following results on the reparability limit: 1) overall residual drift angle was 1/110; 2) maximum residual inter-story drift angle was 1/71; 3) direct restoration cost ratio was 0.86; 4) indirect restoration cost ratio was 0.40. Furthermore, based on the actual data, the relationship of residual drift angle and restoration cost ratio was investigated and the reparability limits synthesizing technical and economic aspects were defined by overall residual drift angle and maximum residual inter-story drift angle as 1/200 and 1/90, respectively.

KEYWORDS: Hyogoken-Nanbu Earthquake, Performance-Based Design, Repair Cost, Reparability Limit, Residual Drift, Steel Structures

1. INTRODUCTION

The Hyogoken-nanbu earthquake on January 17, 1995 brought vast damage to steel structural buildings [1]; however, there were rather few cases which collapsed built after the new seismic design code in 1981 [2] and we can say that the current seismic design code generally fulfilled the crucial role of protecting human life. Meanwhile, it was reported that the economic damage amounted to about 10 trillion yen and there were many cases that building owners suffered great unexpected economic losses [1, 3]. This is attributed to the fact that the usual design method passively ensures both serviceability and life safety of buildings by preserving design specifications and does not fully consider reparability, so that structural designers could not give building owners clear explanations on cost problems related to repair after earthquakes. Therefore, in order to solve this problem in future, the new design process should be required that structural designers preliminarily set the target reparability with building owners considering the relationship to repair cost, confirm the satisfaction of the target reparability through evaluation process, and explain the final performance to building owners.

After seismic events, various damaged states of buildings can be assumed between the serviceability limit and the life safety limit. In these damaged states, it is believed that especially the reparability limit, which refers to whether buildings can be repaired or not is the greatest concern for building owners, because if the buildings are forced to be demolished, they need not only the direct cost to replace the buildings but also suffer the indirect cost, which is associated with the loss of business operation during replacement downtime. Therefore, when we discuss reparability of buildings, the first thing to clarify is the reparability limit in order to avoid the worst situation of demolishing.

---

[1] Researcher, Building Research Institute, Tsukuba-shi, Ibaraki-ken, 305-0802 Japan

[2] Managing Director, Schokbeton-Japan Co., Ltd., Kawagoe-shi, Saitama-ken, 350-1165 Japan

[3] Professor, Dept. of Architecture, School of Eng., the Univ. of Tokyo, Bunkyo-ku, Tokyo-to, Japan

The reparability limit is thought to be relevant to both technical and economic points of view. Therefore, when we refer to the reparability limit, the discussion on deformation and cost related to reparability based on actual data is indispensable. In this paper, for the development of the new design process considering reparability, based on the 12 actual data of repaired or demolished buildings which were damaged by the Hyogoken-nanbu earthquake, we analyzed them in terms of deformation and cost and tried to clarify the reparability limit of steel structural buildings both from technical and economic points of view.

2. INVESTIGATION OF REPAIRED OR DEMOLISHED BUILDINGS

The reparability limit which is determined by the actual data of repaired or demolished buildings is believed to be reliable. In this paper, in order to analyze the reparability limit, we investigated 12 steel moment resisting frame buildings damaged by the Hyogoken-nanbu earthquake. These are mainly low-to-mid-rise office buildings. The basic information of each building (A-L) is listed below with the summary of damage and repair construction. The damage level in the summary is determined by the Japanese standard [1]. The details of damage and repair construction of the buildings are described in [4].

■ Building A
Damage level: Intermediate
Completion Age: 1986
Total Area: 8,643m^2 Height: 28.7m
Usage: Office
Type: Moment-resisting frame
Floor: upper ground 7- penthouse 1 - basement 0
[Summary of damage]
Structural damage concentrated on the 2F-5F. At the end of the beams, the damage of yielding, crack, local buckling and fracture could be seen. The damage of column could scarcely be seen. The maximum residual inter-story drift angle was 1/125 (5F). The tilt of the entire building was 1/216. The serious damage of exterior PC panels could be seen.
[Summary of repair construction]
The 106 damaged parts near beam-to-column connections were effectively repaired by the method shown in [4]. The 104 PC panels were replaced. The building was repaired almost the same as the original one.

■ Building B
Damage level: Intermediate
Completion Age: 1993
Total Area: 1,099m^2 Height: 26.4m
Usage: Office
Type: Moment-resisting frame
Floor: upper ground 7- penthouse 1 - basement 0
[Summary of damage]
Structural damage concentrated on the 3F-5F. At the end of the beams, the damage of yielding, crack, local buckling and fracture could be seen. The damage of column could scarcely be seen. The maximum residual inter-story drift angle was 1/71 (4F). The tilt of the entire building was 1/110.
[Summary of repair construction]
The 16 damaged parts near beam-to-column connections were effectively repaired by the method shown in [4]. As the unusual case, the interior finish work was not conducted during the repair construction and additional work was scheduled on other occasions. The building was repaired almost the same as the original one except the interior parts.

■ Building C
Damage level: Severe
Completion Age: 1978
Total Area: 1,350m^2 Height: 12.3m
Usage: Public train station
Type: Moment-resisting frame (3F)
Civil engineering structure (1F-2F)
Floor: upper ground 3- penthouse 0- basement 0
[Summary of damage]
At the end of the beams, the damage of yielding, crack, local buckling and fracture could be seen. The tilt of the building part was 1/34 (3F).
[Summary of repair construction]

Building C was a public train station. It had a large residual drift (1/34). Although it was judged to be demolished at first, it was straightened by using wire and tension jack because of the public use. The condition that it had one floor and all 32 column bases were pin-connected enabled the straightening repair construction to be a lot easier (cheap repair cost and short repair period). The building was repaired almost the same as the original one.

■ Building D
Damage level: Intermediate
Completion Age: 1992
Total Area: 21,021m^2 Height: 52.8m
Usage: Office
Type: Moment-resisting frame (1F-4F: SRC)
Floor: upper ground 14- penthouse 2- basement 0
[Summary of damage]
Structural damage spread over the 3F-14F. Near beam-to-column connections, the damage of yielding, crack, local buckling and fracture could be seen. The damage of column could scarcely be seen. The maximum residual inter-story drift angle was 1/46 (8F). The tilt of the entire building was 1/120. The serious damage of exterior PC panels could be seen.
[Summary of repair construction]
Building D had a large residual drift (8F:1/46). Although straightening repair construction was studied at first, it was given up in the end because of the technical and economic problems. Instead of straightening repair construction, reinforcing construction using many eccentric braces was adopted. The 54 damaged parts near beam-to-column connections were effectively repaired by the method shown in [4]. As for non-structural members, many exterior panels were partially repaired or replaced. The seismic performance was restored almost the same as the original one.

■ Building E
Damage level: Intermediate
Completion Age: 1989
Total Area: 908m^2 Height: 37.5m
Usage: Office
Type: Moment-resisting frame (BF-1F: SRC)
Floor: upper ground 8- penthouse 2- basement 2
[Summary of damage]
Fracture damage could be seen at the 2 columns of the 1F. Structural damage could scarcely be seen above the 2F except some damaged parts of yielding and local buckling near beam-to-column connections at the 2F. The maximum residual inter-story drift angle was 1/100 (1F). The tilt of the entire building was 1/226. The damage of exterior PC panels could be seen.
[Summary of repair construction]
The 8 damaged parts near beam-to-column connections were effectively repaired by the method shown in [4]. The 2 columns were replaced by jack-up. The all PC panels were replaced. The building was repaired almost the same as the original one.

■ Building F (Demolished)
Damage level: Severe
Completion Age: 1984
Total Area: 1,584m^2 Height: 18.8m
Usage: Office
Structural Type: Moment-resisting frame
Floor: upper ground 5- penthouse 0- basement 0
[Summary of damage]
Structural damage concentrated on the 1F-4F. Near beam-to-column connections, the damage of yielding, crack, local buckling and fracture could be seen. At the 2F-3F in the NS direction, the ratio of fracture of the beams was 54%. The damage of column could scarcely be seen. The maximum residual inter-story drift angle was 1/48 (3F). The tilt of the entire building was 1/100. The serious damage of exterior PC panels and interior finishes could be seen.
[Summary of repair construction]
Building F was demolished.

■ Building G
Damage level: Intermediate
Completion Age: 1983
Total Area: 627m^2 Height: 27.8m
Usage: Office

Type: Moment-resisting frame
Floor: upper ground 8- penthouse 1- basement 1
[Summary of damage]

Structural damage concentrated on the 4F-6F. At the end of the beams, the damage of yielding, crack, local buckling and fracture could be seen. The damage of column could scarcely be seen. The maximum residual inter-story drift angle was 1/98 (7F). The tilt of the entire building was 1/286. The damage of exterior PC panels could be seen.

[Summary of repair construction]

The 11 damaged parts near beam-to-column connections were effectively repaired by the method shown in [4]. The PC panels were repaired. The building was repaired almost the same as the original one.

■ Building H
Damage level: Minor
Completion Age: 1979
Total Area: 18,084m^2 Height: unknown
Usage: Complex facility (Hotel, Store, Station)
Type: Moment-resisting frame + K-brace (BF-5F: SRC)
Floor:upper ground 12- penthouse 2- basement 2
[Summary of damage]

Structural damage could be seen above the 6F. Fracture of braces and shear buckling of beam webs connected with braces could be seen. Some damaged parts near beam-to-column connections could be seen. The damage of column could scarcely be seen. The maximum residual inter-story drift angle and the tilt of the entire building were unknown. The damage of exterior PC panels could be seen.

[Summary of repair construction]

The 13 damaged parts near beam-to-column connections were repaired. The 35 damaged parts by fracture of braces and shear buckling of beam webs connected with braces were repaired. The building was repaired almost the same as the original one.

■ Building I
Damage level: Minor
Completion Age: 1986
Total Area:34,188m^2 Height: unknown
Usage: Parking facility
Type: Moment-resisting frame + Brace
Floor: upper ground 9- penthouse 2- basement 0
[Summary of damage]

Near the column bases connected with braces, 5 cracks could be seen. Serious damage could not be seen in other structural and non-structural members. The maximum residual inter-story drift angle was 1/208 (4F). The tilt of the entire building was 1/416.

[Summary of repair construction]

The repair of the 4 damaged parts near the column bases could be recognized. The building was repaired almost the same as the original one.

■ Building J (Demolished)
Damage level: Severe
Completion Age: 1988
Total Area: 429m^2 Height: 16.0m
Usage: Office
Type: Moment-resisting frame
Floor: upper ground 5- penthouse 0- basement 0
[Summary of damage]

Building J had a large residual drift. The maximum residual inter-story drift angle was 1/48 (1F). The tilt of the entire building was 1/50. These large residual drifts seem to be mainly caused by damage of foundation beams and local buckling of the column at the 1F. Near beam-to-column connections, relatively minor damage could be seen. The serious damage of exterior PC panels and interior finishes could be seen.

[Summary of repair construction]

Building J was demolished.

■ Building K
Damage level: Intermediate
Completion Age: 1988
Total Area: 2,771m^2 Height: 30.7m
Usage: Office
Moment-resisting frame
Floor: upper ground 9- penthouse 0- basement 1
[Summary of damage]

The residual drift could hardly be recognized, but the disorder of the elevators led to the investigation of structural damage. Structural damage concentrated on the 2F-4F. Near beam-to-column connections, the damage of yielding, crack, local buckling and fracture could be seen. The maximum residual inter-story drift angle and the tilt of the entire building was 1/1000.

[Summary of repair construction]

The 67 damaged parts near beam-to-column connections were repaired. The building was repaired almost the same as the original one.

■ Building L

Damage level: Severe

Completion Age: 1977

Total Area: 1,403m^2 Height: 25.0m

Usage: Office

Type: Moment-resisting frame

Floor: upper ground 8- penthouse 0- basement 1

[Summary of damage]

Structural damage concentrated on the 1F. Fracture (3 columns), local buckling (3 columns) of the 1F could be seen. All anchor bolts of exposed-type column bases were fractured. The maximum residual inter-story drift angle was 1/5 (1F). The tilt of the entire building was 1/37. The serious damage of exterior PC panels could be seen.

[Summary of repair construction]

Building L had a large residual drift (1F:1/5). The damage concentrated on the first floor. Although it was judged to be demolished at first, difficult straightening repair construction was conducted because of the owner's strong will to avoid business indirect cost losses. First, the building above the second floor was jacked up. Second, all columns of the first floor were replaced by new ones. Third, new sliding construction technique was introduced to cancel residual drifts. Finally, the building above the second floor was jacked down and all the base parts were welded again. The contractor said that this new construction technique had contributed to much cheaper repair cost and shorter repair period. The building was repaired almost the same as the original one.

3. ANALYSIS OF REPARABILITY LIMIT OF STEEL STRUCTURES

3.1 Analysis from a Technical Point of View

When we discuss reparability in terms of the difficulty of repair construction, we can say that a residual drift angle is one of the most important factors of all engineering parameters. This is because straightening repair construction of an inclined building is extremely difficult, while the repair construction of local damage of the end of beams and columns by local buckling, fracture, yielding and crack can be relatively easy by using the usual methods [5-9]; Besides, the non-structural members and architectural equipment can be partially replaced if damage is severe. Therefore, in this study from a technical point of view, we focused on residual drift and investigated both overall residual drift angle θ_R and maximum residual inter-story drift angle $\theta_{\max,r}$, from the actual data. The overall residual drift angle and maximum residual inter-story drift angle are defined as:

$$\theta_R = \frac{u_R}{H} \tag{1}$$

$$\theta_{\max,r} = \max_{1 \le i \le N}\left[\frac{u_r}{h}\right]_i \tag{2}$$

where u_R is the residual drift of the top of the building and H is the height of the building; $\left[\frac{u_r}{h}\right]_i$ is the residual inter-story drift angle of the i-th story.

The actual data of overall residual drift angle and maximum residual inter-story drift angle are shown in Table 1, 2, respectively. These data are arranged in order of large values. The actual data of building H are unknown. From these tables, we defined the reparability limits of overall residual drift angle and maximum residual inter-story drift angle at general level. This general level means that buildings can be restored by partial repair without any difficult straightening repair construction or large-scale reinforcing construction. Therefore, the reparability limits are determined as the maximum value except the data of building F, J, C, D and L (See chap. 2).

From the analysis of the actual data of these tables, the reparability limits of overall residual drift angle and maximum residual inter-story drift angle are defined as the follows:

$$\theta_{R,\lim} = \frac{1}{110} \tag{3}$$

$$\theta_{\max,r,\lim} = \frac{1}{71} \tag{4}$$

where $\theta_{R,\lim}$ is the reparability limit of overall residual drift angle and $\theta_{\max,r,\lim}$ is the reparability limit of maximum residual inter-story drift angle.

3.2 Analysis from an Economic Point of View

Whether a building can be repaired or not after an earthquake should be determined mainly in terms of cost if it can be technically repaired. In this study, we tried to define the reparability limit in terms of direct restoration cost and indirect restoration cost. Direct restoration cost means the costs required when a building is restored by repair or replacement construction and indirect restoration cost means the costs lost when a building cannot be used during repair or replacement construction period, like business cost losses.

When we discuss the reparability limit from an economic point of view, we can say that the ratio of repair cost to replacement cost (Fig. 1.) is one of the most useful factors of all cost-related indexes.

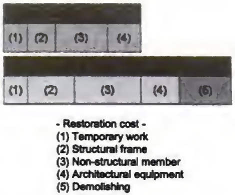

Fig. 1. Breakdown of repair and replacement cost.

Thus, in this study, the reparability limit related to direct restoration cost is determined by the maximum value of the direct restoration cost ratio $R_{c,d}$ which is defined as:

$$R_{c,d} = \frac{C_{repair,d}}{C_{replacement,d}} \tag{5}$$

where $C_{repair,d}$ is direct repair cost and $C_{replacement,d}$ is direct replacement cost.

Similarly, the reparability limit related to indirect restoration cost is determined by the maximum value of the indirect restoration cost ratio $R_{c,ind}$ which is defined as:

$$R_{c,ind} = \frac{C_{repair,ind}}{C_{replacement,ind}} \tag{6}$$

where $C_{repair,ind}$ is indirect repair cost and $C_{replacement,ind}$ is indirect replacement cost.

Table 1. Actual measurement value of overall residual drift angle.

Building	C	L	J	F	B	D	A	E	G	I	K
θ_R	1/34	1/37	1/50	1/100	1/110	1/120	1/216	1/250	1/286	1/416	1/1000

Table 2. Actual measurement value of maximum residual inter-story drift angle.

Building	L	C	D	J	F	B	G	E	A	I	K
$\theta_{\max,r}$	1/5	1/34	1/46	1/48	1/48	1/71	1/98	1/100	1/125	1/208	1/1000

However, indirect cost is very difficult to predict in a design process because it is affected by various indeterminate factors. Therefore, in this paper, on the assumption that indirect cost is approximately proportional to the period of repair or replacement construction, we regarded indirect restoration cost ratio as the ratio of repair construction period to replacement construction period:

$$C_{repair,ind} \approx k \cdot T_{repair} \tag{7}$$

$$C_{replacement,ind} \approx k \cdot T_{replacement} \tag{8}$$

$$R_{c,ind} \approx \frac{T_{repair}}{T_{replacement}} \tag{9}$$

where k is constant, T_{repair} is repair construction period and $T_{replacement}$ is replacement construction period.

On the basis of the above definitions, we investigated direct restoration cost ratio and indirect restoration cost ratio from the actual data by following the next note.

Note :

1) Direct repair cost: Real repair cost (1995) is used.

2) Direct replacement cost: The sum of the initial construction cost (1995) into which is converted from the real initial construction cost by multiplying an age-modification factor and the virtual demolition cost estimated by an expert engineer is used.

3) Repair construction period: Real repair construction period is used. (All buildings were repaired under completely closed condition.)

4) Replacement construction period: The sum of the initial construction period and the virtual demolition period estimated by an expert engineer is used.

5) The values of building B, C, D and L (marked as * in the tables) are reference values. Building B doesn't include the repair of the interior as an unusual construction condition. As mentioned in 3.1, building C, D and L exceed the general technical reparability limits.

The actual data of direct restoration cost ratio and indirect restoration cost ratio are shown in Table 3, 4, respectively. These data are arranged in order of large values. From these tables, we defined the reparability limits of direct restoration cost ratio and indirect restoration cost ratio. The reparability limits are determined as the maximum values except the data of building B, C, D and L (marked as * in the tables). From Table 3, the maximum value of direct restoration cost is 0.86 (building A), which is below 0. This means that there was no case that a building was repaired by using the repair cost above the replacement cost. From Table 4, the maximum value of indirect restoration cost ratio is 0.40 (building A).

From these analyses, the reparability limits of direct restoration cost ratio and indirect restoration cost ratio are determined as 0.86, 0.40, respectively.

$$R_{c,d,\lim} = 0.86 \tag{10}$$

$$R_{c,ind,\lim} = 0.40 \tag{11}$$

where $R_{c,d,\lim}$ is the reparability limit of direct restoration cost ratio and $R_{c,ind,\lim}$ is the reparability limit of indirect restoration cost ratio.

Table 3. Direct restoration cost ratio. (*: Reference value.)

Building	A	G	L*	I	C*	E	D*	H	K	B*
$R_{c,d}$	0.86	0.73	0.62	0.60	0.56	0.55	0.51	0.44	0.18	0.17

Table 4. Indirect restoration cost ratio. (*: Reference value.)

Building	D*	A	B*	L*	E	K	C*	G	H	I
$R_{c,ind}$	0.41	0.40	0.36	0.35	0.28	0.26	0.26	0.24	0.15	0.12

In addition, Eq.12 is confirmed from the fact that both the values of direct restoration cost ratio and indirect cost ratio are below 1.

$$\frac{C_{repair,d} + C_{repair,ind}}{C_{replacement,d} + C_{replacement,ind}} < 1 \qquad (12)$$

4. THE RELATIONSHIP BETWEEN RESIDUAL DRIFT ANGLE AND RESTORATION COST RATIO

Considering the difficulties of the prediction of repair cost and repair construction period in the current database, we tried to predict direct restoration cost ratio and indirect restoration cost ratio (which is defined as the ratio of repair construction period to replacement construction period) from a structural damage index because these ratios within the reparability limits assume to be approximately proportional to a structural damage index. In this study, we used residual drift angle as a structural damage index because it is the only identifiable index which can be obtained from actual data.

Fig. 2 shows the relationship between overall residual drift angle and direct restoration cost ratio. Fig. 3 shows the relationship between overall residual drift angle and indirect restoration cost ratio. The data of building B, C, D, H and L are not plotted in the graphs because of the reasons mentioned in Chap. 2 and 3. The data of demolished buildings (building F and J) are not also plotted in the graphs. The lines in Fig. 2 and 3 show the regression lines. In both graphs, there are some scatters between the plots and the regression line, but from a broader perspective, this relationship can be regarded as linear. It is speculated that one of the reasons of these scatters is that residual drift can become the index to express structural damage to some extent, while it just shows the final damage of a building and does not always perfectly correspond to the damage of the entire building.

When we predict both direct restoration cost ratio and indirect restoration cost ratio from these regression lines, the predicted equations are defined as follows:

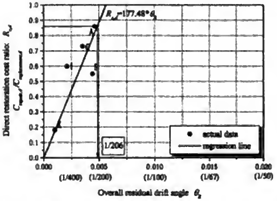

Fig. 2. Relationship between overall residual drift angle and direct restoration cost ratio.

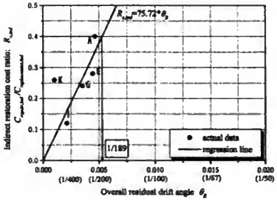

Fig. 3. Relationship between overall residual drift angle and indirect restoration cost ratio.

$$R_{c,d,p} = 177.48 \cdot \theta_R \qquad (13)$$

$$R_{c,ind,p} = 75.72 \cdot \theta_R \qquad (14)$$

where $R_{c,d,p}$ is the predicted value of direct restoration cost ratio; $R_{c,ind,p}$ is the predicted value of indirect restoration cost ratio; θ_R is overall residual drift angle.

From Eq.13, the value of overall residual drift angle corresponding to the reparability limit of direct restoration cost ratio (0.86) is defined as 1/206. From Eq.14, the value of overall residual drift angle corresponding to the reparability limit of indirect restoration cost ratio (0.40) is defined as 1/189. From these two values, the smaller value 1/206 is adopted from a safety viewpoint. Eq.15 shows the definition of the reparability limit of overall residual drift angle recommended for design practices:

$$\theta_{R,\lim,c} = \frac{1}{200} \tag{15}$$

where $\theta_{R,\lim,c}$ is the reparability limit of overall residual drift angle recommended for design practices

Fig. 4 shows the relationship between maximum residual inter-story drift angle and direct restoration cost ratio. Fig. 5 shows the relationship between maximum residual inter-story drift angle and indirect restoration cost ratio. The lines in Fig. 4 and 5 show the regression lines. When we predict both the direct restoration cost ratio and indirect restoration cost ratio from these regression lines, the predicted equations are defined as follows:

$$R_{c,d,p} = 78.35 \cdot \theta_{\max,r} \tag{16}$$

$$R_{c,ind,p} = 31.78 \cdot \theta_{\max,r} \tag{17}$$

where $R_{c,d,p}$ is the predicted value of direct restoration cost ratio; $R_{c,ind,p}$ is the predicted value of indirect restoration cost ratio; $\theta_{\max,r}$ is maximum residual inter-story drift angle.

From Eq.16, the value of maximum residual inter-story drift angle corresponding to the reparability limit of direct restoration cost ratio (0.86) is defined as 1/91. From Eq.17, the value of maximum residual inter-story drift angle corresponding to the reparability limit of indirect restoration cost ratio (0.40) is defined as 1/79. From these two values, the smaller value 1/90 is adopted from a safety viewpoint. Eq.18 shows the definition of the reparability limit of maximum residual inter-story drift angle recommended for design practices:

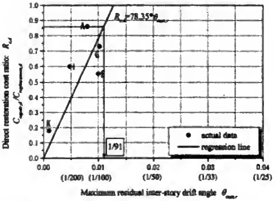

Fig. 4. Relationship between maximum residual inter-story drift angle and direct restoration cost ratio.

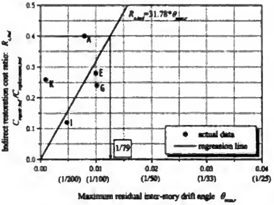

Fig. 5. Relationship between maximum residual inter-story drift angle and indirect restoration cost ratio.

$$\theta_{\max,r,\lim,c} = \frac{1}{90} \tag{18}$$

where $\theta_{\max,r,\lim,c}$ is the reparability limit of maximum residual inter-story drift angle recommended for design practices

5. CONCLUSIONS

In this paper, based on the actual data of repaired or demolished buildings damaged by the Hyogoken-nanbu earthquake, we analyzed residual drift and restoration cost relevant to the reparability and tried to clarify the reparability limit of steel structural buildings from both technical and economic points of view. As for the technical point, we adopted residual drift angle as the index of difficulty of repair construction and analyzed both the overall residual drift angle and maximum residual inter-story drift angle. As for the economic point, we adopted restoration cost ratio and analyzed direct restoration cost ratio and indirect restoration cost ratio. The results obtained by the investigation are shown as follows:

1) The reparability limit of overall residual drift angle was 1/110.

2) The reparability limit of maximum residual inter-story drift angle was 1/71.

3) The reparability limit of direct restoration cost ratio was 0.86.

4) The reparability limit of indirect restoration cost ratio was 0.40.

Furthermore, based on the actual data, the relationship of residual drift angle and restoration cost ratio was investigated and the reparability limits synthesizing technical and economic aspects were defined by overall residual drift angle and maximum residual inter-story drift angle as 1/200 and 1/90, respectively.

6. ACKNOWLEDGEMENTS

This research was funded by the Ministry of Education, Culture, Sports, Science and Technology via a Grant-in-Aid for Scientific Research and was conducted in the committee on steel structures of the Architectural Institute of Japan (Chairperson: Prof. H. Kuwamura, the Univ. of Tokyo). We would like to acknowledge all the project members for their useful advice and suggestions.

7. REFERENCES

1) Architectural Institute of Japan : Report on the Hanshin-Awaji Earthquake Disaster, Structural Damage to Steel Buildings, Building Series Volume 3, 1997.10, (in Japanese)

2) Mitsumasa Midorikawa, Takashi Hasegawa, Akiyoshi Mukai, Isao Nishiyama, Toshibumi Fukuta, Hiroyuki Yamanouchi, Damage investigation of steel buildings in specific areas due to the 1995 Hyogoken-Nanbu Earthquake, Journal of Structural and Construction Engineering, Architectural Institute of Japan, No.493, pp.115-120, 1997.3, (in Japanese)

3) Hitoshi Kuwamura, Naoki Tanaka, Hirokazu Sugimoto, Toshihiko Kouno, Performance description of steel structures -Study on performance based design of steel structural buildings part1-, Journal of Structural and Construction Engineering, Architectural Institute of Japan, No.562, pp.175-182, 2002.12, (in Japanese)

4) Yoshihiro Iwata, Research on Reparability Performance-based Design Methodology of Steel Moment-resisting Frame buildings, Ph. D. thesis of the Univ. of Tokyo, 2004.9, (in Japanese)

5) Hirokazu Sugimoto, Naoki Tanaka, Masaru Teraoka, Yoshihiro Iwata, Hitoshi Kuwamura, Reparable-level of steel buildings based on the actual cost of retrofitting, Annual meeting panel discussion report on the consideration of performance-based design of steel structural buildings, Architectural Institute of Japan, Tokai, pp. 53-72, 2003.9, (in Japanese)

6) Yasuhiko Takahashi, Yoshio Fujitani, Minoru Yoshikawa, Sadaki Yagi, Yoshihiro Fujita, Sanae Fukumoto, Retrofitting technique and modification practice for structural steel building damaged during the Hyogoken-Nanbu Earthquake, Journal of Architecture and Building Science, Vol.1, 1995.12, pp.127-132, (in Japanese)

7) Masaru Teraoka, Hiroshi Shimanuki, Koji Morita, Kazuhiko Komono, Tadayoshi Okada, An Investigation and analysis on a nine-story steel building damaged by the 1995 Hyogoken-Nanbu Earthquake, Journal of Steel Structure, Vol.3, No.11, pp.21-34, 1997.3, (in Japanese)

8) Japan Building Disaster Prevention Association: Guidelines for Seismic Diagnosis and Retrofit of Existing Steel Structural Buildings, 1978.6, (in Japanese)

9) Japan Building Disaster Prevention Association: Guidelines for Evaluation of Damaged Building Structures and Retrofit Techniques, 1991.2, (in Japanese)

Recent Developments on the Design and Evaluation of Steel Structures for Seismic Loads: An NSF Perspective

by

Dr. Douglas A. Foutch[1]

ABSTRACT

There are many sources of uncertainty when designing or evaluating new buildings for seismic loads. Current codes account for these uncertainties in an ad hoc fashion. A new procedure has been developed for design and evaluation of steel moment frame buildings in the U.S. Randomness and uncertainty are accounted for in a rational way. The procedure is performance based and considers Immediate Occupancy and Collapse Prevention performance limits. The goal is to achieve a 90% confidence that the Performance Objective will be achieved under the design hazard level. A large number of design and evaluation examples were investigated. The results indicated that new buildings designed in accordance with the latest IBC specifications are conservative when collapse is considered. The reliability of older buildings, however, is not expected to have the same level of resistance against collapse.

KEYWORDS: Steel Moment Frame Buildings; Reliability-Based Design; Seismic Loads; Performance-Based Design

1.0 INTRODUCTION

Prediction of seismic response of a new or existing structure is complex, due not only to the large number of factors that need to be considered and the complexity of seismic response, but also due to the large inherent uncertainty associated with making these predictions. Clearly the characteristics of future earthquakes can only be approximated leading to very large uncertainties in the loads acting on the structure. Structural properties may differ from those intended or assumed by the designer, or may change substantially during the earthquake (e.g. local fracture of connections). Analysis methods may not accurately capture the actual behavior due to simplifications in the analysis procedure (linear vs. nonlinear for instance) and modeling of the structure. Our knowledge of the behavior of structures during earthquakes is not complete which introduces other uncertainties. Consequently, seismic performance prediction must consider these uncertainties.

Many of these issues are covered to a greater or lesser extent in current codes through the use of load and resistance factors, adjustment of various design parameters following major earthquakes and introduction of new analytical and design procedures as they are developed and verified. In responding to the problems observed in steel moment frame buildings after the Northridge and other earthquakes, the SAC steel project has attempted to develop a comprehensive understanding of the capacity of various moment resisting connections and the demands on these connections. To achieve satisfactory building performance through design, or to evaluate an existing building, one needs to reconcile expected seismic demands with acceptable performance levels while recognizing the uncertainties involved.

Seismic design regulations for new buildings in the United States rely on a very simplified approach for achieving acceptable performance.

---

[1] Program Director
Structural Systems and Hazard Mitigation of Structures
National Science Foundation
4201 Wilson Boulevard Room 585
Arlington, VA 22230

This approach uses several coefficients that may be used in different combinations to satisfy performance goals and objectives. These are the *R* factors, C_d values, drift limits and importance, or occupancy factors. By varying these coefficients several of the factors described above may be accounted for in a crude way. One problem with the current approach is that there has been no rational or quantifiable way to determine these coefficients.

During the 1994 Northridge Earthquake, fractured or cracked beam-column connections were discovered in over 200 steel moment frame buildings. This was a shock to many in the design profession, since steel frame buildings were considered to be the best seismic resisting system. As a result, the Federal Emergency Management Agency (FEMA) sponsored a large research-development project (SAC) that resulted in three reports (FEMA 350, (2000); FEMA 351 (2000); FEMA 351, (2000)). These documents presented a new paradigm for the design and evaluation of steel moment frame buildings. The new procedures allowed for the explicit evaluations of randomness and uncertainties to be included in the design process in a rational manner. The procedure forms the basis for a performance based engineering methodology that recognizes two performance levels, Immediate Occupancy and Collapse Prevention. One main feature of the procedure is that the design professional may calculate the confidence level is satisfying the design objective.

2.0 DEVELOPMENT

The new procedure can be used for new design, evaluation of existing buildings and evaluation of damaged buildings after an earthquake. It is a performance based procedure with two limit states considered, Collapse Prevention and Immediate Occupancy. This paper will deal only with Collapse Prevention. The design object is to have 90% confidence that the chance of not satisfying limit state is less than 2% in 50 (2/50) years. The seismic hazard level for the performance limit is also chosen to be 2/50.

The acceptance criterion is based on a confidence factor,λ, that is used to determine the confidence level. This factor is the ratio of the factored demand over factored capacity. In equation form, this is expressed as:

$$\lambda = \frac{\gamma \cdot \gamma_a \cdot D}{\phi \cdot C} \tag{1}$$

where

D = estimate of median drift demand

C = estimate of median drift capacity

ϕ = resistance factor

γ = demand factor

γ_a = analysis demand factor

The factors, ϕ, γ and γ_a in Equation 15 are based on the reliability work developed by Jalayer and Cornell (1998) for the SAC project. A more detailed derivation of these equations is given by Cornell et al (2002). Equation 1 is essentially the ratio of factored demand divided by factored capacity. The demand, D, is the expected median drift resulting from a series of accelerograms sampled from the chosen hazard level. Details on how to calculate all of the variables for this procedure is given in Yun and Foutch (2000).

The resistance factor, ϕ, accounts for the fact that the estimate of *C* is affected by randomness and uncertainty in the estimation process. The capacity of the building against global collapse is a function of the earthquake accelerograms used in the IDA analyses (Vamvatsikos et. al., 2001). These accelerograms are part of a random process. The capacity is also affected by the uncertainty in the load-deformation behavior of the system determined from tests. The local collapse value is also affected by uncertainties in the response of the components due to variable material properties and fabrication.

The equation for calculating the resistance factor, ϕ is given by (Cornell et al, 2002):

$$\phi = \phi_{RC} \cdot \phi_{UC} \tag{2}$$

$$\phi_{RC} = e^{\frac{-k\beta_{RC}^2}{2b}} \tag{3}$$

$$\phi_{UC} = e^{\frac{-k\beta_{UC}^2}{2b}} \tag{4}$$

where

ϕ_{RC} = Contribution to ϕ from randomness of the earthquake accelerograms

ϕ_{UC} = Contribution to ϕ from uncertainties in measured component capacity

The demand factor, γ, is calculated as:

$$\gamma = e^{\frac{k\beta_{RD}^2}{2b}} \tag{5}$$

where

β_{RD} = $\sqrt{\sum \beta_i^2}$ where β_i^2 is the variance of the natural log of the drifts for each element of uncertainty.

The confidence factor, λ depends on the slope of the hazard curve, k and the uncertainty, but not randomness, associated with the natural log of the drifts. The equation for λ is (Jalayer and Cornell, 1999)

$$\lambda = e^{-\beta_{UT}(K_x - k\beta_{UT}/2b)} \tag{6}$$

where

β_{UT}^2 = $\Sigma\sigma_i^2$ where σ_i is for uncertainties in the demand and capacity but not randomness

k = slope of the hazard curve

K_x = standard Gaussian variate associated with probability x of not being exceeded (found in standard probability tables)

3.0 EXAMPLES

3.1 New Buildings

Twenty steel moment frame buildings were designed in accordance with the 1997 NEHRP provisions. These included eight 3-story, eight 9-story and four 20-story buildings. It was assumed that the buildings were constructed using the beam-column connections that were pre-qualified by the SAC program. All buildings had a greater confidence level than 90% for both Local Collapse and Collapse. Local Collapse occurs when the connections at both end of a beam fracture and the beam falls to the floor below.

3.2 Existing Buildings

A series of 3-, 9-, and 20-story buildings were designed in accordance with the 1973, 1985, 1992 and 1997 Uniform Building Codes. It was also assumed that the connections were the pre-Northridge brittle type. These were then evaluated using the new performance-based procedure. The results are shown in Table 1 for global collapse. The results indicate that the newer that the building is, the higher is the confidence of satisfying the performance objective. The confidence levels range from 99% for buildings built after 1997 to 28% for 20-story buildings built in 1973. The confidence level for avoiding Local Collapse drop as low as 2% for buildings designed and constructed in 1972 or earlier.

4.0 CONCLUSIONS

This paper describes a new performance-based design and evaluation procedure for steel moment frame buildings designed for seismic loads. The procedure allows the designer to estimate the confidence level that the building will satisfy the design objective. It also is based on a rational method for accounting for randomness and uncertainty.

1 The new performance based procedure for designing new steel moment frame buildings is a powerful method for ensuring that the building will satisfy the performance objectives.

2 The new procedure provides a rational way to evaluate existing buildings for seismic loads.

3 Buildings designed by current codes and constructed with the new ductile connections are expected to perform very well during future earthquakes.

4 Older buildings designed before 1997 are more likely to collapse during future quakes.

5.0 REFERENCES

Cornell, C.A., Jalayer, F., Hamburger, R.O. and Foutch, D.A., 2002, "The Probabilistic Basis for the 2000FEMA/SAC Steel Moment Frame Design Guidelines," Journal of Structural Engineering, ASCE, Vol. 128, No. 4, April.

FEMA-350, 2000, Recommended Seismic Design Procedures for New Steel Moment Frame Buildings, prepared by the SAC Joint Venture for the Federal Emergency Management Agency, Washington DC.

FEMA-351, 2000, Recommended Seismic Evaluation and Upgrade Criteria for Existing Steel Moment Frame Buildings, prepared by the SAC Joint Venture for the Federal Emergency Management Agency, Washington, D.C.

FEMA-352 (2000), Recommended Post-earthquake Evaluation and Repair Criteria for Welded Steel Moment-Frame Buildings, prepared by the SAC Joint Venture for the Federal Emergency Management Agency, Washington DC.

Jalayer, F. and Cornell, C. A. (2003). "A Technical Framework for Probability-Based Demand and Capacity Factor Design (DCFD) seismic formats." *PEER Report 2003/8*, Pacific Earthquake Engineering Center, University of California at Berkeley, Berkeley, Calif.

Yun, S. Y. and Foutch, D. A., 2000, "Performance Prediction and Evaluation of Low Ductility Steel Moment Frames for Seismic Loads." SAC Background Report SAC/BD-00/26

Table 1 Collapse capacity, demand and confidence level for different building designs

Year	1997			1992			1985			1973		
Stories	C	D	Conf	C	D	Conf	C	D	Conf	C	D	Conf
3-story	0.10	0.027	99%	0.10	0.047	88	0.10	0.058	72%	0.10	0.056	75%
9-story	0.10	0.034	99%	0.078	0.043	57	0.094	0.048	64%	0.077	0.046	50%
20-story	0.085	0.024	96%	0.072	0.041	57	0.070	0.030	58%	0.069	0.045	28%

Wood Building Collapse Tests Using E-Defense

by

Isao Sakamoto[1], Naohito Kawai[2], Takahiro Tsuchimoto[3] and Chikahiro Minowa[4]

ABSTRACT

This paper presents the wood building collapse tests of NIED E-Defense. In 2002, Ministry of Education, Culture, Sport, Science and Technology (MEXT) began "Special Project for Earthquake Disaster Mitigation in Urban Areas (Dai-Dai-Toku in Japanese)". The test was conducted as one of the project. There were three stages in the test. First stage was "Base Isolated and Recovered Recent Wood House". Second stage was "Traditional Wood Houses". Third stage was "Retrofit and Non retrofit Conventional Wood Houses". In first and second stages, the houses were experienced severe artificial quake on E-defense, and collapsed.

KEYWORDS: Base Isolation, Collapse Test, Seismic Retrofit, Shaking Table, Wood Building

1. INTRODUCTION

In 1995, Hanshin Great Earthquake Disaster occurred. MEXT and NIED started the construction of three-dimensional and six-freedom shaking table for full-scale tests of structures. The table is called E-Defense. The table has scale of 20m by 15m and can move 2m, with velocity of 2m/s in X and Y horizontal directions, 1m with velocity of 0.7m/s in Z vertical direction. Maximum structure weight is 1200ton. Maximum accelerations are 2G in X and Y horizontal directions without structures. Vertical power of the table is 6300tonf.
E-Defense has completed in January 2005. Three types of structures were planned as DAI-DAI-Toku Project in 2002 for E-Defense. One is the test of piles in soil layer, another is concrete building, and the other is wood building.

This paper describes the wood building test. The wood building test had three stages. First stage was "Base Isolated and Recovered Recent Wood House". Second stage was "Traditional Wood Houses". Third stage was "Retrofit and Non retrofit Conventional Wood Houses". At first and second stages, the houses were experienced severe artificial quake on E-defense, and collapsed. The test results of first and third stages are presented here.

2. FIRST STAGE TEST OF BASE ISOLATED AND RECOVERED RECENT WOOD HOUSE

At the opening ceremony of E-Defense, a test of recent style wood house was demonstrated, as shown in Fig. 1. The wood house was quaked by the use of JMA Kobe strong motion record. In the test, small cracks and small partial fracture of walls occurred. There was no heavy damage in the house. The base of the house was designed for the base isolation. When the base isolation system was locked, severe quakes was inputted. The damages of house at the opening ceremony were recovered for the First Stage Test.

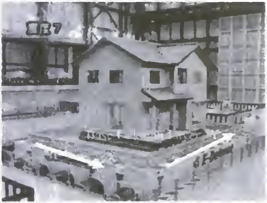

Fig.1 Test Wood House at Opening Ceremony

---

[1] Professor, Keio University

[2] Chief Research Engineer, Building Research Institute

[3] Senior Research Engineer, National Institute of Land and Infrastructure Management, MLIT

[4] Chief Research Engineer, National Research Institute for Earth Science and Disaster Prevention

2.1 Outline of Recent Wood House

The wood house of two stories was built by Japanese post and beam methods. The house had floor spaces of 67.49 ㎡ in first floor, 62.93 ㎡ in second floor. Seismic resistance was provided by bracings. Seismic grade of the house in Quality Verification Law was second. Exterior wall was ceramic siding, and interior wall was gypsum board. The length of seismic resistance wall(LW) and the eccentric ratio(ER) in Quality Verification Law were as follows.

LW of 2nd FL X 49.01m(20.51m), ER 0.036
LW of 2nd FL Y 39.06m(20.51m), ER 0.349
LW of 1st FL X 61.50m(35.73m), ER 0.036
LW of 1st FL Y 46.50m(35.73m), ER 0.332

The length in bracket ( ) was the required seismic resistance wall. Mass above first floor was about 340KN. The plans of house are shown in Fig.2.

The base isolation system was installed between the house base and foundation, as shown in Fig.3. In the system, there were 17 slide bearings, 4 rubber bearrings (horizontal spring 0.5KN/cm) , 8 stainless wire stoppers(fracture strength. 75KN).Special slide plates of moving length 2m were set only for E-defense test.

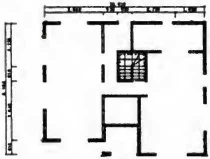

Second Floor

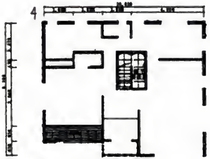

First Floor

Fig.2 Floor Plans of First Stage Test House

2.2 Test Results

2.2.1 Tests of over design input to Base Isolation Large displacement and long period input motions were applied to the house with base isolation system. Fig.4 is the response deformation spectra of input waves used in the tests. The damping 25% and natural period 2 second were roughly estimated the characteristics of the system,

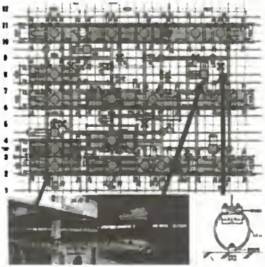

Fig.3 Base Isolation System

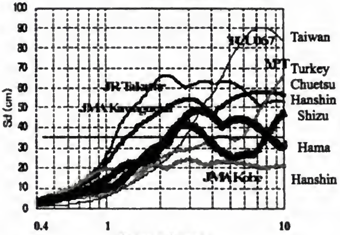

Fig.4 Response Deformation Spectra

Fig.5 presents the base shear coefficient and deformations waves of base isolation layer in shakings of proposal motion Hamamatsu SI(Hama) and 2004 Niigata Chuetsu JMA Kawaguchi inputs. Limit deformation of stopper was 30cm approximately. Stoppers were effective to proposal motion Hamamatsu SI, in which the maximum response deformation was 34cm. However, in the case of JMA Kawaguchi input, stoppers cut by severe motions. The maximum response deformations to JMA Kawaguchi were 62cm without stoppers, 61cm with stoppers.

2.2.2 Collapse Tests of Recent Wood House

After the base isolation tests., the base isolation layer was anchored. The house experienced strong motions before the collapse test. The strong motions made the house soft. At first, the natural frequencies of house were more than 6Hz in X direction, about 5Hz in Y direction. The frequencies right before a collapse test were 2.7Hz in X direction, 2.6Hz in Y direction, approximately. Hanshin great earthquake three dimensional record of JR Takatori, shown in Fig.6, was used for the inputs. The strongest axis motion was adjusted to Y direction input. The maximum input velocities were about 170cm/s in Y direction, 60cm/s in X direction, as 20cm/s in Z direction. The input motion to E-Defense was displacement. The E-Defense performances in displacement inputs were not tuned up. Therefore, the displacement inputs were compensated by the simple methods, in which the shaking table control system was expressed as two degree differential equation. The Fig.7 were velocity response spectra comparisons of shaking table inputs (black) and outputs (red). Long period component more than 0.3 second three direction outputs shows good agreements to inputs. However, the output components of less than 0.3 second in X and Y directions are bigger than input. In Z direction, the output components of less than 0.3 second are smaller than input. The small response of Z direction is supposed to bring from the large flow estimation of servo valves. The peaks of 0.2 second (5Hz) in responses were estimated to be the yawing motion of table.

It took three times of shakings to collapse the house. At first shaking of JR Takatori, a few pieces of wall panel fell down. Permanent deformations were scarcely observed. The photo after first shaking is shown in Fig.8. At second shaking of JR Takatori, big damages occurred. However, the house was standing. Large permanent deformations, shown in Fig.9, were observed. At the third shaking of JR Takatori, the first story of house was completely collapsed, as shown in Fig.10.

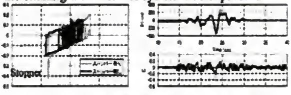

Proposal motion Hamamatsu SI

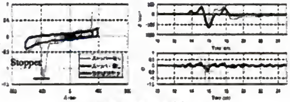

JMA Kawaguchi

Fig.5 Responses of Base Isolation Layer

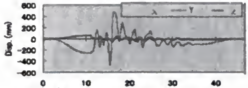

Displacements

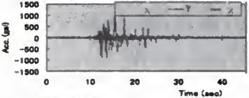

Acceleration

Fig.6 JR Takatori Input Waves

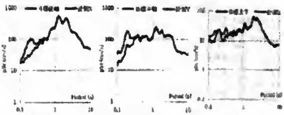

X Direction Y Direction Z Direction

Fig. 7 Comparisons of table inputs and outputs

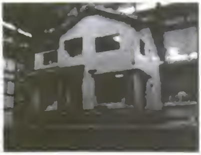

Fig.8 After First Shaking of JR Takatori

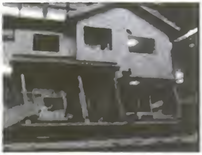

Fig.9 After Second Shaking of JR Takatori

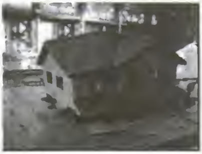

Fig.10 After Third Shaking of JR Takatori

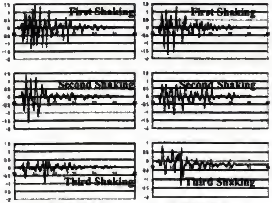

Y Direction X Direction

Fig.11 Roof Accel. Responses to JR Takatori

Fig.11 is the roof acceleration responses to three JR Takatori shakings. The response acceleration went down with progress of shakings.

3. THIRD STAGE OF RETROFIT AND NON -RETROFIT CONVETIONAL WOOD HOUSE

In 2002, the Defense test plan of Retrofit and Non retrofit Conventional Wood Houses" was made. The tests were conducted according to the plan.

3.1 Moving of Existing Houses and Retrofit

In February 2005, the offerings of two conventional wood houses were called around Kobe city, by public media. There were 200 applications approximately. Two conventional wood houses shown in Fig. 12, which built in 1974 at Akashi City in accordance with same drawing, were selected as E-Defense test structures. There were small differences in the houses. The houses were divided into 4 blocks, and moved to E-defense as shown in Fig.13, and rebuilt .The divide lines of moved houses were

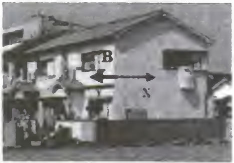

Fig.12 Selected Houses at Akashi City

Fig.13 Moving Works

reinforced with steel plates, steel angles, and additional timber members According to the seismic diagnosis, the houses have the seismic strengths of 22KN in Y axis of A house, 15KN in Y axis of B house, approximately. The required seismic strengths for two houses were same 50KN. The B house was decided to retrofit. According to the publication of "Japan Building Disaster Prevention Association", general retrofit methods of adding structure boards, metal joints and braces were employed. The dimensions, reinforced position and retrofit methods were shown in fig.14 and 15.

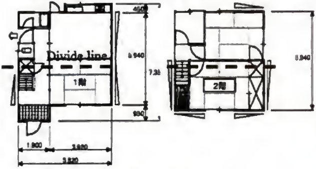

The dimensions of house plan

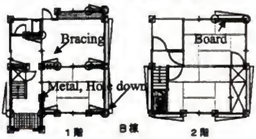

Reinforcement Positions

Fig. 14 Outline of Houses

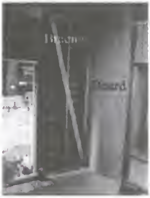

Fig.15 Retrofit Methods

The seismic strength of House B increases to 79KN by the retrofit. The weights were 11ton in roof level, and 15ton in 2nd floor level. Fig.16 shows two houses on the table of E-defense. Micro tremors of two houses were measured for investigating rigidities. Dominant frequencies were estimated as follows.

HOUSE	AXIS	On-site	On-table	Retrofitted
A	X	8.1Hz	7.3Hz	---
A	Y	5.8Hz	4.6Hz	---
B	X	7.1Hz	6.7Hz	7.2Hz
B	Y	5.1Hz	3.9Hz	4.7Hz

3.2 E-Defense Test and Computer Simulation

The three directional strong motions of JR Takator in Hanshin Earthquake, shown in Fig.17, were used as shaking table Inputs. In Fig.17, table response waves and target waves in acceleration were presented. In third stage, displacement wave inputs were adopted, just the same as first stage. Table yawing motion of 5Hz was estimated to occur, and made differences of to two waves.

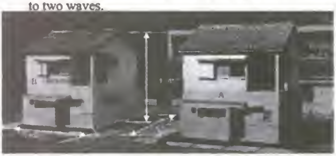

Fig.16 Two rebuilt houses on the table

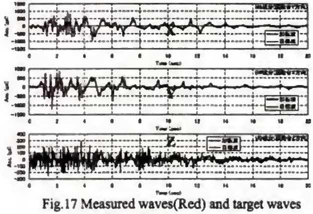

Fig.17 Measured waves(Red) and target waves (Black) of JR Takatori Accelerations.

Maximum velocities of target waves were 149cm/s, 117cm/s, 16.5cm/s in X, Y, Z directions.

In 2003 and 2004, preliminary tests were carried out in the use of middle size 3D shaking table. According to the preliminary test results, computer simulation program was developed, and the computer predictions for E-defense test responses were tried. Computer model of the house is Fig.18. There are 421 analysis points, about 1170 freedoms in the models. Restoring force models are Fig.19 for structure elements, In the model, bracings, mortal walls, mud walls, nailed boards, metal joints were considered.
There were incredible values in the model and the houses. Ratios for house weight mass R=1.0, 0.95, 0.9, 0.75 were used as parameters.

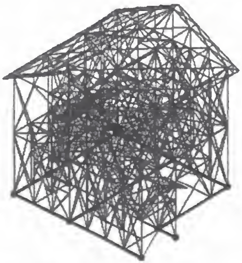

Fig.18 Computer Simulation Model

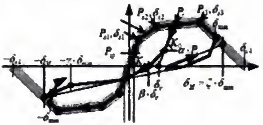

Fig.19 Restoring Force Model

The predicted computer simulations and measured story deformations of two houses are shown in Fig.21. According to the predicted results, there were the possibilities of non-collapse in non-retrofit house A, and the possibilities of collapse in retrofit house B

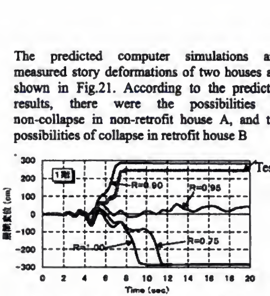

(a) Non Retrofit House A, First Floor, Y

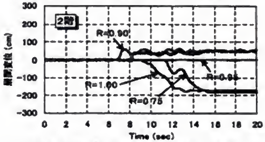

(b) Non Retrofit House A, Second Floor, Y

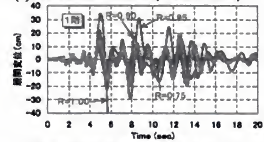

(c) Non-Retrofit House B, First Floor, Y

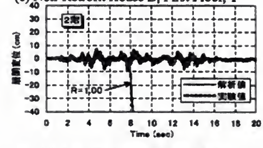

(d) Non-Retrofit House B, First Floor, Y

Fig.20 Story Deformations of Shaking Table Test and Computer Simulations

As test results, the retrofit house B withstand to JR Takatori shakings, and non-retrofit house A collapsed in accord to computer prediction R=0.9. The corrected computer simulation carried out with the use of measured weight data of the house, after tests. Fig.21 is the recorded video and computer simulation graphic. The collapse modes were similar to Hanshin Earthquake damage modes.

Considering after shocks, JR Takatori of 60% amplitude was applied to House B. Mortal walls fell off, however the House B was standing. Next, JR Takatori of 100% amplitude was applied, the house B collapsed.

4. CONCLUSIONS

The base isolation of house is useful to decrease the usual seismic responses of houses. However, safety methods against the earthquake motions of large velocities and large displacements must be developed.

The recent Japanese houses of post-and-beam wood structures were verified to provide enough seismic strength.

E-defense exhibited the efficiency of retrofit, and proved the recommendation of Japan Building Disaster Prevention Association to be correct.

The computer simulation program to be developed in the project was useful to explain the collapse of wood houses.

5. ACKNOLEDGEMENTS

The tests were conducted with NIED, BRI, FRI, Tokyo Denki University, and Nihon System Design. President, Dr. Miyake developed the computer simulation program. We appreciate the cooperation of many peoples, especially Associate Professor Isoda in Shimshu University, Associate Professor Koshihara in University of Tokyo, Mr. Toyoshima of Tokyu Construction.

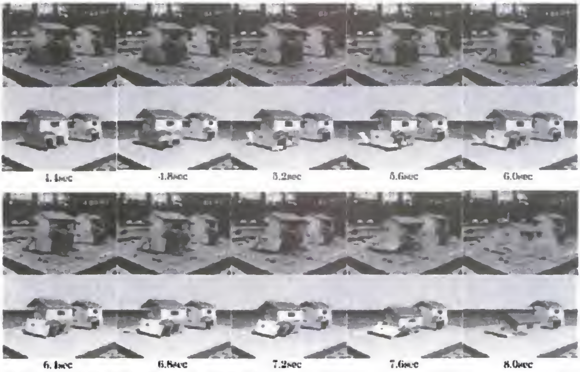

Fig.21 Video Records and Computer Simulation

Civil and Mechanical Systems (CMS) Programs at the NATIONAL SCIENCE FOUNDATION

Shih-Chi Liu, Program Director
Sensor Technology
Division of Civil and Mechanical Systems
Directorate for Engineering

Multi-Hazard Mitigation: New Frontier in Earthquake Engineering

By
Dr. Shih-Chi Liu
Program Director
Sensor Technology
Civil & Mechanical Systems
National Science Foundation

NSF Earthquake Hazard Mitigation Program

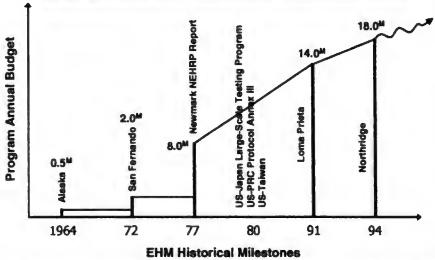

Design For Safety

New Structural Systems

Use of safety Factor—Over design
---Masonry & reinforced Masonry
---R/C
---Steel Framed
---Hybrid/Composite

Cooperative Research US-Japan over 90's

Design with Response Control

- Based Isolation
- Passive Control Systems
- Active/Semi-Active Control Systems
- Future: Smart Structures

Base Isolation

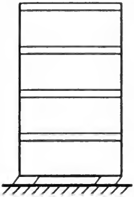

- Seismic hazard mitigation.
- Principle based primarily on deflecting earthquake energy. Requires period separation.
- Passive system, design based on site conditions and assumed ground motion.
- Application to low- and medium-rise buildings. Difficult to achieve period separation in tall buildings (>10 stories)
- Convenient for most retrofits. Limited superstructure modifications.
- Cost effective for retrofit and performance-based designs.
- Independent of outside power supply.
- Codes: UBC (1991), OSHPD (California State), AASHTO (1991)
- Implementation: Hundreds buildings worldwide, new buildings and 10 retrofits
- Basic research at EERC supported by NSF

Passive Control

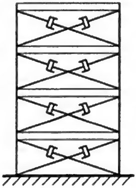

- Multi-hazard mitigation (e.g. wind and earthquake).
- Principle based on enhanced structural energy dissipation.
- Passive system, design insensitive to site conditions and ground motions
- Insensitive to structural type (height, aspect ratio).
- Limited interference with structural functionality in retrofit applications.
- Moderate cost for retrofit. Limited structural intervention as compared to conventional retrofit.
- Systems activated by structural deformation. Require some structure flexibility for maximum effectiveness.
- Independent of external power supply.
- Codes: SEAONC Tentative Guidelines for Passive Energy Dissipation Systems (1995)
- Implementation: a numberr of buildings in USA and Japan
- Basic research at EERC/NCEER supported by NSF

Active Control

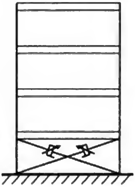

- Multi-hazard mitigation (e.g. wind and earthquake).
- Principle based primarily on added structural energy dissipating capacity and period adaptability.
- Active system, design insensitive to site conditions and ground motions.
- Insensitive to structural type (height, aspect ratio).
- Limited interference with structural functionality in retrofit applications.
- Potentially high costs. Robustness dependent on sensors and algorithms.
- Dependence on external power supply.
- Codes: None
- Implementation: a few buildings in Japan
- Basic research at NCEER supported by NSF

Yokohama Landmark Tower (1993)

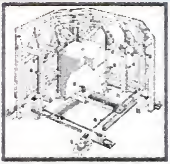

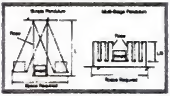

Prototype 20-Ton MR Fluid Damper

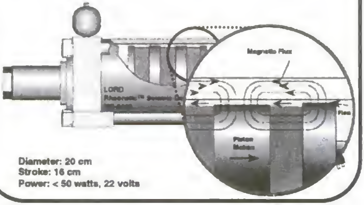

Diameter: 20 cm
Stroke: 16 cm
Power: < 50 watts, 22 volts

Deterioration Science

Material & System Failures (Theories & Models Needed) Due to:

- *Overload (fracture, cracking, etc)*
- *Over use (Fatigue)*
- *Over exposed (corrosion)*
- *Aging*

US EQ Engr Accomplishments

- ❖ **Understanding of Strong-Motion and Effects**
- ❖ **Modeling and Analysis Capabilities**
- ❖ **Design Methods of Structures and Geosystems**
- ❖ **Innovations of Structural Systems**
- ❖ **Innovations of Dynamic Response Control**
- ❖ **Production of Large Talent Workforce**
- ❖ **Successive Transformation of Research Modes and Tactics**

Major Research Milestones

*** Earthquake Engineering & FEM (80's-00's)**

--Ground Motions, Dynamic response & Control , New Structural Systems, Sophisticated Analytical Tools

*** Civil Infrastructure Systems (90's)**

--Deterioration Science, Assessment Technologies, Renewal Engineering, Institutional Effectiveness

--Lead to Intelligent Infrastructure Engineering

*** Sensors & Smart Structure (SSS) Technology**

--Current Global Research Trend

Transformation of US Earthquake Engineering Research

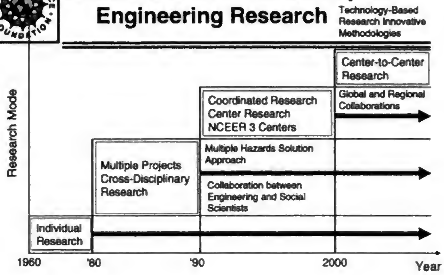
Technology-Based Research Innovative Methodologies
Center-to-Center Research
Global and Regional Collaborations
Coordinated Research Center Research NCEER 3 Centers
Multiple Hazards Solution Approach
Multiple Projects Cross-Disciplinary Research
Collaboration between Engineering and Social Scientists
Individual Research
Research Mode
1960
'80
'90
2000
Year

Transformation of Earthquake Engr Research

- Single investigator research: disciplinary: '70s-'80s
- Coordinated research: 1980--
- Cross-disciplinary research: early '90s (engineers and social scientists, etc)
- Center-based research: '90s--
- Center-to-Center research 2000— (ANCER)

Transformation of Earthquake Engr Research

- *Conventional approaches:* model,analysis, & design (single performance criterion and safety factor)
- *Multi-disciplinary approaches*: engineering plus preparedness and recovery, etc.
- *Technology-based approaches* (added social values: innovations for job and wealth creation)
- *New societal Needs* (blasts & attacks) leading to multiple hazards mitigation approaches

EQ Engr Research Outlook

- Research Responding to Social Demands (Safety, Security, Life Quality, Job and Economy Creation)
- Research Responding to Push by New Technologies (Smart Materials and Smart Structures, Sensors, SHM)
- Cross-Disciplinary Team Research, Center-Base Research
- Integrated Approaches for Multiple Hazard Mitigation and Engineering Design
- Increased Needs for International Collaboration

Push & Pull Between S&E&T

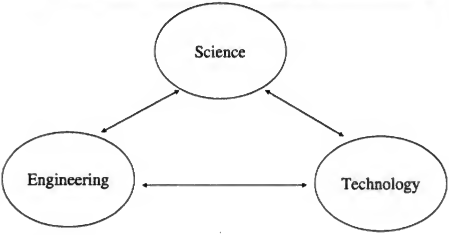

Future Trends

- MULTIPLE HAZARD SOL'NS
- TECHNOLOGY INNOVATIONS
  --information technology
  --new materials & new systems
  --wide use of sensors, actuactors, etc
  -- autoadaptive media
- TRADITIONAL & NONTRADITIONAL APPROACHES

SENSORS TECHNOLOGY RESEARCH

- Sensor technology transforms engineering from the old data-poor practice to the modern data-rich practice.
- Sensor technology closely interfaces a few most transcendental technologies which define our modern living society
- Significant industrial and commercial value.

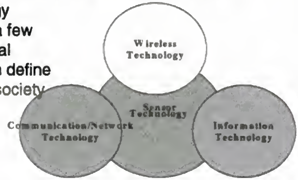

Sensors and Sensor Networks (NSF03-512, 04-522 & 05-526)

- **NSF wide initiative started in 2003.**
  --$45M
- **FY 2004**
  - **~$39M**
- **FY 2005**
  - **-$30M**

Self-Monitoring Structural Composite Materials with Integrated Sensing Networks

University of California, San Diego

Sia Nemat-Nasser, David Meyer, David R. Smith

Objective:

- Embed micro sensors and microcontrollers within fiber braids and weaves used in composite fabrication

- Form networks of interacting sensor nodes to enable structural health monitoring

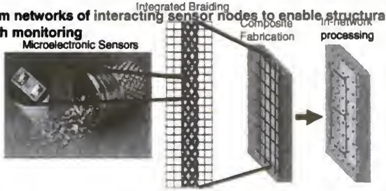

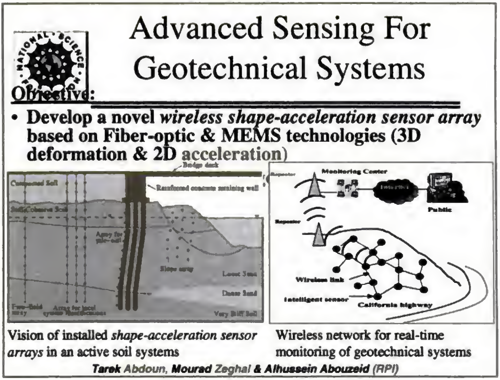

Advanced Sensing For Geotechnical Systems

Objective:

- **Develop a novel *wireless shape-acceleration sensor array* based on Fiber-optic & MEMS technologies (3D deformation & 2D acceleration)**

Bridge deck
Compacted Soil
Reinforced concrete retaining wall
Stiff Cohesive Soil
Array for pile-soil
Slope array
Loose Sand
Dense Sand
Free-field array
Array for local system identification
Very Stiff Soil
Monitoring Center
Repeater
Internet
Public
Repeater
Wireless link
Intelligent sensor
California highway

Vision of installed *shape-acceleration sensor arrays* in an active soil systems

Wireless network for real-time monitoring of geotechnical systems

Tarek Abdoun, Mourad Zeghal & Alhussein Abouzeid (RPI)

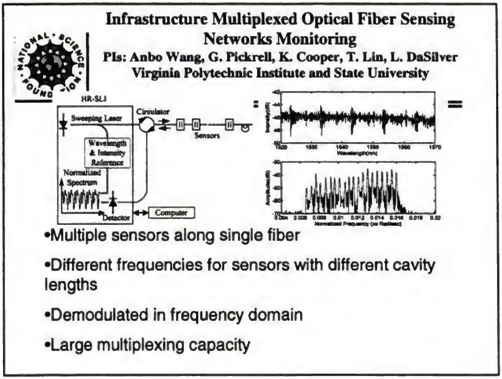

Infrastructure Multiplexed Optical Fiber Sensing Networks Monitoring

PIs: Anbo Wang, G. Pickrell, K. Cooper, T. Lin, L. DaSilver
Virginia Polytechnic Institute and State University

HR-SLI
Sweeping Laser
Circulator
Sensors
Wavelength & Intensity Reference
Normalized Spectrum
Detector
Computer
1520
1530
1540
1550
1560
1570
0.004
0.006
0.008
0.01
0.012
0.014
0.016
0.018
0.02

- Multiple sensors along single fiber
- Different frequencies for sensors with different cavity lengths
- Demodulated in frequency domain
- Large multiplexing capacity

Sensors for the Detection of Explosives

2007 BUDGET REQUEST

$20 million

[illegible], Purdue University School of Civil Engineering

Intellectually Challenging Research Areas

- Re-deployment of strong-motion networks with new wireless micro sensors
- New sensor & actuator technology & integration with structural systems for EQ safety & health monitoring
- Theories & modeling of structural damage
- High-tech warning, control and minimization of disastrous damages (tsunami, landslide, fire, etc.)
- Theories and models on site effects
- Theories and models for nonlinear dynamic response

Noticeable Events

- 2000 Millenniun Conference in Beijing
- International Conferences on Earthquake Engineering (Beijing, Harbin, Nanjing, and Taipei 2006)
- The 2008 World conference in Earthquake Engineering, Beijing
- Asian-Pacific Network of Centers of Earthquake Engineering Research (ANCER)

Useful Web Addresses

- National Science Foundation: www.nsf.gov
- Civil & Mechanical Systems: http://www.eng.nsf.gov/cms/
- Grant Proposal Guide: http://www.nsf.gov/pubsys/ods/getpub.cfm?nsf0423
- FY2004 Guide to Programs: http://www.nsf.gov/pubsys/ods/getpub.cfm?nsf04009
- Sensors and Sensor Networks (FY2004 version): http://www.nsf.gov/pubsys/ods/getpub.cfm?ods_key=nsf04522
- Mathematical Sciences: Innovations at the Interface with the Sciences and Engineering (FY2004 version): http://www.nsf.gov/pubsys/ods/getpub.cfm?ods_key=nsf04538
- Program Officers (Dynamic Systems, Modeling, Sensing and Control)
  - Dr. Shih-Chi Liu sliu@nsf.gov 703-292-7017

Crack Detection Methods Using Radio Frequency Identification and Electrically Conductive Materials

by

Koichi Morita[1] and Kazuya Noguchi[2]

ABSTRACT

In order to reduce life cycle costs of a building from construction to maintenance, it is very effective to monitor the structural health of a building. To generalize structural health monitoring of a building, establishment of a low-cost sensor system is desired. Radio Frequency IDentification (RFID) tag is a promising device for the management of a huge number of products at a very low cost. In this study, two types of electrically conductive materials are considered. In this system, an electrically conductive paint or printed sheet is applied to a part of structure in which crack will occur. Copper wire is connected to the attachment on the structure and a RFID tag. When a crack occurs, the paint or printed sheet is broken, resulting in an increase in resistance of the measured current. Crack width can be estimated by the ability of an RFID transmitter to communicate with the tag,, because electrical resistance value will vary with crack width. By bending tests of concrete specimens, the relationships between crack width and conductivity of the materials applied to the structure are examined. It is shown that the level of crack width which the specimen experienced can be related to the ability of the paint or printed sheet to conduct electricity or not.

KEYWORDS: Crack detection, Electrically Conductive Paint, Health Monitoring, RFID-tag,

1. INTRODUCTION

If we have to reduce life cycle costs of a building from construction to maintenance, it is very effective to monitor structural health of a building. Most buildings built during 1970's construction rush in Japan seem to rapidly deteriorate, and it is necessary to establish structural health estimation of these buildings. In 2002, performance certification mark system of existing housings is started in Japan, and structural performance will be displayed by visual inspection and structural design data, etc. However, in this performance evaluation, measurement such as acceleration is not carried out because of technical difficulties. The decisions from the inspection by experts according to manuals tend to be judged to safe side. It is important to carry out measurement to evaluate damages objectively and quantitatively.

Damage detection and health monitoring are classified into two methods. The first method is based on vibration measurement, and the other one is based on phenomena such as cracking or heat. Each method has its strong points and its weak points. A damage identification system based on vibration measurements is effective for damage detection of whole structures or the story of a structure but it is not effective for damage detection of a specific portion of a building such as its structural members. On the other hand, damage detection based on phenomena such as cracking or heat is effective for damage detection of a specific portion of a building such as its structural members. By combining these two methods, it becomes possible to monitor structural health precisely.

A damage identification system based on vibration measurements has a possibility to find out the process of damage, but in such system, maintenance of sensor and data acquisition system costs very much. In some cases, it is not economical to measure for all time. It is very difficult to install such data acquisition system to many buildings because of high costs.

On the other hand, the techniques which grasp the local damage by use off-line system[1], such as carbon fiber lattice sensor or maximum value memory sensor are much more economical than vibration measurement system. In this study, crack detection sensor using Radio Frequency IDentification (RFID) tag and electrically conductive paint and printed sheets is proposed because of its low costs and easiness of the measurement. The RFID tag is generally used for distinction or management of human or products. By using this RFID tag and transmitter, radio communication is possible. In this proposed system, crack width is estimated by the propriety of this radio communication. In this study, fundamental experiments for the relationship between crack width and the resistance of electrically conductive materials are carried out, and possibility of application of this technique is examined.

---

[1] Senior Researcher, Building Research Institute, Tsukuba-shi, Ibaraki-ken 305-0802, Japan

[2] Researcher, National Institute for Land and Infrastructure Management, Tsukuba-shi, Ibaraki-ken, 305-0802, Japan

2. OUTLINE OF SYSTEM

2.1 Radio Frequency Identification (RFID)

By the radio communication between RFID tag and transmitter with antenna and controller, the object can be recognized. Distance of this communication depends on the type of transmitter and tag. At the present time, there are RFID products whose communication distance is 2[cm] to 9[m]. It is possible to communicate with a myriad tag by one transmitter because of the mobility of the transmitter. The price of tag itself is much more economical than conventional sensors.

2.2 Crack Detection System

Sensing part of this system shown in Figure 1 is a circuit in which electrically conductive material connects with copper wire part of the RFID tag. This sensing part is glued to detection objective part, and communication is carried out between transmitter and RFID tag. If the electrically conductive material is disconnected and the communication between RFID and transmitter is not possible, we can know the level of crack at the point electrically conductive material is applied. That is, the crack width is estimated by the ability of the electrically conductive material to conduct electricity. An example of coin type RFID tag is shown in Figure 2.

2.3 Electrically Conductive Material

What is necessary for electrically conductive material applied to the detection part is shown below:

1)Electrically conductive material is disconnected at the crack width with the purpose.

2) It is comparatively easy to apply.

3) Material is economical.

In this study, two types of electrically conductive materials are tried. One is to apply paint directly which seem to be disconnected most easily, and the other is to glue a printed sheet which is suited to mass production. Both electrically conductive materials are very low cost, and the total installation cost with RFID-tag becomes very economical.

3. BENDING TESTS OF CONRETE SPECIMENS ON RELATIONSHIP OF CRACK WIDTH AND CONDUCTIVITY OF THE ELECTROCALLY CONDUCTIVE MATERIAL

3.1 Material Property and Bending Test

Outline of bending test is shown in Figures 3. Strength of concrete material used for bending test is designed as Fc=21N/mm2 and maximum size of coarse aggregate is 20mm. The dimension of the test specimen is 100mm×100mm×400mm. Fixed tensile force was given to the central part through PC reinforcement rod by a fixed torque. Electrically conductive paint and printed sheet are applied to the bottom of test specimen at midspan. Displacement transducers are respectively installed to both side of test specimen. Loading is carried out by use of 1000kN compression testing machine like Figure 4.

Measurements of load indicator and displacement transducers are carried out through static data acquisition system, and measurements of electrically conductive material resistance are carried out through a tester. Measurement data is acquired every 5kN loading before a crack occurs, and measurement data is acquired every 0.05mm of crack width after cracking. Unloading is started from when crack width exceeds 1.9mm, and measurement data is acquired every 5kN loading until loading returns to the zero.

As a result of cylinder test, concrete compression strength is 37.7N/mm2. Torque pressure is set at 19600Nmm, and axial force of PC reinforcement rod is estimated as 6530N. Bending crack moment Mcr is estimated as following[2];

$$M_{\sigma} = (\frac{5}{3} \times \sigma_t + N / A) \times Z$$

$$\approx (\frac{5}{3} \times \sigma_c / 10 + N / A) \times Z = 1156100\mathrm{N} \cdot \mathrm{mm}$$

where:

σ t = Concrete tensile strength
σ c = Concrete compression strength
N = Axial force of PC reinforcement rod
A = Cross section of specimen
Z = section modulus of specimen

Load F in which bending crack occurs is estimated as following;

$$F = 1156100/75 = 15400N = 15.4kN$$

3.2 Outline of Applied Electrically Conductive Material

In this study, two types of electrically conductive materials are tried as followings;

1) electrically conductive paint applied directly
2) printed sheet adhered with adhesive

In 1), coating material is one liquid acrylic paint (ShintronE-3801 made by SHINTO PAINT Co.) which includes carbon for filler, and 20mm length and 2mm width of paint is applied to specimen directly. Frequency which paint is applied is 1 time and the thickness of paint is about 30 μm as a result of measurements. In 2), the pattern of the electrically conductive printed coating (SS423 made by Nippon Achison) is printed like Figures 5 at a sheet (0.1mm thickness) of polycarbonate. The mesh wire diameter of printing is 35 μm, and thickness of the electrically conductive printed coating is adjusted about 5 μm.

Line widths on the printed sheet are 0.2mm, 0.3mm, 0.4mm and 0.6mm. Test specimen with this printed sheet and paint is shown in Figure 6.

3.3 Adhesive For the Printed sheet

In this crack detection test, printed sheet should break with crack occurring. The following three types of adhesives were examined for their adhesive properties in cracking.

1) two liquid epoxy adhesive
2) instantaneous adhesive for the concrete (CN-E made by Tokyo instrument)
3) instantaneous adhesive for strain gauge (CN made by Tokyo instrument)

In 1) and 2), there are some cases in which adhesive extends without transmitting the rupture. On the other hand, in 3), printed sheet tends to make a brittle fracture with crack occurring. From this fact, printed sheets are glued by instantaneous adhesive for strain gauge.

3.4 Results of Experiments

A crack in this test specimen and electrically conductive material after unloading is shown in Figure 7. In most cases, only one crack occurs like Figure 7 and electrically conductive material breaks by a crack. There are some cases in which two cracks occur. In the following results, only the case in which one crack occurs is shown. An example of the relationship between crack width and load is shown in Figures 8, and an example of relation between crack width and electrical resistance is shown in Figures 9. Crack width is gathered from mean value of installed two displacement transducers, because electrically conductive materials are located at center of test specimen. A crack occurs at about 15[kN] and unloading is started from about 1.9[mm] of crack width as shown in Figures 8. (In Figure 8, residual crack width is 0.37[mm].)

As shown in Figure 9, electrical resistance of electrically conductive material rapidly increases when crack width reaches to some value. The electrical circuit is considered to be broken when the resistance exceeds 10[MΩ]. Resistances over 20[MΩ] are all shown as 20[MΩ] in Figure 9 because of the range of the tester with 20[MΩ]. The resistance value remains over 20[MΩ], even after unloading once if resistance value exceeds 20[MΩ]. From this result, electrical conductivity is not regained after unloading and this sensor seems to have some memory function.

For eleven concrete specimens, static loadings are carried out and crack widths are examined when the electrical circuit is broken. Results of each electrically conductive material are shown in Table 1 and Figures 10. In Table 1 and Figures 10, 2mm shows the case in which electrically conductive paint are applied directly and others show the case in which printed sheets are glued. The 2mm cases in which conductive paint are directly applied to test specimens are most sensitive to cracks and break first from the results of Table 1. In the cases of printed sheets, wire breaking crack width tends to increase, as the line width is generally thicker, though there is variation in the data. The reason for the variation is that the glued condition is not uniform. Though it is difficult to estimate crack width correctly, it is possible to predict the crack width level considering this variation.

4. UTILIZATION OF THE CRACK DETECTION SENSOR

In this crack detection sensor, the crack width is estimated from the line width of electrically conductive material that breaks. From results of experiments, there is some variation at wire breaking crack width. It is necessary to allow some variation in estimation of crack width from these results. For example, by using three types of line width electrically conductive materials, 2mm, 0.2mm and 0.6mm , prediction of crack level is possible such as small, medium or large size crack. Three types of level can be predicted from three types of electrically conductive materials.

It is possible to use this crack detection sensor for the health monitoring of piles in which visual inspection is very difficult. In such cases, the sensor is beforehand installed around at pile top or points of stratum changing in which cracks are predicted to occur. By the propriety of the communication with the RFID tag, the crack width is estimated.

On disconnection of electrically conductive material, it is necessary to prevent disconnection by the factor other than crack. About the printed sheet, it is possible to apply the laminate technology for protection of printed circuit board which is installed in products like cars or housing electric appliances.

5. CONCLUSIONS

Health monitoring is important to attempt life-lengthen and life cycle cost reduction of building structures. For popularization of health monitoring, establishment of more economical sensor system is desired. In this study, crack detection sensor which consists of an RFID tag and electrically conductive materials are examined. Conclusions of this study are shown in the below:

1) By crack detection sensor which consists of an RFID tag and electrically conductive material, continuity of the electrically circuit can be known from the propriety of radio communication. Crack detection is possible from continuity condition.

2) By bending tests of concrete specimens, difference of wiring breaking crack width is examined by glue type or width of electrically conductive material. It is proven that estimation of crack width level in which test specimen has experienced is possible by property of radio communication.

3) Estimation of crack width by this technique is not so accurate, but it is proven that it is possible to estimate crack by allowing some variation.

Static loading experiments at the laboratory level are carried out in this paper. As future problem, following items are mentioned.

1) Examination of loading speed effect
2) Examination of sensors with protects
3) Application to actual structure.

6. REFERENCES

1. Wood, S.L. and Neikirk, D.P., "Development of a Passive Sensor to Detect Cracks in Welded Steel Construction," Proceedings, *U.S.-Japan Cooperative Research in Urban Earthquake Disaster Mitigation*, Third

Grantees Meeting, Seattle, Washington, August 2001
2. Architectural Institute of Japan.: AIJ Standards for Structural Calculation of Pre-stressed Concrete Structures 1998.

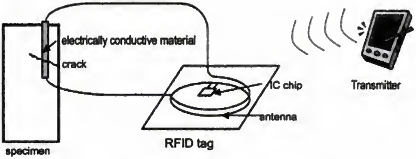

Figure 1 : Outline of crack detection system

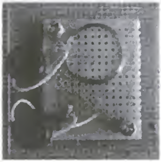

Figure 2 : An example of coin type RFID tag

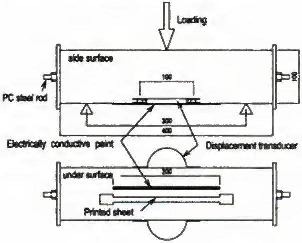

Figure 3 Outline of bending test

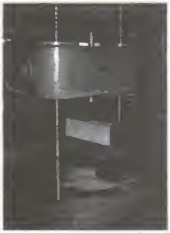

Figure 4 Specimen and testing machine

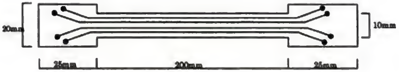

Figure 5 Print pattern .

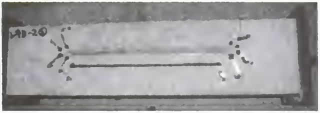

Figure 6 Specimen with printed sheet and paint

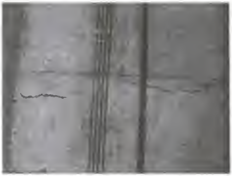

Figure 7 : Crack in this test specimen and electrically conductive materials after unloading

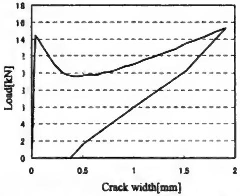

Figure 8 : An example of relationship between load and crack width

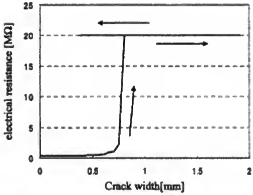

Figure 9 : An example of relationship between electrical resistance and crack width

Table 1 : Wire breaking crack width
(2mm : Paint are directly applied、0.2~0.6mm : Printed sheet are glued)

Case No.	2mm	0.2mm	0.3mm	0.4mm	0.6mm
1	0.14	0.65	1.2	0.88	1.1
2	0.35	0.45	0.95	0.85	1.02
3	0.50	0.65	0.9	0.85	0.95
4	0.30	0.30	0.8	0.45	0.71
5	0.32	0.90	0.70	1.8	1.46
6	0.24	0.93	0.93	0.98	1.1
7	0.33	0.33	0.72	1.13	1.41
8	0.38	0.86	1.51	1.71	1.48
9	0.22	0.67	0.39	0.32	0.68
10	0.45	0.45	0.71	0.71	0.85
11	0.52	1.08	1.08	1.08	1.22
average	0.341	0.661	0.899	0.978	1.089
Standard deviation	0.118	0.260	0.296	0.455	0.283

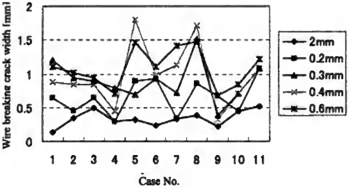

Figure 10 : Wire breaking crack width

Technical Session 3

WIND ENGINEERING

Design and Testing of Iowa State University's AABL Wind and Gust Tunnel

by

Partha P. Sarkar[1] and Fred L. Haan, Jr.[2]

ABSTRACT

A wind tunnel with advanced capabilities will aid research efforts to understand the complex fluid structure interaction problems encountered in wind engineering since wind tunnels remain an integral component of the design process for wind sensitive structures. Whether dealing with the aerodynamics of buildings, bridges or towers many issues remain to be fully resolved—including the role of non-stationary gust interactions, Reynolds number effects, and the significance of small-scale turbulence. Building the next generation of such wind tunnels will contribute to the understanding of these issues and create the research infrastructure necessary to meet the challenges of wind hazards in the USA and elsewhere.

A combination Aerodynamic/Atmospheric Boundary Layer (AABL) Wind and Gust Tunnel with a unique active gust generation capability has been developed for wind engineering and industrial aerodynamics applications. The AABL Wind and Gust Tunnel is primarily a closed-circuit tunnel that can be also operated in open-return mode. It is designed to accommodate two test sections (2.44m x 1.83m and 2.44m x 2.21m) with a maximum wind speed capability of 53 m/s. The gust generator is capable of producing non-stationary gust magnitudes around 27% of the mean flow speed. This paper describes the motivation for developing this advanced wind tunnel and the work related to its design and testing.

KEYWORDS: wind tunnel, active gust generation, non-stationary flow, wind engineering, industrial aerodynamics

1.0 INTRODUCTION

Building wind tunnels with advanced capabilities will aid research efforts to understand the complex fluid structure interaction problems encountered in wind engineering design. Computer simulations currently are inadequate for design of bluff bodies because of the complexity of the fluid dynamics involved. Wind tunnels remain an integral component of the design process for wind sensitive structures.

Boundary layer wind tunnels have played an integral role in the design of wind-sensitive structures for decades. Capable of simulating the lower portion of the earth's atmospheric boundary layer, these tunnels have enabled the safe design of long-span bridges, tall buildings, towers, and a host of other unique structures. With regard to the aerodynamics of these structures, many issues remain to be fully resolved—including the role of non-stationary gust interactions, Reynolds number effects, and the significance of small-scale turbulence. Research into these issues is currently limited by the capabilities of existing wind tunnels.

A combination Aerodynamic/Atmospheric Boundary Layer (AABL) Wind and Gust Tunnel with a unique active gust generation capability has been developed for *wind engineering* and

---

1 Professor and Wilson Chair, 2 Assistant Professor
Wind Simulation and Testing Laboratory, Department of Aerospace Engineering, Iowa State University, 2271 Howe Hall, Room 1200, Ames, IA 50011-2271 USA

industrial aerodynamics applications. The AABL Wind and Gust Tunnel is primarily a closed-circuit tunnel that can be also operated in open-return mode. It is designed to accommodate two test sections (2.44m x 1.83m and 2.44m x 2.21m) with a maximum wind speed capability of 53 m/s. The gust generator is capable of producing non-stationary gust magnitudes around 27% of the mean flow speed. This wind tunnel is one of the several wind tunnels that are housed in the Wind Simulation and Testing Laboratory (WiST Lab) in the Department of Aerospace Engineering at Iowa State University. This paper describes the motivation for developing this advanced wind tunnel and the work related to its design and testing.

The motivation for a tunnel with advanced gusting features arose from the primary assumption in the current practice of boundary layer wind tunnel testing—that atmospheric velocity variations can be adequately modeled by stationary mean and turbulent flow properties. Extreme wind loads, however, result primarily from extreme weather events (such as gust fronts, hurricanes, etc.) where non-stationary gusts, transitional flow structures and rapid wind directionality changes may play a significant role. The current state-of-the-art boundary layer wind tunnels are incapable of physically simulating the transient effects of such events. Building the next generation of such wind tunnels will contribute to the research infrastructure necessary to meet the challenges of wind hazards in this country. Better simulations of atmospheric flows will enhance our understanding of the various fluid structure interaction phenomena involved and greatly enhance our ability to develop mitigation measures.

Understanding how the construction of wind tunnels with advanced capabilities constitutes a worthy endeavor requires some background into the use of wind tunnels in wind engineering and into the technical problems faced by wind engineers. This section provides such background by providing a general introduction to atmospheric boundary layer (ABL) wind tunnels—the wind engineer's tool of choice for the past several decades.

2.0 BACKGROUND

2.1 Boundary-Layer Wind Tunnel

Wind tunnel simulation of the earth's atmospheric boundary layer is a well-established practice. Numerous researchers have contributed to the set of tools now in use for generating wind tunnel boundary layers that are several feet deep (for example, Cermak, 1971; Cook, 1973; Davenport, 1966; Farell and Iyengar, 1999). Conventional approaches employ a combination of passive devices such as spires, barrier walls, and floor roughness to generate boundary layers of the same scale as the geometric scaling of structural models placed in them. These models are then tested in a statistically stationary flow environment where the wind tunnel velocity profile, turbulence intensity profile, integral length scales and velocity spectra are matched to the scaled field values.

It is assumed that atmospheric velocity variations can be adequately modeled by stationary mean and turbulent flow properties. This assumption means that despite the fact that hurricanes and gust fronts can have non-stationary characteristics, wind sensitive structures are tested in stationary flow environments. Wind tunnel turbulence intensities are matched to site values, and wind tunnel integral scales are scaled with the geometric scale of the structural models. While this conventional approach has served (and still serves) research and industrial needs for some time, the following two sections summarize how new tunnel capabilities can answer questions that cannot be addressed with the current generation of wind tunnels.

2.2 Turbulence Effects

The role of turbulence in the relevant fluid-structure interaction problems will influence the wind tunnel design. While some of the characteristics of atmospheric turbulence have been simulated sufficiently well for some time (for example, boundary layer velocity profiles, scaling of turbulence integral scales with model dimensions, etc.) other turbulence characteristics cannot be simulated precisely at all or cannot be simulated without considerable effort. This section briefly describes the role that turbulence plays in wind engineering and how new capabilities in wind tunnels can improve our understanding of these complex fluid-structure interaction problems.

Civil engineering structures do not, in general, have aerodynamic performance as their primary design goal. As a result, most civil engineering structures can be classified as bluff rather than streamlined bodies. Bluff bodies experience flow separation over significant portions of their surface. Bluff body aerodynamics differs from aerodynamics of streamlined bodies in that flow separation and reattachment play primary roles in pressure distributions about bodies of interest.

Free stream turbulence can modify the behavior of shear layers separating from bluff bodies. These modifications lead to flow structure changes and pressure distribution changes.

The role of turbulence in the aerodynamics of bluff bodies has been extensively documented in the literature (e.g., Gartshore, 1973; Kareem & Cermak, 1979; Hillier & Cherry, 1981; Bearman & Morel, 1983; Nakamura & Ohya, 1984; Kiya & Sasaki, 1985; Saathoff & Melbourne, 1997; and others). What is clear is that turbulence scales influence aerodynamic properties (such as rms and peak pressure coefficients). What is not clear is the extent of these influences.

When considering the smallest scales of turbulent velocity fluctuations, the inertial subrange is a relevant concept. The "inertial subrange" of a turbulent flow refers to that range of turbulent eddy scales between the large inviscid energy-containing scales and the small viscous diffusion scales. The size of the small, energy dissipating scales decreases with increasing Reynolds number—which accompanies an increase in the size of the inertial subrange. The size of the inertial subrange is relevant to bluff body aerodynamics because the size of the subrange impacts the amount of turbulent energy residing at small scales. Small scale content—particularly scales on the order of the thickness of the separated shear layer—has been shown by a number of researchers to have a significant effect on separated shear layer flow structure (Gartshore, 1973; Tieleman & Akins, 1990).

A significant difference in small-scale turbulence content can exist between wind tunnel and full-scale flows because wind tunnel Reynolds numbers can be as much as three orders of magnitude lower than those of atmospheric flows. To quantify small-scale content, a "small-scale spectral density parameter" was originally suggested by Melbourne (1979) and subsequently used by Tieleman and Akins (1990). This parameter is essentially a *scale-specific* turbulence intensity. Tieleman and Akins reported that wind tunnel simulations with insufficient small scale content resulted in poorer comparisons of pressure coefficients between model and full-scale results.

The above may not fully address all issues relating to Reynolds number mismatches. Rather, it illustrates one of the ramifications of failing to match Reynolds numbers in wind tunnel simulations. Decreasing Reynolds number disparities between model and prototype flows will increase our confidence in test results. Understanding the physics of *how* flows depend on Reynolds number will decrease the uncertainty associated with imperfect turbulence simulation. Wind tunnels capable of higher Reynolds numbers would enable study of such questions.

2.3 Non-Stationary Flow Simulation

In addition to Reynolds number and small-scale turbulence issues, large-scale turbulent gusts also constitute an important aspect of wind tunnel simulation. Passive turbulence generation techniques (such as the obstacles described previously) have been shown to produce only a limited range of possible integral scales (Bienkiewicz et al., 1983). These scales are often not large enough to match prototype scales. As a result, active turbulence generation schemes have been developed to produce integral scales up to an order of magnitude larger than those of passive techniques. These techniques generally involve grids, flaps, airfoils (and combinations of them) that are forced to oscillate (Bienkiewicz et al., 1983; Kobayashi et al., 1994; Cermak et al., 1995).

While such devices are useful for generating stationary velocity fluctuations, they have not generally been used to simulate the non-stationary gusts that can occur in hurricanes and thunderstorms. Anemometry data from hurricanes has shown that velocity records are non-stationary at times (Schroeder & Smith, 1999). Thus far, however, no wind tunnel studies have investigated the impact of such non-stationarity on aerodynamic pressures on structures. While advanced analytical simulation methods for non-stationary wind fluctuations are being developed (Chen and Letchford, 2005; Wang and Kareem, 2005), little experimental work in this area has been attempted. The next generation of ABL wind tunnel should have the capability to conduct such tests.

In addition to simulating large-scale gusts, wind direction changes can be simulated with active turbulence generation equipment. Wind direction changes have been observed to significantly affect pressure distributions on building models in wind tunnels (Wu et al., 2001a; Wu et al., 2001b). Next generation ABL wind tunnels will also be used for furthering research of this type.

3. DESIGN OF THE WIND TUNNEL

This section describes the various components of the Aerodynamic/Atmospheric Boundary Layer (AABL) Wind and Gust Tunnel and discusses their performance. The conception and design of the wind tunnel began in August 2000 and was completed in February 2003. The construction of the wind tunnel began in November 2003 and was completed in October 2005. The design objectives were set on the basis of research needs and two main considerations which were minimizing the cost of construction and accommodating the wind tunnel within the available building space. It was desired to have two test sections, one for uniform flow with low turbulence and the other for atmospheric boundary layer flow with moderate to high turbulence, with a gust generation capability.

The design included non-stationary flow capability, a reasonably high-speed capacity and a large cross-section to accommodate realistic models. The wind tunnel was conceived as a closed-circuit type with the option of running it in an open-circuit mode. The dimensions were fixed as 2.44 m (8 ft) wide by 1.83 m (6 ft) high for the Aero (aerodynamic) test section followed by 2.44 m (8 ft) wide by 2.21 m (7.25 ft) high ABL test section to simulate atmospheric boundary layer wind. The maximum desirable speed in the Aero test section was 47.8 m/s (107 mph) and the maximum desirable speed in the ABL test section was 40 m/s (90 mph). High velocity capability combined with a relatively large test section would allow larger Reynolds numbers—with the accompanying increase in small-scale turbulent spectral content. A large working cross section would accommodate both large-scale models and large-scale velocity structures.

3.1 Component Description

Details of various components including the test sections, plenum, contraction, turning sections, heat exchanger, diffusers, and fan are given below and shown in Figure 1.

3.1.1 Fan and Motor

The fan is a Howden-Buffalo 108-50-710 model with 2.74m (9 ft or 108 in.) tip-to-tip blade diameter, 1.27m (4.2 ft or 50 in.) hub diameter with a specific flow rate of 214 m^3/s (452,000 cfm) generated at a static pressure of 870 Pa (3.5 in. water) and rotating speed of 710 rpm. The fan is driven by a 260 kW (350 hp) 3-phase, 460 volts AC motor.

3.1.2 By-Pass Duct

The By-Pass Duct is the most innovative portion of the AABL Wind and Gust Tunnel. In most wind tunnels, air speeds can be changed by increasing the speed of the fan, which causes a relatively slow change in test section velocities. However, the By-Pass Duct allows the wind and gust tunnel to change the test section velocity almost instantaneously - creating wind gust which more accurately represents the natural wind. This type of unsteady flow simulation is extremely important and opens up a new world of testing opportunities for research in unsteady-flow aerodynamics. This component is described in detail later.

3.1.3 Diffusers

There are three diffusers in this wind tunnel. These diffusers are located downstream of the test sections where maximum speed is generated. The function of a diffuser is to slow down the flow speed so that the pressure loss is minimized. The flow speed decreases as a result of gradual increase in the area of cross section of a diffuser along its length that is obtained by providing inclination angles to the side walls and/or the ceiling and floor. The first of the three diffusers is a two-dimensional plane-walled diffuser with constant width (area ratio is 1.10) and inclined ceiling that connects the ABL test section to the first corner, where its ceiling increases from 2.21m (7.25 ft) to 2.44m (8.00 ft) in 2.29 m (7.5 ft) length. The second diffuser is a three-dimensional plane-walled diffuser with area ratio of 3.5 and overall length of 19.1m (62.5 ft). It connects the 2.68m (8.80 ft) wide x 2.44m (8.02 ft) high rectangular end of the transition (first component) to a 5.03m (16.5 ft) wide x 4.1m (13.5 ft) high cross section before the heat exchanger and the third turn. The third diffuser is two-dimensional plane-walled diffuser with constant width and area ratio of 1.03. It connects 5.03m (16.5 ft) wide by 4.1 m (13.5 ft) high section at the exit of the third corner to 5.18m (17 ft) wide by 4.1m (13.5 ft) high section at the entry of the fourth corner over a length of 2.06m (6.75 ft). There is a constant section between the third diffuser and the fourth corner to accommodate a screen that will be used only if it is required. This section is 0.152m (0.5 ft) in length.

3.1.4 Heat Exchanger

The heat exchanger makes it possible to maintain a constant temperature inside the wind tunnel. Heat released by the fan and motor would cause the temperature inside a closed-circuit tunnel to continuously rise – leading to inaccuracies in experiments. The heat exchanger operates in a similar fashion as a radiator of a car, except that in this case the "radiator" is absorbing heat from the air instead of releasing it into the air, i.e. it functions as a heat sink. It is essentially made of a coil to which numerous fins are attached. Chilled water is run through the coil to remove the unwanted heat produced by the fan and motor. This heat exchanger requires 80 gpm (gallons per minute) of chilled water at 45°F to remove 9,200 BTU/min. of heat produced in the wind tunnel at 85% of the design flow capacity to maintain a constant temperature of 75 deg. F. Six coils were used with two side-by-side units of three coils stacked one above another in a staggered configuration to reduce blockage area.

3.1.5 Turning Vanes

Turning vanes help to change the direction of the air flow as it goes through a corner by directing it in the proper direction. There are 34 vanes (curved pieces of sheet metal) at each of the first two corners, as shown (Figure 1h), and 70 and 72 vanes, respectively, at the third and fourth corners. The benefits of using turning vanes include: retaining the velocity profile as the flow turns at the corner and minimizing the pressure loss at the corner.

3.1.6 Plenum

The plenum section (17 feet wide by 13.5 feet high) of the wind tunnel precedes the contraction, and its main purpose is to reduce the turbulence and increase the uniformity in the flow. This section consists of three screens (Mesh10 or M10) with spacing between the screens to reduce turbulence and a honeycomb that acts as a "flow straightener." The porosity or open area ratio of the screens is 64%. It is planned to add up to two additional screens, if necessary. The aluminum honeycomb (HEXCEL) has hexagonal cells, 12.7mm (0.5 inch) in cell size and 20.3cm (8 inches) in length.

3.1.7 Contraction

The contraction is that section of the wind tunnel in which the cross section is greatly reduced to speed up the flow and make the flow more uniform. The mass of air per unit time that flows through the large end of the contraction must exit out of the smaller end of the contraction (principle of conservation of mass). The only way this can happen is if the air speeds up as the cross sectional area is reduced. The result is that the air moving in the test section is moving much faster than the air in the sections before contraction. The contraction ratio (ratio of the inlet area to the exit area of the contraction) is 4.78 that means the flow speeds up from 10 m/s or 22.4 mph to 47.8 m/s or 107 mph before it exits the contraction at full speed. The length of the contraction, L_c, is 5.94m (19.5 ft). Two cubic shaped profiles with matching point at a distance of $0.45L_c$ from the inlet of the contraction were used for each of the four walls.

3.1.8 Test Sections

The AABL Wind and Gust Tunnel's test section is different from most wind tunnels because the section allows for two types of testing. The first portion of the test section, 2.44m (8 ft) wide by 1.83m (6 ft) high (*Aero* test section) that immediately follows the contraction is for testing aerodynamic models. Typical aerodynamic models would be airplanes, wings of airplanes, cars, etc., that often require minimum turbulence and high speed for testing. The second portion of the wind tunnel, 2.44m (8 ft) wide by 2.21m (7.25 ft) high (*ABL* test section), is devoted to atmospheric boundary layer simulation. Buildings, bridges, and other structures encounter a more turbulent flow than airplanes. It also requires the mean velocity to increase and turbulence levels to decrease with height. The ceiling of the test section is adjustable, to allow the boundary layer growth without accelerating the flow.

3.1.9 Closed and Open-Return Modes

Most wind tunnels are either Open Return – which means air is taken in at one end and expelled from the other - or Closed Return – which means the air circulates inside the wind tunnel in a loop. Both open- and closed- return tunnels have pros and cons and that is why the AABL Wind and Gust tunnel is designed to work both as an open- and a closed-return tunnel.

The facility's open-return mode is configured by eliminating the sets of turning vanes at the two successive corners that follow the test sections. Both sets of turning vanes have wheels at their base to allow them to be moved into the 4.9m (16 ft) duct that connects these corners. This duct is then isolated from the rest of the wind tunnel by two hinged doors, one at each corner. Each door forms part of one side of the corner section which becomes its perpendicular side once rotated, thereby opening the corner section to the outside and forming a U-shaped wind tunnel flow circuit.

3.2 Active Gust Generation using a By-Pass Duct Configuration

It has been stated previously that a number of different methods of turbulence generation have been implemented by other researchers. To create the flow features, as specified in the objectives of this work, conventional means like the oscillating vanes or airfoils used in the past by others would not be practical. Changing the mean flow speed using "lossy" devices such as vanes requires the fan to operate well off of optimal conditions and induces sudden changes in electrical power requirements. Flow speed changes could also be accomplished by changing the speed of the fan—but the inertia of the fan precludes speed changes on time scales required (25% test section speed change in 1-5 sec).

The basic design that was chosen to achieve the requirements was a bypass duct. The bypass duct (conceptually similar to the transition facility described in Saric, 1992) diverts flow from the main duct. This diversion reduces the flow velocity in the main test section. Computer-controlled dampers dictate the amount of flow diverted and the time scales involved. Several configurations of ducting were tested using small scale physical models. Hot wire probes were used to obtain velocity profiles to determine how uniformly air could be diverted from the main duct. The final concept can be seen in the wind tunnel layout diagram shown in Figures 1 and 2.

Several issues guided the design of the bypass duct. First, the amount of flow diverted through the duct had to result in a reasonable amount of velocity change in the main test section. Two rectangular ducts 4.12m (13.5 ft) high by 0.46m (1.5 ft) wide were designed for the bypass ducts. The size of these ducts was rather seriously constrained by the building geometry. They were designed to be as large as possible given the room size. These ducts run parallel to the main duct just outside the fan and represent a bypass area of 84% of the main test section's area. Second, the bypass duct and its accompanying transition sections must minimize the amount of flow non-uniformity introduced into the main duct of the wind tunnel. This issue had two major ramifications. Removing air from the stream downstream of the fan—and upstream of the test section—may introduce large non-uniformities in the mean flow profile at the test sections that would adversely affect testing. Also, reintroducing air just upstream of the fan could inject non-uniform profiles into the fan and subject the fan to damaging unsteady periodic loading.

To address these issues—and to accommodate the building geometry—the duct transition sections were designed to take air out of and put air into the main duct evenly around its entire perimeter. The two sections of the main duct on each side of the fan have circular cross sections, so this was accomplished using a 0.61m (2 ft.) wide slot along the circumference of each of these sections. Surrounding each slot is a large plenum that acts as a transition from the slot to the bypass ducts. The plenum allows the flow to reorganize from the slot to the bypass duct. These slots can be completely covered to allow the wind tunnel to operate like a regular wind tunnel—as if the bypass ducts do not exist. They are only open when the gusting capability is required.

Each bypass duct is designed with a set of electromechanically controlled dampers to open and close the duct. They consist of Ruskin heavy duty, opposed-blade airfoil dampers. Each duct has 20 blades in a 46 cm by 411 cm (18 in. by 162 in.) configuration. The dampers can be fully open, fully closed, or fixed partially open. The damper system also has a dynamic response capability for more complex gust simulations.

3.1.1 Gust Magnitude Predictions

To predict the performance of the bypass duct concept, a set of analytical tools was derived. A small scale prototype system to test the bypass duct concept was also designed and built. By validating the analytical predictions with the results of the prototype tests, reasonable performance estimates for the full scale system were obtained. This section briefly describes the analytical tools that were developed to test them.

To predict the magnitude of the gusts that could be generated with this system, estimates had to be made of the difference in wind tunnel *Aero* test section velocity, V_{WT}, when the bypass duct was open or closed. Wind tunnel velocities (again, in the *Aero* test section) for the bypass duct open and closed are denoted here as V_{WTopen} and $V_{WTclosed}$, respectively.

To estimate the test section velocity when the bypass duct is closed, one must estimate the pressure drop through the entire tunnel circuit and use the fan curve to estimate total flow rate. To estimate the pressure drop, loss coefficients were calculated for each element of the wind tunnel—diffusers, ducts, turns, screens, etc. These loss coefficients were summed into an overall loss coefficient for the wind tunnel. This loss coefficient was then related to the pressure drop through the tunnel as:

$$\Delta p_{WTclosed} = \frac{1}{2}\rho V_{WTclosed}^2 K_L^{WT_{closed}} \qquad (1)$$

where $\Delta p_{WTclosed}$ is the total pressure drop of the main circuit when the bypass ducts are closed and

$K_L^{WT_{closed}}$ is the loss coefficient (referenced to the *Aero* test section velocity) of the main circuit when the bypass duct is closed. One issue should be noted here. The loss coefficient, K_L^{WT}, will have three different values depending on the configuration of the wind tunnel for each mode of operation (closed or open return). When the exit and entry slots of the bypass duct are covered, you have one loss coefficient denoted $K_L^{WT_{clean}}$. The design velocity, design static pressures and loss coefficients (with respect to Aero test section), as estimated for each component of the wind tunnel with these slots closed, is given in Table 1 where $K_L^{WT_{clean}}$ was estimated as 0.64. When the slots are open, then the loss coefficients are denoted as $K_L^{WT_{open}}$ and $K_L^{WT_{closed}}$ corresponding to the bypass duct dampers being open and closed, respectively. Values for each coefficient are listed in Table 2 (all for the wind tunnel in closed-return mode). K_L^{BD} was estimated by modeling the bypass duct as a series of individual components such as dividing flows, area contractions, etc. The details of these calculations are beyond the scope of this paper (see Haan et al., 2006, for more details).

4.0 EXPERIMENTAL STUDY OF GENERAL PERFORMANCE

The AABL Wind and Gust Tunnel facility became operational in October of 2005. This section reports the results of testing the bypass-duct gust generator of this facility. These results include overall performance parameters, velocity profiles in the aerodynamic test section, time dependence of the gusts and static pressure distribution around the circuit. The atmospheric boundary layer mode and open-return mode of the tunnel were not tested for this project, and hence not reported here. Testing these modes is planned for the future.

4.1 Gust Generator Performance Parameters

Table 3 lists comparisons between predictions made for gust generator performance parameters and the values measured in the AABL Wind and Gust Tunnel. The changes being quantified are differences in test section velocity, fan pressure drop and fan motor power when one switches from having the bypass duct open to having it closed. The design estimates were made before the facility was built using the original fan curve provided by the vendor. Once the facility was complete, it was found from in situ measurements that the vendor-provided fan curve predicted performance somewhat below the as-built performance of the system. In situ testing found that the fan flow rate was approximately 20% greater than that predicted by the vendor's fan curve. A fan curve adjusted for this in situ performance was used to identify the measured value of K_L^{BD}. The measured velocity change in the test section was used to estimate K_L^{BD} as given in Table 2.

Overall, the design estimates compared very well with measurements. The increased gust magnitude is primarily due to the lower than expected bypass duct loss coefficient, K_L^{BD}. The small change in the pressure drop across the fan will minimize the unsteady loading on the fan and will minimize the pressure fluctuations due to the actuation of the dampers.

4.2 Test Section Velocity

The maximum velocity in the Aero test section was measured to be 53 m/s (188 mph). During the design process, the uniformity of the velocity profile in the test section was a priority. The goal was to produce a uniform flow both with and without gust generation. Mean velocity and turbulence intensity profiles were measured in the AABL tunnel.

Velocity profiles were measured using an A.A. Labs constant temperature anemometer and a straight, hot wire probe. Figure 4 shows the horizontal profile of mean velocity and turbulence intensity in the test section with the bypass ducts open and closed. The velocity across the test section is within 1.5% of the centerline velocity and the turbulence intensity is less then 0.15%. This same degree of uniformity and low turbulence is evident in the vertical velocity profiles (not shown). Clearly, the tunnel's flowconditioning devices (three screens and a honeycomb) is adequate to generate gusts while maintaining very uniform flow. The profiles show very little difference in turbulence intensity whether the bypass duct was open or closed. This shows that the bypass duct system is not generating unwanted turbulence in the test section.

4.3 Static Pressure Distribution

The design static pressures, as given in Table 1, are compared with those measured at each section of the wind tunnel (Figure 3). The comparison was found to be reasonable. The total wind tunnel loss coefficients compare very well between design and estimated values (Table 2).

4.4 Fan Section Velocity Profiles

The nature of non-uniformities ingested by the fan was quantified using an 18-hole pressure probe (a Dantec model PS18 Omniprobe) that could measure three components of velocity just upstream of the fan. Since the fan rotates through velocity asymmetries, it is subject to unsteady loading. The purpose of this test was to quantify any asymmetries induced by the bypass duct. The largest asymmetry going from a bypass open to closed configuration was approximately 17%. All other bypass-induced asymmetries were less than this—many were significantly less than this. It was assumed that if the flow asymmetries generated by the bypass duct were less than that generated by a typical ABL profile (30%-60%) then the bypass performance would be deemed acceptable. The level of inflow asymmetry of the system was therefore considered acceptable.

4.5 Time Dependence of Gusts

A hot wire anemometer was used to quantify the time scales of the gusts in the main test section. Figure 5 shows a velocity time series during a ramp up gust event. In this event the damper valves in the bypass duct go from fully open to fully closed causing an increase in the test section velocity of approximately 27%. The velocity magnitude reaches 97% of the increased steady-state (or gust) value in 2.2 seconds. In this case, the initial velocity was about 20 m/s and the final steady-state value was 25.4 m/s. This results in a velocity acceleration value of about 2.45 m/s^2. It was observed that this 2.2 second time interval decreases approximately linearly when the initial wind tunnel velocity is increased. Testing the gusts with initial wind tunnel velocities from 10 m/s to 25 m/s reduced the time interval for velocity change from 5.5 sec. to about 1 sec. The lower time interval will result in a velocity acceleration of 5.4 m/s^2. If the velocity is increased further it is possible to achieve the higher velocity acceleration limit of 10 m/s^2 that was set for the design.

5.0 SUMMARY

A unique wind tunnel with a active gust generation mechanism has been developed. The tunnel's performance has been at par with the design. The maximum test section velocity in the tunnel (53 m/s, 118 mph) will exceed the design estimate of 107 mph because the fan's performance was found to be slightly better than that initially specified by the vendor. The velocity in the Aero test section was found to be very uniform with turbulence less than 0.15%. A wide range of non-stationary flow structures can be simulated in the wind tunnel using a bypass duct with flow diverted through the use of computer-controlled vanes. The current design allows for gusts between 25% and 30% of the mean flow velocity with time and velocity acceleration scales comparable to a wide range of full scale thunderstorm and hurricane gust events.

6.0 ACKNOWLEDGMENTS

The authors are grateful for the support of the Department of Aerospace Engineering, T.A. Wilson and Grace Miller Endowment and the College of Engineering at Iowa State University. The support of the U.S. National Science Foundation (Grant # CMS-0201510) is also gratefully acknowledged. The authors would like to thank Professor Cesar Farell for his help designing the facility. In addition, the authors thank technician Bill Rickard and undergraduate students Joshua Clemens, John Stronck and Kevin

Houstman in the Aerospace Engineering department for their work on building and testing components of the system.

7.0 REFERENCES

Bearman, P.W., Morel, T. (1983), "Effect of free stream turbulence on the flow around bluff bodies," *Progress in Aerospace Sci.*, v. 20, 97-123.

Bienkiewicz, B., Cermak, J.E., Peterka, J.A., Scanlan, R.H. (1983), "Active Modeling of Large-Scale Turbulence." *Journal of Wind Engineering and Industrial Aerodynamics*, v. 13, 465-475.

Cermak, J.E. (1971), "Laboratory simulation of the atmospheric boundary layer," *AIAA Journal*, 9 (9), 1746-1754.

Cermak, J.E., Leighton, S.C., Leffler, R.D. (1995), "Wind-tunnel modeling of the atmospheric surface layer." *Journal of Wind Engineering and Industrial Aerodynamics*, v. 54/55, 505-513.

Chen, L., Letchford, C. (2005), "Simulation of Extreme Winds from Thunderstorm Downbursts," *Proc. 10th America's Conference on Wind Engineering*, Baton Rouge, Louisiana.

Cook, N.J. (1973), "On Simulating the Lower Third of the Urban Adiabatic Boundary Layer in a Wind Tunnel." *Atmospheric Environment*, v. 7, 691-705.

Davenport, A.G. (1966), "The treatment of wind loading on tall buildings," *Proc. Symposium On Tall Buildings*.

Farell, C., Iyengar, A.K.S. (1999), "Experiments on the wind tunnel simulation of atmospheric boundary layers," *Journal of Wind Engineering and Industrial Aerodynamics*, v. 79, 11-35.

Gartshore, I.S. (1973), "*The effects of free stream turbulence on the drag of rectangular two-dimensional prisms*," Boundary Layer Wind Tunnel Laboratory 4-73, University of Western Ontario.

Haan, Jr., F.L., P.P. Sarkar, N. Spencer-Berger, "Development of an Active Gust Generation Mechanism on a Wind Tunnel for Wind Engineering and Industrial Aerodynamics Applications," in review for publication in *Wind and Structures*.

Hillier, R., Cherry, R.J. (1981), "The effect of stream turbulence on separation bubbles," *Journal of Wind Engineering and Industrial Aerodynamics*, v. 8, 49-58.

Kareem, A., Cermak, J.E. (1979), "Wind-tunnel simulation of wind structure interactions," *ISA Transactions*, v. 18, n. 4, 23-41.

Kiya, M., Sasaki, K. (1985), "Structure of large-scale vortices and unsteady reverse flow in the reattaching zone of turbulent separation bubble," *Journal of Fluid Mechanics*, v. 154, 463-491.

Kobayashi, H., Hatanaka, A., Ueda, T. (1994), "Active simulation of time histories of strong wind gust in a wind tunnel." *Journal of Wind Engineering and Industrial Aerodynamics* v. 53, 315-330.

Melbourne, W.H. (1979), "Turbulence effects on maximum surface pressure – A mechanism and possibility of reduction," *Wind Engineering, Proc. of Fifth International Conference.* Pergamon Press.

Nakamura, Y., Ohya, Y. (1984), "The effects of turbulence on the mean flow past two-dimensional rectangular cylinders." *Journal of Fluid Mechanics*, v. 149, 255-273.

Saric, W.S. (1992), "The ASU Transition Research Facility," AIAA 17th Aerospace Ground Testing Conference, AIAA-92-3910.

Saathoff, P.J., Melbourne, W.H. (1997), "Effects of free-stream turbulence on surface pressure fluctuations in a separation bubble," *Journal of Fluid Mechanics*, v. 337, 1-24.

Saric, W.S. (1992), "The ASU Transition Research Facility," *AIAA 17th Aerospace*

Ground Testing Conference, AIAA-92-3910.

Schroeder, J.L., Smith, D.A. (1999), "Hurricane Bonnie wind flow characteristics as determined from WEMITE." *Wind Engineering into the 21st Century, Proc. of Tenth International Conference on Wind Engineering*, 329-335.

Tieleman, H.W., Akins, R.E. (1990), "Effects of incident turbulence on pressure distributions on rectangular prisms," *Journal of Wind Engineering and Industrial Aerodynamics*, v. 36, 579-588.

Wang, L., Kareem, A. (2005), "Modeling and Simulation of Transient Winds in Downbursts/Hurricanes," *Proc. 10th America's Conference on Wind Engineering*, Baton Rouge, Louisiana.

Wu, F., Sarkar, P.P., Mehta, K.C. (2001a), "Full-scale study of conical vortices and roof corner pressures," *Wind & Structures*, v. 4, n. 2,131-146.

Wu, F., Sarkar, P.P., Mehta, K.C., Zhao, Z. (2001b), "Influence of incident wind turbulence on pressure fluctuations near flat-roof corners," *Journal of Wind Engineering and Industrial Aerodynamics*, v. 89, 403-420.

Table 1. Design static pressure and estimated loss coefficients for tests in aerodynamic test section in closed-return mode of operation (with gust generator slots closed)

Exit Section of Components Listed	**Area m^2 (ft^2)**	**Length m (ft)**	**Local Design Velocity m/s**	**Design Static Pressure N/m^2**	**Estimated Loss Coefficient $K_L^{WTclean}$**
ABL Test Section	5.39 (58)	10.36 (34.00)	39.6	249.9	0.044
First Diffuser	5.95 (64)	2.29 (7.50)	35.9	342.6	0.055
First Corner	5.95 (64)	2.88 (9.45)	35.9	232.6	0.080
Duct between First and Second Corners	5.95 (64)	4.88 (16.00)	35.9	215.2	0.0126
Second Corner	5.95 (64)	2.88 (9.45)	35.9	105.2	0.080
First Transition	6.36 (68.4)	1.83 (6.00)	33.6	194.5	0.0053
First By-Pass Connector	6.36 (68.4)	1.52 (5.00)	33.6	189.0	0.0040
Fan/Motor/Nacelle	5.91 (63.6)	3.51 (11.50)	36.1	956.4	
Second By-Pass Connector	5.91 (63.6)	1.52 (5.00)	36.1	950.9	0.0040
Second Transition and Second Diffuser	20.7 (222.75)	19.1 (62.5)	10.3	1521.2	0.1080
Heat Exchanger	20.7 (222.75)	0.30 (1.0)	10.3	1431.8	0.0075
Third Corner	20.7 (222.75)	5.47 (17.95)	10.3	1421.5	0.0040
Third Diffuser and Duct	21.32 (229.5)	2.21 (7.25)	10.0	1419.6	0.00407
Fourth Corner	21.32 (229.5)	5.62 (18.45)	10.0	1410.0	0.0070
Plenum	21.32 (229.5)	2.90 (9.50)	10.0	1248.3	0.1176
Contraction	4.46 (48)	5.94 (19.50)	47.9	-87.1	0.0150
Aero Test Section	4.67 (50.3)	61.10 (20.00)	45.7	0.00	0.026
TOTAL		79.3 (260.1)			0.64

Table 2. Loss coefficients for wind tunnel main circuit (closed-return mode) and bypass duct circuit in different configurations.

	Description	**Design Estimate**	**Measured**
$K_L^{WT_{clean}}$	Slots covered	0.64	0.67
$K_L^{WT_{closed}}$	Slots uncovered, bypass duct closed	0.71	0.72
$K_L^{WT_{open}}$	Slots uncovered, bypass duct open	1.07	1.11
K_L^{BD}	Bypass duct loss coefficient	15.2	13.9

Table 3. Gust generator performance when conducting a change from a bypass-duct open condition to a bypass-duct closed condition.

	Velocity Change	**Fan Pressure Change**	**Fan Power Change**
Design Estimate	21%	4%	1%
Measured	27%	-2%	7%

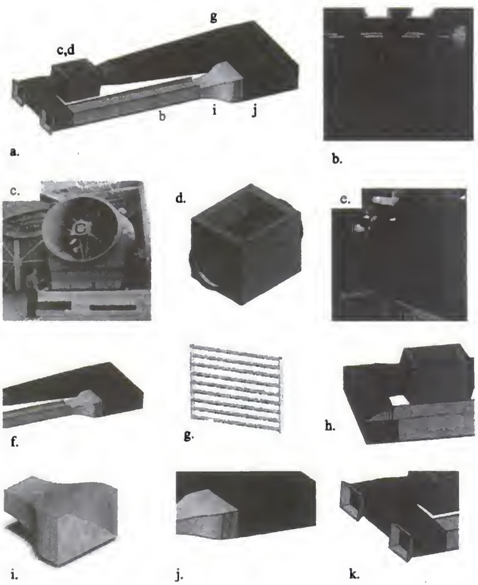

Figure 1. a. Layout of the AABL Wind and Gust Tunnel, b. Test sections as seen from downstream end, c. Fan section, d. By-pass gust generator-schematic, e. By-pass gust generator, f. Diffusers-schematic, g. Heat exchanger-schematic, h. Corner-schematic (first and second corners), i. Contraction-schematic, j. Plenum-schematic, k. Inlet and outlet for open–mode operation-schematic

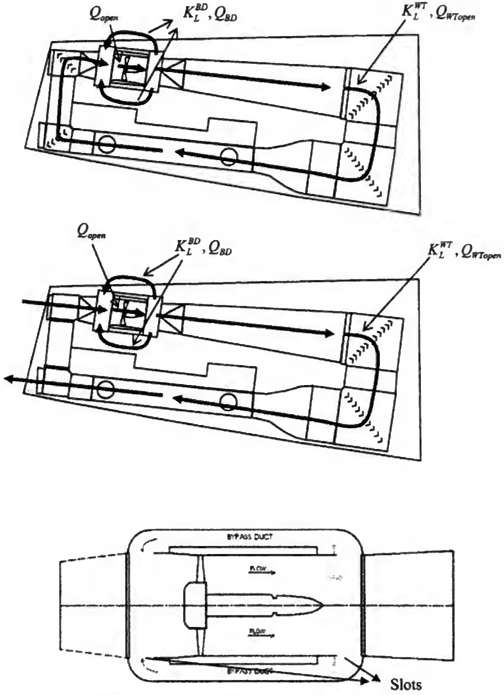

Figure 2. Diagrams showing the wind tunnel's main circuit and bypass duct in both closed and open circuit modes and the bypass duct surrounding the portion of the main duct containing the fan. The slots that allow flow through the bypass duct are covered when the gusting mode is not used.. K_L^{WT} and K_L^{BD} represent the loss coefficients through the wind tunnel test section and bypass duct circuits, respectively. Q_{BD}, Q_{WTopen} and Q_{open} are the flow rates through the bypass duct, the test section and the fan section, respectively.

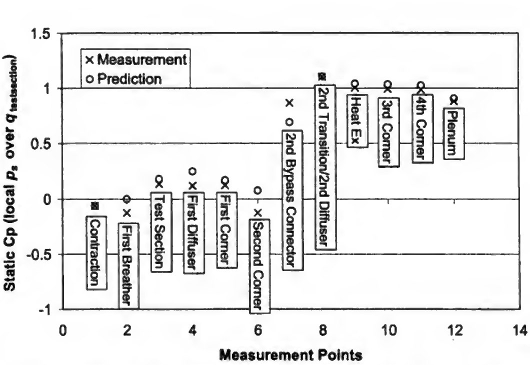

Figure 3. Comparison of static pressures at different sections of the ISU-AABL Wind and Gust Tunnel between design and measured values (closed-circuit mode, slots covered).

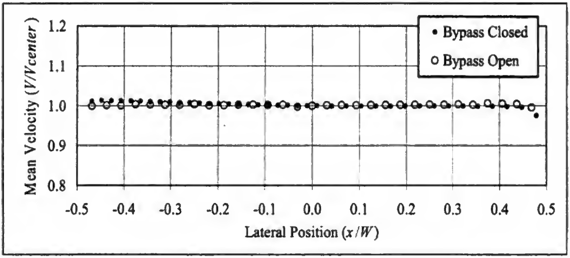

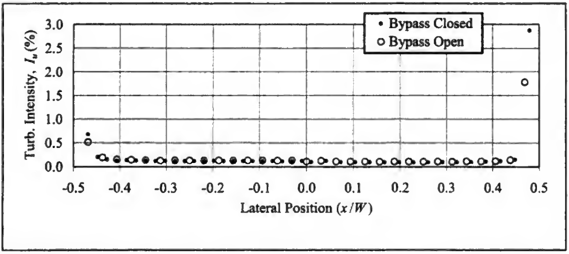

Figure 4. Horizontal profiles of mean test section velocity and turbulence intensity for bypass open and bypass closed cases.

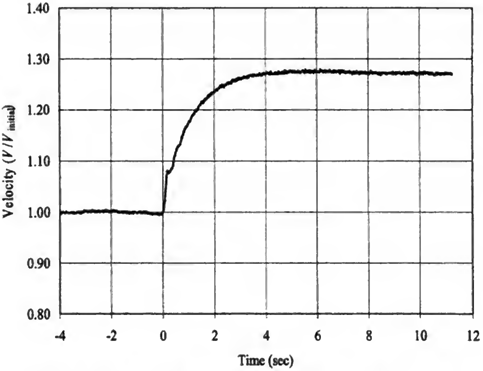

Figure 5. Time series of test section velocity during a ramp-up gusting event. 97% of the higher-speed velocity is attained within 2.2 seconds.

High Wind Damage to Buildings Caused by Typhoon in 2004

by

Yasuo Okuda[1], Yukio Tamura[2], Hiroaki Nishimura[3], Hitomitsu Kikitsu[1] and Hisashi Okada[1]

ABSTRACT

In 2004, Japan experienced noticeable damage by 10 typhoons, especially in western part. Severe damage to various buildings and structures occurred due to high wind during the passing of typhoons. The damage to roofing material or roof system of large-scale buildings was remarkable. Investigation on such damage in buildings is considered to be useful to prevent and to mitigate from similar damage.

KEYWORDS: Repeated Temperature Fluctuation, Roofing Material, Roof System, Typhoon

1. INTRODUCTION

In 2004, 29 typhoons were bone on the South Pacific Ocean and 10 typhoons struck Japan, which holds the annual record for the number of typhoons striking Japan. Fig.1 shows tracks of the typhoons in 2004.

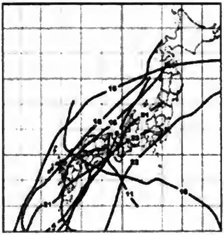

Fig.1 Tracks of Typhoons Striking Japan in 2004

In Japan, 214 people were killed and more than 2,000 people were injured by these typhoons. Houses more than 200,000 were collapsed or damaged by high wind and flooding. Serious financial losses exceeded $5 billion. Furthermore, lots of large-scale public or commercial buildings were damaged, which were remarkable for damage to roofing materials and system.

2. EXAMPLES OF HIGH WIND DAMAGE[1),2)]

2.1 Public Facility

Public facility named Yamaguchi Center for Arts and Media (YCAM) at Yamaguchi Prefecture in the southwestern part of Japan is a new building constructed in March, 2003. The main structure is steel frame with metal roof system which has a unique shape expressing three big waves. The roofing materials cover the roof with the length of 170m and the width of 30m. About half of the whole roofing materials were blown off due to high wind of Typhoon 0418 in September 7, 2004. Maximum 10 minutes mean wind speed of 24.4m/s and maximum instantaneous wind speed of 50.5m/s were observed at the local meteorological observatory. Fig.1 shows the failure observed in YCAM.

As a typical failure, lots of screws were observed to be pulled off from wood-wool cement board located on the edge of roof. On the other hand, screws attached to mortal slab at the center part of roof were tone. It is considered that the failure of roofing materials started from the edge of roof, and then they were subjected to increasing wind force and peeled from the roof one after another. A team of storm investigators concluded that the main cause of the failure is inadequate estimation of the design wind loads and the use of fasten materials whose strength is inadequate. The design wind load was evaluated using a wind force coefficient for a typical

---

[1] Department of Structural Engineer, Building Research Institute, Tsukuba-shi, Ibaraki-ken 305-0802 Japan

[2] Tokyo Polytechnic University

[3] General Building Research Corporation of Japan

semi-cylindrical roof such as sports gymnasiums. Furthermore, it is found that the wind force could be increased by backpressure of roofing materials through under machinery space.

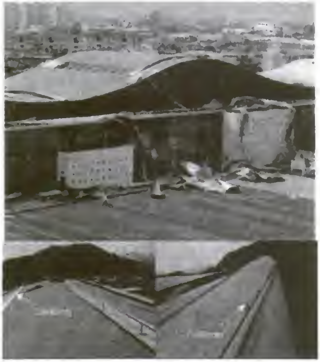

Fig.1 Failure of Roofing Materials of YCAM due to Typhoon 0418

Based on a number of tests to certify the strength of fastener as shown in Fig.2, it was found that the dispersion of the strength of fastener is larger than we expected. Some of them have the value less than the permitted strength of the fastener. It is also found, furthermore, that a remarkable strength reduction in the fastener may be appeared by the stretch of metal roof for daily heat fluctuation suffered by sunshine. Subsequently, the renovation of roof just after damage was assured to satisfy the wind design load considering a sufficient safety margin based on the research results including the wind tunnel experimental result.

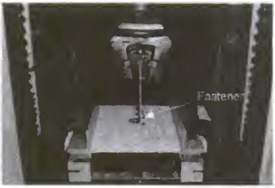

Fig.2 Tensile Test for the Fastener of YCAM

2.2 Large-scale Experimental Facility

The roof of a large-scale experimental facility named SPring-8 was damaged by two Typhoons 0416 (August 30, 2004) and 0418 (September 7, 2004). Fig.3 shows the damage of its roof. The plan of the building is donut-shaped. It is approximately 1,500m in circumference and 30m in width and was constructed in 1997. The roof system consists of two-layer folded steel plates and with thermal insulating materials between them, and the gorge and ridge lines of the folded plates are in the radial direction. The southern part of the roofing material was damaged over an area 270m long-by-10m wide by typhoon 0416, and the eastern part of the roofing material was damaged over an area 100m long-by-10m wide by typhoon 0418.

According to the precise post-disaster investigations, the main cause of the damage was attributed to the fatigue effect on the bolts connecting the roof system to the tight frames due to daily solar heating effects on the upper layer. Fig.4 shows the fracture surface of damaged bolt. Striations and dimples are both observed in the fracture surface of it. Striations are basically observed in fatigue fracture surfaces caused by repeated loads, and dimples are generally observed in the normal fracture surfaces caused by tensile loads. Dimples also took place on the center with striations on both sides.

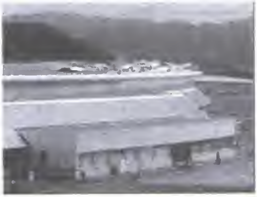

Fig.3 Failure of the roof of SPring 8

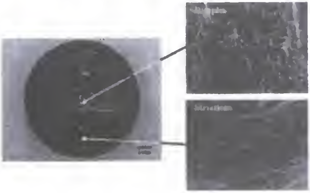

Fig.4 Fracture Surface of Damaged Bolt after Takeuchi, *et al.* 3)

2.3 Warehouse

A large-scale commercial warehouse at Kobe was damaged due to high wind by Typhoon 0423 in September 27, 2004. The size of this building is 70m in width, 40m in depth and 30m in height. The wall was caved in and the roof was severely damaged due to strong wind pressures as shown in Fig.5. Many stocked goods resulted in suffering heavy losses by water intrusion.

The wall made of ALC (Autoclaved Light-weight Concrete) board, which was supported by light steel frame, was connected to solid rack in the building. The buckling of the connecting steel pipe which seems to have insufficient strength caused this failure. The roof system of a double metal roof deck filled with insulation glass wool was adopted. On this roof system, remarkable differences in temperature arise between the upper and the lower deck by incident sunshine on the roof. The repeated occurrence of significant difference in stretch of decks affected by fluctuation of temperature may cause the metal fatigue in bolts fastened between the upper and the lower deck.

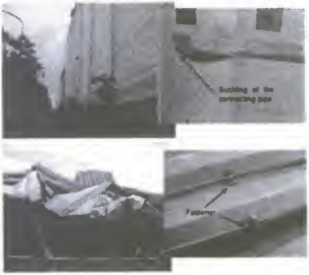

Fig.5 Failure of Large-scale Warehouse at Kobe

2.4 Public Gymnasium

Okawa Taiikukan is a public gymnasium with ridged roof covered by metal roofing material located at Shikoku in southwestern part of Japan. This building was damaged three times in a year by Typhoons 0406, 0410 and 0423. At first, a quarter of roofing materials were blown off during Typhoon 0406. Subsequently, a few and a half cladding got blown off when Typhoon 0410 and 0423 were passing, respectively. Observed wind speeds were relatively small, i.e. the maximum instantaneous speed of 28.4m/s in Typhoon 0406 and 26.9m/s in Typhoon 0423, respectively. Fig.6 shows the failure of the gymnasium by Typhoon 0423.

Metal roofing materials were fixed to ALC board by using an aluminum anchor that spreads itself two wards inside the ALC board to resist against pulling force. The roofing materials, however, were damaged when high wind attacked to the building. It was observed that lots of anchors were broken without pulled off from the board. It suggests that somewhat substantial trouble in anchors occurred, which may be affected by an influence of temperature fluctuation. As described above, the effect of temperature causes metal fatigue, since a stretch of roofing material raises shear stresses in the anchor. Considering that this type of public building is generally used as a public shelter for local people, it is important to meet wind resistant performance not only in the structural elements but also in claddings such as roof coverings.

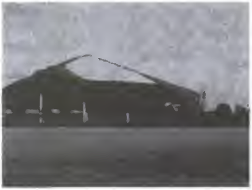

Fig.6 Failure of Public Gymnasium

2.5 Dome with Membrane Roof

Izumo Dome was constructed in 1992 at Shimane Prefecture in northwestern part of Japan. This building has a wooden-arch dome supported membrane structure of 148m in diameter at base and 48m in height. The membrane with the thickness of 0.8mm is made of glass fiber coated with Teflon, and the suspended cable with the diameter of 52mm is also finished with Teflon coating in order to reduce the friction to each other.

When the membranes were severely vibrated induced by high wind during Typhoon 0418, one of 36 sheets of membrane was suddenly punctured as shown in Fig.7. The maximum instantaneous wind speed was observed 38.8m/s at a nearby fire station. Since the punctured membrane was subjected to nearly normal to wind and the breakage started from a point under the cable near the top of the dome, it can be estimated that any flying debris did not attack the punctured area. Fragments of punctured membrane scattered outside and inside of the building and some parallel lines were observed on the surface of them. It implies that severe friction between the cable and the membrane apparently occurred.

In a long time, sand and dust ridden with wind had been stuck in a gap between the cable and the membrane. Those accumulations may act such as a sandpaper to tear the Teflon coating from the surface of the membrane when the building is vibrated by high wind. When high wind due to Typhoon 0418 hardly shook the building, significant reduction of the strength of the membrane might occur.

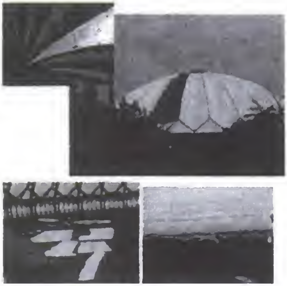

Fig.7 Punctured Membrane Roof of Izumo Dome

2.6 Inn

Typhoon 0406 struck Kinki area of Japan in June 21, 2004. A metal roofing covered on a motor inn at Shiga Prefecture was blown off from the building due to high wind and flew on to neighboring railway track of the Shinkansen super express as shown in Fig.8.

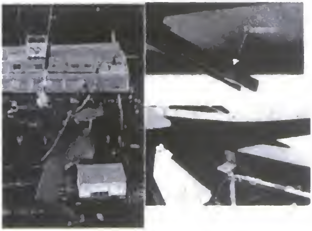

Fig.8 Blown Roofing Material from the Motor Inn

The size of the roofing material is 9 meter-by-41 meter and its weight is 7 ton. The Shinkansen service was suspended during 7 hours. The maximum 10 minutes mean wind speed of 16.0m/s and the maximum instantaneous speed of 36.4m/s were observed at the local meteorological observatory. The roof jumped upward and surprisingly passed over the signboard and the antenna on board apart and 10m in height 4m from the roof. Matsui *et al.*[4] carried out wind tunnel experiment to confirm the phenomenon as shown in Fig.9.

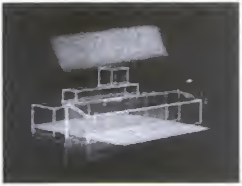

Fig.9 Experiment of Flying Roof Model by Matsui *et al*[4]

The blown roofing material was constructed on the original roof a few months before the damage in order to repair the rain leakage remaining the original one. The new roofing material was fixed to the original roof by using small fasteners and screws as shown in Fig.8. It was observed that the original roof was corroded and the number of fasteners was too small, and moreover a few screws did not reach to the beam in the existing roof system. Thus obviously, the strength of holding the roof was insufficient to resist wind pressure. The mean wind speed to start the flight of the roofing material is estimated to be 13.5m/s to 23.5m/s.

3. CONCLUSIONS

The investigation of wind damage to various buildings due to typhoons in 2004 indicates that actual wind speed on each site did not exceed the design wind speed based on the Building Standard Law of Japan. In many cases, the causes of the damage attribute to some reasons on buildings, e.g. the design of structure, the strength of materials, the consideration of effects on repeated temperature fluctuation on the roofing materials, and so on. Some of them are common problems to be solved for many other buildings.

4. REFERENCES

1. Nishimura H., Okuda Y. and Tamura Y., "High Wind Damage to Buildings in Japan by Typhoons in 2004", *Proceedings of the Sixth Asia-Pacific Conference on Wind Engineering*, pp. 2935-2944, 2005.
2. Tamura Y., Ohkuma K., Sakamoto I., Yagi K., Okuda Y., Ohno H., Kumagai N. and Shibata T., "Lessons from Wind-induced Damage to a Long-span Steel Roof due to Two Typhoons in 2004", *Proceedings of the Sixth Asia-Pacific Conference on Wind Engineering*, pp. 2907-2916, 2005.
3. Takeuchi E., Matsuoka S., Sumiyoshi E. and Yagi, K., "Investigation report on IS bolts caused damage to SPring-8 roof due to Typhoons No.16 and No.18 in 2004", Committee Report submitted at Committee on Typhoon Damage on SPring-8, 2004. (in Japanese)
4. Matsui M., Tamura Y and Cao S., "Wind tunnel experiments for a damaged flying

shed roof due to typhoon 0406 (DIANMU), JWA, Vol.30, No.2, pp.121-122, 2005.(in Japanese)

5. ACKNOWLEDGEMENTS

The authors express sincere gratitude to supporting members of the post disaster investigation. The authors also express gratitude to Mr. Kenji Ohkuma, Prof. Isao Sakamoto, Dr. Koichi Yagi, Mr. Hideo Ohno, Dr. Noritaka Kumagai and Mr. Tsutomu Shibata for their kind collaborations in post disaster investigations of SPring 8.

Table A.1 Lists of Typhoons Striking Japan in 2004

No (Name)	Date	Struck Site	Minimum Pressure [hPa]	Maximum Instantaneous Wind Speed [m/s] (Observed Site)
0404 (Conson)	June 11	Kochi	994	40.4 (Tanegashima)
0406 (Dianmu)	June 21	Kochi	965	57.1 (Muroto)
0410 (Namtheum)	August 1	Kochi	980	60.9 (Muroto)
0411 (Malou)	August 4	Tokushima	996	30.3 (Muroto)
0415 (Megi)	August 20	Aomori	980	48.7 (Izuhara)
0416 (Chaba)	August 30	Kagoshima	950	58.3 (Muroto)
0418 (Songda)	September 7	Nagasaki	945	60.2 (Hiroshima)
0421 (Meari)	September 29	Kagoshima	970	52.7 (Kagoshima)
0422 (Ma-on)	October 9	Shizuoka	950	67.6 (Ishirozaki)
0423 (Tokage)	October 20	Kochi	955	63.7 (Unzendake)

Meteorological Aspects of the Gulf of Mexico Hurricanes

by

John E. Gaynor[1]

ABSTRACT

The 2004 and 2005 Atlantic and Gulf of Mexico hurricane seasons were unprecedented in the length of the seasons, the number of named storms and landfalls, and the amount of damage.

A tropical storm becomes a hurricane when winds reach 74 mph (64 kt). There are on average six Atlantic hurricanes each year; over a three-year period, approximately five hurricanes strike the United States coastline from Texas to Maine. When hurricanes move onto land, the heavy rain, strong winds and heavy waves can damage buildings, trees and transportation systems.

According to FEMA, hurricanes account for seven of the top ten most costly disasters in U.S. history. The State of Florida was struck by four major hurricanes in 2004 with losses totaling $42B (Meade and Abbot, 2003). This was considerably more than the losses resulting from Hurricane Andrew in 1992, which had been the standard for single hurricane losses in the U.S. The 2005 season included 27 named storms and 15 hurricanes, 6 of which struck the U.S.[2] The losses due to Hurricanes Katrina, Rita and Wilma in 2005 are still being determined, but early estimates place losses from Hurricane Katrina upwards of $200B. This dwarfs the losses due to any disaster in the U.S. and approaches a significant percentage of the U.S. Gross Domestic Product.

Recent storms demonstrated how hurricanes can affect the entire U.S. and its economy, from energy, to raw materials, to food supplies. The impacts of hurricanes are the dependent on response immediately prior to storm landfall and on the years and decades of decisions and development preceding the storm impact. Better forecasts, better warnings and better preparedness plans in the days and hours before a storm makes landfall are needed, as are better development policies, long-term mitigation strategies and long-term assessments of risk and vulnerability.

KEYWORDS: hurricane winds, hurricane damage

1.0 INTRODUCTION

When hurricanes enter the Gulf of Mexico from the Atlantic Ocean or develop in situ in the Gulf, they have no where to go but make landfall, if not in the United States, then in Mexico, Central America, and/or the Caribbean Islands.

When the steering winds of these storms are light, there is very little skill in predicting their track. These slow moving storms are often the most destructive from wind damage and especially from flooding. For any hurricane in the Gulf, there is very little skill in predicting the intensity of the storm at landfall, its rate of weakening after landfall, or its potential for spawning tornadoes. Tornadoes in hurricanes or tropical storms after landfall tend to be of the weaker variety (F0 to F2), but they can locally significantly add to wind damage.

Added to wind and freshwater flooding damage is the storm surge and shallow water wave damage on the coast. The U.S. National Oceanic and Atmospheric

---

[1] Senior Meteorologist and Program Director, U.S. Weather Research Program, National Oceanic and Atmospheric Administration, Office of Weather and Air Quality, 1313 East West Highway, Silver Spring, Maryland, 20910

Administration (NOAA) runs an operational storm surge model (Sea, Lake, and Overland Surges from Hurricanes or SLOSH) (http://www.nhc.noaa.gov/HAW2/english/surge/slosh.shtml) (Jelesnianski, 1992) which provides a reasonable forecast for relatively simple coastlines, but does not do well in complex coastlines, such as with small bays and estuaries with complex bathymetry, and does not include the additional effects of fresh water flooding in estuaries nor the effects of shallow water waves. Currently, there is work being done to incorporate shallow wave into the next generation NOAA operational air-sea-land-coupled hurricane prediction model (hurricane weather and research forecast, or HWRF, model) (Surgi and Evans, 2003)

2.0 CONDITIONS LEADING TO THE ACTIVE 2005 GULF OF MEXICO HURRICANE SEASON

The seasonal conditions were primed for an active Gulf hurricane season (Fig. 1). The "loop current", a prevalent feature in the Gulf during the warm season, was considerably larger and warmer than normal. Also, a persistent tropical circulation was set up that helped steer the Atlantic hurricanes northwestward into the Gulf. The number of Atlantic hurricanes was above normal due to the unusually warm tropical Atlantic sea surface temperatures and weak wind shear at least partially due to a weak La Niño.

3.0 CURRENT U.S. HURRICANE WIND FORECASTING CAPABILITIES

Two years ago, the U.S. National Weather Service (NWS)/Tropical Prediction Center officially began extending its hurricane forecasts (more accurately described as "outlooks") to five days. The motivation to do so emerged from a requirement of the U.S. Navy who needed long lead times to move their ships in port out of harm's way. These longer lead times necessitated describing the uncertainty of hurricane track forecasts

3.1 Hurricane Track

A skillful forecast of hurricane track at landfall is essential. If the track forecast is not correct, the wind, rain, storm surge, and shallow wave forecasts will also not be correct. Through strategic U.S. investment in research on hurricane forecast model development through the U.S. Weather Research Program and through improvements in operational global model predictions of steering currents in the tropical Atlantic and Gulf of Mexico, significant improvements have been realized in hurricane track forecasts within the past decade (Fig. 2).

The global model (NWS Global Forecast System, or GFS) improvements in the tropics has mainly been realized by improved satellite measurements of moisture in the tropics, which has, in turn, greatly improved precipitation and wind forecasts. The NWS hurricane model, currently the Geophysical Fluid Dynamics Laboratory's (GFDL's) model, which is embedded in the GFS was updated to by compatible with the improved GFS dynamics.

As seen in Figure 3, coupling the hurricane model with an ocean wave model also improves the track. The fully coupled GFDL model will be run operationally in the 2006 hurricane season.

3.2 Hurricane Intensity

Of most direct importance to hurricane winds is improving the hurricane intensity forecasts at landfall. There is currently little skill for any lead time in predicting hurricane intensity. Coupling hurricane models with an ocean model (Falkovich and Ginis, 2005; Bender and Ginis, 2000), as has been done with the GFDL operational hurricane forecast model, has provided an improvement in skill (Fig. 4).

The fully coupled GFDL model, with a deep ocean wave model and an improved Gulf of Mexico loop current model, which will be operational in the 2006 hurricane season, holds promise of significant improvement in intensity forecast skill (Fig. 5). However, missing is knowledge of hurricane inner core processes and detailed knowledge of the small-scale interactions between a hurricane and its immediate environment which are also critical to changes in intensity.

4.0 CURRENT HURRICANE SURFACE WIND MEASUREMENT CAPABILITIES

The measurement of surface winds within a hurricane is extremely challenging, whether over land or over water.

Over water, the most accurate, but not necessarily the most reliable or representative winds are observed by anemometers on buoys. However, in high winds, these observations are plagued by the damping effects of breaking waves and sea spray, let alone the extreme oscillations of the buoy. In addition, due to their maintenance costs, ocean buoys in the Gulf that measure winds are quite sparse.

Also over water, GPS dropsondes from aircraft (Uhlhorn and Black, 2003) are now observing winds close to the ocean surface without the previous need to extrapolate winds to the surface. In addition, the airborne Stepped Frequency Microwave Radar (SFMR) has been used for many years, but recently is being used operationally. It remotely senses the ocean surface foam and can be calibrated for surface wind speed and direction and corrected for interference from rain (Uhlhorn and Black, 2003).

The GPS dropsondes and the SFMR have revealed that the surface winds over the ocean in strong hurricanes are higher than previously determined by models using estimated drag coefficients at high winds (French et al., 2006). The sea-surface drag coefficients appear to be nearly constant with wind speed rather than increase at high winds as older parameterizations have indicated. These new drag coefficients are now being used in the GFDL operational model and contribute to improved track and intensity forecasts (Moon et al., 2006).

Sea surface wind observations are derived from Quickscat (NASA) and Windsat (Navy) which are passive microwave sensors that are not affected by clouds, but do have some interference in heavy rain conditions. However, the spatial resolution of these observations is not particularly high – 12.5 km for Quickscat and about 60 km for Windsat. These instruments sense the capillary surface waves and the sea-surface foam to derive wind speeds and directions.

Along the coast and inland, the bulk of the surface wind observations come from Automated Surface Observing System (ASOS) operated at airports by the Federal Aviation Administration and the NOAA. In terms of the instrumentation itself, these are high quality measurements, but they are subject to power outages and lost data, which often happens in hurricanes and other severe storms. There also is a question about exposure. Some sites are subject to wind blockage in certain directions. The spatial coverage of these systems is rather sparse.

A new source of near surface wind measurements over land and to some distance over water are from Doppler radars. The largest source of such data are the WSR-88D (or NEXRAD) operational radars. Although the coverage is excellent, the spatial resolution is poor for structural engineering applications and, because the winds are usually derived from single Doppler velocity-azimuth data (VAD), except where radar ranges overlap, the observations only provide one wind dimension and can be many 10s of meters above the surface, increasing with distance from the radar. Although much more robust with respect to power sources than ASOS, they do lose power and, more importantly, can lose data communication at which point the data is usually not recoverable.

A more experimental, but potentially very rich data set comes from the mobile, deployable Doppler radars such as the SMART or Doppler on Wheels (DOW) radars (Biggerstaff et al., 2006; Knupp et al, 2005) and portable towers with *in situ* wind instruments (Masters et al., 2004; Masters et al., 2003; Howard et al., 2003). These systems have been deployed for the past several years by U.S. universities in collaboration with NOAA, along the Gulf and Atlantic Coasts at critical times and locations relative to forecasted hurricane landfalls. They are very robust with respect to winds measurements with their own power sources and designed for the very high surface winds expected at landfall in the more powerful hurricanes. The radars are KU band radars with less than one kilometer resolution. Figure 6 shows a Doppler display that clearly reveals small scale streaks representing the wind gusts. The disadvantages of these systems are that they are not operational and therefore are not continuously available, the systems are few in number, and their funding source is not secure.

5.0 SOME CURRENT HURRICANE WIND PRODUCTS

NOAA's Tropical Prediction Center/National Hurricane Center has offered the hurricane track "cone of uncertainty" (Fig. 7) operational products, introduced about three years ago, that provide probabilistic hurricane track information. Although these products do not directly forecast surface winds, they do indirectly provide information on the possible location and timing of hurricane force winds. These cones are derived from ensembles of hurricane models from operational centers and experimental models from U.S. universities.

Tested during the 2005 hurricane season and to become operational during the 2006 season are the surface wind probabilities, an example of which is shown in Figure 8. These contours are derived by using similar ensemble forecasts and provide 34 Kt (tropical storm wind), 50 Kt, and 64 Kt (hurricane force wind) thresholds. A corresponding text product provides information on the probable timing of these thresholds at selected coastal communities.

A wind product that has been used experimentally for several years is the NOAA-developed HWIND surface wind analysis that uses data buoys, dropwindsonde, SFMR, and Quikscat data over the ocean and ASOS, any available *in situ* wind data, and Doppler radar derived winds over land (Powell et al., 1996; Powell et al., 1998). An example of this product is shown in Figure 9. Among other users, it is used by insurance companies and FEMA for damage estimation.

6.0 FUTURE SURFACE WIND OBSERVING SYSTEMS IN HURRICANES

An effort is emerging in the U.S., led by NOAA and called the Integrated Surface Observing System (ISOS) initiative, to nationally integrate surface observing systems and provide data quality control. Although, if successful, this effort will provide more reliable and more easily available wind data, among other parameters, it will not necessarily provide higher time and spatially resolved wind observations, nor will the instrumentation be more resilient to the extreme conditions in hurricanes.

Although there is some delay, the SFMR will be installed on the Air Force C-130 reconnaissance aircraft to provide a much richer source of ocean surface wind measurements.

In the "hoped for" category, but not yet definitely planned due to the lack of a funding source, is the deployment of more buoys that will have sea surface wind and even wind profiles from wind profiling radars in the Gulf and off of the Gulf coast.

There are also discussions for the deployment of unmanned aerial systems (UAS) to provide more continuous monitoring of the development, track, and intensity changes in hurricanes while over the ocean and to provide a richer data set for assimilation into numerical models. Finally, using nanotechnology, a system of Global Environmental Micro Sensors (GEMS) is being developed. These would be very small Lagrangian balloons with micro sensors that could be deployed by the 100s into developing tropical system and follow it through all of its stages.

7.0 THE FUTURE OF OPERATIONAL HURRICANE MODELING

The National Weather Service's new Hurricane Weather Research and Forecasting (HWRF) community model will be operational for the first time during the 2007 hurricane season. It is essentially based on the GFDL hurricane model and, like the GFDL model, will be fully coupled to an ocean model and ocean wave model. It will initially have a four kilometer resolution and will be in a moving grid nested in the operational GFS model.

In the next few years, HWRF will be coupled with an improved land surface model that will include coastal wetlands and even ground water from previous flooding. In addition, coupling with a shallow wave model will also be added. Finally, if operational computer capabilities allow, the resolution of HWRF will be increased.

8.0 CONCLUDING REMARKS

When tropical depressions, tropical storms, or hurricanes form within or move into the Gulf of Mexico, forecasters become concerned. Very often, during hurricane season, the Gulf waters are warm with relatively deep warm mixed layers and the winds are light. These are the ingredients for the development of major hurricanes. Two ingredients that sometimes foil this development are entrainment of drier air into the storm or wind shear, often due to the weak southern edge of a mid-latitude trough. Since these subtle changes are very difficult for models to predict, it is a challenge to forecast both the direction of the track and the intensity changes. At the same time, forecasters know that a storm in the Gulf must make landfall somewhere in some form.

9.0 ACKNOWLEDGEMENTS

I would like to thank Drs. Mark Powell and Peter Black of the NOAA Hurricane Research Division, Mr. Kevin Kelleher of the NOAA Severe Storms Laboratory, Dr. Eric Blake of the NWS Tropical Prediction Center, and Dr. Naomi Surgi of the NWS National Centers for Environmental Prediction for their contributions to this paper. Part of the support for the hurricane research described in this paper has come from the U.S. Weather Research Program.

10.0 REFERENCES

Bender, M. A., Ginis, I., 2000: "Real-case simulations of hurricane-ocean interaction using a high-resolution coupled model: effects on hurricane intensity", *Mon. Wea Rev.*, 128, 917-946.

Biggerstaff, M., Wicker, L.J., Guynes, J., Ziegler, C., Straka, J.M., Rasmussen, E.N., Doggett IV, A., Carey, L.D., Schroeder, J.L., and Weiss, C., 2005: "The Shared Mobile Atmospheric Research and Teaching Radar: A collaboration to enhance research and teaching", *Bull. Amer. Meteor. Soc.*, **86**, 1263 - 1274.

Falkovich, A., Ginis, I., 2005: "Implementation of data assimilation and ocean initialization for the coupled GFDL/URI hurricane prediction system", *J. Atmos. and Ocean. Tech.*, 22, 1918–1932.

French, J.R., Drennan, W.M., Zhang, J., and Black, P.G., 2006: "Turbulent Fluxes in the Hurricane Boundary Layer, I. Momentum Flux", submitted to *J. of Atmos. Sci.*

Howard, R., Dodge, P., Doggett, A., Finney, J., K. Gurley, Levitan, M., Reinhold, M.T., Schroeder, J., and Stone, G., 2003: "The Landfall of Hurricane Dennis in Louisiana: A Summary of Cooperative Data Collection Efforts", 11th International Conference on Wind Engineering, Lubbock, TX, June 2-5, 2003.

Jelesnianski, C. P., Chen, J., and Shaffer, W.A., 1992: "SLOSH: Sea, Lake and Overland Surges from Hurricanes", NOAA Technical Report 48, National Oceanic and Atmospheric Administration, U.S. Department of Commerce, 71pp.

Knupp, K. R., Walters, J., and Biggerstaff, M., 2006: "Doppler profiler and radar observations of boundary layer variability during the landfall of Tropical Storm Gabrielle", *J. Atmos. Sci.*, 63, 234 - 251.

Masters, F., Aponte, L., Gurley, K. and Reinhold, T. "Gust factors observed in tropical cyclones Isabel, Dennis, Isidore Gabrielle and Irene during the 1999-2003 Atlantic hurricane seasons," 9th Annual ASCE Joint Specialty Conference on Probabilistic Mechanics and Structural Reliability, Albuquerque, New Mexico, July 26-28, 2004.

Masters, F, Gurley, K., and Reinhold, T. (2003). "Ground level wind characteristics of Isidore and Dennis", 11th International Conference on Wind Engineering, Lubbock, Texas, June 2-5, 2003.

Meade, C., and Abbot, M., "Assessing Federal Research and Development for Hazard Loss Reduction", RAND Report, 2003, 65pp.

Moon, I.-J., Ginis, I, and Hara, T., 2006: "Physics-based parameterization of air-sea momentum flux at high wind speed and its impact on hurricane intensity prediction", *Mon. Weather Rev.*, submitted.

Powell, M. D., Houston, S.H., Amat, L.R., and Morisseau-Leroy, N., 1998: "The HRD real-time hurricane wind analysis system", *J. Wind Engineer. and Indust. Aerodyn.*, 77&78, 53-64.

Powell, M. D., Houston, S.H., and Reinhold, T.A., 1996: "Hurricane Andrew's Landfall in South Florida. Part I: Standardizing measurements for documentation of surface wind fields", *Weather Forecast.*, 11, 304-328.

Surgi, N., and Evans, J., 2003: Hurricane Weather and Research Forecast (WRF) Model Workshop Report, Arlington, Virginia, 29-30 May 2002, available from http://www.mmm.ucar.edu/uswrp/, 31 pp.

Uhlhorn, E., and Black, P.G., 2003: "Verification of Remotely Sensed Sea Surface Winds in Hurricanes", *J. of Atmos. and Oceanic Tech.*, 20, 99-116.

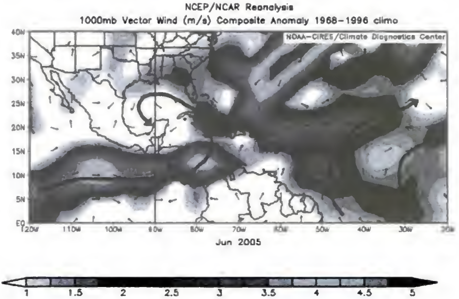

Figure 1: Favorable tropical steering currents for Gulf of Mexico hurricanes during the 2005 hurricane season.

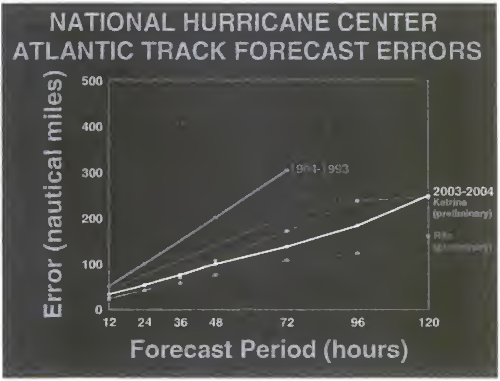

Figure 2: NOAA National Weather Service operational forecast skill of hurricane tracks

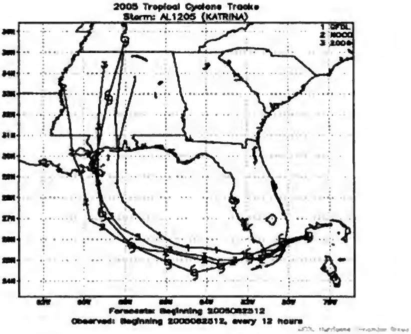
2005 Tropical Cyclone Tracks
Storm: AL1205 (KATRINA)
1 GFDL
2 NOCO
3 2006
Forecasts: Beginning 2005082512
Observed: Beginning 2005082512, every 12 hours

Figure 3: Forecasted tracks from Katrina: Actual track (black); GFDL hurricane model without ocean coupling (red); GFDL model with ocean coupling (green); GFDL model with ocean and wave coupling and other improved physics (blue).

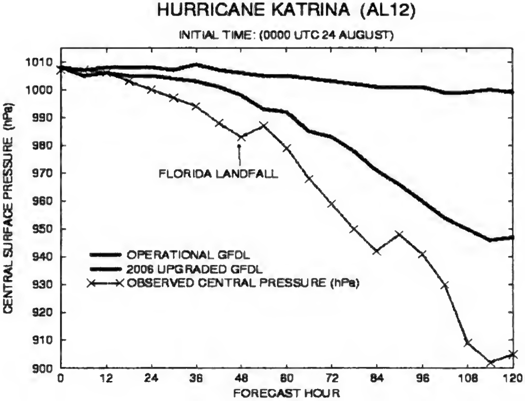

Figure 4: Improvement in hurricane intensity prediction with a fully ocean coupled hurricane model.

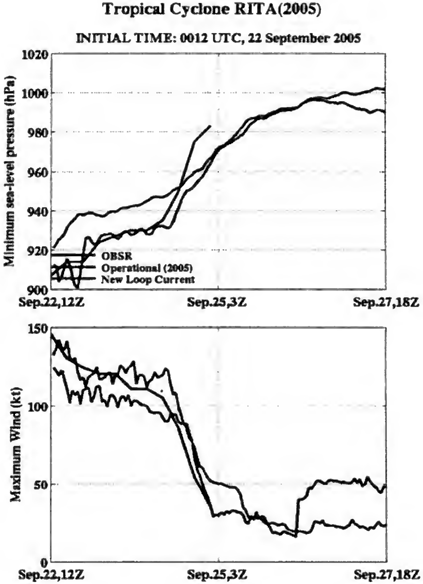

Figure 5: Improvement in hurricane intensity forecast with inclusion of more accurate depiction of the Gulf of Mexico loop current in an ocean coupled hurricane model.

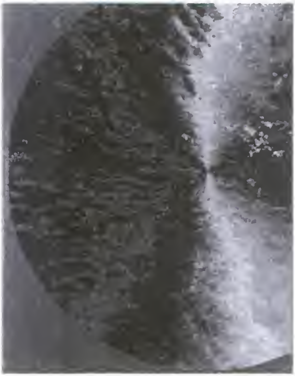

Figure 6: Doppler on Wheels (DOW) Doppler wind display during Hurricane Rita showing role vortices representing gustiness in the near surface winds.

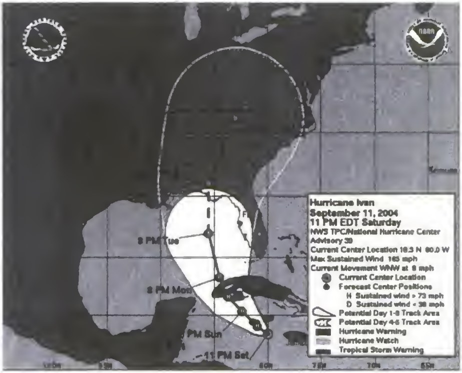
8 PM Tue
8 PM Mon
PM Sun
11 PM Sat
Hurricane Ivan
September 11, 2004
11 PM EDT Saturday
NWS TPC/National Hurricane Center
Advisory 39
Current Center Location 18.3 N 80.0 W
Max Sustained Wind 165 mph
Current Movement WNW at 8 mph
Current Center Location
Forecast Center Positions
H Sustained wind > 73 mph
D Sustained wind < 39 mph
Potential Day 1-3 Track Area
Potential Day 4-5 Track Area
Hurricane Warning
Hurricane Watch
Tropical Storm Warning
75w
70w
65w

Figure 7. Example of the U.S. National Weather Service, National Hurricane Center's "cone of uncertainty" hurricane product.

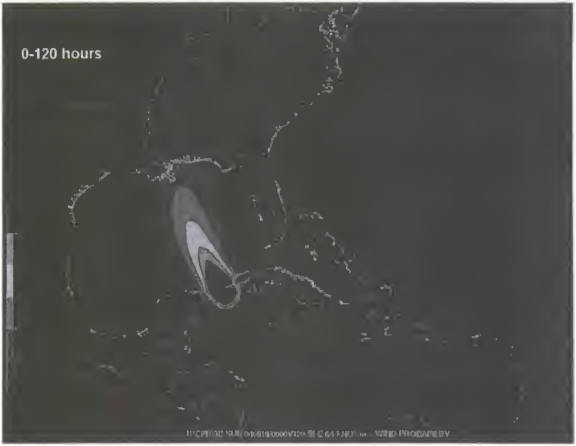

Figure 8. Example of the new U.S. National Weather Service, National Hurricane Center's 120-hr cumulative surface wind speed forecast probability product.

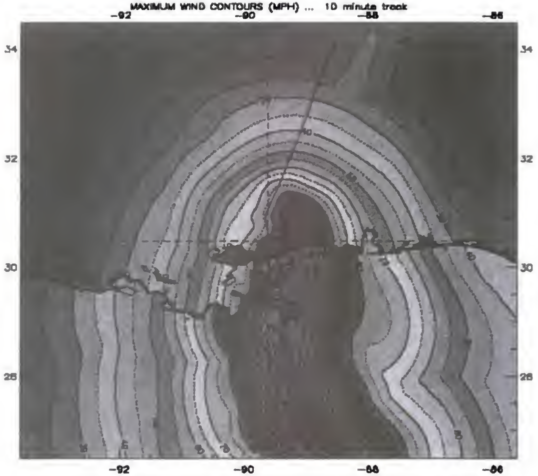

Figure 9. Example of HWIND surface wind swath from Hurricane Katrina. Contours are in miles per hour.

Technical Session 4

STORM SURGE AND TSUNAMIS

Application of Storm Surge and Tsunami Simulator in Oceans and Coastal Areas (STOC) to Tsunami Analysis

by

Takashi Tomita[1], Kazuhiko Honda[2] and Taro Kakinuma[3]

ABSTRACT

The numerical simulator named STOC (Storm surge and Tsunami simulator in Oceans and Coastal areas) has been developed to estimate the damages by tsunamis and storm surge. It includes non-hydrostatic and three-dimensional models of STOC-IC and STOC-VF to estimate the flow velocity and wave force of tsunamis. In this study, STOC was applied to tsunami analysis; especially, the sub-model of STOC-IC that adopted the vertically-integrated continuity equation to determine the free water surface was verified in comparison with the physical model experiments in which the tsunami reduction around an opening section of breakwaters, tsunami transformation on a slope and tsunami wave forces were investigated. The non-hydrostatic model, STOC-IC, was able to estimate the tsunami reduction by structures with the use of the suitable eddy viscosity model, and calculate tsunami wave pressure on a vertical wall in the fine computational grid whose size was a few meters in real scale.

KEYWORDS: Numerical Simulation, Three Dimensional Model, Tsunami, Tsunami Flow, Tsunami Wave Pressure

1. INTRODUCTION

The Indian Ocean Tsunami on 26 December 2004 caused severe damages in many coastal areas along the Indian Ocean. Tsunami fluid motion on land was complicated depending on local topography and existence of structures. The resultant tsunami action caused various types of damage. For example, in Banda Aceh, Northern Sumatra, Indonesia, almost houses within 2-3 km of a beach were broken by the tsunami more than 4m on the ground and a large vessel whose length and width were approximately 60m and 20m respectively was floated into the land as well as small fishery boats. On the other hand, field surveys on the tsunami damages showed that some structures such as breakwaters, coastal mounds, rigid houses etc. were effective in reduction of tsunami momentum behind them. As shown in Picture 1, a high mound, which was a road connecting to a bridge, reduced the destruction of the first floor of a shop against the 10 m tsunami. To understand and estimate these tsunami damages and to consider suitable measures for the reduction of damages, it is necessary to estimate fluid velocity and wave pressure of tsunami as well as inundation area and its water depth.

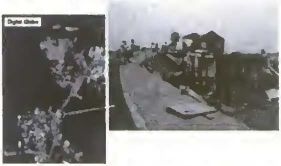

Picture 1 Reduction of tsunami damage by a road mound in Banda Aceh

In general, tsunamis can be estimated by horizontally two-dimensional numerical model with the use of the hydrostatic pressure assumption, because the tsunamis are extreme long waves. However, Fujima et al. [1] showed that the tsunamis had non-hydrostatic feature around an opening section of breakwaters in which a submerged breakwater was installed and non-hydrostatic numerical model calculated such a behavior accurately. Yoneyama et al. [2] also accomplished the calculation of 30 m-runup on a v-shaped valley in the 1993 Okushiri Tsunami Disaster with the use of their non-hydrostatic model. These results suggest that the tsunamis have non-hydrostatic features depending on complicated topography and the interaction with structures and therefore the non-hydrostatic models are capable of estimating them.

---

[1] Tsunami Research Director, Tsunami Research Center, Port and Airport Research Institute, Yokosuka, Kanagawa 239-0826 Japan

[2] Project Researcher, Tsunami Research Center,, ditto

[3] Special Researcher, Littoral Drift Division, Marine Environment and Engineering Department, ditto

In this study a numerical simulator, STOC (Storm surge and Tsunami simulator in Oceans and Coastal areas), which includes non-hydrostatic and three-dimensional fluid models, was applied to tsunami analysis and verified in comparison with some physical model experiments. Especially, the performance of a non-hydrostatic model named STOC-IC was examined.

2. NUMERICAL MODEL

2.1 Model Components

The numerical simulator, STOC, has been developed to estimate tsunami behavior including the interaction with structures such as coastal defense facilities and buildings. The simulator is a hybrid model consisting of three-dimensional and non-hydrostatic models of STOC-IC and STOC-VF and a multilevel model of STOC-ML. The discrepancy between STOC-IC and STOC-VF is in the calculation method of free water surfaces. Figure 1 shows an example of model arrangement of STOC.

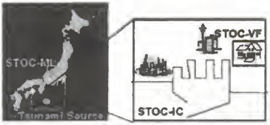

Fig. 1 Example of model arrangement of STOC

STOC-ML is the multi-level model to compute the tsunamis in a wide sea area in less computation time. In this model, the water area is vertically divided to some levels. The governing equations of the model are the continuity equation and Reynolds-averaged Navier-Stokes equations as the momentum equations, as described in Sec 2.2. Instead of calculation of the vertical momentum equation, the hydrostatic pressure is computed, since the assumption of hydrostatic is applied in each level.

STOC-IC is the non-hydrostatic pressure model in three-dimensions to estimate tsunamis in a wide area whose size is a coastal city where there are many structures and non-hydrostatic behavior of tsunami is induced by them. To reduce computational time and memory than another non-hydrostatic model of STOC-VF, STOC-IC uses the integrated continuity equation to analyze the position of free water surface and can be connected to STOC-ML. The governing equations are also the continuity equations and the Reynolds-averaged Navier-Stokes equations in three-dimensions.

STOC-VF is also the non-hydrostatic pressure model in three-dimensions. The difference of STOC-IC is in calculation of the position of the free water surface. STOC-VF adopts the method of volume of fluid (VOF) [3] to determine the free water surface in order to calculate tsunami overtopping and impulsive wave forces. It is, therefore, applied to analysis of .structural destruction by the tsunami and so on.

2.2 Governing Equations

Basic governing equations of all sub-models of STOC are the Reynolds-averaged Navier-Stokes equations and the continuity equation in three dimensions for incompressible fluids as follows:

- Reynolds averaged Navier-Stokes equations in x, y and z directions, respectively

$$\gamma_v \frac{\partial u}{\partial t} + \frac{\partial}{\partial x}(\gamma_x uu) + \frac{\partial}{\partial y}(\gamma_y vu) + \frac{\partial}{\partial z}(\gamma_z wu) - f_0 v$$

$$= -\gamma_v \frac{1}{\rho_0}\frac{\partial p}{\partial x} + \frac{\partial}{\partial x}\left(\gamma_x \nu_e 2\frac{\partial u}{\partial x}\right)$$

$$+ \frac{\partial}{\partial y}\left\{\gamma_y \nu_e \left(\frac{\partial u}{\partial y} + \frac{\partial v}{\partial x}\right)\right\} + \frac{\partial}{\partial z}\left\{\gamma_z \nu_e \left(\frac{\partial u}{\partial z} + \frac{\partial w}{\partial x}\right)\right\} \quad (1)$$

$$\gamma_v \frac{\partial v}{\partial t} + \frac{\partial}{\partial x}(\gamma_x uv) + \frac{\partial}{\partial y}(\gamma_y vv) + \frac{\partial}{\partial z}(\gamma_z wv) + f_0 u$$

$$= -\gamma_v \frac{1}{\rho_0}\frac{\partial p}{\partial y} + \frac{\partial}{\partial x}\left\{\gamma_x \nu_e\left(\frac{\partial v}{\partial x} + \frac{\partial u}{\partial y}\right)\right\} +$$

$$\frac{\partial}{\partial y}\left(\gamma_y \nu_e 2\frac{\partial v}{\partial y}\right) + \frac{\partial}{\partial z}\left\{\gamma_z \nu_e\left(\frac{\partial v}{\partial z} + \frac{\partial w}{\partial y}\right)\right\} \qquad (2)$$

$$\gamma_v \frac{\partial w}{\partial t} + \frac{\partial}{\partial x}(\gamma_x uw) + \frac{\partial}{\partial y}(\gamma_y vw) + \frac{\partial}{\partial z}(\gamma_z ww)$$

$$= -\gamma_v \frac{1}{\rho_0}\frac{\partial p}{\partial z} + \gamma_v \frac{\rho - \rho_0}{\rho_0} g +$$

$$\frac{\partial}{\partial x}\left\{\gamma_x \nu_e\left(\frac{\partial w}{\partial x} + \frac{\partial u}{\partial z}\right)\right\} + \frac{\partial}{\partial y}\left\{\gamma_y \nu_e\left(\frac{\partial w}{\partial y} + \frac{\partial v}{\partial z}\right)\right\}$$

$$+ \frac{\partial}{\partial z}\left(\gamma_z 2\frac{\partial w}{\partial z}\right) \qquad (3)$$

- Continuity equation

$$\frac{\partial}{\partial x}(\gamma_x u) + \frac{\partial}{\partial y}(\gamma_y v) + \frac{\partial}{\partial z}(\gamma_z w) = 0 \qquad (4)$$

in which (x, y, z) are the Cartesian coordinates, (u, v, w) the velocity in the directions of x, y and z, ρ the fluid density, ρ_0 a reference density, p the pressure, g the gravitational acceleration, ν_e the eddy viscosity, and f_0 the Coriolis coefficient. The porosity ε and transmissivity γ_x, γ_y and γ_z in each direction of x, y and z introduced by Sakakiyama and Kajima [4] are imposed to express configurations of the sea bottom and structure faces smoothly.

In STOC-IC and STOC-ML, the free water surface is determined by the vertically integrated continuity equation:

$$\gamma_v \frac{\partial \eta}{\partial t} + \frac{\partial}{\partial x}\int_{-h}^{\eta} \gamma_x u dz + \frac{\partial}{\partial y}\int_{-h}^{\eta} \gamma_y v dz = 0 \qquad (5)$$

in which η is the free water surface elevation, and h the still water depth.

In STOC-VF, the free water surface is analyzed by the calculation of the function of volume of fluid on the water free surface.

2.3 Numerical Scheme

The governing equations are solved by the finite difference method in which a staggered mesh in space and leapfrog method in time are used. The diffusion terms are discretized with the second-order central scheme, while the advection terms are expanded with a hybrid scheme where the first-order upwind scheme is combined with the second-order central scheme for stability.

To calculate of pressure in STOC-IC and STOC-VF, the method of SMAC (Simplified Marker And Cell) [5] is applied

Connection between STOC-IC and STOC-ML is made in overlapping zones in which the physical quantities such as the water surface displacement, velocities, pressure etc. in each computational area of STOC-IC and STOC-ML are adjusted using the interpolation technique.

3. APPLICATION TO TSUNAMIS IN PHYSICAL MODEL EXPERIMENTS

3.1 Tsunami around an Opening Section of Breakwaters

The model validation of STOC was investigated in comparison with the results of physical model experiments by Tanimoto et al. [6], in which the water surface elevations of the tsunamis were measured around an opening section of breakwaters with a submerged breakwater as shown in Fig. 2.

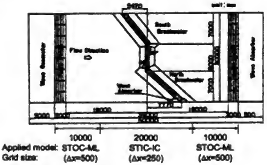

Fig. 2 Experimental basin with breakwaters

In the computations, STOC was applied in the range of 10 m in front and back of the submerged breakwater in which the size of computational grid was 0.25 m. In both sides of it STOC-ML was applied and the grid size was 0.50 m. The grid size of the transverse direction was 0.25 m in all of the computational area. The vertical grid sizes were varied so as to be fine grid near the free water surface. The tsunami in the computation was reproduced as a uniform flow whose speed was 1.00 m/s, because in the experimental cases the tsunamis were produced by uniform flows of 0.98 m/s and 1.05 m/s.

The comparison of the tsunami water surface variation in space is shown in Figure 3. In the figure, Cal. (-2, -4), for example, indicates the numerical result using the horizontal and vertical eddy viscosity coefficients of 10^{-2}m^2/s and 10^{-4}m^2/s, respectively, and Cal. (SGS) shows the numerical result with the eddy viscosity like the subgrid scale (SGS) model of in large eddy simulation (LES) as shown by (6) in the same way as Fujima et al. [1] following Nakatsuji et al. [7].

$$\nu_e = (C_s\Delta)^2\sqrt{\left(\frac{\partial u_i}{\partial x_j}+\frac{\partial u_j}{\partial x_i}\right)\left(\frac{\partial u_i}{\partial x_j}+\frac{\partial u_j}{\partial x_i}\right)} \qquad (6)$$

in which $\Delta = (\Delta x\times\Delta y\times\Delta z)^{1/3}$ and $C_s = 0.2$ that is the ordinal value for the SGS model.

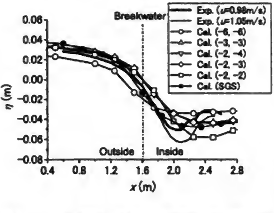

Fig. 3 Free water surface around the opening section of breakwaters

The use of eddy viscosity coefficient like SGS-type depending on spatial variation of flow provided good results in the numerical simulation by STOC-IC. However, it was necessary to investigation on the turbulent model more since the combination of STOC-IC and SGS-type eddy viscosity could not express the recovery of water surface elevation behind the breakwaters well.

3.2 Tsunami transformation on slope

Since Tsuruya and Nakano (Tanimoto et al. [8]) investigated tsunami transformation on a uniform slope (Fig. 4) experimentally, the computation results by STOC-IC were compared with their experimental results in Fig. 5. Corresponding to the experimental condition, the slope angle was 1/200 and the tsunami wave period was 40 s, and wave steepness was approximately 1.9 × 10^{-4} at Point H whose water depth was 1.0 m. In the computation, the dimensionless grid sizes $\Delta x/L$ and $\Delta z/H$ were 4 $\times 10^{-3}$ and 0.5, respectively, in which L was the wavelength at 1.0 m depth and H the incident wave height of 0.02 m based on the wave steepness in the experiment.

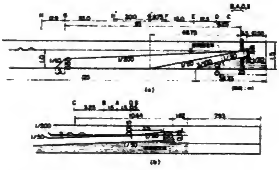

Fig. 4 Tsuruya and Nakano's experiment set up

The computed tsunami forms as a whole were quantitatively comparable with the experimental forms. However, considerably high tsunami was calculated at Point C when the second incident tsunami wave encountered with the reflected wave of the first tsunami. This discrepancy indicates that there are some improvements on the numerical scheme to calculate the free water surface when the incident and reflected waves meet each other.

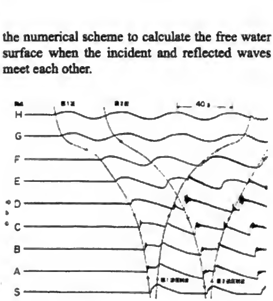

(a) Experimental result

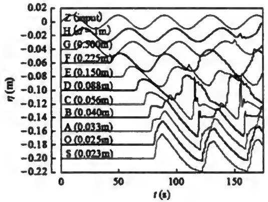

(b) Numerical result

Fig. 5 Tsunami transformation on slope

3.3 Tsunami Wave Pressure

Computed tsunami wave pressures acting on a seawall were compared to experimental results by Tanimoto et al. [8] in which the wave pressures due to the main body of tsunamis shown as P_s in Fig. 6 acting on a vertical wall on uniform slopes were analyzed.

In the time variations of the experimental tsunami wave pressures in Fig. 6, the tsunami wave pressure were categorized into three types: impulsive wave pressure, P_i, solitaly wave pressure, P_p, and wave pressure of tsunami main body, P_s. The wave pressure, P_s, is significant to investigate the stability of mass structures against tsunamis.

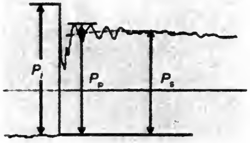

Fig. 6 Analyzed tsunami wave pressure P_s

In the computations, the tsunami wave pressure was calculated by STOC-IC, and the model topography as shown in Fig. 7 was adopted from the experimental cases.

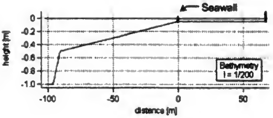

Fig. 7 Model topography to calculate tsunami wave pressure on seawall

In the computations, the computational grid sizes around the seawall were 0.01 m in the tsunami propagation direction, 0.5 m in the transverse direction, and 0.01 m in vertical direction. The time marching step was 0.002 s. If the model scale is 1/200, the grid size is 2.0 m in front of the seawall and the time step is 0.028 s.

Figure 8 shows the vertical distribution of the tsunami wave pressure, P_s, by the experimental and numerical simulations. The data was the maximum value in each experimental and numerical run, and then did not always appear each other in the same time. The computed tsunami wave pressures were in good agreement with the experimental pressures. Moreover, the computed tsunami wave pressures were also well comparable with other experimental pressures by Ikeno et al. [9]. Therefore, it confirmed that the non-hydrostatic model of STOC-IC had performance to estimate the sustainable tsunami pressure following the impulse pressure, which might be predominant force for movement of massive structures like a breakwater.

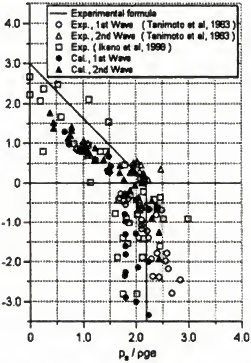

Fig. 8 Experimental and numerical tsunami wave pressures acting on a vertical wall

4. CONCLUSIONS

The main conclusions in this study are as follows:

1) The numerical tsunami simulator, STOC, was developed to estimate hydraulics and hydrodynamics of tsunami. Especially non-hydrostatic model of STOC-IC showed good performance in comparison with the hydraulic experiments.
2) The non-hydrostatic model was capable of estimating the reduction of tsunami by structures using the suitable eddy viscosity model.

In the study proceeding at present, we are going to apply the numerical simulator of STOC to real topography in order to understand what happen there by the tsunami striking under the interaction with structures and to develop "Tsunami Dynamic Hazard Map" which gives tsunami features including tsunami hydrodynamics as well as hydraulics visually to the citizens, policy makers etc. Figure 8 is an example of the numerical output which shows the tsunami flooding in an imaginary coastal city under the interaction with structures. This may be one of tsunami dynamic hazard map.

Moreover, we must modify the numerical scheme to calculate the water surface when the incident tsunami wave encounters the reflected wave of the previous tsunami wave. Considering the tsunami form in front of the seawall, the tsunami wave pressure on the seawall is also verified in point of variation in time.

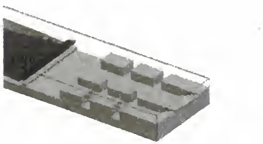

Fig. 9 Example of demonstration of tsunami flooding in a coastal city

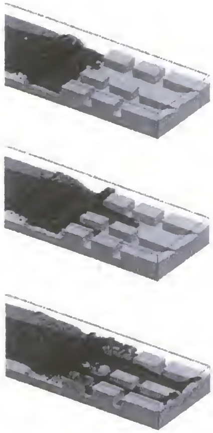

Fig. 9 (cont.) Example of demonstration of tsunami flooding in a coastal city

5. REFERENCES

1. Fujima, K. et al.: Development of the 2d/3d Hybrid Model for Tsunami Numerical Simulation, *Coastal Eng. Jour.*, 44(4), 373-397, 2002.
2. Yoneyama N., M. Matsuyama and H. Tanaka: Numerical analysis for Locally High runup of 1993 Hokkaido Nansei-Oki Seismic Tsunami, *Jour. JSCE*, 705/II-59, 139-150, 2002 (in Japanese).
3. Hirt, C. W. and B. D. Nichols: Volume of Fluid (VOF) Method for the Dynamics of Free Boundaries, *Jour. Computational Physics*, 29, 201-225, 1981.
4. Sakakiyama, T. and R. Kajima: Numerical Simulation of Nonlinear Wave Interacting with Permeable Breakwaters, *Proc. 23rd Int. Conf. Coastal Eng.*, ASCE, 1517-1530, 1992.
5. Amsden, A.A. and F.H. Harlow: A Simplified MAC technique for Incompressible Fluid Flow Calculations, *Jour. Computational Physics*, 6, 322-325, 1970.
6. Tanimoto, K et al.: Study on Stability of Submerged Dike at the Opening Section of Tsunami Protection Breakwaters, *Rep. Port and Harbour Res. Inst.*, 27(4), 93-121, 1988 (in Japanese).
7. Nakatsuji, K., S. Karino, and H. Kurita: Finite Element Analysis of Tidal Flow in the Osaka Bay with Subgrid Scale Eddy Coefficient, *Proc. Hydraulic Eng.*, JSCE, 36, 693-696, 1992 (in Japanese).
8. Tanimoto, K et al.: Field and Laboratory Investigations of the Tsunami Caused by 1983 Nihonkai Chubu Earthquake, *Tech. Note Port and Harbour Res. Inst.*, 470, 1983 (in Japanese).
9. Ikeno, M., M. Matsuyama and H. Tanaka: Shoaling and Soliton Fission of Tsunami on a Shelf and Wave Pressure for Tsunami-Resistant Design of Breakwater by Large Wave Flume-Experiments, *Proc. Coastal Eng.*, JSCE, 45, 366-370, 1998 (in Japanese).

Experimental and Numerical Modeling of Storm Surge and Tsunami Effects on Structures

by

Solomon C. Yim[1] and Kwok Fai Cheung[2]

ABSTRACT

The joint research work at Oregon State University and the University of Hawaii at Manoa on experimental and numerical modeling of storm surge and tsunami interaction with structures for both model basin test and prototype scenarios are described in this paper. The numerical modeling capabilities for storm surge, and storm waves as well as tsunami propagation and runup using a nested-grid approach are presented first. Modeling capabilities at Oregon State University for coupled fluid-structure interaction using the computational fluid dynamics and computational structural dynamics approaches are then delineated. A roadmap to combine the computational and experimental capabilities for the analysis and design of prototype structures in future research is finally presented.

KEYWORDS: Storm surge, storm waves; tsunami; structures; numerical modeling; coupled; fluid; structure; interaction.

1.0 INTRODUCTION

Natural disasters caused by hurricanes and tsunamis, notably Katrina in 2005 and the India Ocean Tsunami in 2004 in the last couple of years, are vivid evidence that the design codes of coastal infrastructure, including those in the inundation zone, need to take into account these extreme events. However, current design codes (FEMA, CEM, UBC, etc.) in the US rarely mention hydrodynamic effects due to storm surge and waves or tsunami. In an effort to mitigate the effects of tsunami on coastal cities, the US government is implementing a series of measures including installation of additional tsunami measurement buoys in the Pacific and Atlantic oceans by NOAA. A number of conferences and workshops on the survey of the devastating effects of tsunami and hurricane have been held worldwide in the past decade, and much more frequently in 2005 to present. The 100th Anniversary San Francisco Earthquake Conference held this April attracted approximately 4,000 scientists, engineers and academicians from many countries (see web site in reference).

Recently, intense research activities on various aspects of storm surge and waves, and tsunamis as well as their effects on coastal infrastructure are underway. A complete account of these events is necessary to link the statistics of their occurrences to the mitigation efforts or design code revisions. These include modeling of generation at the source, propagation across the ocean, near-shore transformation, and fluid-structure interaction. In support of the experimental research at the Hinsdale Wave Research Laboratory at Oregon State University, 2-D and 3-D numerical models including tsunami runup and inundation effects on coastal structures are being developed. In the following sections, numerical modeling and its challenges are discussed.

2.0 STORM SURGE AND WAVES

Complete and accurate modeling of coastal overwash due to hurricanes requires simultaneous simulation of physical processes that include surface winds and pressure, storm surge, astronomical tides, swell and seas, surf-zone processes, and wave runup onto dry land. These processes, with different time and length scales, have been modeled separately with reasonable accuracy. Cheung *et al* (2003) described linkages of the processes to produce a forecast package for storm-induced coastal flooding. The package

---

[1] Professor, Dept. of Civil Engineering, Oregon State University, Corvallis, OR 97331, USA

[2] Professor, Dept. of Ocean Resource Engineering, University of Hawaii at Manoa, HI 96822, USA

produces good agreement with measured wind velocity, wave conditions, and storm-water levels in the Pacific and Atlantic basins as well as the overwash evidence in Hawaii and Southern New England.

The coupling of the four model components and their interface with supporting models and utilities is illustrated in Figure 1. Each simulation covers three levels of nested geographic regions of increasing resolution: ocean, coastal, and nearshore. Hurricane wind and pressure fields, which can be generated by a parametric or numerical model, provide the environmental forcing over the ocean and coastal regions. A third-generation spectral wave model generates and propagates the waves in the ocean region. The simulation results define the boundary conditions for another spectral wave model to describe transformation of the storm waves as well as the subsequent wave setup in the coastal region. A shallow-water model simulates the storm surge and astronomical tides, while a Boussinesq model provides wave-by-wave simulation of the surf and swash zone processes at the coastline. The four-layered nested grid for the New England area for a model of the 1991 Hurricane Bob is shown in Figure 2. The grid size ranged from the coarsest of 10 Km for the ocean scale to the finest of 10 m for the runup on land (with 1 Km and 100 m in between).

3.0 TSUNAMIS

A number of the numerical nonlinear long-wave models currently used do not conserve flow volumes and underestimate runup when breaking occurs. However, a fully conservative model with shock-capturing capability is a prerequisite to producing sensible runup results. Wei *et al* (2006) makes use of the surface-gradient method and a Godunov-type scheme with an exact Riemann solver to track directly the moving waterline and to capture flow discontinuities associated with bores or breaking waves, which are essential for runup calculations. This provides accurate descriptions of the conserved variables and small flow-depth perturbations near the moving waterline. The computed surface elevation, flow velocity, and runup show very good agreement with previous asymptotic and analytical solutions as well as laboratory data. The model accurately describes breaking waves as bores or hydraulic jumps and conserves volume across flow discontinuities.

A nested grid is employed in the numerical simulation with four levels of nested grids. As an example, the nested-grid model of a tsunami inundation simulation of the northshore of Oahu due to the 1946 Alaska tsunami is shown in Figure 3. The largest is ocean grid, with a size of approximately 10 Km. (top left, Figure 3). It contains the regional grid, with a size of 1 Km (top right, Figure 3). Within the regional grid is the island grid, which has a size of approximately 100 m (bottom left, Figure 3). Finally, the finest grid is used in the area, where runup calculations are performed. It is nested within the island grid and has an approximate grid size of 10 m (bottom right, Figure3).

Accurate modeling of tsunamis from seismic sources to runup is a challenging task. Deformation of the earth surface due to internal faulting is an idealization based on elastic theory of dislocation, in which the earth is treated as an isotropic and elastic material. The determination of the initial tsunami waveform from the seafloor deformation is not trivial and depends on a number of factors. The most important is the rupture time, which affects the transfer of energy from the seafloor deformation to the water. The standard approach is to assume a short rupture time, as a result, the initial tsunami waveform is identical to the vertical component of the seafloor deformation due to faulting. In recalibration of the seismic source intensity is necessary to reconcile errors from tsunami source modeling to match historical runup records.

4.0 TSUNAMI WAVE BASIN FACILITY

The multidirectional tsunami wave basin (TWB) at OSU is 48.8m long by 26.5m wide by 2m deep (Figure 4). It is a reinforced concrete reservoir with unistrut inserts placed in rows at 2.1m spacing to affix models, instrumentation, and the wave generator throughout the basin. The wave generator consists of 29 wave-board segments, each paddle 0.9m wide by 2m high. Each wave board is capable of a 2m displacement and a maximum velocity of

2m/sec. It is able to generate a clean solitary wave approximately 0.8m high in a water depth of 1m. Each wave board is powered by an AC electric motor. The wave generator digitally controls the paddles on an individual basis, making it possible to generate arbitrary wave profiles and arbitrary wave directions. Control of the wave board is achieved through displacement and velocity feedbacks. Velocity control utilizes a wave profile measurement at the front of the wave board, comparing it to the desired long-wave profile; board velocity is adjusted via an algorithm that relates wave profile and board velocity. This velocity control has the capability of absorbing reflected waves in the basin and optimizing the wave shape beyond that available by means of the displacement control. The 3-D TWB creates a unique large-scale experimental testing laboratory for tsunami-hazard mitigation research. This basin, together with the existing directional (2-D) large wave flume (LWF), supports high resolution, unprecedented-scale experiments with very dense instrumentation. The OSU WRL facility provides coastal, offshore, earthquake and tsunami researchers with critical means to conduct large-scale experiments and validate advanced analytical and numerical models.

5.0 FLUID-STRUCTURE INTERACTION

Storm surge and waves, and tsunami models define the boundary conditions at the coastline for more detailed analysis of fluid-structure interaction. The environmental loads on a structure include hydrostatic pressure, fluid impingement, form and viscous drag, and impact due to waterborne debris. These loads often induce large structural deformation, yielding, fracture, and collapse or dislodgement. Accurate modeling of coupled fluid-structure interaction is therefore a very challenging problem. Traditionally, the study of coastal waves and structures belong to two separate disciplines and their analysis and numerical techniques usually cannot be coupled. Since the inception of the Tsunami Wave Basin (TWB) construction project in FY2000, researchers at OSU have been developing computational fluid-structure interaction software suitable for use by both environmental and structural engineers (Yuk *et al* 2006). Selected ongoing developments related to this goal are briefly summarized here.

The software package LS-DYNA, which contains modules for very large strain deformation, nonlinear materials, fracture, shearing detachment, contact and impact, appears to be a suitable computational structural dynamic (CSD) code for the structural analysis needs. It also contains a fluid module based on the NS equations to model wave impact as well as surface piercing and re-submergence of multiple flexible bodies. Recently, a finite-element based formulation to model the fluid domain; called the particle finite element method (PFEM) (Del Pin 2003) shows promising signs of unifying the simulation of fully coupled fluid-structure interaction. In PFEM method, the continuity and momentum balance equations in the fluid domain are modeled using the Lagrangian formulation and discretized using particle finite-elements. The boundaries at the free surface and at the interface between the fluid and the structure can be modeled exactly with a moving FE grid that is remeshed at every time step.

A combination using the CSD and CFD (computational fluid dynamics) codes from the industry for their proven robustness and nonlinear capabilities for the analysis of structural behavior and the PFEM methods for modeling fluid motions in Lagrangian form may provide the best solution for the development of a robust code for simulation of storm wave and tsunami basin experiments and prototype events. This choice allows a unified Lagrangian formulation and computation for both fluid and structural domains. More importantly, it allows for exact means of tracking the fluid-structure interfaces that determines: (1) the energy input to the wave field by the wave generator; (2) the wave forces on the coastal structures and floating debris; and (3) energy dissipation at the bottom boundary and the beach that may contain porous media and/or movable sediments.

A glimpse of the current capability of LS-DYNA for modeling the US National Science Foundation supported Network for Earthquake Engineering Simulation Tsunami Wave Facility at Oregon State University is shown here. Figure 5 shows the physical 3-D wave basin and the LS-DYNA numerical model with the exact dimension and number of wave paddles. The numerical model accepts prescribed motions of each individual paddle. Using the same prescribed motions as those of the physical wave generator, the subsequent wave motions in the basin are observed to be predicted accurately when appropriately fine grids are employed.

LS-DYNA is also capable of modeling a complex system by first modeling the components of the system as individual modules and then assembling them together to form the system. With this capability, we are able to model an experiment to be conducted at the NEES Tsunami Wave Facility as follow. We first model the wave basin including wave paddles and water as a single module (Figure 6a), and separately an instrumented cylinder including its components as another module (Figure 6b), and then insert the cylinder module inside the tsunami wave basin module to form the experimental model (Figure 6a). Once the system is in place, we can simulate a test run and compute the strains inside the cylinder (Figure 6c). Thus, LS-DYNA is used as a design and simulation tool for experiments at the NEES Tsunami Wave Basin Facility.

An issue that needs to be addressed is computational resources. To model a fluid-structural interaction experiment at the TWB using $1cm^3$ elements would lead to the number of fluid and structural elements approximately 3×10^9. Using 20-node solid element with 3 degrees of freedom (d.o.f.) at each node would lead to approximately 4×10^{10} d.o.f. An explicit computation of the numerical model for a typical transient experimental test of approximately 20 seconds would exceed the capability of many existing parallel computer clusters. The use of high-end vector supercomputer is necessary.

6.0 FUTURE RESEARCH

We are currently conducting research to develop a methodology to couple the numerical simulation capabilities at both universities and to extend the LS-DYNA capability to model fully coupled fluid-structure interaction. The key piece to be developed is the transfer of information at the boundary of the environmental domain containing the fluid and structure. The boundary conditions have to take into account the incoming wave (runup) from the ocean side and the out-going wave (rundown). When the research is complete, we expect to utilize the resulting software for practical applications to study the effects of storm surges and tsunamis on coastal infrastructure including bridges and buildings. For these cases, an existing finite-element model of a full-scale bridge (e.g., Figure 7) or a building, if available, may be directly inserted into the model of the coastal environment subjected to storm surge or tsunami boundary conditions. The resulting finite-element model will likely contain hundreds of thousands to millions of nodes and elements. Parallel and supercomputing will be needed. Results of this joint research will be reported in future workshops.

7.0 ACKNOWLEDGMENTS

Financial support from the National Science Foundation (CMS-0086571), NEESinc. (OMSA-2004-OSU), and from the Office of Naval Research (N00014-92-J1221 and N00014-04-10008) is gratefully acknowledged.

8.0 REFERENCES

http://www.1906eqconf.org/

Cheung, K.F., Phadke, A.C., Wei, Y., Rojas, R., Douyere, Y., Martino, C.D., Houston, S.H., Liu, P.L.-F., Lynett, P.J., Dodd, N., Liao, S., and Nakazaki, E. "Modeling of storm-induced coastal flooding for emergency management," *Ocean Engineering*, 30(11), 1353-1386, 2003.

Del Pin, F., "The Meshless Finite Element Method Applied to a Lagrangian Formulation of Fluid Flows," Ph.D. Thesis, Universidad Nacional del Litoral, 2003.

Yuk, D., Yim, S.C., and Liu, P.L-F., "Numerical Modeling of Submarine Mass-Movement Generated Waves Using RANS Model," *Computers and Geosciences*, in press, 2006.

Wei, Y., Mao, X.Z., and Cheung, K.F. "Well-balanced finite volume model for long-wave runup," *Waterway, Port, Coastal, and Ocean Engineering*, 132(2), 114-124, 2006.

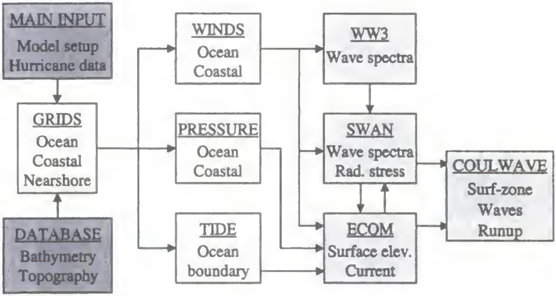

Figure 1. Storm Surge and Storm Waves Model Structure.

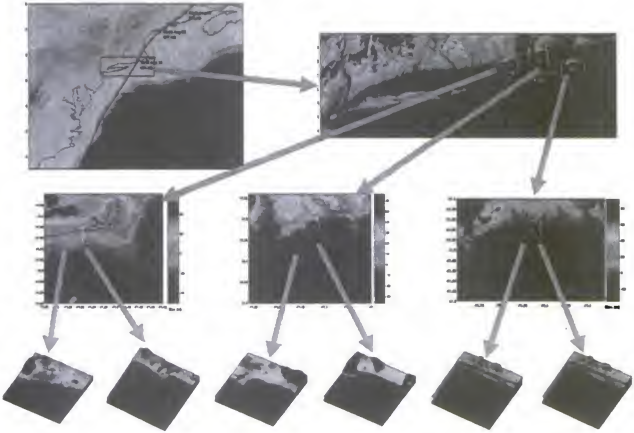

Figure 2. Nested Grid of Storm Surge and Storm Waves Model Structure for New England Area.

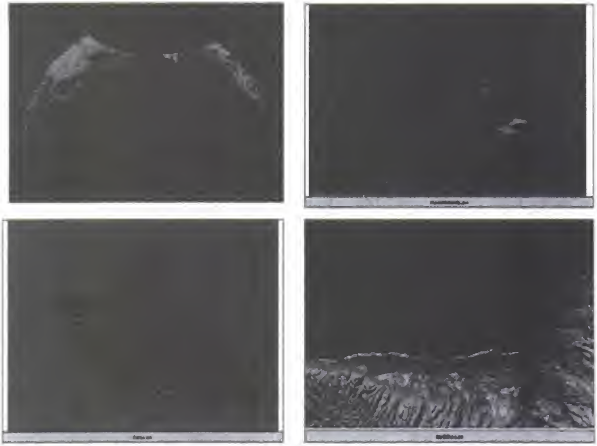

Figure 3. Nested grid with four scales and grid sizes.

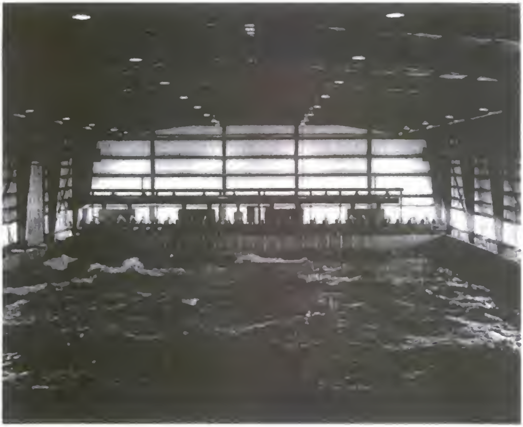

Figure 4. The Oregon State University NEES Tsunami Wave Basin Facility.

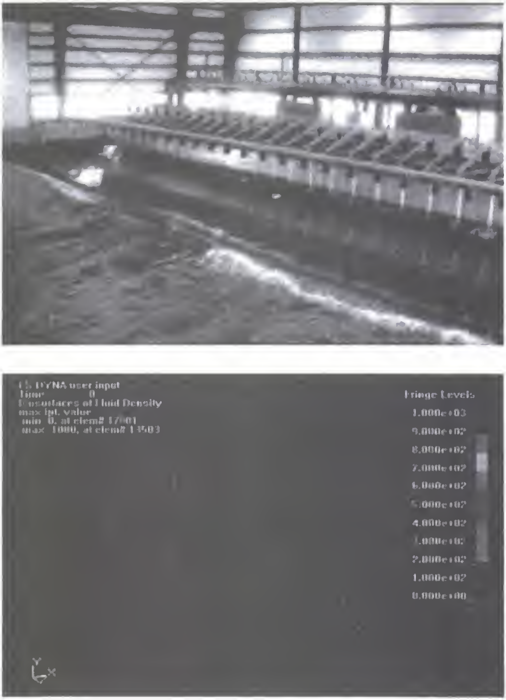

Figure 5. LS-DYNA model of tsunami wave generation at the OSU NEES 3-D basin.

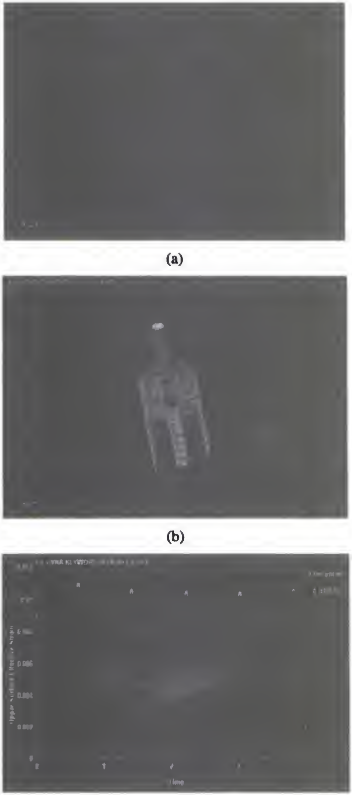

(a)

(b)

(c)

Figure 6. Numerical modeling of tsunami wave effect on a cylinder.

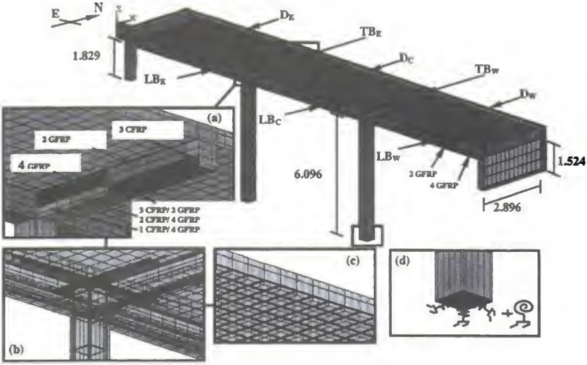

Figure 7. An example finite-element model of a coastal bridge.

Development of Estimation Method on Drift and Collision Behaviors of Debris Caused by Tsunamis

by

Katsuya Oda[1], Osamu Okamoto[2] and Kentaro Kumagai[3]

ABSTRACT

In order to reduce tsunami damage, it is necessary to appropriately estimate the potential damage caused by the collision of tsunami debris such as maritime cargo containers, small boats or timbers, drifting out to sea or onto land. This paper reports on the development of a simple method for estimating the drift and collision behavior of tsunami debris. The method combines the flow field modeled using a horizontal two-dimensional simulation of a tsunami, with floating debris modeled using the distinct element method. The applicability of this estimation method is further discussed using the results of model experiments on the drift behavior of maritime cargo containers.

KEYWORDS: Debris, Drift and Collision Behavior, Maritime Cargo Container, Tsunami Disaster Mitigation

1. INTRODUCTION

Japan is prone to the threat of interplate earthquakes and large-scale tsunamis caused by these earthquakes. A tsunami could cause flood damage along the Japanese coastal regions, notably in harbor areas where there are many cargo containers, large quantities of stored lumber, and moored boats and ships that could be set adrift. The potential damage that facilities and infrastructures, such as buildings and seawalls along the coast, could sustain from collision with such debris must be considered. Monetary loss of drifting objects is not the only concern. Greater damage could be caused by the collision of debris with seawalls and other costal structures, harbor structures, houses behind the harbors, and the outflow of hazardous material from dangerous goods storage. When waterways and anchorages are littered with drifting and submerged debris, navigation must be halted and the harbor may cease functioning until the debris is removed and the safety of navigation is confirmed. Damage from a tsunami could have such far-reaching effects.

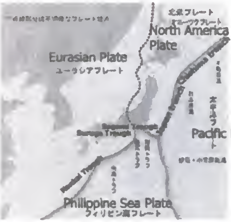

Fig. 1 Earthquakes In and Around Japan

To reduce potential damage, structural measures such as installing fences to prevent drifting, and non-structural measures such as planning the layout of the cargo storage area and consolidating the mooring sites for small boats, must be implemented. This requires an understanding of the drift and collision behavior of cargo containers, lumber and small boats. It is also necessary to develop a relatively simple method for estimating and assessing the potential collision damage. Therefore, in this research, a model was developed for simulating the drift behavior, when subject to external forces from the flow, and reproducing the collision of debris with fixed structures. This was achieved using data on the flow field in water and on land that was obtained from an often-used tsunami inundation simulation model based on the nonlinear long-wave theory. The debris, the shape of which was reproduced according to the distinct element method (DEM), is placed in this flow field. The applicability of this model was further studied using the results from a separate experiment on the drift and collision behavior of cargo containers conducted by Nagoya University and MLIT.

---

[1] Head, Coastal Disaster Prevention Division, National Institute for Land and Infrastructure Management (NILIM), Ministry of Land, Infrastructure and Transport(MLIT), Yokosuka-shi, Kanagawa-ken 239-0826 Japan

[2] Senior Researcher, ditto

[3] Researcher, ditto

2. EXPECTED DAMAGE CAUSED BY TSUNAMI DEBRIS IN JAPAN

2.1 Risk of Tsunami from Large-Scale Earthquakes

Many plates collide around the Japanese Islands. It is known that earthquakes occur where plates meet. So, many earthquakes and tsunamis attack Japan periodically. Fig. 1 shows that the plates; the Pacific Plate, Philippine Plate, North American Plate and Eurasian Plate all meet at the sea off Japan, making this country prone to large-scale interplate earthquakes. In the past century, there have been seven tsunamis with more than a hundred fatalities. Six of these tsunamis occurred in the adjacent seas, and one was from the 1960 Great Chilean Earthquake. The earthquake occurrence probability in various regions of Japan is assessed and publicized by a government organization, the Headquarters for Earthquake Research Promotion. The hypocentral regions, occurrence probability and expected magnitude of earthquakes such as trench earthquakes with subsequent tsunami are shown in Fig. 2. Notably, the Pacific Coast region is at high risk of sustaining damage from large-scale tsunamis, and there are concerns over large-scale distant tsunamis such as those that followed the Cascadia earthquake and the next Chilean earthquake.

2.2 Distribution of Potential Tsunami Debris throughout the Country

Population and industry in Japan are destined to be concentrated on the alluvial plains and along the coast because only about 10% of the total area is suitable for such uses. These may be dangerous regions, but the cities are highly developed with meticulous use of available land,

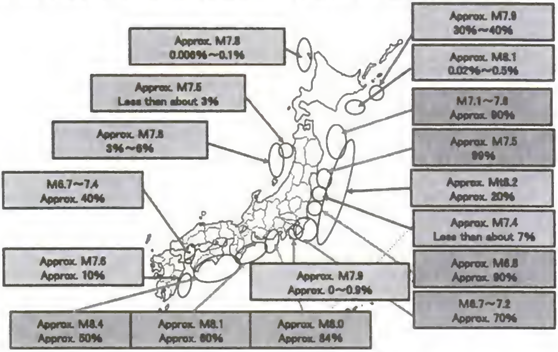

Fig.2 Probability of Major Earthquakes in Japan

such as the vertical development of underground space. Just as the land is intensively utilized, the city waterfront is highly developed mainly as ports. With their functional requirements, ports must be located outside the tsunami defense line, and are consequently at risk of inundation damage from tsunamis. Furthermore, many cargoes in these ports such as cargo containers, lumber, and small boats are highly prone to be set adrift in a tsunami and could cause damage. Fig. 3 shows the location of major ports handling maritime cargo containers and lumber. About 30 ports handle cargo containers and 35 ports handle more than ten thousand tons of lumber in 2004. The major part of these ports that handle cargo containers and lumber are located in regions where tsunami damages concern. Together with these cargoes, small boats could also be set adrift in a tsunami. Notably, many small boats are illegally moored without proper registration and with their owners unidentified. Since they are not properly overseen and often inadequately moored, these boats are prone to drift, but taking immediate action to prevent this is difficult. There are approximately 134,000 small boats illegally moored throughout the country.

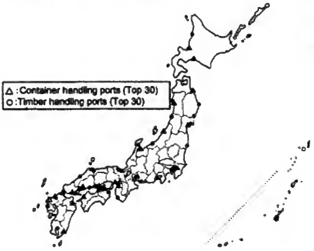
△ :Container handling ports (Top 30)
○ :Timber handling ports (Top 30)

Fig.3 Location of Major Ports Handling Maritime Cargo Container and Timber

3. MODELING THE DRIFT AND COLLISION BEHAVIOR OF CARGO CONTAINERS

3.1 Simulation Method

The method for tracing the drift behavior of debris such as cargo containers by assuming a particle without mass was already established. However, a simple and practical model for estimating drift and collision behavior that considers the mass and size of the debris and the acting hydrodynamics was yet to be developed. Therefore, in this research, a model was developed for reproducing the drift and collision behavior. The debris was modeled according to the distinct element method, using the water level and horizontal distribution of flow velocity from the calculation for estimating a tsunami at sea and calculating the run-up based on the nonlinear long-wave theory. Inertial force and drag force are also assumed to act on the debris. Fig. 4 shows the calculation procedure using this model. Fig. 5 shows the schematic illustration of the cargo container that was modeled according to DEM. For this model, in order to drift as a single structure and reproduce the drift and collision behavior, the debris has to be elastoplastic rather than rigid. As shown in Fig. 6, the distinct element method applied the model where each element consists of connected elements such as springs, dashpots, and link element [1].

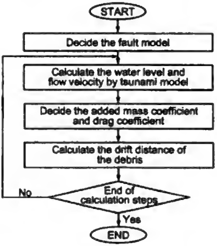
START
Decide the fault model
Calculate the water level and flow velocity by tsunami model
Decide the added mass coefficient and drag coefficient
Calculate the drift distance of the debris
No
End of calculation steps
Yes
END

Fig.4 Calculation Procedure for the Drift Model

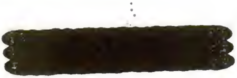

Fig.5 Schematic Illustration of Container Modeled Using DEM

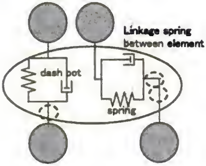

Fig.6 DEM Model

The hydrodynamic force (in the x-direction) from the fluid acting on the debris is according to the Morison's formula as shown below:

$$F_x = C_M \rho V \frac{\partial u}{\partial t} + C_D \frac{\rho u^2}{2} A_x$$

Where,

ρ is the water density; V is the volume of the portion in water; u is the flow velocity in the x-direction; A_x is the projected area (cross section) in the flow direction; C_M and C_D indicate the added mass coefficient (inertia coefficient) and drag coefficient.

3.2 Calculating the Drift and Collision Behavior According To the Modeled Topography

The simulation of container drift and collision behavior with other structures was performed by first calculating the water level and flow velocity in the modeled topography that assumes a harbor.

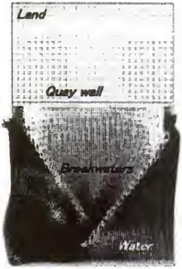

Fig.7 Example of Calculated Flow Field (Velocity)

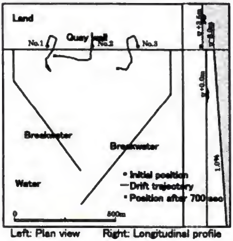

Fig.8 Drift Trajectory of Containers (Calculated Example)

Fig. 7 shows the flow velocity vector at the moment of tsunami beginning to run-up onto land. With this drift model, the added mass coefficient and drag coefficient, which changes according to factors such as the relative angle of the debris to the flow, must be precisely determined. These were decided by considering previous research [2]. Fig. 8 shows an example of the calculated drift trajectory for the center point of the container. This reproduced, to a certain level, the phenomenon where the container drifts in the container yard, collides with the wall, and then drifts out to sea with the reversed flow. To assess the impact force, damage behavior, and other factors affecting land structures, a more precise study should be conducted through verification and improvement of the model utilizing the results of large scale experiments.

4. VERIFYING THE APPLICABILITY OF THE ESTIMATION MODEL WITH THE MODEL EXPERIMNT ON CONTAINER DRIFT

4.1 Calculated Reproduction of the Model Experiment

At Shimizu Port, which is located along the Pacific Coast, there are concerns over potential large-scale tsunami damage. The Ministry of Land, Infrastructure and Transport, and Nagoya University have jointly performed experiments on tsunami-based drifting of a container from the container terminal of this port [2], [3]. The scale of the test model was 1/150. The topographical conditions were: two cases with collapsed breakwaters, assuming the collapse of the breakwaters from the earthquake; and three cases with the breakwaters intact, assuming the breakwaters were not affected by the earthquake. The wave conditions were: periodic waves and solitary waves.

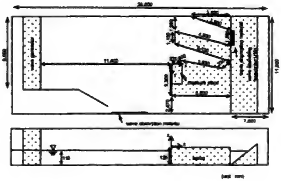

Fig.9 Outline of Experiment Model

As shown in Fig. 9, two cases are used to study the applicability of the estimation model by assuming that the seawalls have completely collapsed from the earthquake, and therefore, have no effect on tsunami propagation. The wave conditions are solitary waves with different periods. A nonlinear dispersive wave model was used for the water, and a nonlinear long-wave model was used for land, and then the measured water level and waveform were used as boundary conditions. One of the cases is shown in Figs. 10 and 11, and changing tsunami heights with time over the apron were obtained from the experiments and the calculation.

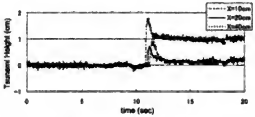

Fig.10 Tsunami Height (Observed)

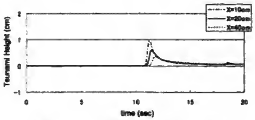

Fig.11 Tsunami Height (Calculated)

In the calculated results, the peak in run-up water level over the apron was slightly less than that of the results of the experiments, but it is believed that changes in the run-up water level with time were successfully reproduced to a certain level. On the other hand, the calculated Froude number over the apron (x = 10 cm) was a maximum of about 2.0. Since this was estimated to be similar in the experiment results, it is believed that flow velocity over the apron could be reproduced to a certain level with the calculation as well.

4.2 Verification of Container Drift Behavior

The drift calculation for the container was performed according to the tsunami wave forces acting on the container and calculated with the Morison's formula. The drag coefficient and inertia coefficient were decided by referring to the experiment by Mizutani, et al. (2005) [2]. There are two types of containers lengths: 20 ft and 40 ft; and two types of weight: half-loaded and fully loaded. Fig. 12 shows the drift trajectory from the model test when the 20-ft container was either half or fully loaded.

Fig. 13 shows the calculated position of drifting container in x-direction (drift distance) when the 20-ft container was either half or fully loaded. The calculated result, when the container was half-loaded, was a drift of about 25 cm in the x-direction and about 1 cm in the y-direction. When the container was fully loaded, the drift was about 20 cm in the x-direction, which was smaller than when the container was half-loaded, and about 1 cm in the y-direction. The calculated drift distance was rather small compared to the test results, but this was successful in reproducing the trend where the drift of the container over the apron showed a large movement in the x-direction, while being affected by the flow in the y-direction.

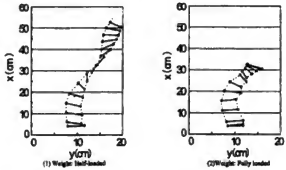

Fig.12 Drift Trajectory of the Container (Observed, 20-ft Container)

With the 40-ft container, the drift distance in the x-direction showed a similar trend as shown in Fig. 14. In the calculation, the container floated (the z-value became positive) and drifted, and then stopped when the bottom dragged. This is believed to be reproducing the behavior where the container started to drift with the increase in water depth at the apron. Then the drifting stopped with the decrease in water depth that caused friction between the bottom of the container and the surface of the apron.

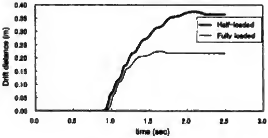

Fig.13 Drift Distance in the x-Direction (Calculated, 20-ft Container)

5. SUMMARY OF RESULTS

1) Simulation of drift and collision behavior of cargo containers and other debris, in model topography that assumes a harbor, was performed by establishing a drift model of the container considering factors such as the mass and size of the debris, and the hydrodynamics that will be acting on it from the tsunami. The results showed that this could be successfully reproduced to a certain level.

2) The friction at the container bottom and the drift behavior including rotation were modeled by comparing the calculated results from the estimation model and the results from the model test of the container. The established model reproduced the behavior where the container started to drift with the increase in water depth at the apron, and although the drift distance was rather small, it reproduced the trend according to differences in weight and length of the container.

6. CONCLUSION AND FUTURE ISSUES

With the use of this proposed method, estimating the drift and collision behavior of tsunami debris became possible with relative ease and low cost. The use of this method is anticipated in planning and designing structures

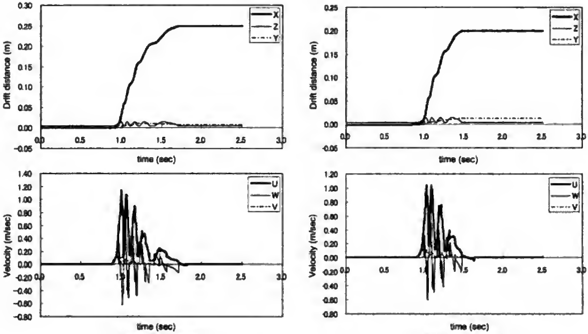

(1) Weight: Half-loaded

(2)Weight: Fully loaded

Fig.14 Drift Distance and Velocity of Container (Calculated, 40-ft Container)

such as debris protective barriers, as well as in estimating potential damage to buildings and other social infrastructures. Furthermore, this could be used in studying measures that do not rely on protective structures such as cargo storage that considers the effects from tsunami debris, and planning the layout of mooring sites and storage for small boats.

On the other hand, this method has limited ability for reproducing the behavior of large debris such as ordinary cargo ships, because the interaction between the flow field and debris is not considered. It is necessary to clarify how far this method could be used with large debris through comparisons with model experiments and other methods that could reproduce the phenomenon more logically and precisely. Furthermore, this requires verification through large-scale experiments to reproduce the collision more accurately. The National Institute for Land and Infrastructure Management will be actively involved in further research of these issues.

7. REFERENCES

1. Meguro, K., Hakuno, M.: Fracture Analyses of Concrete Structures by Granular Assembly Simulation, *Bulletin of the Earthquake Research Institute*, University of Tokyo, Vol. 63, 1988 (in Japanese)
2. Mizutani, N., Takagi, Y., Shiraishi, K., Miyajima, S., Tomita, T.: Study on Wave Forces on a Container on an Apron Due to Tsunami and Collision Force of Drifting Container, *Annual Journal of Coastal Engineering*, JACE, Vol. 53, 2005
3. MLIT: Report of the experimental study on influence of tsunami debris on port structures, 2005(not yet open to public)

Technical Session 5

RECENT NATURAL DISASTERS AND NATURAL DISASTER MANAGEMENT PLAN

Toward the Establishment of a Regional Society that is Safe and Secure against Disasters

by

Tsuneyoshi Mochizuki[1], Kiyoshi Minami[2], Koichi Yamashita[3], Keiichi Tamura[4],
Koh-ichi Fujita[5] and Katsuya Oda[6]

ABSTRACT

Japan has suffered and recovered from numerous and varied disasters in the past, and has made constant efforts to ensure safety in a range of areas towards to a safer society. These efforts ensure the basic requirements for every aspect of living. However, the country still suffers much human and property damage every year, and sees the emergence of additional detrimental or restricting factors in ensuring greater safety and security. This paper proposes, in the form of ten challenges, guidelines for establishing a regional society that is safe and secure against disasters under the current conditions.

KEYWORDS: Disaster, Regional Society, Safety, Security

1. INTRODUCTION

Japan has suffered and recovered from numerous and varied disasters in the past, and has made constant efforts to ensure safety in a range of areas towards to a safer society. These efforts ensure the basic requirements for every aspect of living.

However, the country still suffers much human and property damage every year, and sees the emergence of additional detrimental or restricting factors in ensuring greater safety and security. In this context, the country needs dramatic technological advances along with their application and operation in local communities in close collaboration with the human and social sciences. This will help to bring an enhanced social resistance to risk events and build a safer and more secure society, thereby providing the infrastructure for a decent quality of life.

In the United States, the Subcommittee on Disaster Reduction, which was established within the National Science and Technology Council's Committee on Environment and Natural Resources, published a report called the *Grand Challenges for Disaster Reduction* in June 2005 [1]. This report identified a set of hazard-mitigating measures and policies known as the Grand Challenges to develop a ten-year strategy for disaster reduction through science and technology. The Subcommittee also plans to develop a hazard-mitigating strategy on 15 priorities identified and an implementation schedule for it in Phase II of the Grand Challenges program in around June of 2006.

In Japan, the Working Group on Science and Technology Policy for a Safe and Secure Society, which was established by the Ministry of Education, Culture, Sports, Science and Technology, developed a set of priorities for a safe and secure society in April 2004. The Council for Science and Technology Policy, established by the Government, specified the implications of the development of safety science and technology and clarified the guiding principles and implementation of its steps. The council also proposed that the achievements of science and technology which contribute to security should be shared through a range of applications to achieve the policy objective (Goal 6), "The world's safest country – making Japan the world's safest country" under Concept 3, "Protect nation's health and security – to become a nation that secures safety and quality of life" set out in the Third Science and Technology Basic Plan.

---

[1] Director-General, National Institute for Land and Infrastructure Management, Ministry of Land, Infrastructure and Transport, Tsukuba-shi, Ibaraki-ken 305-0804 Japan

[2] Research Coordinator for Evaluation, ditto

[3] Research Coordinator for Codes and Standards, ditto

[4] Research Coordinator for Earthquake Disaster Prevention, ditto

[5] Head, River Environment Division, ditto

[6] Head, Coastal Disaster Prevention Division, ditto

With these points in mind, this paper proposes Japanese efforts to provide guidelines addressing the perceived needs for the development of a comprehensive policy towards a society resilient to natural disasters. We hope that this proposal will help develop a shared key understanding that allows all concerned to address the issues in a concerted manner.

2. WHAT IS A SAFE AND SECURE COMMUNITY?

The Working Group on Science and Technology Policy for a Safe and Secure Society, which was established by the Ministry of Education, Culture, Sports, Science and Technology, defined a safe and secure community in an April 2004 report as having the following qualities:

1) A community to minimize risk and withstand actualized risks

Continuous efforts should be made to reduce risk to a socially acceptable level in order to ensure safety, and an appropriate risk management system should be developed to maintain risk at the lowest level. At the same time, in the event that a risk does materialize, the community should be able to limit its consequences and maintain normal function.

2) A community for flexible response and international cooperation

Anticipating that safety may be threatened at any time in ways that are unpredictable, the community should develop a dynamic system to ensure flexible and timely response to any emerging threat, and should participate in international cooperation towards safety.

3) A community whose members have an increased level of safety-consciousness

Organizations should be responsible for building a safer community, and individuals should have a knowledge and awareness of safety and be able to fulfill appropriate roles in community's efforts towards safety.

4) A community that reassures individuals through confidence

A socially acceptable level of safety should be continuously maintained, and mutual confidence should be increased among organizations involved in security and individuals through coordinated activities, thus enhancing the feeling of safety.

5) A community with the capacity to consider the positive and negative aspects of policies for a safer and more secure community and to make rational decisions

The community should be able to closely consider the positive and negative aspects of policies for a safer and more secure community, and should be able to make rational decisions about the level of safety and security to be achieved through these policies.

It should be noted that the term *safety* refers to any objectively verifiable absence of injury or damage, either tangible or otherwise, to humans, organizations and public domains.

The term *security* refers to a belief that no events significantly different from predictions based on knowledge and experience will occur, and that the resulting conditions can be accepted even if such events do occur.

3. PRESENT ISSUES IN CREATING A SAFE AND SECURE SOCIETY

The disaster environment of Japan and its surrounding countries has recently undergone significant changes. To ensure a safe and secure lifestyle, the contemporary issues arising from these changes should be carefully considered and appropriately handled. The issues are outlined as follows:

1) Emergence of new critical phenomena

Recent advances in research into the generation mechanisms of dangerous phenomena such as earthquakes, volcanic eruptions and tsunami have clarified previously unknown phenomenon generation patterns, and new measures for these patterns should be now considered. In addition, the frequent occurrence of large-scale disasters around the world has created the need to consider measures to address the effects of new disasters. New emergency issues also need to be handled, such as chemicals whose harmful effects have only recently been discovered and newly detected infectious diseases.

2) Increased harmfulness of some dangerous phenomena

As an example, abnormal local weather phenomena such as concentrated heavy rains are found in relation to global warming.

3) Reduction of regional resistance to disasters

There are indications that disaster resistance in each region decreases explicitly according to inhabitant ageing, depopulation, changes in the regional community, the deterioration of social systems such as flood prevention teams, the scattering or loss of experimental knowledge saved in each region and the popularization of urban lifestyle.

4) Increased vulnerability due to the enlargement, deepening and complexifying of urban systems

Our society may have gradually evolved a vulnerability to dangerous phenomena in the consistent flow of enlargement, deepening and complexifying of urban systems. In particular, such vulnerability may be actualized as unstable actions in and damage to systems caused by unexpected external factors, or as a chain reaction and amplification of simultaneously caused damage.

5) Delays in the supply of scientific diagnosis and technical solutions to handle new issues

A number of issues threatening the safety and security of our society have been pointed out. For example, can disaster prevention equipment developed in the past also function effectively today? Do the devastation of forests and the abandonment of plowlands increase the risk of landslides and floods? Could watershed degeneration from human activities have destroyed the continuation of near shore water ecosystems? Can the effects of chemical pollution on humans and ecosystems be ignored? It is necessary to properly diagnose these risks and propose solutions to prevent unnecessary alarm over a range of disputed problems whose risk is not sufficiently clear.

6) Occurrence of restrictions on assuring safety and security

It can be considered that the capacity for investing in disaster prevention systems may decrease in the long term, and the number of function-deteriorated disaster prevention facilities may increase. In this light, there is an increasing worry that enhancements to disaster prevention facilities may remain insufficient for possible external forces. It is becoming clearer that disaster prevention measures depending solely on disaster prevention facilities are dangerous.

4. WHAT CONSTITUTES A REGIONAL SOCIETY THAT IS SAFE AND SECURE AGAINST DISASTERS?

Referring to the US's *Grand Challenges for Disaster Reduction* activities outlined above and the report issued by the Working Group on Science and Technology Policy for a Safe and Secure Society, we propose the following three basic recognitions to consider Japan's disaster prevention measures:

- Checking the requirements of safety and security in regional society.
- Comprehensively arranging the issues to be resolved.
- Viewing these measures as a process in which a common awareness is developed between all the related parties, leading to evolution based on the present conditions and a steady increase in cooperation.

Based on these recognitions, we first clarify the issue of what constitutes a regional society that is safe and secure against disasters. Then we show how all the parties can create and maintain a regional society that satisfies the following three requirements:

1) The capability to safeguard human life to the maximum
2) The capability for resistance to danger (above a certain level)
3) The capability for speedy recovery from disasters

The conditions to be achieved (or maintained) for a safe and secure regional society will be outlined according to the above three requirements: 1) safeguarding life, 2) increasing resistance, and 3) increasing recovery capacity. These conditions must also be established and maintained in line with the following three factors:

a) A continued grasp and understanding of the necessary information and knowledge
b) Maintaining the means and environment necessary for fulfillment
c) Keeping a sense of belonging between the parties concerned

Table 1 lists these conditions in detail.

5. INTERIM APPROACHES (DRAFT PROPOSAL) – TEN CHALLENGES –

The draft proposal of approaches towards realization of the content in Table 1 is suggested in the form of ten challenges.

As described in the basic acknowledgement above, this draft evolves constantly in response to current status by considering how to widen the coalition circle while developing a common view among the parties involved across a range of fields. For this purpose, the Ministry of Land, Infrastructure and Transport should encourage the parties to collaborate with each other. This draft also shows the nature of such encouragement and the direction of the approaches undertaken by the Regional Development Bureau. By reviewing this information, it is considered possible to identify areas that have not yet been studied or researched by research institutes such as the National Institute for Land and Infrastructure Management. Examples of research and development issues to be addressed in the future are also provided.

– Ten challenges –

Classification	Ten challenges
1. Knowledge	1-1 Learning from disasters 1-2 Supporting communications that lead to risk-preventive behavior 1-3 Knowing the effects on the economy and business activities in disaster-stricken region
2. Cooperation	2-1 Sharing information and knowledge with regional communities even under normal circumstances 2-2 Promoting the creation of communities capable of disaster prevention through self- and co-support
3. Real-time information	3-1 Providing information in real time 3-2 Utilizing emergency earthquake information
4. Recovery	4-1 Improving the resistance and recovery power of basic infrastructures as a whole 4-2 Developing innovative technologies to improve the resistance of facilities 4-3 Preparing for recovery

1. Knowledge

1-1 Learning from disasters

o Encouraging local governments to share information on successful (or failed) case examples of disaster control to accumulate technical knowledge.

- Accumulating technical knowledge which cannot be stylized.
- Accumulating information on actual action taken in response to disasters, such as whether proper evacuation was carried out or proper information given.

Table 1 Conditions to be achieved for a safe and secure regional society

Conditions to be achieved Requirements of safe and secure regional society	a) A continued grasp and understanding of the necessary information and knowledge	b) Maintaining the means and environment necessary for fulfillment	c) Keeping a sense of belonging between the parties concerned.
1) The capability to safeguard life	1. People are aware in advance of the nature of each danger (i.e., the present state of resistance, future prospects and degree of threat), proactive measures and action to be taken when necessary. 2. People have a continued grasp of the present state of danger and can understand the level of threat.	3. People execute proactive measures including seismic inspection and retrofit of houses. Safe evacuation zones, routes, procedures and emergency measures are established.	4. People trust the information and action of disaster prevention agencies and can take appropriate action in response to instructions given by them. 5. People are able to lend assistance to others.
2) The capability for continued efforts to increase resistance	1. Disaster prevention agencies know the mechanism and level of threat for each danger, and are aware of the present situation of resistance and any resistance-related issues of the facilities in their jurisdictional area. 2. Disaster prevention agencies know the degree of people's knowledge, the proactive measures they are capable of, their level of trust in the agencies, and their co-support awareness. 3. Disaster prevention agencies know the nature and degree of effect that each danger will have on the private sector and industries, and have strategies such as BCPs (Business Continuity Plans) to minimize these effects. 4. Disaster prevention agencies know the process of the mutual effects of infrastructure damage.	5. Disaster prevention agencies can acquire measurement data on each dangerous phenomenon and the status of resistance using an appropriate observation system. Agencies can save such data for use as needed and are able to analyze it. 6. Disaster prevention agencies have means such as visualization techniques to obtain a visceral understanding of disaster information, and can utilize these means for internal and external notification. 7. Disaster prevention agencies have a standard analytical method for actual disasters, and can accumulate experience by utilizing this method. 8. Disaster prevention agencies have the technical knowledge to develop co-support awareness, and can support regional societies by using this knowledge. 9. Disaster prevention agencies can use innovative techniques for increasing resistance. Examples may include minimization of the disaster area or network creation of a physical distribution infrastructure to secure overall function. 10. Disaster prevention agencies can make and execute plans for increasing resistance that are appropriate to the level of threat, the degree of effect and the current state of resistance and any issues related to it. Such plans include prevention measures against the mutual effects of infrastructure disaster and measures by land induction.	11. Disaster prevention agencies can share information and act as a unit.
3) The capability to acquire ideas for increasing recovery power	1. The private sector and industries know the nature of each danger (i.e., the present state of resistance, future prospects and degree of threat).	2. The private sector and industries have strategies such as BCPs (Business Continuity Plans) to minimize the effects of danger in collaboration with the parties concerned, and can update such plans as necessary. 3. The private sector and industries have plans in conjunction with disaster prevention agencies for effective measures to recover from disaster. The private sector and industries can also update such plans as necessary and can reserve the executive organizations and materials required. 4. Disaster prevention agencies have recovery plans that determine the priority of infrastructure recovery, and can reserve the executive organizations and materials required. 5. Disaster prevention agencies can make and execute new plans for easy recovery as necessary in addition to the above plans for increasing resistance.	6. The private sector, industries, disaster prevention agencies and inhabitants share necessary information.

Interim approaches (draft)

RDB, etc.	• Collecting successful (or failed) case examples of disaster control, diffusing successful examples • Conducting field surveys on evacuation and the supply of information
NILIM	• Analyzing the successful (or failed) case examples collected • Studying how to interpret or quantify the information accumulated

RDB: Regional Development Bureau, Ministry of Land, Infrastructure and Transport

NILIM: National Institute for Land and Infrastructure Management

1-2 Supporting communication that leads to risk-wise behavior

- o Encouraging local governments to engage a common view on the importance of information services that lead to risk-wise behavior, and collecting and utilizing successful examples while reflecting on failed examples.
- o Upgrading visual indication technologies to promote awareness of dangerous phenomena among people, and conducting research into methods of supplying such information by considering types of human bias in collaboration with the fields of arts and social sciences.

Interim approaches (draft)

RDB, etc.	• Conducting survey on actual conditions (i.e., case examples) of the relationship between risk-wise behavior and information
NILIM	• Analyzing case examples collected • Studying methods of upgrading visual indication technologies • Conducting research into methods of supplying information by considering types of human bias, in collaboration with the fields of arts and social sciences

1-3 Knowing the effects on the economy and on business activities in a disaster-stricken region

- o Encouraging local governments (at a prefectural level), the private sector and economic communities to have a common awareness to grasp the effects of disasters on the local economy as a whole and on business activities, and clarifying the procedures for this purpose.
- Preparing a macro analysis method for the whole region utilizing an economic model, applying the model to a disaster area and establishing a quantification method.
- Preparing a research method to determine the spreading process of direct/indirect disaster impact (e.g., questionnaire research involving the representative private sector and industries), applying the method to a disaster area and establishing a method of understanding the effects.

Interim approaches (draft)

RDB, etc	• Using a macro-analysis method in a disaster area • Developing and utilizing a micro-analysis method (such as questionnaires) according to regional characteristics
NILIM	• Developing a macro-analysis method and analyzing the application results • Developing a micro-analysis method and analyzing the application results

2. Collaboration

2-1 Sharing information and knowledge with regional communities even under normal circumstances

- o Encouraging inhabitants, local governments and the private sector to share information and knowledge related to disasters, as well as information on the level of damage to be expected from each type of disaster and the actual status of facilities.
- Knowing the depth of inhabitants' current awareness and understanding of hazard maps and so forth, and taking measures to improve the level of awareness.
- Knowing the actual status of and issues related to regional governments' disaster measures, and presenting methods to enhance regional resistance such as information collection/analysis abilities.
- Knowing the current status of and issues related to each private sector's Business Continuity Plan (BCP), and supplying basic information to enable the private sector to make their BCP consistent with others.

- Providing a progress indicator for realization of the desired community through these activities, and reflecting this into new technological development and academic activities.

Interim approaches (draft)

RDB, etc.	• Continuously enhancing the information-sharing ability of inhabitants, local governments and the private sector through daily activities (e.g., disaster drills, disaster prevention meetings, facility inspections, various events etc.) • Continuously measuring the indicator provided to show progress towards a desirable society
NILIM	• Researching methods of developing, analyzing and improving the indicator to show progress towards a desirable society • Researching the new technology necessary to provide the information and knowledge required by the parties concerned

2-2 Promoting the creation of a disaster-preventive community through self- and co-support

- o Encouraging inhabitants to have a common awareness of the importance of creating a disaster-preventive community through self- and co-support, raising awareness of disaster prevention through regional activities, and supporting the development of a disaster-preventive community.
- Analyzing the relationship between community changes and co-support awareness, and presenting measures to improve co-support awareness (preventing decreases in awareness).
- Collecting and diffusing good case examples of activities linked with daily regional activities.

Interim approaches (draft)

RDB, etc.	• Collecting and familiarizing the good case examples of creating a disaster-preventive community by self- and co-support • Surveying the relationship between community alteration and co-support awareness • Supporting the creation of disaster-preventive communities linked with daily regional activities
NILIM	• Collecting and analyzing the good case examples of a disaster-preventive community by self- and co-support • Analyzing the relationship between community alteration and co-support awareness, and studying about measures to improve co-support awareness (reduction prevention)

3. Real-time information

3-1 Providing information in real time

- o Encouraging inhabitants, local governments and the private sector to have a common awareness of the importance of real-time disaster information for all including the unspecified majority who are not constituent members of the regional society, and building a mechanism for providing/ receiving such information.
- Pinpointing areas for improvement in existing methods of transferring disaster information to a wide range of people, indicating how to use it under normal conditions and developing a new media method of utilization.
- Developing a system to provide information to the unspecified majority such as users of cars or public transportation, seaside visitors, and so on at facilities in the jurisdictional area, and encouraging the relevant authorities to take appropriate measures in places with a high number of visitors such as downtown areas.

Interim approaches (draft)

RDB, etc.	• Pinpointing areas for improvement in existing methods and indicating how to utilize information under normal circumstances in accordance with current regional conditions • Executing social testing of new information media • Solving the issues of how to provide information to the unspecified majority at facilities in the jurisdictional area
NILIM	• Analyzing/presenting areas for improvement in existing methods and how to utilize information under normal conditions • Developing an application of new information media • Studying how to provide information to the unspecified majority at facilities in the jurisdictional area

3-2 Utilizing emergency earthquake information

- Encouraging facility managers to have a common awareness of the importance of utilizing emergency earthquake information, and conducting research and development into new methods of applying this information to the field of ITS etc.

Interim approaches (draft)

RDB, etc.	• Exploring the possibility of using emergency earthquake information for facility management
NILIM	• Researching a method of using emergency earthquake information for facility management

4. Recovery

4-1 Improving the resistance and recovery capacity of the basic infrastructure as a whole

- Encouraging each infrastructure manager to have a common awareness of the mutually dependent relationships between infrastructures, analyzing this mutual dependence and presenting a method of damage reduction (i.e., a proactive program).
- Presenting a framework of broad-based collaboration across a range of fields to prepare a method for the temporary storage, transportation and disposal of waste and debris caused by a disaster.

Interim approaches (draft)

RDB, etc.	• Surveying/analyzing the mutual dependent relationship between key infrastructures in the area • Studying the current conditions and issues related to the temporary storage, transportation, and disposal methods of waste and debris from a disaster area
NILIM	• Developing a method of analyzing the mutually dependent relationships between key infrastructures and presenting a method of damage reduction • Presenting a framework of broad-based collaboration across a range of fields for the temporary storage, transportation and disposal of waste and debris from a disaster area

4-2 Developing innovative technologies to improve the resistance of facilities

- Encouraging the private sector and facility managers to understand the needs and seeds of innovative technologies to improve the resistance of facilities, and collaborating in the development of such technologies.

(Examples)

- Development of structures using high-strength steel with nanotechnology.
- Performance improvements in seismic isolation technologies and reductions in their cost.
- Large-scale emergency recovery work from the air for breached dykes.
- Minimization of flooded areas using existing structures such as roads etc.
- Collective use of facilities with functions for local revitalization and environmental conservation, with the aim of preventing or reducing disasters.

Interim approaches (draft)

RDB, etc.	• Grasping the needs of innovative technologies to improve the resistance of facilities • Grasping the needs for multiple methods
NILIM	• Grasping the needs and seeds of innovative technologies to improve the resistance of facilities, and conducting technology development • Grasping the needs for multiple methods, and researching the necessary technologies

4-3 Preparing for recovery

○ Encouraging local governments to have a common awareness of the importance of creating highly disaster-preventive towns based on changes in the social environment, and beginning research by clarifying the topics, methods and period of discussions to prepare a recovery plan.

Interim approaches (draft)

RDB, etc.	• Surveying the awareness of local governments of the preparations necessary for recovery
NILIM	• Researching a range of issues to prepare a recovery plan in advance

6. CONCLUSION

This paper proposes, in the form of ten challenges, guidelines for establishing a regional society that is safe and secure against disasters under current Japanese conditions. The following actions are planned:

1) Establishing the content of each challenge more specifically.
2) Encouraging inhabitants, regional societies, local governments, infrastructure managers, the private sector and economic communities to execute these challenges jointly with the parties concerned. This should be done in accordance with general instructions from the Regional Development Bureau or other organizations of the Ministry of Land, Infrastructure and Transport.

7. REFERENCE

1. Subcommittee on Disaster Reduction, Committee on Environment and Natural Resources, National Science and Technology Council: *Grand Challenges for Disaster Reduction*, 2005.

Recovery and Monitoring Challenges with Water Quality Issues in New Orleans During Hurricane Katrina Recovery Operations

by

William E. Roper[1] Kevin J. Weiss[2] and James F. Wheeler[2]

ABSTRACT

Following the passage of Hurricane Katrina, New Orleans was left with eighty percent of its land area flooded. In some locations the flood waters were over thirty feet deep. In the heat and stagnation that followed the waters quickly became heavily polluted with petroleum products, industrial chemicals, raw sewage, dead animals etc. In addition, a super fund cleanup site was flooded and contributed to the water pollution problem. Pump out operations began in early September 2005 as a high priority to get the city dried out and on the road to recovery. Lake Pontchartrain was the primary receiving water body with the Mississippi River as a secondary receiver. A variety of approaches and technologies were evaluated to achieve treatment with minimal impact on pumping operations. Some of these methods and technologies included; sorbet booms in the channels and the lake near outfalls, oil and debris removal skimmers in channels and near outfalls, floating and bottom anchored containment screens around outfalls, sediment control devises for hot spots within the city, application of flocculation chemicals in contained areas, aerators in the channels and near the outfalls, application of specialized bacteria, etc. Over 100 water quality sampling sites were setup throughout the city to characterize water conditions as the pump out proceeded. High risk areas were identified in a dynamic process and decisions make for best corrective action. Lake Pontchartrain continues to be monitored and long term rehabilitation efforts will be predicated on water quality monitoring results. Lessons learned from a water quality perspective during this massive disaster is presented with the goal of assisting future recovery efforts.

KEY WORDS: Hurricane Katrina recovery, New Orleans, water quality, sediment sampling, expedient pollution controls, dewatering operations

1. INTRODUCTION

Hurricane Katrina made landfall on the coast of Louisiana near Buras, Louisiana as a category 4 hurricane during the early hours of August 29, 2005. The storm crossed the Mississippi River Delta, and Mississippi Sound, and came back ashore near the Louisiana-Mississippi border. Winds were recorded as high as 140 mph in the near shore areas of Louisiana and Mississippi. Storm surges of over twenty five feet were developed in some coastal area causing extreme damage for miles inland. New Orleans was hit particularly hard. Hurricane Katrina left the Crescent City with no poser, so drinking water, no wastewater treatment, dwindling food supplies and, because of levee breaches, rapidly rising floodwaters. By September 1, almost eighty percent of New Orleans was under water, in some places by more than twenty feet (figure 1). Thousands of people sought shelter from the rising waters on rooftops; thousands more gathered in shelters or in groups on high ground.

---

[1] George Mason University, 4400 University Drive, MS 5C3, Fairfax, VA 22030

[2] Environmental Protection Agency, Office of Wastewater Management, 1200 Pennsylvania Avenue, N.W., Washington, DC 20460

2. DEWATERING OPERATIONS

The U.S. Army Corps of Engineers had primary responsibility through FEMA for the dewatering of New Orleans as well as many other missions in response to Hurricanes Katrina and Rita. The Corps Mississippi Valley Division (MVD) had developed a Hurricane Contingency Plan in 1998 following Hurricane Georges that was updated annually and used as a starting point for this emergency. Under the MVD contingency plan for a hurricane hit on New Orleans, New Orleans District, as the "impacted" district, would have reconstitution as its primary initial mission. The plan also assumed there would be a "dewatering" mission for New Orleans. In this case Rock Island District was brought in to handle the dewatering mission. Memphis and Vicksburg districts would handle the primary FEMA mission for Louisiana and Mississippi, respectively. St. Louis District would execute civil works missions such as levee repairs. The Motor Vessel Mississippi was used as the forward headquarters for MVD and positioned in Port Allen, LA just across the Mississippi River from Baton Rouge. This allowed for close interaction with state and federal agencies in Baton Rouge. Quarter boats from the Corps' Mat Sinking Unit were also positioned at Port Allen to feed and house first responders.

Dewatering operations began soon after hurricane Katrina passed New Orleans. Some of the initial actions involved notching levees to allow flood water to drain out by gravity in some areas. Portable pumps were installed and put into operation throughout the city (figure 2) and work was started to repair the main pumping stations. GIS maps were used to track the daily progress of the dewatering effort. Figure 3 illustrates the dewatering condition on September 2 and figure 4 illustrates the progress made in dewatering by September 15. The plan was to have major pumping operations begin as soon as the levee breaches were closed. Pumping began at the 17th Street Canal site on September 5, at the London Avenue canal location on September 10, and at the other locations throughout the city using portable pumps. Working twenty four hour days throughout September New Orleans was close to being pumped out when Rita swept through on September 24, reflooding almost forty percent of the area again, causing more damage to Southeast Louisiana. But even with the Rita set back, the New Orleans dewater effort was completed on October 11. Dewatering was completed in just forty three days, less than half the time estimated by some.

For the water quality aspects of the dewatering operation EPA emergency response personnel worked in partnership with FEMA and state and local agencies and the Corps to help assess the test results and evaluate health and environmental conditions to water quality from Hurricanes Katrina and Rita. In emergency situations such as this, EPA serves as the lead Agency for water quality including the cleanup of hazardous materials such as oil and gasoline. EPA national and regional Emergency Operations Centers were activated 24 hours a day. The Corps had employees embedded with the EPA/LDEQ team in Baton Rouge and onsite teams locally in New Orleans for rapid and effective communication regarding water quality issues. There were also numerous conference calls involving Corps and EPA Headquarters representatives with field personnel to advise and assist on water quality issues during dewatering.

The large amounts of water resulting from the hurricanes may have actually helped some of the water pollution concerns particularly in Lake Pontchartrain due to dilution. The large volumes of water from outside the city also provided dilution to the flood waters, and the time consuming process of dewatering allowed many solids to settle, likely removing some sorbed constituents from the water column. Lake Pontchartrain seems to have survived its hurricane-induced direct hit, but longer term data will be needed for the final assessment. Concerns have also been raised about impacts on the Gulf of Mexico. From a volumetric standpoint, these impacts are minimal - more water enters the Gulf from the Mississippi River every day than was moved out of New Orleans over the 43-day dewatering operation.

New Orleans pumps water into Lake Pontchartrain instead of the Mississippi River because the lake level is lower than the river's level. The estimated 5000 billion gallons (BG) of rain from Hurricane Katrina that fell on the continental US is based on the assumption of an average rainfall of 4" across the 90,000 square miles of federally declared disaster areas. Lake Pontchartrain, the chief receiving water for the waters removed from New Orleans, is a 640- square mile tidal basin with an average depth of about ten feet. The lake receives about ten billion gallons a day of freshwater inflows from its 4,500 square mile watershed. Its volume of 1,300 billion gallons would fit in a cube 5,600 feet on a side - slightly more than a cubic mile. By contrast the long-term average volume passing New Orleans in the Mississippi River every day is 400 billion gallons. The Corps of Engineers directed the removal of an estimated 200 billion gallons of floodwaters through dewatering breaches and pumping. About a quarter to a third of this volume was removed from inside New Orleans' levees. The average daily volume dewatered over the 43-day operation was about five billion gallons.

The floodwaters removed from New Orleans proper consisted of a mixture of rain, Gulf of Mexico and Lake Pontchartrain waters, and other constituents. The rainfall estimate assumes16 inches of Katrina and Rita rainfall across New Orleans' 75 square miles. Under normal conditions, New Orleans is able to pump 25 billion gallons per day - out of the city into Lake Pontchartrain. This is about the same volume that the Ohio River carries by Cairo, IL every day. However, Hurricane Katrina caused major damage to all of New Orleans pumping stations that significantly delayed getting them back into full operation.

3. EXPEDIENT WATER QUALITY MEASURES

EPA coordinated closely with the Corps in consideration of a number of alternative measures for the treatment of floodwaters and mitigation of potential environmental impacts on Lake Pontchartrain, from New Orleans floodwaters. The objective was to dewater New Orleans as quickly as possible but to do it in an environmentally sound manner. The major concern was minimizing the environmental impact of the pumped floor water. A number of treatment processes were evaluated for application in New Orleans.

An interagency technical sub-group (water quality/ecosystem restoration management experts) collaboratively identified an array of recommendations for preventative and remedial mitigation management actions during dewatering for both inside and outside the levees. Based on the interagency recommendations and the dewatering mission, the Corps deployed sorbent booms with sorbent skirts inside the levees at appropriate intake points. There was a special management strategy for appropriate containment and treatment of HOT-SPOT areas identified by personnel on the ground as the water lowers.

One was the deployment of temporary "floating passageways" for in-canal treatment. This configuration of floating passageway curtains in conjunction with injected flocculants and disinfectants was proposed for the 10,000 cfs discharge from Pumping Station #6 on the 17th Street Canal. The curtains lengthen the flow path and augment settling; trash and debris are captured by the net curtain at the end of the canal. An illustration of the approach is shown in figure 5. Dosing requirements for the suggested mix of a cationic coagulant in conjunction with an anionic polymer would be matched to the application. Similar configurations were developed for direct discharges to Lake Pontchartrain. Another was the use of Sequestration, Flocculation and Sedimentation materials for Removing Contaminants from Flooded Areas of New Orleans.

In addition to floating debris of various size many contaminants associated with flooding are essentially small colloidal particulates that are suspended in the water column. These include many organic contaminants, metals, and disease causing microorganisms. In addition, suspended clay particulates can hold adsorbed contaminants. Due to electrostatic charges found on the colloids, these particles can remain suspended indefinitely. However, coagulation, flocculation, and sedimentation (CFS) are accepted, established and commonly used set of methodologies to remove colloidal contaminants. CFS involves adding a chemical to overcome the electrostatic barriers between the particles, allowing the colloids to interact with each other to form larger particles, following by gravity settling of the larger particles. Large-scale applications of CFS have been conducted at lakes in Washington and Idaho to remove excess nutrients causing eutrophication, demonstrating its applicability in an environment with relatively low control. The large pools of floodwaters in New Orleans were an excellent opportunity to apply these methods to remove these colloidal contaminants.

The technology was deployed at the 95 acre Agriculture Street Landfill Superfund Site, which is a submerged CERCLA site in New Orleans. The treatment consisted of the addition of powdered activated carbon (PAC) and a synthetic polymeric coagulant, such as polystyrene sulfonate (a jar test would be conducted to select the exact coagulant and dosage). Based on experience with dredge waters in the same area, relatively modest dosages of these chemicals were needed to treat relatively large water volumes. Low tech barriers to reduce the sediment migration such as submerged sandbags, were used to create sedimentation areas are reduce off-site migration of contamination.

Though most of the City was dry by Sept 30, the Corps still is treating water in the three main canals, Orleans, London and 17th Street. The Corps has deployed artificial aeration devices in major channels to reduce biological oxygen demand (BOD) and support healthy dissolved oxygen concentrations in the water column. Two aerators in each of the three main channels draining to Lake Pontchartrain were strategically placed and operating successfully prior to Hurricane Rita and 20 more aerators are being placed in these and other strategic locations, even in the outfall areas of Lake Pontchartrain. More aerators also are being planned – about an additional 20, or total of 40. After a suspension of pumping operations during Hurricane Rita the Corps has resumed the aeration operations, and coordinated with the U.S. Coast Guard to deploy booms, skimmers, and suction at pumping stations where oil was observed. Based on input from EPA, the Corps is doing its best to address bacteria, suspended solids, and petroleum in storm water runoff. Options include more booms, silt screens, aerators, and possibly adding some mobile treatment plants. EPA and the Corps jointly formulated approaches to manage known and suspected areas of hazardous materials production and storage, and areas with contaminant sequestration materials such as flocculation, disinfection, and sorption.

The Corps also developed a comprehensive non-point source control program to manage the first flush of rainfall from contaminated residuals as well as developing and executing programs to clean streets, canals, storm drains of contaminated residuals to minimize their flushing when receiving waters during rainfall events. This approach was formulated collaboratively between the Corps and EPA and coordinated with State and Local governments and water boards.

In addition to the floodwaters, the EPA and State of Louisiana are sampling and monitoring the sediments left behind from the New Orleans floodwaters for possible contaminants and infectious agents. Sampling site locations within New Orleans are shown in figure 6. Effective sampling and analysis are critical to effective evaluation and characterization to assure proper handling and disposal. The Corps and its contractors are working closely with the EPA and state of Louisiana to assure that this is achieved in a safe manner.

4. WATER QUALITY SAMPLING

EPA in coordination with the Louisiana Department of Environmental Quality performed chemical sampling of New Orleans flood waters for over one hundred priority pollutants such as volatile organic compounds (VOCs), semi volatile organic compounds (SVOCs), total metals, pesticides, herbicides, and polychlorinated biphenyls (PCBs). More than 190 water quality data parameters are constantly being updated, reviewed and validated through an EPA quality assurance process to ensure scientific accuracy. Example results are shown in tables 1 – 4 for testing of Primary pollutants. Table 1 lists the one pollutant, lead, that was found in this testing data that exceeded the EPA standard. Table two lists pollutants that were present but did not exceed EPA standards. Lead was the one pollutant most often found at measurement sites. However, when measured it was at locations that have historically been high in lead content. Table three lists material present but there are no standards at this time. Table four lists pollutant that was not present. Concerns about potential water-quality issues prompted discussions among the U.S. Environmental Protection Agency (EPA), Louisiana Department of Environmental Quality (LDEQ), and the LWSC to coordinate sampling locations and constituents sampled. The LWSC sampled fecal-indicator bacteria in Lake Pontchartrain in support of the LDEQ monitoring effort and water and bed-sediment samples from those areas in the lake not sampled by LDEQ. Dewatered sediments deposited by floodwaters were sampled in New Orleans and St. Bernard Parish as floodwaters retreated to determine what chemicals were in these sediments. At the same time high water marks along the north shore of Lake Pontchartrain, and in St. Bernard and Plaquemines Parishes were collected.

EPA, USGS and the State of Louisiana assessed Lake Pontchartrain as part of the broad, multi-agency assessment of damages to the region. Many of Katrina's impacts will emerge over different time spans and this mid- to long-term monitoring plan has been designed to detect effects as they appear. Most Pontchartrain sampling was done by the USGS and the State in collaboration with EPA. The Louisiana Department of Environmental Quality sampled Lake Pontchartrain and found no exceedances of water quality standards for organic and toxic compounds. Dissolved oxygen and bacterial impacts were most pronounced along the North Shore, while toxicity testing of New Orleans floodwaters showed little effect on fish and invertebrates.

Understanding why the floodwaters were not the toxic "witches brew" reported in the media depends on consideration of where the floodwaters came from. Perhaps 20 billion gallons (BG) of the New Orleans floodwater was rainfall, carrying little or no contamination. Human waste in the form of raw sewage was certainly present, but the total volume of effluent is not likely to be much beyond the 0.22 BG daily capacity of New Orleans' Dunbar WWTP. An additional small volume (with disproportionately large potential water quality impact) can be attributed to petroleum products and household wastes leaking out of cars and containers. The remainder - nearly 40 BG - must have been a combination of Lake Pontchartrain waters and the storm surge from the Gulf of Mexico.

The waters entering from outside the levees are likely to have been heavily laden with resuspended bottom sediments. However, extensive pre-1990 shell dredging covering two-thirds of Lake Pontchartrain may have helped bury deposited metals and other toxics, making these waters comparatively clean from a human health risk standpoint (Mannheim). If so, the 1+ BG of sewage, petroleum products, and household wastes inside New Orleans were mixed with 60 BG of comparatively clean water. The 1300 BG volume of Lake Pontchartrain also acted as a buffer to water quality impacts, providing an additional opportunity for dilution.

4.1 Contaminant metals

Except for samples in the vicinity of New Orleans canal mouths, means of contaminant metals in analyzed sediment samples from Lake Pontchartrain were found to be lower than those from Mississippi River suspended matter, and in the range of pristine sediments. This surprising result can be explained by the fact that an estimated 2/3 of the total area of Lake bottoms had been dredged for clam shells prior to 1990. Core profiles were analyzed for trace metals. The profiles revealed that dredging had mixed pristine sediments with very low metal concentrations with shallow surficial sediments that had increased contaminant levels (but below toxicity guidelines) down to depths of nearly 3 m.

Water sampling by the Louisiana Department of Environmental Quality and partner organizations has found detectable contaminant metals rare in city flood waters. Unless increased concentrations of hazardous metals emerge in the rain water flushes from the city, the likelihood of significant enhanced contamination by metals in the sediments outside areas immediately adjacent to pumping station outfall appears small.

4.2 Toxic organic compounds

EPA in coordination with the Louisiana Department of Environmental Quality performed chemical sampling of New Orleans flood waters for over one hundred priority pollutants such as volatile organic compounds (VOCs), semi volatile organic compounds (SVOCs), total metals, pesticides, herbicides, and polychlorinated biphenyls (PCBs). Flood water sampling data for chemicals are being posted from September 3, 2005 on as they become available. The data has been reviewed and validated through a quality assurance process to ensure scientific accuracy.

Principal toxic compounds can be divided into three categories: polyaromatic hydrocarbons (PAHs) found in petroleum and coal tar products, polychlorinated biphenyls (PCBs), and pesticides and miscellaneous chemicals (see tables 1-4). PAH concentrations studied in the previous database were far lower than might have been expected, but for reasons different than in the case of metals. Unchlorinated hydrocarbons are broken down rapidly by microbial attack in warm salty waters like those of Lake Pontchartrain (about 1/10 to 1/8th the saltiness of seawater). Even stations near earlier creosote spills on the north coast of Lake Pontchartrain showed only faint traces of what must have been earlier heavy contamination from former Superfund sites, and former sites of offshore oil wells in Lake Pontchartrain. Recent reports by the Louisiana Department of Environmental Quality (DEQ) and partner agencies have reported no oil sheen in offshore water sampling sites investigated. This suggests that evaporation and biochemical breakdown of petroleum has already removed much of the oil reported to be dispersed in the flood waters. Early, alarming newspaper reports of spill of 78,000 barrels of oil in New Orleans posed much more serious concern. This spill turns out to have occurred not in New Orleans, but well downstream in the Mississippi River, at storage tanks Cox Bay.

Chlorinated hydrocarbons are 100 times or more resistant to bacterial breakdown than

PAHs in the natural environment. However, the earlier inventory showed that these compounds too were well below toxic levels in sediments, except for isolated occurrences in the immediate vicinity of New Orleans' canals. In the decades since the early 1970s, PCBs and long-lived pesticides like DDT, dieldrin, and aldrin have been systematically removed from use in the U.S., and none were detected in the initial DEQ samplings.

4.3 Biological (sewage-related) and nutrient loads.

Two contaminants prominently identified in New Orleans flood waters were fecal coliform bacteria of sewage origin, and oil. Pathogens dispersed and diluted in Lake waters are expected to be broken down quickly. The load of sewage-derived organic matter is reflected in reduced oxygen levels in DEQ-sampled waters at. However, stations ½ mile from shore showed oxygen levels within the normal range. Table five shows E. coli testing results for September 8 at locations throughout New Orleans.

Once the sewage-derived organic matter is broken down into its component nutrients – especially nitrogen, a secondary bloom of phytoplankton is expected – which may extend farther into the Lake through normal dispersion and mixing. Information on this secondary productivity is not yet available. It could be tracked synoptically by multispectral satellite data as reported in by Stumpf in the abovementioned report and shown in the oral presentation.

The efforts of relevant New Orleans and Louisiana agencies, stimulated by the urgings and studies of public organizations like *Save Our Lake*, coastal New Orleans beaches became swim able and fishable in recent years. Hurricane Katrina also caused large-scale sediment and bottom topographic changes that remain to be assessed However, assuming appropriate restoration and upgrading of water treatment facilities and other appropriate measures in New Orleans, and barring factors not currently known, there should be few long-lasting contaminant influences that would inhibit restoration and future recreational use of New Orleans' shoreline.

Flood water samples for September 16, 2005 indicated that slightly elevated levels of hexavalent chromium were detected in two samples and manganese was detected at elevated levels in seven samples. Lead and arsenic were also found in two samples at levels which exceed the drinking water action levels. The Center for Disease Control (CDC) concluded that exposures at these levels during response activities would not be expected to cause adverse health effects.

4.4 Sediment Sampling

When Hurricane Katrina flooded the city of New Orleans, one of many concerns in its wake was contamination. Several chemical plants, petroleum refining facilities, and contaminated sites, including Superfund sites, were covered by floodwaters. In addition, hundreds of commercial establishments, such as service stations, pest control businesses, and dry cleaners, may have released potentially hazardous chemicals into the floodwaters. Figure 7 shows potential petroleum-related release points, including refineries, oil and gas wells, and service stations in the city relative to water inundation damage. There were also major hazardous-materials storage locations, Superfund sites, and Toxic Release Inventory reporting facilities located in the larger New Orleans area. Some of these sites located within the city are shown in figure 8.

Adding to the potential sources of toxics and environmental contaminants are metal-contaminated soils typical of old urban areas and construction lumber preserved with creosote, pentachlorophenol, and arsenic. Compounding these concerns is the presence of hazardous chemicals commonly stored in households and the fuel and motor oil in approximately 400,000 flooded automobiles.

Uncontrolled biological wastes from both human and animal sources also contributed to the pollutant burden in the city.

Sediment, for the purposes of the hurricane response sampling effort, are defined as residuals deposited by receding flood waters which may include historical sediment from nearby water bodies, soil from yards, road and construction debris, and other material. Preliminary results indicate that some sediment may be contaminated with bacteria and fuel oils and human health risks may therefore exist from contact with sediment deposited from receding flood waters. As sediments begin to dry, EPA performed air sampling to monitor potential inhalation risks and will also assess long-term exposure scenarios.

E. coli was detected in sediment samples but no standards exist for determining human health risks from E. coli in soil or sediment. The presence of E. coli, however, does imply the presence of fecal bacteria and exposure to sediment should therefore be limited if possible. In the event contact occurs, EPA and the Centers for Disease Control (CDC) strongly advised the use of soap and water, if available, to clean the exposed areas, and the removal of contaminated clothing.

Of the 430 sediment samples collected by EPA between September 10 and October 14, a number exceeded screening criteria of the local regulatory authority, the Louisiana Department of Environmental Quality (LDEQ Risk Evaluation/Corrective Action Program or RECAP) (LDEQ, 2005). These criteria were developed to meet objectives similar to those of the EPA Health Specific Screening Levels and are similarly derived. The constituents most often found to exceed the RECAP screening criteria were arsenic, lead, several PAHs (including benzo[a]pyrene), and diesel range organics. Figure 9 illustrates the sediment sampling sites that were in operation in the New Orleans area.

On November 19 and 20, EPA resampled areas where previous sampling had indicated contaminant concentrations in excess of screening criteria and where sediment depth equaled or exceeded 0.5 inches (EPA, 2005b). Because of the complex nature of the storm surge and levee breaches and overtopping, the amount of sediment deposited in flooded areas varied widely, and only 14 of the 145 locations had sufficient sediment depth. Three samples showed arsenic concentrations higher than 12 mg/kg (14.4–17.6 mg/kg); one sample showed benzo[a]pyrene concentration of 0.77 mg/kg; and one sample showed a concentration of diesel range organics of 2,100 mg/kg. Other samples were below applicable screening values.

Samples were also collected at specific sites where there were known or potential leaks of hazardous materials. Elevated concentrations of total petroleum hydrocarbons and a variety of crude oil-associated contaminants were observed in the vicinity of the Murphy Oil crude oil tank failure and spill, which had a clearly identifiable source and could be easily differentiated from the general flooding-related contamination. This area is being managed separately from the rest of the flooded area and is not considered further here.

4.5 Tissue Sampling

In response to public concern for the water quality and related sea food contamination of Lake Pontchartrain and in the Gulf following Hurricane Katrina, the U.S. Geological Survey (USGS), in collaboration with the Louisiana Department of Environmental Quality (DEQ), U.S. Environmental Protection Agency (EPA), National Oceanic and Atmospheric Administration (NOAA), and the Food and Drug Administration (FDA), is conducting intensive studies of water, sediment, and seafood quality of Lake Pontchartrain and the Gulf coastal region. Seafood harvesting in most of this area was stopped following the hurricane events and was reopened after tissue testing showed no presents of contamination. Figure 10 shows the location of sampling sites in the Gulf coastal region that were used in to evaluate the condition of sea organisms.

Findings suggest that, despite expectations that hurricane-related flooding in New Orleans could cause uniformly high concentrations of fecal bacteria in Lake Pontchartrain, water samples from sites in and around the lake commonly were within limits acceptable for recreational waters.

These results represent a first round of testing following Hurricanes Katrina and Rita. The Louisiana DEQ is continuing to monitor bayous along the north side of Lake Pontchartrain, areas found to be 'hot spots' in samples collected immediately following Hurricane Rita. USGS scientists measured fecal-indicator bacteria *Escherichia coli* (*E. coli*), enterococci, and fecal coliforms over a 3 week period. These indicator bacteria are not themselves pathogens, but scientists monitor for them because they are useful indicators of fecal contamination and the possible presence of pathogens. Concentrations in samples they collected in the third and fourth week after passage of Hurricane Katrina commonly were less than U.S. EPA criteria for *E. coli* and enterococci in fresh or marine waters and also met the Louisiana DEQ standard for fecal coli form bacteria. A week later, following the passage of Hurricane Rita, concentrations at several tributary sites were well above the criteria and standard, while concentrations in the lake remained generally below or near those limits.

Scientists collected water samples at 22 sites—including most inflows to the lake, sites within the lake, and the major outflows to the Gulf of Mexico by way of Lake Borgne and the Mississippi Sound. Nineteen of the sites are routinely sampled as part of the Louisiana DEQ ambient monitoring network. Corresponding data on water temperature, specific conductance (a measure of salinity), pH, and dissolved oxygen also were collected at each site at the time of sampling.

The scientists were especially interested to find the highest concentrations of fecal contamination in north shore tributaries rather than in the south shore canals that carried flood water from New Orleans into Lake Pontchartrain. Dennis Demcheck, the USGS hydrologist at Baton Rouge, La., who led the sampling effort, attributed this to a "settling pond" effect in New Orleans, which held flood waters during the weeks prior to pumping them back into Lake Pontchartrain.

The study included an extensive quality-control data set, and that data set largely indicates satisfactory analytical performance, even though scientists were working out of a mobile lab in less than ideal field conditions. These results are intended to help in completing the regional Interagency Environmental Assessment underway by USGS, U.S. EPA, NOAA and FDA.

5. CONCLUSIONS

The flooding in New Orleans resulted in the potential for unparalleled exposure to toxics and contaminants. Initial concerns about a "toxic gumbo," however, have not been supported by sampling and analyses to date. Although floodwaters did contain significant short-term biological hazards that posed risks to stranded residents and relief workers, they did not contain chemical toxicants at levels that are expected to lead to long-term impacts on the surroundings beyond the impacts expected of a similar volume of stormwater from the city. The floodwaters undoubtedly redistributed some contaminants, but the contaminant burden in soils and sediments appears to have generated few concerns for acute exposure and risk. However, although acute generalized hazards have not been identified, the population of New Orleans faces localized areas of more serious contamination, such as the neighborhoods impacted by failure of a crude-oil storage tank in St. Bernard Parish. The most serious continuing issue facing most residents is the presence of high concentrations of mold and airborne mold spores. However, respiratory protection during the removal of all mold-contaminated materials and reconstruction can mitigate the risk.

Ultimately, the lessons learned from Katrina should be crystallized in a generic form so that the country as a whole will be better prepared for the next natural disaster, major industrial accident, or act of terrorism. Thus, every effort should be made to focus on the way information is processed in emergency situations and to make sensible, safe, and equitable cleanup/habitability decisions in an environment of great uncertainty. Because existing institutions were largely unprepared for a disaster of the scale of Katrina, it may not be possible to implement these principles in New Orleans. However, we can learn from Katrina and provide more effective responses to future catastrophes.

6. REFERENCES

EPA (U.S. Environmental Protection Agency). 2005a. EPA Region 6: Human Health Medium-Specific Screening Levels. Available online at: http://www.epa.gov/earth1r6/6pd/rcra_c/pd-n/r6screenbackground.pdf at 3 of 37 (Region 6 Screening Value Guidance).

EPA. 2005b. Hurricane Response 2005: Environmental Assessment Summary for Areas of Jefferson, Orleans, St. Bernard, and Plaquemines Parishes Flooded as a Result of Hurricane Katrina Available online at http://www.epa.gov/katrina/testresults/katrina_env_assessment_summary.htm.

EPA. 2005c. Hurricane Response 2005: Murphy Oil Spill. Available online at: http://www.epa.gov/katrina/testresults/murphy/index.html.

EPA. 2005d. Summary of Testing at Superfund National Priority List Sites: Agriculture Street Landfill, Orleans Parish, New Orleans, LA. Available online at: http://www.epa.gov/katrina/superfund-summary.html#2.

EPA. 2005e. Superfund Information Systems: Record of Decision System (RODS). Available online at: http://www.epa.gov/superfund/sites/rods/index.htm.

EPA. 2005f. Updated EPA Region 6 Internet Version of Risk-Based Human Health Screening Values. Available online at: http://www.epa.gov/earth1r6/6pd/rcra_c/pd-n/screen.htm.

Gustavsson, N., B. Bølviken, D.B. Smith, and R.C. Severson. 2001. Geochemical Landscapes of the Conterminous United States—New Map Presentations for 22 Elements. U.S. Geological Survey Professional Paper 1648. Denver, Colo.: U.S. Geological Survey. Available online at: http://pubs.usgs.gov/pp/p1648/p1648.pdf.

Janda, J.M., and P.S. Duffey. 1988. Mesophilic aermonads in human disease: current taxonomy, laboratory identification and infectious disease spectrum. Reviews of Infectious Diseases 10(5): 980–997.

LDEQ (Louisiana Department of Environmental Quality). 2003. Risk Evaluation/Corrective Action Program (RECAP). Final Report. Available online at: http://deq.louisiana.gov/portal/Portals/0/technology/recap/2003/RECAP%202003%20Text%20-%20final.pdf.

Louisiana Department of Environmental Quality, Water Quality Assessment Division. *Post-Katrina Water Quality Assessment*. Web Release Date: 11-Sep-2005; http://www.deq.louisiana.gov/news/pdf/Post-KatrinaWaterQualityAssessment9-20-05.ppt

LDEQ. 2005. RECAP: Risk Evaluation/Corrective Action Program. Available online at: http://deq.louisiana.gov/portal/tabid/131/Default.aspx.

Manheim, Frank T. *Interpreting the Influence of Contaminants in Flood Waters from New Orleans on Lake Pontchartrain.* Geological Society of America, 2005 Annual Meeting Paper #LB1-5. http://gsa.confex.com/gsa/2005AM/finalprogram/abstract_98411.htm

Mielke, H.W., G. Wang, C.R. Gonzales, E.T. Powell, B. Le, and V.N. Quach. 2004. PAHs and metals in the soils of inner-city and suburban New Orleans, Louisiana, USA. Environmental Toxicology and Pharmacology 18(3): 243–247.

NIEHS (National Institute of Environmental Health Sciences). 2005. Geographic Information Systems. Environmental Health Science Data Resource Portal: Hurricanes Katrina and Rita. Available online at: http://cleek.ucsd.edu:8080/gridsphere/gridsphere?cid=gisimages.

NRDC (Natural Resources Defense Council). 2005a. Mold: Health Effects of Mold. Available online at: http://www.nrdc.org/health/effects/katrinadata/mold.asp.

NRDC. 2005b. New Orleans Environmental Quality Test Results. Available online at: http://www.nrdc.org/health/effects/katrinadata/contents.asp.

NRDC. 2005c. Sampling Results: Bywater/Marigny Including Agriculture Street Landfill. Available online at: http://www.nrdc.org/health/effects/katrinadata/bywater.asp.

Pardue, J.H., W.M. Moe, D. McInis, L.J. Thibodeaux, K.T.
Valsaraj, E. Maciasz, I. Van Heerden, N. Korevec, and Q.Z. Yuan. 2005. Chemical and microbiological parameters in New Orleans floodwater following hurricane Katrina. Environmental Science and Technology 39(22): 8591–8599.

Pelley, J. 2006. Lead: a hazard in post-Katrina sludge. Environmental Science and Technology 40(2): 414–415. Available online at: http://pubs.acs.org/subscribe/journals/esthag-a/40/i02/html/011506news3.html.

Presley, S.M., T.R. Rainwater, G.P. Austin, S.G. Platt, J.C. Zak, G.P. Cobb, E.J. Marsland, K. Tian, B. Zhang, T.A. Anderson, S.B. Cox, M.T. Abel, B.D. Leftwich, J.R. Huddleston, R.M. Jeter, and R.J. Kendall. 2006. Assessment of pathogens and toxicants in New Orleans, LA following Hurricane Katrina. Environmental Science and Technology 40(2): 468–474.

WSDA (Washington State Department of Agriculture). 2001. Pesticide Management Database. Olympia, Wash.: WSDA.

Louisiana Department of Environmental Quality, Water Quality Assessment Division. *Post-Katrina Water Quality Assessment*. Web Release Date: 11-Sep-2005; http://www.deq.louisiana.gov/news/pdf/Post-KatrinaWaterQualityAssessment9-20-05.ppt

Manheim, Frank T. *Interpreting the Influence of Contaminants in Flood Waters from New Orleans on Lake Pontchartrain.* Geological Society of America, 2005 Annual Meeting Paper #LB1-5. http://gsa.confex.com/gsa/2005AM/finalprogram/abstract_98411.htm

Pardue, J.H. ,W. M. Moe, D. McInnis, L. J. Thibodeaux, K. T. Valsaraj, E. Maciasz, I. van Heerden, N. Korevec, and Q. Z. Yuan. *Chemical and Microbiological Parameters in New Orleans Floodwater Following Hurricane Katrina.* Environ. Sci. Technol.; 2005; ASAP Web Release Date: 11-Oct-2005; http://pubs.acs.org/cgi-bin/sample.cgi/esthag/asap/abs/es0518631.html

US EPA. EnviroMapper for Hurricanes Katrina and Rita. http://www.epa.gov/enviro/katrina/

US Geological Survey. Environmental Atlas of the Lake Pontchartrain Basin. USGS Open File Report 02-206. http://pubs.usgs.gov/of/2002/of02-206/index.html

Table 1: Sampled, Found Exceeds EPA Limits

CASNumber	Name	Measured Level (μg/L)	EPA Limit (μg/L)
7439-92-1	Lead	20	15

Table 2: Sampled, Found meets EPA Limits

CASNumber	Name	Measured Level (μg/L)	EPA Limit (μg/L)
7440-39-3	Barium	210	2000
7440-50-8	Copper	62	1300
57-12-5	Cyanide	29.7	200

Table 3: Sampled & Found No EPA Limits

CASNumber	Name	Measured Level (μg/L)
7429-90-5	Aluminum	1290
7440-70-2	Calcium	111000
7439-89-6	Iron	1930
7439-95-4	Magnesium	99200
7439-96-5	Manganese	669
7440-02-0	Nickel	22
7440-09-7	Potassium	52700
7440-22-4	Silver	12
7440-23-5	Sodium	724000
7440-66-6	Zinc	292

Table 4: Toxic Organic Compounds and Metals Sampled & Not Found

Name
.alpha.-Endosulfan
.alpha.-Hexachlorocyclohexane
.beta.-Endosulfan
.beta.-Hexachlorocyclohexane
.delta.-Hexachlorocyclohexane
1,1,1-Trichloroethane
1,1,2,2-Tetrachloroethane
1,1,2-Trichloroethane
1,1-Dichloroethane
1,1-Dichloroethylene
1,2,4-Trichlorobenzene
1,2-Dichloroethane
1,2-Dichloropropane
1,2-Diphenylhydrazine
1-Propene, 1,3-dichloro-, (Z)-
2,4,5-T
2,4,6-Trichlorophenol
2,4-D, Dichlorophenoxyacetic acid
2,4-Dichlorophenol
2,4-Dimethylphenol
2,4-Dinitrophenol
2,4-Dinitrotoluene
2,5-Dichlorophenol
2,6-Dichlorophenol
2,6-Dinitrotoluene
2-Chloroethyl vinyl ether
2-Chloronaphthalene
3,3'-Dichlorobenzidine
3,4-Dichlorophenol
Hexachlorobutadiene
Indeno[1,2,3-cd]pyrene
Mercury
Methylene chloride
Naphthalene
Phenanthrene
Selenium
Thallium
Tribromomethane
Vinyl chloride
Acenaphthene
Acenaphthylene
Acrolein
Acrylonitrile
Aldrin
Anthracene
Antimony
Aroclor 1016
Aroclor 1221
Aroclor 1232
Aroclor 1242
Aroclor 1248
Aroclor 1254
Aroclor 1260
Arsenic
Benz[a]anthracene
Benzene
Benzidine
Benzo(b)fluoranthene
Benzo[a]pyrene
Benzo[ghi]perylene
Benzo[k]fluoranthene
Benzoic acid
Beryllium
Bis(2-chloroethoxy)methane
Bis(2-chloroethyl) ether
Bis(2-chloroisopropyl) ether
Bis(2-chloroisopropyl) ether
Butyl benzyl phthalate
Hexachlorocyclopentadiene
Isophorone
Methoxychlor
N-Nitrosodi-n-propylamine
Nitrobenzene
Phenols
Silvex
Toluene
Trichloroethylene
m-Chlorophenol
Carbazole
Carbon tetrachloride
Chlordane, technical
Chlorobenzene
Chlorodibromomethane
Chloroethane
Chloroform
Chloromethane
Chromium
Chromium(VI)
Chrysene
Cobalt
Di(2-ethylhexyl) phthalate
Di-n-octyl phthalate
Dibenz[a,h]anthracene
Dibutyl phthalate
Dichlorobromomethane
Dieldrin
Diethyl phthalate
Dimethyl phthalate
Dinitro-o-cresol
Endosulfan sulfate
Endrin
Endrin aldehyde
Endrin ketone
Ethylbenzene
Fluoranthene
Fluorene
Heptachlor
Hexachloroethane
Lindane
Methyl bromide
N-Nitrosodimethylamine
Pentachlorophenol
Pyrene
Tetrachloroethylene
Toxaphene
Vanadium
m-Dichlorobenzene

Table 5: Example of EPA Biological Water sample data for New Orleans on September 8, 2005

Sample Date	County	Location Description	Sample Number	Bacteria	Colonies/100mL
9/8/2005	JEFFERSON	Bonneville Canal	15178	E. coli	5818
9/8/2005	JEFFERSON	Outfall	15561	E. coli	6260
9/8/2005	JEFFERSON	Outfall	15562	E. coli	7568
9/8/2005	ORLEANS	Louisa & Almonaster	15172	E. coli	462
9/8/2005	ORLEANS	Independence & Marais	15175	E. coli	7308
9/8/2005	ORLEANS	Independence & Marais	15176	E. coli	8212
9/8/2005	ORLEANS	Kenilworth Canal	15177	E. coli	5702
9/8/2005	ORLEANS	610 & I-10 split	15180	E. coli	11588
9/8/2005	ORLEANS	W610 Exit 4	15181	E. coli	9768
9/8/2005	ORLEANS	Chantilly & Chef HWY	15184	E. coli	610
9/8/2005	ORLEANS	Wilson & Chef HWY	15185	E. coli	1820
9/8/2005	ORLEANS	Schinduie Dr & Chef HWY	15188	E. coli	264
9/8/2005	ORLEANS	I-510 & Chef HWY	15189	E. coli	462
9/8/2005	ORLEANS	Mayo Rd & Dwyer Rd	15192	E. coli	2356
9/8/2005	ORLEANS	Louisa & Chef Menteur	15196	E. coli	976
9/8/2005	ORLEANS	Paris Ave & Prentiss Ave.	15198	E. coli	3348
9/8/2005	ORLEANS	Paris Ave & Prentiss Ave.	15202	E. coli	4210
9/8/2005	ORLEANS	Marais & Poland Ave	16190	E. coli	8704
9/8/2005	ORLEANS	W610 Exit 2C	16198	E. coli	6896
9/8/2005	ORLEANS	610 & Elysian Fields	16199	E. coli	5226
9/8/2005	ORLEANS	Croader Blvd & Chef HWY	16200	E. coli	576
9/8/2005	ORLEANS	Hickerson Dr. & Chef HWY	16201	E. coli	346
9/8/2005	ORLEANS	E. AdamsCt & Chef HWY	16202	E. coli	4196
9/8/2005	ORLEANS	LakeForestBlvd & SamOvar Dr.	16203	E. coli	862
9/8/2005	ORLEANS	Dwyer Rd & I-10	16204	E. coli	1970
9/8/2005	ORLEANS	StephenGirard & St Ferindad	16205	E. coli	1508
9/8/2005	ORLEANS	Chef Menteur & Iroquois St	16206	E. coli	3870
9/8/2005	ORLEANS	Paris Ave & Lafreniere St.	16207	E. coli	4718
9/8/2005	ORLEANS	Paris Ave & Mirabeau Ave	16208	E. coli	2402
9/8/2005	ORLEANS	Franklin Ave & Gentilly Rd	16209	E. coli	992
9/8/2005	ORLEANS	Franklin Ave & Mirabeau Ave	16210	E. coli	5702

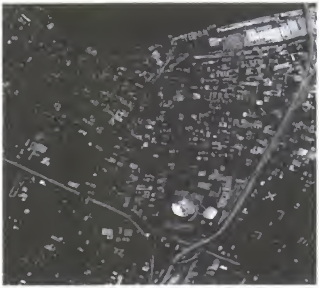

Figure 1: Aerial view of New Orleans Flood

Figure 2: Portable Pump Operation

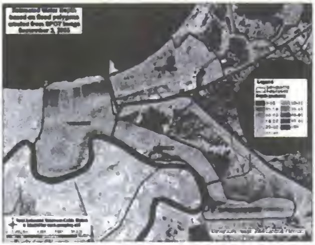

Figure 3: Flooded Area on Sept 2

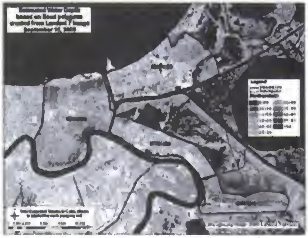

Figure 4: Flooded Area on Sept 15

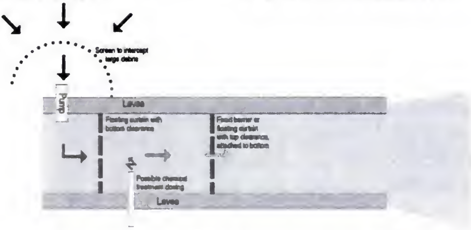
Screen to intercept large debris
Pump
Levee
Floating curtain with bottom clearance
Fixed barrier or floating curtain with top clearance, attached to bottom
Possible chemical treatment dosing
Levee

Figure 5. Illustration on in-canal expedient water treatment system

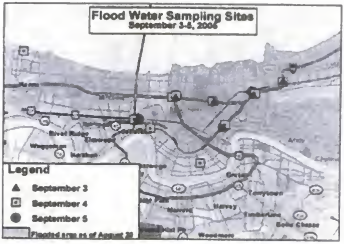

Figure 6: Flood Water Sampling Sites

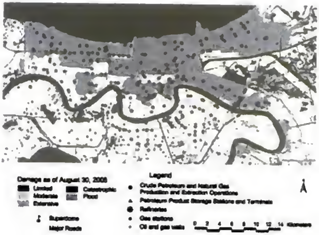
Damage as of August 30, 2005
Limited
Catastrophic
Moderate
Flood
Extensive
Superdome
Major Roads
Legend
Crude Petroleum and Natural Gas Production and Extraction Operations
Petroleum Product Storage Stations and Terminals
Refineries
Gas stations
Oil and gas wells
0 2 4 6 8 10 12 14 Kilometers

Figure 7: Petroleum Risk Sites

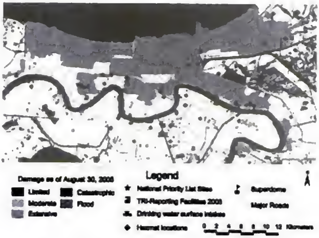
Damage as of August 30, 2005
Limited
Catastrophic
Moderate
Flood
Extensive
Legend
National Priority List Sites
TRI-Reporting Facilities 2003
Drinking water surface intakes
Hazmat locations
Superdome
Major Roads
0 2 4 6 8 10 12 Kilometers

Figure 8: Critical Infrastructure Risk Sites

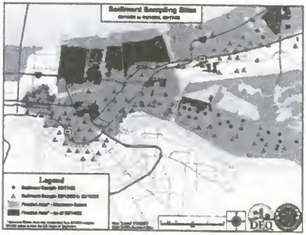

Figure 9: Sediment Sampling Sites

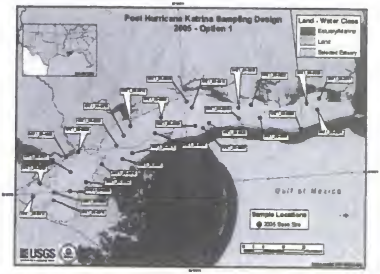

Figure 10: Tissue Sampling Sites in the Gulf Coastal Area

PWRI's New Organizations and Research Projects on Natural Disasters

by

Tadahiko Sakamoto[1] and Hiroshi Sato[2]

ABSTRACT

The second medium-term plans with the new 17 Priority Research Projects started in April 2006 at the Incorporated Administrative Agency, Public Works Research Institute (IAA-PWRI). In addition to the change of medium-term plans, the IAA-PWRI made two big changes in its organization. One is the foundation of the International Centre for Water Hazard and Risk Management under the auspices of UNESCO (ICHARM), and the other is the unification with the Civil Engineering Research Institute of Hokkaido. It is hoped that the new Priority Research Projects and these changes in the organization will increase the IAA-PWRI's capacity for research on natural disasters.

KEYWORDS: International Centre for Water Hazard and Risk Management under the auspices of UNESCO (ICHARM), Natural Disasters, Organization, Priority Research Projects

1. INTRODUCTION

In April 2001, the old Public Works Research Institute (PWRI) that had belonged to the Ministry of Land, Infrastructure and Transport (MLIT) was reorganized to the Incorporated Administrative Agency, Public Works Research Institute (IAA-PWRI). The IAA-PWRI should carry out research and development

- that must be surely performed to promote the public welfare,
- and that need not be carried out directly by the national government,
- but that might not be always carried out by the private sector.

The IAA-PWRI should achieve the medium- term goals that are given by the Minister in charge. To achieve the medium- term goals, the IAA-PWRI prepare the medium- term plans, and carry out research and development according to the plans. One of the most important parts of the medium-term plans are the Priority Research Projects, which deal greatly required research topics, which should be conducted quickly, and whose results will contribute greatly to advance in civil engineering technologies and public welfare.

The first medium-term plans were for the period from April 2001 to March 2006. The second medium-term plans should be formulated before the end of the first plans. In this paper described are the new Priority Research Projects, the most important parts of the plans.

In addition to the change of medium-term plans, we made two big changes in our organization. One was the foundation of the International Centre for Water Hazard and Risk Management under the auspices of UNESCO (ICHARM) on the 6th of March 2006, and the other was the unification with the Civil Engineering Research Institute of Hokkaido on the first of April 2006. It is hoped that these changes in the organization will increase our capacity for research on natural disasters. The changes in our organization are described first, then follows the new Priority Research Projects.

2. INTERNATIONAL CENTRE FOR WATER HAZARD AND RISK MANAGEMENT UNDER THE AUSPICES OF UNESCO (ICHARM) [1]

2.1 Background

The UNESCO International Hydrology Programme (IHP) is contributing to solving global water-related problems through the foundation of UNESCO Centres in every corner of the earth. The Centres serve as an international base for every specific theme of water-related field and aim to promote exchange of international information, partnership and cooperation. On the other hand, the Public Works Research Institute

---

[1] Chief Executive, Public Works Research Institute, Minamihara 1-6, Tsukuba-shi, Ibaraki-ken 305-8516 Japan

[2] Executive Research Coordinator, Public Works Research Institute, ditto

has greatly contributed to solving diversified water management problems, including flood control, water resources, quality management of public waters and river ecology. Recently, international research projects, such as the flow prediction of the Mekong River basin are also done successfully.

In 2003 on the occasion of the Ministerial Conference of the Third World Water Forum, Mr. Koichiro Matsuura, the UNESCO Director-General, proposed the foundation of UNESCO Centre for Water Hazard and Risk Management, in agreement with the Japanese government. Recognizing the positive role of such international contribution and willing to make use of its accumulated technical knowledge in solving global water-related problems, the Public Works Research Institute founded an International Center for Water Hazard and Risk Management under the auspices of UNESCO (ICHARM) inside the institute on March 6, 2006, following its recognition by the UNESCO general meeting on October 2005.

2.2 Objectives

The goal of the Center is to be the world Centre of Excellence to provide best practicable strategies to localities, nations, regions and the globe to manage the risk of water related disasters including flood, drought, landslide, debris flow, storm surge, tsunami and water contamination.

This centre aims to promote Research, Training and Information Networking activities, focusing on the issues and problems related to water hazard and risk management (Fig. 1). These three activities will be developed in integrated manner. For instance, the daily research results will be applied to the capacity building for researchers and professionals mainly from developing countries. The human network to be formed through the training activities will become a permanent core of the future information networking. The information networking will boost mutual flow of information, enabling the outcome to be reflected accurately in the research and capacity building

2.3 Principles and Strategies

The guiding principles of the ICHARM are:

- To be needs driven rather than supply driven, responsive to respective local realities.
- To prescribe tailored strategies to realize integrated risk management under the multifaceted social, economical, institutional and cultural conditions as well as technological availability.
- To produce policy effective information and raise public awareness to promote societal action.
- To promote Research Development and Capacity Building jointly, to bring science where most needed.
- To work in alliance with all the related organizations of the world to mutually complement resources and expertise and to create synergy in implementation.
- To serve as a think-tank of water hazards and risk management of the world and play a central role of its strategic promotion.

The management strategies of the ICHARM are:

- To be the clearinghouse of information and the broker of knowledge and technology of the world to deliver whatever available to wherever needed in the world.
- To make the Japanese and PWRI's experiences and human network available worldwide.
- To promote joint work with researchers and engineers in developing countries in alliance with universities and related institutes worldwide.
- To function, in substance, as a UNESCO Centre with internationally recruited staff and English as an operation language.
- To promote external fundraising jointly with the researchers and administrators of various nations and international institutes.

2.4 Present Activities

Initially, ICHARM will place its priority on "risk management regarding flood-related disasters". Specifically, the centre conducts activities of "research, training and information networking."

Based on the Japanese and PWRI's experiences and technologies, the centre integrates and carries out those activities in collaboration with relevant organizations in Japan and abroad.

3. NEW PUBLIC WORKS RESEARCH INSTITUTE

3.1 Unification with the Civil Engineering Research Institute of Hokkaido

The Civil Engineering Research Institute of Hokkaido was originally established as the Laboratory of the Civil Engineering Department, Hokkaido Agency, Ministry of Internal Affairs in 1937. In 1947, it was reorganized as the Civil Engineering Laboratory of Hokkaido. It was renamed as the Civil Engineering Laboratory, Hokkaido Developing Bureau, Hokkaido Developing Agency in 1951. After changing its name several times, it was reorganized to the Incorporated Administrative Agency, Civil Engineering Research Institute (IAA-CERI) of Hokkaido in 2001.

The objective of the IAA-CERI was to contribute to the promotion of development of Hokkaido by improving civil engineering technologies. Hokkaido's climate is severe and cold. Soft peat covers considerable part of plains in Hokkaido. The IAA-CERI has developed civil engineering technologies suitable for the natural conditions of Hokkaido.

On the other hand, the objective of the IAA-PWRI was to contribute to the promotion of effective construction and maintenance of quality infrastructures by improving civil engineering technologies. The improvement of civil engineering technologies was common to the both institutes. Because of their common missions, it was recommended to unify the IAA-PWRI and IAA-CERI to the new IAA-PWRI. The new IAA-PWRI was established on the first of April 2006.

3.2 New Organization

The objective of the new IAA-PWRI is to contribute to the promotion of effective construction and maintenance of quality infrastructures and of development of Hokkaido by improving civil engineering technologies. The new organization chart is shown in Fig. 2. The new IAA-PWRI consists of three sub-institutes, namely the Tsukuba Central Research Institute, the Civil Engineering Research Institute for Cold Region and the ICHARM. Most of the research groups of the old IAA-PWRI belong to the Tsukuba Central Institute. Most of the research departments of the old IAA-CERI belong to the Civil Engineering Research Institute for Cold Region. For comparison, the old organization charts of the two old agencies are shown in Fig. 3. It goes without saying that the unification with the IAA-CERI has increased the IAA-PWRI's capacity to make research on natural disasters in the cold region, and that the foundation of the ICHARM has increased the IAA-PWRI's capacity to disseminate its expertise and research results on natural disasters to the world.

4. PRIORITY RESEARCH PROJECTS IN THE NEW MEDIUM-TERM PLAN

4.1 Medium-term Goals, Medium-term Plans and Priority Research Projects

The medium-term goals are operating goals that should be achieved by an Incorporated Administrative Agency during a period ranging from 3 years to 5 years. The Minister in charge gives these goals. The Incorporated Administrative Agency must prepare the medium-term plans, which are plans for the Agency to achieve the medium-term goals.

In the medium-term plans, the research projects, which are greatly required, which should be conducted quickly, and whose results will contribute greatly to advance in civil engineering technologies and public welfare, are defined as Priority Research Projects. The Priority Research Projects in the previous medium-term plans of the IAA-PWRI are shown in the Table 1.

4.2 Development of the New Priority Research Projects

In the new medium-term goals, it was directed by the Ministers in charge to conduct research and development that will realize the following goals:

a) To prevent or mitigate damages caused by earthquakes, tsunami, eruption, storm and flood-related disasters, sediment-related disasters, snow and ice-related disasters, and traffic accidents

b) To decrease risk of life environment remarkably and to improve quality of living space

c) To renew infrastructures safely and efficiently and to improve management of infrastructures

d) To utilize energy and natural resources efficiently, to reduce wastes, and to preserve sound water quality and ecological systems

e) To construct infrastructures suitable in the snowy and cold climate of Hokkaido

f) To construct stable agricultural infrastructures utilizing local resources and harmonizing with beautiful nature of Hokkaido

To realize these goals, 17 Priority Research Projects were formulated. The Priority Research Projects in the present medium-term plans are shown in the Table 2. Seven Priority Research Projects are dealing with natural disasters in the present medium-term plans, while there were only two Projects dealing with natural disasters in the previous medium-term plans.

5. CONCLUSIONS

The second medium-term plans with the new Priority Research Projects started in April 2006 at the Incorporated Administrative Agency, Public Works Research Institute (IAA-PWRI). In addition to the change of medium-term plans, the IAA-PWRI experienced two big changes in its organization. One is the foundation of the International Centre for Water Hazard and Risk Management under the auspices of UNESCO (ICHARM), and the other is the unification with the Civil Engineering Research Institute of Hokkaido. It is hoped that the new Priority Research Projects and these changes in the organization will increase the IAA-PWRI's capacity for research on natural disasters.

6. REFERENCES

1. http://www.icharm.pwri.go.jp/centre/icharm_newsletter/i-newsletter1_e.html

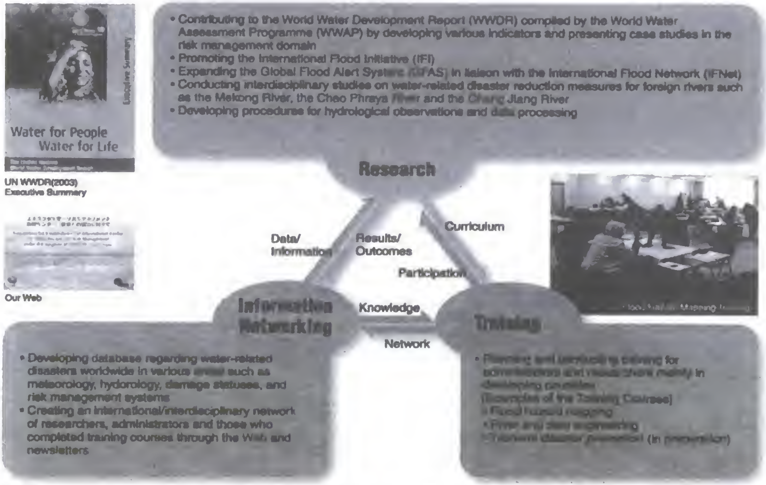

- Contributing to the World Water Development Report (WWDR) compiled by the World Water Assessment Programme (WWAP) by developing various indicators and presenting case studies in the risk management domain
- Promoting the International Flood Initiative (IFI)
- Expanding the Global Flood Alert System (GFAS) in liaison with the International Flood Network (IFNet)
- Conducting interdisciplinary studies on water-related disaster reduction measures for foreign rivers such as the Mekong River, the Chao Phraya River and the Chang Jiang River
- Developing procedures for hydrological observations and data processing

- Developing database regarding water-related disasters worldwide in various areas such as meteorology, hydrology, damage statuses, and risk management systems
- Creating an international/interdisciplinary network of researchers, administrators and those who completed training courses through the Web and newsletters

- Planning and conducting training for administrators and researchers mainly in developing countries
[Examples of the Training Courses]
• Flood hazard mapping
• River and dam engineering
• Tsunami disaster prevention (in preparation)

Fig. 1 Three Activities of the International Center for Water Hazard and Risk Management under the auspices of UNESCO (ICHARM)

Incorporated Administrative Agency, Public Works Research Institute (IAA-PWRI)

- Chief Executive
  - Executive Members
  - General Affairs Department
  - Planning and Research Administration Department
  - Tsukuba Central Research Institute
    - Construction Technology Research Department
    - Material and Geotechnical Engineering Research Group
    - Earthquake Disaster Prevention Research Group
    - Water Environment Research Group
    - Hydraulic Engineering Research Group
    - Erosion and Sediment Control Research Group
    - Road Technology Research Group
    - Structures Research Group
  - Civil Engineering Research Institute for Cold Region
    - Administration Department
    - Cold Region Construction Engineering Research Group
    - Cold Region Hydraulic and Aquatic Environment Engineering Research Group
    - Cold Region Road Engineering Research Group
    - Cold Region Agricultural Development Research Group
  - The International Centre for Water Hazard and Risk Management under the auspices of UNESCO (ICHARM)
    - Water-related Hazard Research Group

Fig. 2 The Organization Chart of the New Incorporated Administrative Agency, Public Works Research Institute (IAA-PWRI)

Incorporated Administrative Agency, Public Works Research Institute (IAA-PWRI)

Chief Executive
- Executive Members
- General Affairs Department
- Planning and Research Administration Department

- Construction Technology Research Department
- Material and Geotechnical Engineering Research Group
- Earthquake Disaster Prevention Research Group
- Water Environment Research Group
- Hydraulic Engineering Research Group
- Erosion and Sediment Control Research Group
- Road Technology Research Group
- Structures Research Group

- Secretariat for Preparatory Activities of UNESCO-PWRI Centre

Civil Engineering Research Institute of Hokkaido (IAA-CERI)

Chief Executive
- Executive Members
- General Affairs Department

- River and Port Department
- Structures Department
- Road Department
- Agricultural Engineering Department

Fig. 3 The Organization Chart of the Old Incorporated Administrative Agency, Public Works Research Institute (IAA-PWRI) and the Incorporated Administrative Agency, Civil Engineering Research Institute (IAA-CERI) of Hokkaido

Table 1 The Priority Research Projects of the Old PWRI for the Medium-Term Plans during 2001-2005

1. R&D for ensuring safety
    - 1.1 Research on economical seismic retrofit technologies for civil infrastructures.
    - 1.2 Research on enhancing techniques for mitigating damage caused by slope collapse and fluidization.
    - 1.3 Research on evaluating water quality risks.
    - 1.4 Research on techniques for conserving ground environment.

2. R&D for conserving and restoring the environment
    - 2.1 Research on comprehensive hydrologic models for river basins.
    - 2.2 Research on restoring the natural environments of lakes and rivers.
    - 2.3 Research on techniques for controlling water quality and soil at dam reservoirs and downstream sections of rivers.
    - 2.4 Research on techniques for treating bottom sediment at enclosed water areas.
    - 2.5 Research on evaluating heat island phenomena reduction alternatives.

3. R&D for efficiently preserving and improving infrastructure
    - 3.1 Research on improving the durability of structures and evaluating their performance.
    - 3.2 Research on evaluating the soundness of infrastructure stock and its remedial techniques.
    - 3.3 Research on improving infrastructure using new, untapped, and recycled materials.
    - 3.4 Research on efficient construction and redevelopment of dams considering surrounding environment.
    - 3.5 Research on reducing construction costs of super-long highway structures.

Table 2 The Priority Research Projects of the New PWRI for the Medium-Term Plans during 2006-2010

I. R&D for preventing or mitigating damages caused by earthquakes, tsunami, eruption, storm and flood-related disasters, sediment-related disasters, snow and ice-related disasters, and traffic accidents

1. Research on prevention and mitigation of flood-related disasters in the world by utilizing integrated risk management approaches
2. Development of technologies for strengthening river levees against floods
3. Development of seismic resistant technologies for existing highway and river infrastructures against strong earthquakes
4. Development of technologies for predicting or mitigating sediment-related risks posed by severe rainfalls or earthquakes
5. Research on efficient utilization of coastal areas in the cold region
6. Research on improvement of road safety against large-scale rock slope failure
7. Research on winter road safety and efficiency

II. R&D for decreasing risk of life environment remarkably and for improving quality of living space

8. Development of technologies for decreasing risk of life environment

III. R&D for renewing infrastructures safely and efficiently and for improving management of infrastructures

9. Research on improvement of design methods for efficient construction of highway infrastructures
10. Research on improvement of maintenance and management technologies of highway structures
11. Research on durability of infrastructures in the cold region

IV. R&D for utilizing energy and natural resources efficiently, reducing wastes, and preserving sound water quality and ecological systems

12. Development of recycling technologies in construction for efficiently utilizing natural resources and reducing wastes
13. Development of preservation and restoration techniques for aquatic ecosystems
14. Development of technologies on dams that reduce effects on the natural environments
15. Development of design technologies on rivers and basins in snowy climate

Table 2 The Priority Research Projects of the New PWRI for the Medium-Term Plans during 2006-2010 (contd.)

V. R&D for construction of infrastructures suitable in the snowy and cold climate of Hokkaido

5. Research on efficient utilization of coastal areas in the cold region
6. Research on improvement of road safety against large-scale rock slope failure
7. Research on winter road safety and efficiency
11. Research on durability of infrastructures in the cold region
15. Development of design technologies on rivers and basins in snowy climate

VI. R&D for construction of stable agricultural infrastructures utilizing local resources and harmonizing with beautiful nature of Hokkaido

16. Development of the cyclic utilization system of local biomass that has the centralized biogas plant in its core
17. Research on preservation of structural function and on improvement of water supply function of agricultural water use infrastructures in the cold region

Reconnaissance of Damage to Physical Structures in the Gulf States from Hurricanes Katrina and Rita

by

William P. Fritz[1]

ABSTRACT

The National Institute of Standards and Technology (NIST) led reconnaissance to assess the performance of physical structures during Hurricane Katrina and Hurricane Rita. This paper summarizes 1) the major findings of the NIST-led reconnaissance team, 2) analysis of environmental actions (wind speed, storm surge, and flooding) that were present during the hurricanes in regions that were affected by the hurricanes, and 3) the team's observations of damage to major buildings, infrastructure, and residential structures resulting from wind and wind-borne debris, storm surge and surge-borne debris, and flooding. Storm surge and flooding caused the most extensive damage, completely devastating most physical structures in their paths. Damage due to wind and wind borne debris was also prevalent in most areas of the reconnaissance.

KEYWORDS: building codes and standards; building practices; flooding; hurricane; major buildings; physical infrastructure; residential structures; storm surge; surge-borne debris; wind; wind-borne debris.

1.0 BACKGROUND

On August 29, 2005, Hurricane Katrina made landfall along the Mississippi-Louisiana border. During its movement through the Gulf of Mexico, Hurricane Katrina reached a Category 5 intensity on the Saffir-Simpson Hurricane Intensity Scale, with maximum sustained winds of 77.3 m/s (173 mph). The storm began to weaken about 18 hours before landfall, and was a Category 3 hurricane with maximum sustained winds of 56.3 m/s (126 mph) when it made landfall. However, the storm generated a significant storm surge, particularly along the Mississippi Gulf Coast, where in some locations the storm surge reached heights of 28 ft. The storm surge caused extensive damage to buildings, residential structures, and physical infrastructure along the Mississippi Gulf Coast. Damage from wind and storm surge extended east into Alabama's coastal areas. To the west, the storm surge caused breaches in the levees and floodwalls surrounding New Orleans, Louisiana, in several locations. These breaches caused flooding of approximately 75 % of the city and led to extensive damage to buildings, infrastructure and residential structures. In areas beyond the storm surge debris line, wind and wind-borne debris damage was extensive. Hurricane Katrina is the costliest hurricane to strike the United States.

Less than one month later, Hurricane Rita made landfall near the Texas-Louisiana border as a Category 3 hurricane with maximum sustained winds of 44.7 m/s (100 mph). During Hurricane Rita's path through the Gulf of Mexico but prior to landfall, the storm reached Category 5 intensity with maximum sustained winds of 78.2 m/s (175 mph). Hurricane Rita began weakening 36 hours before landfall. While Hurricane Rita did not generate the same level of storm surge as Hurricane Katrina, storm surge did cause significant damage in some developed coastal areas. Wind and wind-borne debris were the dominant causes of damage in the affected area.

The National Institute of Standards and Technology (NIST) is a non-regulatory agency of the Department of Commerce. NIST supports U.S. industry and public safety by providing critical tools

---

[1] Research Structural Engineer, Materials and Construction Research Division, Building and Fire Research Laboratory, National Institute of Standards and Technology, Gaithersburg, MD, 20899-8611.

– metrics, models, and knowledge – and the technical basis for standards and codes, and practices. Disasters such as Hurricane Katrina and Hurricane Rita provide an opportunity to learn from the performance of structures exposed to extreme loads and to derive lessons that can lead to improvements in standards, codes, and practice that will reduce losses in future events.

NIST began preparation for conducting reconnaissance in the hurricane affected areas on August 29, 2005. NIST coordinated with the Federal Emergency Management Agency (FEMA), and other agencies to begin planning for an initial deployment to the region. During the week of September 6, 2005, a NIST roofing expert deployed as part of a team assembled by the Roofing Industry Committee on Weathering Issues (RICOWI). This team conducted reconnaissance of damage to commercial and residential roofing systems in the Alabama and Mississippi coastal areas. During the week of September 26, 2005, four NIST structural engineers deployed in cooperation the FEMA Mitigation Assessment Team to conduct reconnaissance of damage in the coastal areas between New Orleans and the Biloxi-Gulfport, Mississippi, area. Two of the NIST team members went to New Orleans during the last two days of this deployment to document damage to the levees and floodwalls in New Orleans. These initial deployments provided valuable input to NIST in planning a more comprehensive reconnaissance effort.

NIST, working with the Applied Technology Council (ATC) under a contract, assembled a team of twenty-six experts to conduct reconnaissance in the areas affected by Hurricane Katrina and Hurricane Rita. The team consisted of experts from NIST, Federal Highway Administration (FHWA), U.S. Army Corps of Engineers (USACE), as well as a diverse and balanced group of experts from the private sector and academia. The team deployed during the weeks of October 10, 2005 and October 17, 2005. Based upon the earlier reconnaissance efforts and other available data, the team selected the Mississippi Gulf Coast, New Orleans, and Southeast Texas-Southwest Louisiana area for conducting reconnaissance and collecting perishable data. The scope of the reconnaissance included major buildings, physical infrastructure, and residential structures. The team subdivided into three smaller teams, each of which deployed to one of the selected areas to conduct reconnaissance. In addition to collecting perishable data in the field, the team analyzed environmental data (e.g., wind speeds, storm surge, and flooding), and analyzed observations made by other teams working in the affected areas.

2.0 MAJOR FINDINGS

In coastal areas and in New Orleans, storm surge was the dominant cause of damage. Storm surge heights, in general, exceeded historical records. Storm surge led to breeches in three major canals in New Orleans resulting in significant structural damage to residences in the immediate vicinity of breeches due to high-velocity water and flooding in approximately 75 % of the city. In coastal Mississippi, storm surge and surge-borne debris caused extensive structural damage to buildings and residences in the surge zone, damage to casino barges that either sank in place or broke free of moorings and floated inland. Storm surge also caused significant damage to bridges in the coastal areas of Mississippi and Louisiana. Currently, storm surge is not considered as a design load for buildings, residences, and transportation structures in coastal areas.

Away from the immediate coastal areas, wind and wind-borne debris were the dominant causes of damage to buildings, residences, and infrastructure. Major buildings suffered damage to glazing (windows) as a result of aggregate surfacing on nearby roofs, debris from damaged equipment screens, and debris from damaged buildings. Wind also caused damage to roofing and rooftop equipment providing paths for water ingress into buildings. Wind-driven rain through wall and around intact windows was also responsible for water damage to the interiors of buildings.

It was also observed that both Hurricane Katrina and Rita generated storm surges that were higher than would be expected for hurricanes of their intensity at landfall. While wind speeds diminished rapidly as the hurricanes approached landfall, the storm surge did not dissipate as rapidly and led to significant damage to structures located in the areas of greatest storm surge height.

Based upon its data collection in the field during the reconnaissance, analysis of observation made by other teams, and analysis of environmental data, NIST has identified a number of key findings related to environmental actions, major buildings, infrastructure and residential structures.

3.0 ENVIRONMENTAL ACTIONS

3.1 Wind Speeds

In general, for all locations studied in this reconnaissance report, the observed and modeled/estimated wind speeds for both hurricanes were less than the design wind speeds prescribed in the ASCE 7-02 (2005) Standard.

Hurricane Katrina. Wind speed estimates taken from the National Oceanic and Atmospheric Administration (NOAA) and Applied Research Associates (ARA) indicate that the maximum sustained wind speed at landfall along the Mississippi coast was estimated between 49.2 m/s (110 mph) and 53.6 m/s (120 mph) (2005). In New Orleans, the ARA maps suggest that wind speeds reached 40.2 m/s (90 mph), while the NOAA maps indicate that winds were 35.8 m/s (80 mph) or less. Furthermore, according to a recent National Hurricane Center (NHC) report (2005), the maximum sustained wind speed produced by Katrina was approximately 56.3 m/s (126 mph). Based on wind speed information from these data sources, Hurricane Katrina was a Category 3 event on the Saffir-Simpson (SS) scale.

Hurricane Rita. At landfall, Hurricane Rita's sustained winds had diminished to a SS Category 2 intensity, with the exception of a small area on the coast of extreme Southwestern Louisiana that was to the east of the eyewall, where wind speeds were a Category 3 intensity. However, most of the affected area in Southwest Louisiana and Southeast Texas was exposed to wind speeds of SS Category 1 or 2 intensity. The highest 3 s peak gust observed for Hurricane Rita was 51.9 m/s (116 mph) at Port Arthur, Texas. Based on an assessment of maximum sustained wind speeds (NOAA wind speed map), the highest level estimated was less than 49.2 m/s (110 mph). Hurricane Rita was officially classified as a Category 3 hurricane. However, most of the effected area in southwest Louisiana and southeast Texas was exposed to hurricane wind speeds of Category 1 or 2 intensity.

3.2 Storm Surge

Hurricane Katrina. A number of locations experienced storm surge heights greater than 20 ft. NOAA's National Climatic Data Center estimated that the coastal surge along Mississippi exceeded 25 ft. Observations by the NIST-led reconnaissance team also suggest that in some locations between Biloxi and Long Beach, Mississippi, the surge reached as high as 30 ft. Estimates of surge heights in New Orleans ranged from 9 ft to 10 ft. This information is based on High Water Mark data collected by FEMA investigators and on other observations as well. These surge heights are consistent with a SS Category 5 hurricane.

Hurricane Rita. The National Climatic Data Center estimated surge levels of 8 ft in New Orleans and about 15 ft along the Texas/Louisiana border flooding coastal towns in the region. Surge heights observed by the NIST-led reconnaissance team are consistent with a SS Category 3 to SS Category 4 hurricane.

3.3 Flooding

The depth of flooding in New Orleans based on several independent sources (NOAA, 2005) indicates that many areas of New Orleans were covered by at least 7 ft to 9 ft of water with some areas exceeding 20 ft (as of August 31, 2005). The NIST-led reconnaissance team observed flood depths of up to 10 ft in some areas of New Orleans.

4.0 MAJOR BUILDINGS

4.1 Structural Systems

Storm surge caused partial collapse of concrete parking structures located in Biloxi. These structures were constructed of concrete columns, precast concrete girders and beams, and pretensioned, double-tee beams for decks. Decks subjected to storm surge were lifted and displaced off of their beam seats due to uplift forces (either directly or in combination with the pre-stressing forces in the beams) and poor connection details.

Unreinforced brick parapet walls were observed to have partially collapsed in New Orleans and Port Arthur. Failure of the rooftop parapets due to wind likely initiated failure of the exterior wall. There was an apparent lack of proper reinforcement within the walls or a framing system to resist lateral movement.

The collapse of masonry walls by strong winds was due to the lack of proper reinforcement within the walls or due to insecure attachment of these walls to the building frame. Instances of failure due to storm surge were also observed.

The NIST-led reconnaissance observed damage to metal buildings ranging from minimal damage to partial collapse. The roof purlins in the windward, end bay of several large, steel-framed warehouses buckled upwards due to wind pressures and the end frame collapsed inward. These failures allowed rain and winds to devastate the building's interior.

Casino barge structures along the Mississippi coast broke free of their moorings during Hurricane Katrina and caused extensive damage. Barges were observed to have 1) partially collapsed all levels to the corner bay of an otherwise structurally sound, reinforced concrete parking garage, 2) drifted inland with the storm surge, 3) collided with multi-story hotels causing partial collapse of these buildings, and 4) sank in place.

4.2 Roofing

Conventional bituminous membranes with and without gravel surfacing, and polymer-modified bituminous membranes generally with granule surfacing were the predominant roof systems on major buildings. Other systems included metal roofing, synthetic single ply roofing, and spray polyurethane foam (SPF) roofing. Damage to all types of roofing was observed but the extent of the damage varied according to the system. Examples of typical damage included: failure of flashings, puncturing of roof coverings or the total roof system, blow-off of the roof coverings often accompanied by loss of insulation, blow-off of the insulation and covering accompanied by loss of deck, failure of metal roof panels with and without damage to structural members, and combinations of these types of damage.

Where detailed observations of roofing damage were made, the failures were in many cases attributed to installation that did not comply with currently accepted practice as given in manufacturers' literature and association guidelines. Examples included lack of an adequate number of fasteners, and mis-location of fasteners, and inadequate heating of bituminous membranes.

The predominant damage to bituminous membrane roofing was blow-off of some section of the membrane. Damage was generally associated with three modes of failure that have been commonly observed in past hurricanes: (1) poor performance of perimeter metal flashing, (2) inadequate inter-laminar strength of insulation and inadequate adhesion between membranes and insulation, and (3) poor attachment of bituminous base sheets to decks and other substrates. The three are associated with selection of a membrane roofing system that does not have adequate resistance to the maximum winds expected for the given geographic location or misapplication of the roofing during installation.

Many metal roofs performed well, particularly standing seam metal roofs installed on commercial and industrial buildings and schools. Often where damage to such metal roofing occurred, it was limited to a small portion of the roof area whereby some panels on the structure were bent away or blown off. Where metal roofing sustained considerable damage, it often, although not exclusively, occurred at industrial-type facilities including the roofs and structural supports of all metal buildings.

A limited number of spray polyurethane foam (SPF) roofing systems was observed in the Hurricane Rita damage zone. Such roofing was found, with minor exception, to have sustained the winds well without blow-off of the SPF or damage to flashings.

Damage to rooftop equipment was observed in all study areas. In some cases, equipment and portions of rooftop mechanical screens became windborne, causing damage to the building itself, or to other buildings downwind.

4.3 Window Systems

Many buildings in areas of the NIST-led reconnaissance had roofs with aggregate surfaces. The aggregate typically became wind-borne during the hurricanes and caused damage to the windows of neighboring downwind buildings. The aggregate caused extensive damage to window systems in many high-rise buildings, particularly in New Orleans, and in many critical facilities such as schools and hospitals.

Wind-driven water penetration through exterior masonry and other undamaged cladding and glazing elements combined with water from other sources forced closure of important hospital facilities as a result of Hurricane Rita. Facilities remained partially or totally out of operation for weeks, indicating a need to review resistance of exterior cladding and glazing systems for wind-driven water.

4.4 Cladding

The NIST-led reconnaissance observed damage to exterior insulation and finish systems (EIFS) throughout the reconnaissance areas, in many cases without evidence of wind- or waterborne debris, suggesting that wind pressure caused the observed damage.

Damage to masonry veneer due to high winds was observed throughout the hurricane affected areas. Damage was associated with a lack of reinforcement to resist lateral loads and inadequate or deteriorated mechanisms that anchor the masonry cladding to the building.

4.5 Water Damage to Building Contents and Equipment

Flood damage to New Orleans hospitals, especially to critical equipment and facilities (e.g., chiller plants, backup generators, kitchen facilities) located below flood elevations in basements or at ground level, was responsible for extended closure of these facilities as a result of Hurricane Katrina.

Flooding of the basement and ground levels of buildings damaged key facilities and equipment critical to the building's operation, such as back up generators, electrical equipment, water chillers, kitchen facilities, vacuum pumps and 9-1-1 call centers.

5.0 PHYSICAL INFRASTRUCTURE

5.1 Levees and Floodwalls

Floodwall failures in New Orleans, either due to sliding or overturning instability, appeared to be the results of failure of the supporting soil. Sliding instability, likely triggered by increased outboard lateral pressure combined with loss of soil strength due to saturation by preceding rain and possibly underground water seepage, was the principal mode of floodwall failure along the 17th Street and the London Avenue Outfall Canals. Overturning instability, likely triggered by full outboard lateral pressure combined with loss of embankment material due to scour trench along the inboard toe of the floodwalls, was the principal mode of failure of floodwalls along the Inner Harbor Navigation Canal (IHNC).

The loss of embankment material due to erosion and scour trenches was widespread at breaches along the IHNC and the Intercoastal Waterway (IWW, part of the Mississippi River Gulf Outlet), where overtopping occurred. None of the sites inspected, where erosion and scour trenches occurred, was armored. Scour trenches, due to either overtopping or flow disturbance or both, were observed on both the protected and unprotected sides of the floodwall. At many breaches along the

IHNC, the scour trenches were measured at more than 6 ft deep. This represented a loss of up to half of the total embedment depth of the floodwall at these locations, thus amplifying the applied moment due to full outboard pressure and making it much more vulnerable to overturning instability.

The earthen levee at the transitional junction between the levee and the floodwall, as currently designed and constructed (perpendicular transition between the concrete I-wall/ railroad closure monolith and the earthen levee), is highly susceptible to erosion due to flow disturbances. This led to complete failure of the earthen levees at the breaches on both sides of the IHNC at France Road and Jordan Road. Provisions to armor the earthen levee at this transitional junction to limit the effect of flow disturbances, with consequent erosion and scour, should be considered.

No structural failure at the connection between the concrete I-walls and steel sheet piles was observed, except for the 17th Street Outfall Canal breach where it appeared that the concrete I-walls might have been disconnected from the steel sheet piles. Where the connections between the concrete cap wall and the steel sheet piles can be inspected, the reinforcements between the concrete floodwall and the steel sheet piling appeared to be in place as shown on typical drawings. Concrete I-wall panels of the floodwalls along the 17th Street and London Avenue Outfall canals separated from adjacent panels along the vertical water stop joints at failure.

5.2 Transportation Systems

The most extensive and obvious damage to bridges was caused by the uplift and lateral displacements of the superstructure spans, many of which fell into the water. The bridge construction that is most susceptible to this type of damage is the segmental bridge construction where individual superstructure spans (deck, curb rail, and girders) were prefabricated and simply supported on the bridge piers without adequate provisions for restraint against uplift or lateral transverse displacements. This is a common damage scenario that has also been observed after many earthquakes when the bridge is subjected to dynamic loading and cannot accommodate the resulting displacements. While simply-supported bridge spans are easier and less expensive to design and build, they are vulnerable to damage due to direct effects of storm surge and wave actions in coastal regions.

Bridges with continuous spans and positive connection between the superstructure and the substructure, or even single span segmental bridges with adequate provisions for restraint against lateral transverse displacements, were observed to have sustained only minor, non-structural damage even with the direct effects of surge and wave forces caused by Hurricanes Katrina and Rita.

Besides structural damage, moveable bridges are also susceptible to damage due to flooding of motors and control mechanisms when subjected to high storm surge. The loss of control mechanisms of moveable bridges severely impacted some recovery efforts.

Impacts from surge-borne debris (barges, vessels, etc.) and scour of approach pavement and embankments also led to loss of functionality of bridges. In some instances the pier fender systems did not afford protection at the elevated water levels due to storm surge or flooding.

The entire Gulf Coast region suffered extensive loss of traffic control devices such as traffic lights, road lighting, regulatory signs, and directional signs. Failure of these signs also generated debris that impacted surrounding structures. Most obvious were large advertising sign failures adjacent to U.S. Interstate 10 in Louisiana and cable-suspended traffic lights in many coastal communities.

5.3 Sea Ports

Storm surge, rather than extreme wind, was the most destructive force to port facilities in with Hurricanes Katrina and Rita; however, most structural design of these facilities focuses on wind effects. The height and force of the surge—which reportedly reached upwards of 30 ft above mean sea level—along with wave impacts and saltwater inundation of coastal areas, caused widespread damage to buildings and facilities along the Louisiana, Mississippi, and Alabama coastline. Storm surge damage affected wharfs and warehouse structures in Gulfport moored casino barges in Biloxi and Gulfport and anchorage and motor-driven equipment of container cranes in Mobile, Alabama, and Gulfport. Wind was responsible for container crane anchorage failures in New Orleans and warehouse failures in Orange and Port Arthur, Texas.

5.4 Utilities

The loss of over one million timber power distribution poles in Hurricanes Katrina and Rita through a combination of storm surge, wind, and impacts of debris and falling trees seriously affected the ability to restore power quickly. There was a significant loss of lattice and steel high voltage transmission lines that also delayed restoration of electric power. Many of these failures were in exposed locations, across rivers and marshland, which further complicated replacement of fallen structures. Cascade failures were also observed.

Underground components of the natural gas distribution system did not sustain damage. However, in buildings and houses that sustained significant damage, uncontrolled venting of natural gas often occurred as a result of damage to fixtures or appliances within these structures.

Restoration of water service was hampered by the scope of damage, difficulty in gaining access to cut-off valves due to debris, and insufficient repair part inventories to respond to an event of such magnitude. Restoration of service was further challenged by the loss of system pressure due to massive damage to distribution networks at the user level in storm surge zones, resulting in uncontrolled flow of water.

Sewage treatment plants in the Gulf Coast region became inoperable when their pumps and generators were submerged in saltwater and damaged.

Both landline and cellular telephone service was severely disrupted. Landline services were lost primarily due to damage to lines and poles from wind and debris. There were few cellular tower failures, but loss of backup power disrupted service.

The major disruption to radio and television communication services was due to loss of power.

5.5 Other Industrial Facilities

Many oil storage tanks south of New Orleans (in the vicinity of Port Sulphur) were destroyed and did not float off their supports, implying that they suffered wind-induced damage. This region experienced some of the highest land-based wind speeds during Hurricane Katrina.

In many other cases, smaller oil storage tanks had no hold-down mechanisms and floated off their foundations upon inundation of the diked area meant to contain spills.

The greatest damage observed to storage tanks was loss of insulating cladding to walls and roofs, leading to the potential to inject debris into the wind field, causing further damage downwind.

More damage was apparent on the periphery of tank farms, indicating that exposure is an important consideration in design of such structures.

Observed damage to major industrial facilities included the loss of shrouds on approximately 50 % of all cooling towers.

The NIST-led reconnaissance team was able to adequately document damage that was visible in aerial photographs and from outside the perimeter fences of the facilities.

6.0 RESIDENTIAL STRUCTURES

6.1 Structures

The types of damage observed in each broad geographic area did not vary greatly.

The predominant causes of damage to residential structures were direct storm surge impacts, surge inundation, and inland flooding. Direct surge impacts extended as much as half a mile inland; surge inundation extended up to several miles inland along the gulf coast, and inland flooding was concentrated in the New Orleans area.

Nearly all non-elevated residential structures exposed to storm surge impacts were completely destroyed. Many houses were swept off their foundations by surge and floodwaters.

For residential structures on elevated foundations, the super-structure of the single family dwellings was completely destroyed. In most cases, it appeared that the failures stemmed from inadequate connections between the building structure and the foundation piers. Concrete, timber, and steel piers exhibited very little damage, except where impacted by surge-borne debris.

Damage due to wind loading was not as severe when compared with damage caused by storm surge and flooding. Damage due to hurricane winds was observed to roofing materials, siding, windows, soffits, porches, doors, and garage doors. Wind-borne debris was not a significant contributor to overall damage.

Damage to manufactured housing was similar to that observed for site-built structures. Reconnaissance team members observed some instances where anchoring systems for manufactured homes failed, however, the team also observed cases where anchoring systems performed well (e.g., portable classrooms in Port Arthur, TX).

6.2 Roofing

The extent of damage to residential roofing in the impact zones for Hurricanes Katrina and Rita was found to be extensive with an estimated 20 % to 30 % of the dwellings observed having some level of damage. With very few exceptions, the damage was limited to the coverings with underlayment remaining on the structure.

For many homes, particularly those in the Hurricane Rita impact zone, damage to roof coverings was the only visible damage to the dwelling.

In virtually all cases where damage to individual roofs was extensive, and the observers were able to make detailed observations, roofing failures were attributed to improper installation that did not follow acceptable practice such as given in typical manufacturers' instructions and association guidelines.

The most prevalent roof covering for residential structures was asphalt shingles. Loss of those shingles was the predominant damage observed to residential roofs. Three-tab asphalt shingle roofing suffered significantly more damage than did laminated shingle systems. Reasons for the relative difference in performance of the two types of shingles were not ascertained. The reconnaissance observations clearly support a recommendation that asphalt shingles carry a wind resistance classification appropriate for the geographic area, and that they be installed according to acceptable practice and current design standards.

Relatively little metal roofing was observed on residential construction in the hurricane areas. Overall, however, observed damage to metal roofing was less than that for other types of roofing, and most residential metal roofs appeared to be undamaged. Where damage attributed to direct wind force was seen, it was relatively minor, limited to small roof areas where a panel or two were missing or bent away from the roof structure.

6.3 Cladding

Little direct wind damage to exterior cladding of residential structures was observed.

Brick veneer used an exterior cladding to residential structures sustained less damage than other cladding systems.

The effects of aging (corrosion, decay, rot) were evident in many cases where cladding system failures were observed.

7.0 SUMMARY

Hurricanes Katrina and Rita had devastating effects on the Gulf States in August and September, 2005. A NIST-led reconnaissance assessed the performance of physical structures during to these events. This paper summarized the major findings, the analysis of environmental actions (wind speed, storm surge and flooding) that were present during the hurricanes, and the team's observations of damage to major buildings, infrastructure, and residential structures. Storm surge and flooding caused the most extensive damage, completely devastating most physical structures in their paths. Damage due to wind and wind borne debris was also prevalent in most areas of the reconnaissance. NIST is preparing a written report detailing the reconnaissance and its findings. NIST plans to include recommendations in the report that focus on topics that require immediate action with respect to the reconstruction process that is currently underway in the Gulf Coast, topics that should be addressed to assess whether codes, standards or practices need to be changed or modified, and topics requiring further study or investigation.

8.0 REFERENCES

Applied Research Associates (ARA), "Wind Speed Maps for Hurricane Katrina and Hurricane Rita", (2005).

ASCE Standard 7-02, "Minimum Design Loads for Buildings and Other Structures", Virginia: American Society of Civil Engineers, (2005).

NOAA, "Climate of 2005: Summary of Hurricane Katrina, NOAA's National Climatic Data Center," U.S. Department of Commerce, lwf.ncdc.noaa.gov/oa/coimate/research/2005/katrina.html, (2005).

National Hurricane Center, www.nhc.noaa.gov/, (2005

Establishing a Disaster Information System to Practically Support Disaster Countermeasures: Conducting and Reviewing Demonstration Experiment

by

Akihiro Sanada[1], Takaaki Kusakabe[2] and Keiichi Tamura[3]

ABSTRACT

Although information systems are used in order to collect and share information at a time of disaster, such systems are not always effective. In this context, after analyzing the reasons for such ineffectiveness and current problems in disaster countermeasures, we established an information system as well as our disaster countermeasures business model that would be put into operation after introducing such an information system. Then, we also conducted a demonstration experiment in order to evaluate the practical usefulness and effectiveness of the information system and task model. Our experiment revealed that the information system would contribute to quickly collecting and sharing disaster information, but the operationality and operational rules require some improvements and modifications. After addressing these problems, the Chubu Regional Bureau will start full-scale operation of the system and business model. We also outlined these outcomes in the system's basic specifications and some other documents. These documents will contribute to mitigating system development costs if policymakers refer to them when they establish new disaster information systems in the future.

Keywords: Disaster information system, Gazetteer, Information Gathering & Sharing Platform, Interface among systems

1. BACKGROUND

Information systems are used in order to collect and share disaster information. However, such systems do not always bring about the intended outcomes in many cases because of inadequate or inappropriate reporting system and rules, which include the following problems: Operators doubly enter data in the existing systems; and staff still communicate over the phone or by fax even after implementing a new system.

To solve these problems, the Earthquake Disaster Prevention Division and the Information Technology Division, NILIM (National Institute for Land and Infrastructure Management), as well as the Information Access Division, GSI (Geographical Survey Institute) jointly began efforts in FY2003 to analyze potential problems that prevent effective operations of disaster information systems and identify proper solutions for these problems. As FY2005 is the last fiscal year for these efforts, we have been working with Chubu Regional Development Bureau since the beginning of FY2005 to improve the practical outcomes of setting up the joint review working group. On February 16, 2005, we conducted a demonstration experiment on the new disaster countermeasures, assuming that we would employ the new disaster information system derived from our research. Then, we evaluated the practicability and effectiveness of operating such a new system and business model derived from our research.

For more information on the detailed background of our research, research process and the business model, refer to the document listed as [1] in the references.

2. OUTLINE OF DEVELOPED DISASTER INFORMATION SYSTEM

---

[1] Senior Researcher, Earthquake Disaster Prevention Division, National Institute for Land and Infrastructure Management, Tuskuba-shi, Ibaraki-ken 305-0804 JAPAN

[2] Team Leader, Earthquake Disaster Prevention Research Group, Public Works Research Institute, Tsukuba-shi, Ibaraki-ken, 305-8561 JAPAN

[3] Research Coordinator for Earthquake Disaster Prevention, National Institute for Land and Infrastructure Management, Tuskuba-shi, Ibaraki-ken 305-0804 JAPAN

2.1 Examining Proper Functions of Such New System

Even if a new information system is installed, it does not always bring about the intended outcomes in some cases. This is partly because the existing disaster information system prevents user friendliness if the system has too many functional capabilities. In our research, we analyzed problems in collecting and sharing information by holding a hearing session with staffs in MLIT regional development bureau that have actually handled disaster countermeasures during major earthquakes in the past. Then, we identified the requirements for system functions by examining whether or not an information system would properly contribute to solving these problems and, if so, what kind of functional capabilities the information system should have.

2.1.1 Problems in Collecting and Sharing Information during a Disaster

We held a hearing session with MLIT regional development bureau staffs that actually handled disaster countermeasures during the Sanriku Minami Earthquake in May 2003, the Tokachi-oki Earthquake in September 2003, the Niigataken-Chuetsu Earthquake in October 2004 and some other earthquakes. We held this hearing sessions to identify actual countermeasures and problems. Among the hearing results, Table 1 shows the problems in collecting and sharing disaster information.

2.1.2 Necessary Functions for Solving Problems

When solving the problems listed in Table 1, the information system would make contributions from the following aspects.

(1) Collecting disaster information

From various systems, operators will be able to collect information useful for disaster countermeasures.

(2) Analyzing information

Operators will be able to analyze from various perspectives, paying attention to the information's roles in disaster countermeasures. Operators will be able to properly select and display the necessary information.

(3) Managing information

Operators will be able to manage information in terms of time and location. Operators will be able to easily categorize reported information.

(4) Distributing information

Operators will be able to view particular information at multiple organizations or departments at the same time. With a single data processing task, operators will be able to provide information to many stakeholders. (An increase in such stakeholders should not lead to heavier workload on data operators.)

From these viewpoints, the disaster information system should have the following functional capabilities.

(1) Requirement 1

By collaborating with information systems and database systems used under usual circumstances, operators will be able to search for and cite necessary information.

[Example 1] By associating damage information, and the affected facility's drawings with damage location or the affected facility's name as a key, operators will be able to quickly collect the necessary information.

[Example 2] By using a camera system to capture visual images of the site that are necessary for disaster countermeasures, the disaster information system will display a camera icon on its map. The system provides visual images captured with the camera system if a data operator clicks on the camera icon.

(2) Requirement 2

The information system should have "maps" and a "bulletin board" as its basic capabilities. Operators will be able to view necessary information according to each aspect of disaster countermeasures.

(3) Requirement 3

The disaster information system should manage "time" and "location" data, which are included in the reported information. For example, the disaster information system should be able to import temporal or location data from fax messages and store up these data in the system.

(4) Requirement 4

By using a web-based approach, multiple disaster countermeasure staff will be able to view the data on their browser at the same time.

For example, if an operator receives information from a local office and enters it in the system, staff at the MLIT regional development bureau and the MLIT headquarters will be able to view the data at the same time.

(5) Requirement 5

In order to reduce the data entry workload as much as possible, the information system should employ the current fax-based data transmission where possible, and minimize data entries. The system should also replace telephone communication because it is difficult to make a phone call during disaster countermeasures.

Newly developed disaster information system is characterized by the following four points show: (Fig.1)

(1) Platform for sharing disaster information

This platform electronically provides the same functions as the traditional maps and whiteboard, which are currently used for showing damage information at the disaster countermeasures headquarters. Fig.2 provides the outline of the electronic map, which electronically displays the territory map, as well as the electronic bulletin board, which electronically assumes the same roles as the whiteboard.

They have the following main functions.

[Electronic map]

i) It is able to display the map at a designated contraction scale. It is also able to designate map levels, such as overall areas that the MLIT regional development bureau or local offices are in charge of, or a prefecture-wide map. The system has six contraction scales, ranging from 1/300,000 to 1/2,500.

ii) As it employs an indirect location reference database (gazetteer), the system is able to search for an intended location by using a portion of the location name as a keyword, and it displays a list of intended location candidates. When an operator selects one of these locations, the system will display a map so that the selected location lies at its center.

[Electronic bulletin board]

i) The electronic bulletin board has three elements: the newest data portion on its top page, the list data screen and the detail data screen.

ii) The list data screen is able to sort data on a time-series basis, responsible local office basis or prefectural basis.

iii) The system is able to print out its input data in a designated list format. It is also able to export data to spreadsheet software and automatically generates a proper format reportable to higher organizations.

iv) It is difficult to identify newer information on the traditional fax sheets, because faxes arrive one after another. On the other hand, the information system provides easily viewable data because it displays a new data element in red.

v) An operator is able to easily confirm incoming data.

vi) When entering follow-up data, an operator needs only enter a new data element because the system automatically imports the previously-entered data from the previous report.

[Data link between Electronic map and electronic bulletin board]

The information system provides a data link between the electronic map and electronic bulletin board. If an operator selects a location on the map, the system displays data on the selected location. From the detail data screen that provides the detailed information on a certain location, an operator is able to view and confirm its location on the map.

(2) Interface among systems

If the existing system contains and manages information, our new system prevents double data entry because the system imports such data from the existing system. In our project, we developed a data exchange rule for intersystem data exchange (i.e., intersystem interface specifications). In our experiment, we actually used the new rule, collected applicable data from road closure database and specific systems that handle CCTV camera images, and displayed these data on the system screen.

(3) Indirect location reference database (gazetteer)

If an operator inputs location data of affected area by using mile posts that are currently used for managing rivers and roads, the new system converts it into longitude and latitude data, and displays such data on the map. When an operator inputs a distance mark in the new system, the operator is able to search for data related to such distance mark.

(4) FAX-OCR

Disaster countermeasures staff usually use drawings that show handwritten disaster damage information. On the other hand, when an operator sends a paper document via fax in the same manner as the traditional approach, the new system automatically imports the received data into its scanner, and electronically displays and manages the data, rather than printing out paper-based data.

3. OUTLINE AND OUTCOMES OF DEMONSTRATION EXPERIMENT

Applying the disaster information system and our system usage stated in Section 2 above, we conducted a demonstration experiment in order to evaluate the effectiveness and practicability of the disaster information system.

3.1 Purposes of Demonstration Experiment

The demonstration experiment has the following main purposes.

First, we intended to evaluate the outcomes of our research by actually operating our new system and business model under a certain disaster scenario.

As the first aspect in our evaluation process, we focused on evaluating the practicability of our developed system. This would reveal the practicability and feasibility of our new approaches, such as the FAX-OCR functions, as well as the new disaster countermeasures business model that incorporates the new information system. As the second aspect in our evaluation process, we focused on evaluating the effectiveness of our development efforts. In other words, we compared the new disaster countermeasures tasks with the new disaster information system installed and the traditional telephone- or fax-based approach. By doing so, we evaluated to what degree we could reduce the workload. Our evaluation revealed necessity of some improvements in the system, which would contribute to enhance the practicability of our new system.

Second, we intended to provide experiment participants with some information on the beneficial points of employing our new business model and information system.

3.2 Outline of Demonstration Experiment

(1) Demonstration experiment

i) Participants

The following participants took part in the experiment: Planning Department in charge of coordinating the overall tasks of the MLIT regional development bureau, the River Department in charge of managing river-related facilities, and the Road Department in charge of managing roads, as well as river offices and national road offices in charge of disaster countermeasures on site.

ii) Player levels

Our demonstration experiment has two player levels at departments in the MLIT regional bureau and participating local offices.

1) Data reader: Decision makers

They mainly check out input data and communicate with related departments/local offices.

2) Data operator: Data operators, such as staff in charge of entering system data

They mainly enter or coordinate data and prepare documents.

(2) Disaster and scenario assumed

i) Outline of assumed earthquake

- Date/time: Around 11:00 a.m., February 16, 2006
- Seismic center: In the waters off Tokaido
- Others: No aftershock assumed. Assumed that tsunami had arrived after the earthquake.

ii) Damages assumed

We assumed that some rivers and national roads would suffer damage resulting from the earthquake.

iii) Outline of scenario

Our scenario has two phases: Phase I and Phase II.

1) Phase I

Phase I starts with setting up a countermeasure framework and ends at initial inspection. Players entered and viewed inspection data. In Phase I, we finally confirmed how well the entire system would work and also evaluated how familiar data readers and data operators were with their own tasks.

2) Phase II

Phase II starts with when data operators would have entered inspection/damage data to some extent and ends at when they would start emergency recovering tasks. We handled disaster countermeasures by using our information system.

iv)How to assume disasters and scenario

1) We assumed certain disaster countermeasures tasks, which would bring about positive impacts on disaster countermeasures if our disaster information system were employed. (Table 2)

2) In addition, we also set up certain tasks so that we would be able to evaluate the performance of our new system capabilities and explicitly understand some positive impacts. In addition to our assumption as stated in 1) above, we also assumed some tasks that would explicitly bring about positive impacts on the system's functional capabilities.

(3) How to allocate tasks for players

We allocated player's tasks by distributing a (pink color) card that specifies the player's tasks. In the experiment, the controller basically did not orally specify the player's tasks over the phone. Fig.3 shows an example of the card specifying the player's tasks.

3.3 Experiment Results

When considering the experiment as whole, participants from MLIT regional development bureau staff that mainly acted as data readers in the experiment provided positive responses, stating that the new disaster information system was helpful in their tasks. Local office workers, who mainly acted as data operators, highly evaluated that the new system provided an easily viewable data screen, but they also pointed out many problems that would require improvements.

Positive responses are shown at 3.3.1 to 3.3.3

3.3.1 Overall Evaluation

- The new system is good because it only imposes a smaller amount of workload than the current system and also eliminates data input errors.
- It is highly user-friendly and provides significant positive impacts.

3.3.2 Supporting Capabilities in Collecting, Analyzing and Sharing Information

- It is good because the system provides the newest real-time information.
- It is possible to share information with many stakeholders.
- By using the system, it becomes easier to coordinate disaster-related data.
- It becomes easier to understand affected locations.

3.3.3 Impacts of Specific Functional Capabilities

- The indirect location reference database enables a map-based data search. With the new system, it becomes easier to collect data on a certain location (a specific mile post).
- FAX-OCR is effective if a local office has a poor network connection or if staff are unfamiliar with how to use a PC. It is good because a fax document is attached to the map (on the top of the screen).

Participants also indicated the following problems that require some improvements.

(1) In some cases, the system is difficult to operate or provides some confusing data screens.

[Examples]

i) The button names do not represent functional capabilities intuitively understandable.

ii) Icon marks are not intuitively understandable.

iii) Some improvements are necessary for switching over multiple screens, screen locations and screen sizes when there is more than one screen on the display. (Operator sometimes needs to find the screen he/she was working on, as another screen may appear on the top by some data process.)

(2) Some improvements are necessary to prevent data operator's errors.

[Examples]

i) Buttons should be properly located to prevent data operator's errors. (These buttons are located close to one another, which could easily result in pushing the wrong button.)

ii) Updating the map is different from updating the bulletin board. (I had wrongfully thought that updating the map or bulletin board would automatically update both.)

(3) The system has way too many operation steps.

[Examples]

i) It is troublesome to confirm incoming data because I need to do it by opening the detail data screen. (It would be better if we could do that on the list.)

ii) As an decision maker, I have two different screens for inspection data and for damage data because I like to manage them separately. However, as a data-input operator, the system would be better if we could enter the inspection and damage data at the same time.

iii) Operators could easily select a wrong data entry screen and enter the wrong data. As the data screens look similar to one another, operators could easily make a mistake (e.g., damage data might be entered on the inspection data screen).

(4) It is necessary to have a function to ensure timely confirmation of new incoming data.

[Examples]

i) It is difficult to distinguish between already-read data and unread data.

ii) The system should have an alarm to let us know when new data arrive at the system.

(5) It is necessary to modify or supplement the current rules.

[Examples]

i) Each division should check out their data when sending or reporting their data. (A report from a local office to a regional bureau requires the approval of the head of the local office. However, a new approval rule is necessary in order to operate the new system in a better manner.)

ii) Report titles are not coherent. We don't have a proper rule on describing data even though this kind of rule is a must for proper data analysis.

(6) Others

i) It would be better if we could customize screen shots or functional capabilities for each user.

[Examples]

-Some data displays or functional capabilities are not necessary at the local office level. (It was necessary to select the necessary data at the local offices.)

-Two data categories (river and road) would be okay for the Planning Department, but the Road Department will need more detailed data categories of only road.

ii) Proper screen shot or expression is necessary

[Examples]

-The system would be better if it calculates some data so that we could answer routine questions from the MLIT headquarters. (For example, the system should be able to calculate the inspection progress percentage.)

iii) Some improvements are necessary in the indirect location reference database.

[Example]

-The system would be better if we could search an intended location by using the intersection name as a keyword.

iv) It is necessary to provide easily viewable maps.

[Examples]

-The system provides many unnecessary data displays. (It is possible to set the data items for dispaly, but the default data shot provides so many data items.)

- When we have an increased number of data showing on the screen, it is difficult to identify the selected data items.

v) Problems in FAX-OCR

[Examples]

-The system should have an alarm to let us know that the data have arrived.

-The data entries in OCR format should be fully optimized.

vi)The system should have more functional capabilities in the future.

[Examples]

-The system should automatically import data by using sensor-based systems.

-The system would be better if it imported data from GPS mobile phones.

-We need applications for our tasks under usual conditions.

We have been making efforts to solve the aforementioned problems after setting up our priorities.

4. FUTURE EFFORTS

After some modifications in line with our experiment outcomes, the Chubu Regional Development Bureau will start operating its new disaster information system in FY2006.

We also intend to develop a new operational manual and specifications after correcting some problems, paying attention to the results of our demonstration experiment (Fig4). The outcomes of our efforts will contribute to reducing R&D costs if they are effectively used for developing a new system or expanding the system functional capabilities.

5. REFERENCES

1. Kusakabe, T. and Sanada, A. : Application of Information & Communication System for Better Coordination among the Emergency Responders, *Proc .the 37th Joint Panel Meeting of U.S.- JAPAN Panel on Wind and Seismic Effects UJNR*, pp297-310, 2005

Table 1 Problem in Collecting and Sharing Disaster Information

Tasks	Current problems
Collecting Information	**1) The system does not provide visually apparent data.** **2) We also need various data such as damages on facilities outside our responsible areas, but such data are very difficult to get.** **3) It is difficult to effectively use our data available under normal conditions.**
Analyzing Information	**4) Information will become deteriorated. Data processing is difficult.** **5) Some redundant tasks are emerging.**
Managing Information	**6) The system is difficult to manage data temporally or spatially.** **7) Processing a massive amount of data is difficult.**
Distributing Information	**8) Telephone line convergence emerges.** **9) Inefficiencies, workload and artificial mistakes will increase because the staff need to provide multiple stakeholders with data.** **10) Data communication channels have been designed, merely by paying attention to data management needs.**

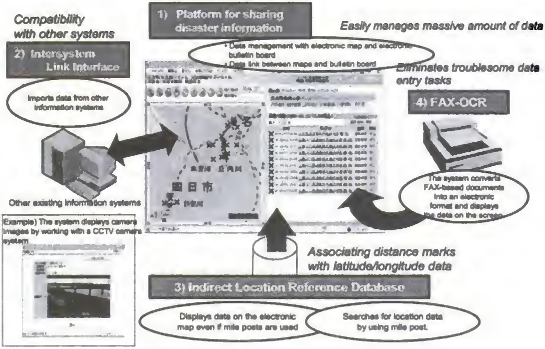
Compatibility with other systems
1) Platform for sharing disaster information
Easily meneges massive amount of data
2) Intersystem Link Interface
• Data management with electronic map and electronic bulletin board
• Data link between maps and bulletin board
Eliminates troublesome data entry tasks
Imports data from other information systems
4) FAX-OCR
The system converts FAX-based documents into an electronic format and displays the data on the screen
Other existing information systems
Example) The system displays camera images by working with a CCTV camera system
Associating distance marks with latitude/longitude data
3) Indirect Location Reference Database
Displays data on the electronic map even if mile posts are used
Searches for location data by using mile post.

Fig.1 Main Characteristics of Disaster Information System in our Development and Demonstration Experiment Efforts

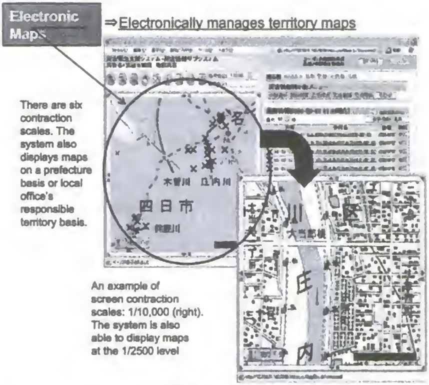

There are six contraction scales. The system also displays maps on a prefecture basis or local office's responsible territory basis.

An example of screen contraction scales: 1/10,000 (right). The system is also able to display maps at the 1/2500 level

(1) Electronic maps

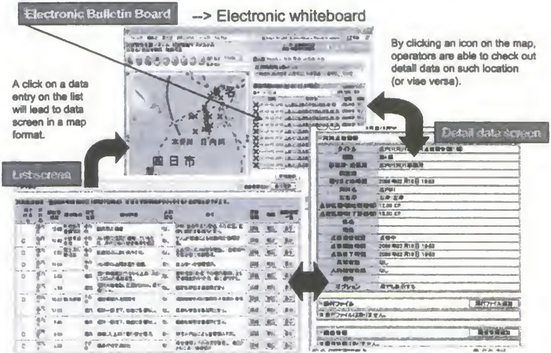

By clicking an icon on the map, operators are able to check out detail data on such location (or vise versa).

A click on a data entry on the list will lead to data screen in a map format.

A list of various categories, such as inspection progress and damages

Detail data on inspection zones and affected locations

(2) Electronic Bulletin Board
Fig.2 Outline of Platform for Sharing Disaster Information

Table 2 Scenarios assumed (details)

Collecting information

[All staff are able to check out information once the data is entered in the system]

- Staff would answer questions from mass media, local governments and other organizations.
    - ◆ They would provide information (without making inquires to pertinent organizations) based on the data displayed on the system.
- River office staff would confirm detours.
    - ◆ They would provide information (without making inquires to pertinent organizations) based on the data displayed on the system.
- By using media information (residents evacuation to river area or tsunami residues accumulation at coastal areas) when little information is available, the staff would provide inspection-related instructions to check out these locations.
    - ◆ The system would provide data that have been difficult to use so far.

Analyzing information

[Easily manages information]

- Staff would answer questions from local governments about XXX River, Route XX or a certain location.
    - ◆ The system would identify the location in question from address data or distance marks and display the data relating to such location.
- Staff would coordinate data available as of XX o'clock and report them to senior officials and the Ministry headquarters.
    - ◆ They would coordinate the data entries (without transcribing or re-typing them).
    - ◆ The system would automatically sort out the data in the bureau's jurisdiction into a report format acceptable to the Ministry headquarters.
- Staff would answer questions from XX Prefecture about prefectural information, XXX River or National Route XX.
    - ◆ The system would display a map on a prefectural basis or local office's responsible territory basis.
    - ◆ The system would display a list of bulletin boards by using prefectural, river or route name.

[Others]

- We assumed serious damages, less serious damages and death of passengers or users.
    - ◆ Evaluates priority in sending data

Table 2 Scenarios assumed (details) (Continued)

Managing information

[Easily manages information]

- Road or river administrators would address the damages after receiving a report from residents. They would manage data, associating them with resident reports or actual disaster countermeasures.
  - ◆ The system would comprehensively manage related data in a category, such as unidentified data or administrator's confirmed data.
- Damages would occur at the same time at an embankment at adjacent distance marks.
  - ◆ The system would properly manage data by enlarging maps or displaying a bulletin board list even if multiple affected locations exist nearby.
- The system would easily convert data into an electronic format because it has FAX-OCR.
  - ◆ The system would manage data that are difficult to use so far.

[Real-time data and historical data on disaster countermeasures are available]

- Data operator would enter wrong damage data in the system and then correct them.
  - ◆ They would easily search for data entry (sorting out the data on a time-series basis, facility basis, or mile post basis).
  - ◆ The system would also display the data correction process. It is available to any staff at the site.
- As some other departments have provided disaster data, staff would instruct a local office to collect data on site and conduct subsequent countermeasures.
  - ◆ As the system would display actual disaster countermeasures at affected locations, system users would easily confirm actual countermeasures that are taken in line with their own instructions.

Distributing information

[Proper role sharing between information system and FAX/phone]

- River office staff would identify a road disaster.
  - ◆ They would report such damage, and they would be able to check out the data on the system (without making a phone call or sending a FAX).
- They would make the first report of damage over the phone and check out detailed data on the system.
  - ◆ Proper role sharing between the phone call and the information system
- Staff would state necessary equipment over the phone and enter equipment data in the system for the purpose of data management.
  - ◆ Proper role sharing between the phone call and the information system

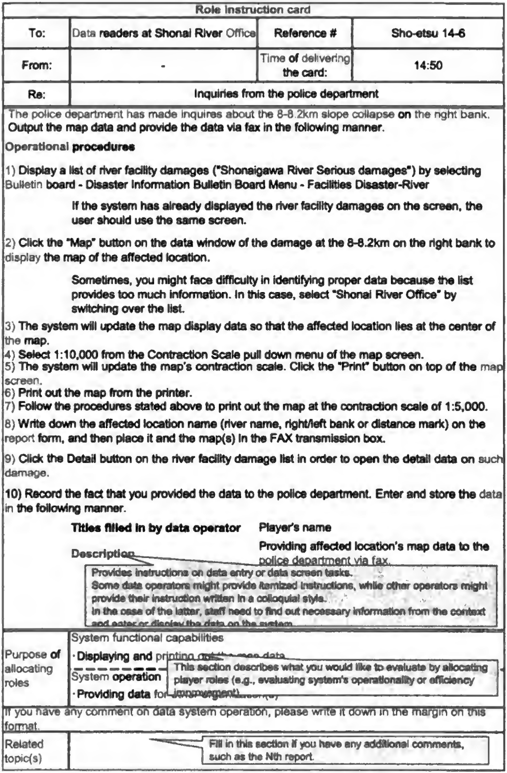

Role instruction card			
To:	Data readers at Shonai River Office	Reference #	Sho-etsu 14-6
From:	-	Time of delivering the card:	14:50
Re:	Inquiries from the police department		

The police department has made inquires about the 8-8.2km slope collapse on the right bank. Output the map data and provide the data via fax in the following manner.

Operational procedures

1) Display a list of river facility damages ("Shonaigawa River Serious damages") by selecting Bulletin board - Disaster Information Bulletin Board Menu - Facilities Disaster-River

If the system has already displayed the river facility damages on the screen, the user should use the same screen.

2) Click the "Map" button on the data window of the damage at the 8-8.2km on the right bank to display the map of the affected location.

Sometimes, you might face difficulty in identifying proper data because the list provides too much information. In this case, select "Shonai River Office" by switching over the list.

3) The system will update the map display data so that the affected location lies at the center of the map.
4) Select 1:10,000 from the Contraction Scale pull down menu of the map screen.
5) The system will update the map's contraction scale. Click the "Print" button on top of the map screen.
6) Print out the map from the printer.
7) Follow the procedures stated above to print out the map at the contraction scale of 1:5,000.

8) Write down the affected location name (river name, right/left bank or distance mark) on the report form, and then place it and the map(s) in the FAX transmission box.

9) Click the Detail button on the river facility damage list in order to open the detail data on such damage.

10) Record the fact that you provided the data to the police department. Enter and store the data in the following manner.

Titles filled in by data operator	**Player's name**
Description	**Providing affected location's map data to the police department via fax.**

Provides instructions on data entry or data screen tasks.
Some data operators might provide itemized instructions, while other operators might provide their instruction written in a colloquial style.
In the case of the latter, staff need to find out necessary information from the context and enter or display the data on the system.

Purpose of allocating roles	System functional capabilities · **Displaying and** printing out the map data System **operation** · **Providing data** for other organization(s)

This section describes what you would like to evaluate by allocating player roles (e.g., evaluating system's operationality or efficiency improvement).

If you have any comment on data system operation, please write it down in the margin on this format.

Related topic(s)	

Fill in this section if you have any additional comments, such as the Nth report.

Fig 3 Sample of Card to Specify Players' Task

[Studied contents]	[Final Results]
Disaster countermeasures task model	Use case chart
	Disaster countermeasures manual
System basic specifications	Standard specifications
Data dictionaries	JPGI-compatible standard specifications
System interface specifications	Standard specifications (draft)
FAX-OCR	Project book, functional specifications, user manual
Indirect location reference database	Project book, functional specifications, user manual

If decision makers refer to these documents (including the definitions for system capability requirements) when establishing a new system or adding capabilities of their existing systems, cost to define system function requirements and to design system will be reduced.

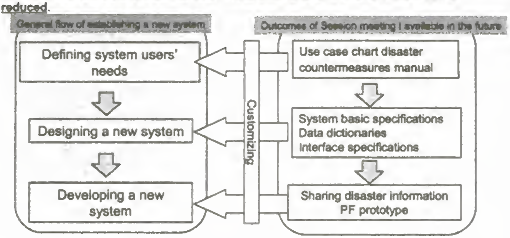
General flow of establishing a new system
Outcomes of Session meeting I available in the future
Defining system users' needs
Designing a new system
Developing a new system
Customizing
Use case chart disaster countermeasures manual
System basic specifications
Data dictionaries
Interface specifications
Sharing disaster information PF prototype

Fig 4 Final Result and Its Contribution in Developing New Disaster Information System

Health Concerns Associated with Mold in Water-Damaged Homes After Hurricanes Katrina and Rita — New Orleans Area, Louisiana, October 2005

by

Clive Brown[1], Margaret Riggs[2], Carol Rao[3], Kristin Cummings[4]

ABSTRACT

Breaches in the levees after Hurricanes Katrina and Rita in August and September, 2005 led to flooding in the New Orleans area making the likelihood of mold contamination a certainty. The Louisiana Department of Health and CDC assessed mold exposure in homes and mold remediation knowledge and behaviors of residents and workers. A convenience sample of residents and remediation workers with potential exposure to mold were asked questions about their knowledge, attitudes, and practices regarding mold. One consenting adult from a random selection of 112 of the 440,269 households in the New Orleans area responded to questions on demographics, home occupancy, and participation in remediation activities a visually assessment of water damage and mold growth was done. Samples were collected from a subset of homes and tested for culturable fungi, endotoxins, glucans and fungal spores. A total of 235 (70.1%) of the 332 workers and residents approached were for interviewed. Most workers and residents were aware that exposure to mold could affect health, but neither workers nor residents consistently wore personal protective equipment (PPE). An estimated 46% or about 110,000 homes had some mold growth. Although typical molds were found, environmental markers of mold and other micro-organisms were above levels typically reported with an inversion of the outdoor/indoor ratio. Novel approaches are needed to increase the availability of PPE and to communicate health prevention strategies to reduce exposure to mold in post disaster situations that involve floods.

KEYWORDS: mold, hurricane, flooding,

1.0 INTRODUCTION

On August 29 and September 24, 2005, Hurricanes Katrina and Rita respectively made landfall along the Gulf Coast. After both instances, levees were breached leading to massive flooding in New Orleans and surrounding parishes. The duration and extent of flooding, and the number of structures flooded in New Orleans, made the likelihood of massive mold contamination a certainty.

Recent parallels to the degree of flooding seen in New Orleans as a result of Hurricanes Katrina and Rita occurred in 1997 in Grand Forks, North Dakota, and in 1999 in North Carolina after Hurricane Floyd (CDC 2004). In North Carolina there was a reported increase in persons presenting with asthma symptoms and this was postulated to be due to exposure to mold (CDC 2004). In 2001, flooding and subsequent mold growth on the Turtle Mountain reservation in Belcourt, North

---

[1] Medical Epidemiologist, Centers for Disease Control and Prevention, Atlanta, GA 30333, USA

[2] Epidemiologist & Epidemic Intelligence Service Officer, Centers for Disease Control and Prevention, Atlanta, GA 30333, USA

[3] Epidemiologist & Epidemic Intelligence Service Officer, Centers for Disease Control and Prevention, Atlanta, GA 30333, USA

[4] Medical Epidemiologist & Epidemic Intelligence Service Officer, Centers for Disease Control and Prevention, Atlanta, GA 30333, USA

Dakota was associated with self-reports of rhinitis, rash, headaches, and asthma exacerbation (Stock 2005). The Institute of Medicine report on Damp Indoor Spaces and Health (IOM 2004) determined that exposures to mold are associated with respiratory illnesses, and that immunocompromised persons are at risk for fungal colonization and opportunistic infections. Although there have never been reports of increased fungal infections related to floods in the United States, anecdotal case-reports of fungal infection after floods include *Apophysomyces elegans* wound infection in a man who sustained traumatic injuries after the southeast Asian tsunami in December 2004 (Andresen 2005). In addition, there is an endemic area of Blastomycosis in Washington Parish, Louisiana, about 70 miles from New Orleans (Lowry 1989).

CDC, state public health officials and the general public were therefore concerned about possible health effects for returning residents due to the anticipated mold contamination of homes and other structures along the U.S. Gulf Coast associated with massive flooding after these hurricanes (CDC 2005). Because of these concerns, CDC was invited by the Louisiana Department of Health and Hospitals (LA-DHH) to assist in an investigation of the respiratory health effects of mold exposure. The epidemiologic investigation was planned to determine if there were increased respiratory symptoms, assess mold exposure, and determine mold remediation knowledge and behaviors of residents and workers. This report summarizes partial results and findings from the investigation.

2.0 METHODS

During October 2005, a team composed of CDC personnel assisted LA-DHH to conduct a variety of public health surveillance activities in and around hospitals, worksites, and communities in the Greater New Orleans area.

2.1 Knowledge, Attitudes, and Practices Survey of Residents and Workers

During October 18--23, the assessment team conducted interviews in English and Spanish with residents and remediation workers in recently flooded communities at the FEMA Disaster Recovery Center in St. Bernard, a home improvement store in West Jefferson, and a grocery store in East Jefferson and at worker gathering sites. A convenience sample of residents and remediation workers with potential exposure to mold were asked questions about their knowledge, attitudes, and practices regarding mold; non-identifying demographic information was also collected. A display of respirators was used for reference during the interviews. Statistical analyses were done using SAS (version 9.12) software packages (SAS Institute, Cary, NC, USA) to generate means, medians and frequency distributions for questionnaire items. Comparative analyses were done using Chi-squared and Fisher's exact tests.

2.2 Survey of New Orleans Residences to Assess Level of Flooding and Mold Growth

2.2.1 Selection of Residences

During October 22--28, the team assessed a sample of a cross-section of the 440,269 households in the four-parish area (on the basis of the 2000 U.S. Census). Sampling was restricted to blocks with more than 20 housing units yielding 239,949 potential households. Blocks were classified into three strata (mild, moderate, and severe) on the basis of Federal Emergency Management Agency (FEMA) flood and damage maps. Geographic information system (GIS) mapping software was used to select a random number of waypoints (latitude and longitude) proportionate for each stratum. A sample size of 88 homes was required to obtain estimates within 10% accuracy. Global positioning system (GPS) units were used to locate each waypoint as the random starting point to locate the nearest home at or north of the waypoint.

2.2.2 Investigation of Residences

A questionnaire on demographics, home occupancy, and participation in remediation activities was administered to one consenting adult from the homes in which someone was in the home. A standard instrument designed for this study was used to visually assess water damage and mold growth. Statistical analyses were done using SAS (version 9.12) software packages (SAS Institute, Cary, NC, USA) to generate means and frequency distributions for questionnaire and visual assessment items.

2.2.3 Environmental Sampling and Laboratory Analysis

Between October 22—27, 2005, samples were collected indoors and outdoors at a subset of participating homes. Indoors, samples were collected in the "moldiest" room of the residence, as visually assessed by an industrial hygienist, using 0.4 μm pore size, 37 mm closed-faced filters, sampling at a rate of 3 liters per minute. Sampling time ranged from 36 to 144 minutes.

The filters were analyzed for culturable fungi, (1→3, 1→6)-β-D-glucan (a cell-wall component of many fungi) (Blanc 2005), endotoxin (a cell-wall component of gram-negative bacteria) (Thorne 2000) and fungal spores. For statistical analyses, post priori, residences were grouped into mild and moderate/heavy-damaged categories. Statistical analyses were done using SAS (version 9.12) software packages (SAS Institute, Cary, NC, USA). Concentrations were expressed as geometric means (GM) and geometric standard deviations (GSD).

3.0 RESULTS

3.1 Survey of Residents and Workers

A total of 332 persons (workers and residents combined) were approached for interviews; 235 (70.1%) participated. Of 159 residents interviewed, 82 (51.6%) were male; the overall mean age was 51 years (range: 18--81 years). Nearly all (96.2%) residents responded affirmatively to the question, "Do you think mold can make people sick?" One hundred eight (67.9%) correctly identified particulate-filter respirators as appropriate respiratory protection for cleaning of mold. Sixty-seven (42.1%) had cleaned up mold; of these, 46 (68.7%) did not always use appropriate respirators. Reasons for not using respirators included discomfort (10 [21.7%] respondents) and lack of availability (10 [21.7%]). For public communications about potential risks from exposure to mold and the use of personal protective equipment, 139 (87.4%) respondents recommended the use of television or radio.

Seventy-six persons who self-identified as remediation workers were interviewed. Of these, 14 (18.4%) were self-employed, and 62 (81.6%) worked for a company doing remediation. Of the 76 workers, 70 (92.1%) were male; the mean age of respondents was 33 years (range: 18--57 years); 41 (54%) spoke only Spanish. Seventy-two (94.7%) thought mold causes illness. Sixty-five (85.5%) correctly identified particulate-filter respirators as appropriate protection for cleaning of mold. Sixty-nine (90.7%) had already participated in mold remediation activities at the time of the interview. Of these, 34 (49.3%) had not been fit tested for respirator use and 24 (34.8%) did not always use appropriate respirators; 13 (54.2%) cited discomfort as the reason for not using respirators. For worker communications about potential risks from exposure to mold and the use of personal protective equipment, 36 (47.4%) recommended use of television or radio and 17 (22.4%) recommended communication through employers.

3.2 Environmental Survey of New Orleans Residences to Assess Level of Flooding and Mold Growth

In the sampled areas, 141 homes were found to be occupied. The questionnaire was administered to an adult from 113 of the 141 homes in which someone was in the home. One assessment was abandoned resulting in a final sample of 112.

Of 112 homes inspected (Table), flood levels were assessed from the outside for 105 homes as been high (>6 feet) in 21 (20%) homes, medium (3--6 feet) in 18 (17.0%), and low (<3 feet) in 66 (63%) (including 38 [36%] homes with no flooding). Flood levels were assessed as been high indoors for 16 (15%) of 109 homes. Seventy-six (67.9%) homes had roof damage with water leakage. Visible mold growth occurred in 51 (45.5%) homes, and 19 (17.0%) had heavy mold coverage (>50% coverage on interior wall of most-affected room). The distribution of homes with heavy mold coverage was 10 (52.6%), seven (36.8%), and two (10.5%) in high, medium, and low flood areas, respectively.

Participants reported being indoors doing heavy cleaning an average of 13 hours since the hurricanes (range: 0--84 hours) and 15 hours doing light cleaning (range: 0--90 hours). Sixty-eight (60.7%) participants reported inhabiting their homes overnight for an average of 25 (standard deviation: +13.7) nights since the hurricanes.

3.2.1 Environmental Samples

Samples were collected indoors from 20 of the 112 residences that participated in the survey, and also outdoors from 11 of these 20 residences. Of the 20 residences sampled, 5 were in mild-damaged areas and 15 were in heavy-damaged areas. Moderately to heavily-damaged residences had higher measures of microorganisms compared to mild-damaged residences. However, only for culturable fungi were they significantly different (Table 1). Indoors, for culturable fungi, Penicillium and Aspergillus were the most commonly identified fungal species. In outdoor samples, Penicillium, Aspergillus and Cladosporium were most commonly identified.

3.2.2 Household Factors and level of Mold and Micro-organisms

As noted, level of flooding was associated with observed and culturable mold growth. Though not statistically significant, for the 20 homes where samples were taken, there were differences in the levels of endotoxin, glucan and mold growth by the type of material used for wall, ceiling or flooring (Table 2). The amount of endotoxin, glucan and mold growth was greater for drywall or wood compared to plaster or tile. However, no similar relation was seen for observed mold growth and type of wall or floor material in analyses including all surveyed homes (table 3). In a logistic regression model of the full sample controlling for remediation, observed indoor flood level was associated with mold wall coverage whether the wall material was drywall or not. When indoor flooding was greater than 3 feet, both drywall/wood paneling (odds ratio, OR=26; CI 6.0-114.3, p<0.05) and plaster/tile (OR=36; CI 2.5- 527.0, p<0.05) were associated with mold wall coverage of >50%.

4.0 DISCUSSION

The typical molds found indoors and outdoors in all regions and all climates in the United States are *Aspergillus, Cladosporium and Penicillium* (Shelton 2002). Indoor concentrations are generally lower than outdoor levels and for culturable fungi, median indoor levels are approximately 80 CFU/m3 ranging from the lower limit of detection to 10,000 CFU/m3 (Shelton 2002). Indoor concentrations were found to be lowest in the Northeast and highest in the Southwest, Far west and Southeast (Shelton 2002).

We estimate that in New Orleans there were at least 110,000 homes with elevated mold and bacteria levels and at least 40,000 homes that were heavily contaminated with mold and bacteria. Based on samples taken from a limited number of homes, typical fungi were found indoors and outdoors. However, the levels indoors and outdoors were much higher than typically found and indoor levels were higher than outdoors.

Similarly, levels of glucan and endotoxin were higher than typically reported. In this assessment, a newer assay for (1→3, 1→6)-β-D-glucan (Douwes 2005) which has a higher specificity for fungi, yielded higher indoor than outdoor levels in New Orleans homes, confirming the findings from visual assessment of homes and measurements of culturable fungi and spore counts. Levels of airborne endotoxin inside homes in post-hurricane New Orleans averaged more than 20 times higher than the usual 1.0 EU/m3 average (Park 2000), with an inversion of the expected indoor-outdoor relationship. Thus in addition to mold, these environments most likely had other micro-organisms and possibly their toxic metabolites.

As expected the main factor associated with mold growth was the extent of flooding. However, though not statistically significant, drywall and wood were more likely to be found with higher levels of mold growth, glucan and endotoxin. However, observed mold growth in all homes surveyed was not associated with type of building material. These results could imply that elevation of homes and type of building materials may be important when building in flood prone areas such as New Orleans, but more data is needed to resolve this question.

Although a variety of clinical syndromes and symptoms are reportedly associated with mold and microorganisms in damp environments, the Institute of Medicine report on Damp Indoor spaces (IOM 2004) found sufficient evidence of an association for a limited number of conditions. Exposures, especially to mold were often determined by self-report. Associated conditions included: upper respiratory tract symptoms (such as nasal congestion, sneezing, runny or itchy nose, and throat irritation); lower respiratory tract symptoms of cough and wheeze; asthma symptoms in sensitized people with asthma; hypersensitivity pneumonitis in a small proportion of susceptible people; invasive respiratory and other fungal infections in severely immunocompromised people; and fungal colonization of the respiratory tract or infection in individuals with chronic pulmonary disorders.

In some homes, the measured indoor endotoxin levels were comparable to those of certain industrial settings in which declines in pulmonary function have been demonstrated (Douwes 2002). The levels of mold found were well above levels reported as being associated with symptoms of respiratory tract illnesses in children (Stark 2003). However, based on the currently available evidence, we cannot determine a level of mold that is either safe or likely to be associated with adverse health effects (IOM 2004) and there are no standards that relate health effects to specific levels of molds in the air (Rao 1996).

In October 2005, the CDC Mold Work Group published guidelines for remediation workers and the public on preventing mold-associated illness (CDC 2005, CDC 2006). Recommendations included avoiding exposure when possible and using a particulate-filter respirator during activities that create mold-contaminated dust. Despite the apparent risk of exposure to mold and other microorganisms in New Orleans homes post Katrina and a seeming awareness by workers and residents about the potential for adverse health outcomes from exposures, PPE was not consistently used. This was despite the fact that residents reported spending a lot of time inside homes doing clean-up work. Disruption of normal communication channels made the dissemination of public health messages difficult immediately post Katrina. Novel measures to increase awareness of appropriate respiratory protection among the public are warranted in the immediate post disaster settings. As conditions return to near normal, communication could be carried out via traditional media announcements and educational sessions for employees of home improvement stores and other commercial entities that sell respirators. Public availability of particulate-filter respirators might be increased through partnerships with respirator manufacturers. For remediation workers, the importance of appropriate respiratory protection should be emphasized via traditional media announcements and/or employers, with messages in both English and Spanish. Fit testing should occur according to the OSHA Standard (OSHA 2004); making such services available to small or individual operators might increase compliance with requirements.

5.0 ACKNOWLEDGEMENTS

The authors would like to thank GL Chew, ScD, Mailman School of Public Health, Columbia University, New York, New York; PS Thorne, PhD, College of Public Health, University of Iowa, Iowa City, Iowa; and M Muilenberg, MS, School of Public Health, Harvard University, Boston, Massachusetts, who contributed data used in part to prepare this report; D Van Sickle, PhD, J Ferdinands, PhD, David Callahan MD, R Moolenaar, MD, Air Pollution and Respiratory Health Branch, National Center for Environmental Health, CDC.

6.0 REFERENCES

D Andresen, A Donaldson, L Choo, A Knox, M Klaassen, C Ursic, et al. Multifocal cutaneous mucormycosis complicating polymicrobial wound infections in a tsunami survivor from Sri Lanka. The Lancet, 2005;365;876-878.

Blanc PD, Eisner MD, Katz PP, et al. Impact of the home indoor environment on adult asthma and rhinitis. J Occup Environ Med 2005;47:362–72.

CDC. Morbidity and Mortality Associated With Hurricane Floyd — North Carolina. MMWR 2000;49:369-372.

CDC. Interim recommendations: respiratory protection for residents reentering previously flooded areas and homes. Atlanta: US Department of Health and Human Services; 2005. Available at: http://www.bt.cdc.gov/disasters/hurricanes/katrina/respiratorypub.asp

CDC. Mold: Prevention Strategies and Possible Health Effects in the Aftermath of Hurricanes and Major Floods. MMWR Recomm Rep. 2006 June 2;5x(RR-y):1-zz.

Douwes J, Pearce N, Heederik D. Does environmental endotoxin exposure prevent asthma? Thorax 2002;57:86–90.

Institute of Medicine Committee on Damp Indoor Spaces and Health. Damp Indoor Spaces and Health. Washington DC: The National Academies Press 2004:183-269.

Lowry P, Kelso K, McFarland L. Blastomycosis in Washington Parish, Louisisna, 1976-1985. American J Epidemiology 1989;130:151-159.

Park JH, Spiegelman DL, Burge HA, Gold DR, Chew GL, Milton DK. Longitudinal study of dust and airborne endotoxin in the home. Environ Health Perspect 2000;108:1023–8.

Occupational Safety and Health Administration (OSHA). Fit testing procedures (mandatory). Washington, DC: US Department of Labor, Occupational Safety and Health Administration; 2004. Available at http://www.osha.gov/pls/oshaweb/owadisp.show_document?p_table=standards&p_id=9780.

Rao CY, Burge HA, Chang JC. Review of quantitative standards and guidelines for fungi in indoor air. J Air Waste Manag Assoc. 1996;46:899-908.

Shelton BG, Kirkland KH, Flanders WD, Morris GK. Profiles of airborne fungi in buildings and outdoor environments in the United States. Applied and Environmental Microbiology 2002; 68:4; 1743-1753.

Stark PC, Burge H, Ryan LM, et al. Fungal levels in the home and lower respiratory tract illnesses in the first year of life. Am J Respir Crit Care Med 2003; 168; 232-237.

Stock AL, Davis K, Brown CM, et al. An investigation of home dampness and adverse health effects on a Native American Reservation. The Toxicologist CD —Journal of the Society of Toxicology 2005: 84 (S-1).

Thorne PS. Inhalation toxicology models of endotoxin- and bioaerosol-induced inflammation. Toxicology 2000;152:13-23.

Table 1: Geometric means (GM) and geometric standard deviations (GSD) of indoor microbiological measurements by FEMA classification of water damage and outdoor microbiological measurements,

	Indoors					Outdoors		
	Mild	Moderate/ Heavy	Mild vs mod/heavy	Overall				Indoor vs Outdoor
Measurement (units)	**GM (GSD)**	**GM (GSD)**	**P-value**	**GM (GSD)**	**Min-Max**	**GM (GSD)**	**Min-Max**	**P-value**
Endotoxins (EU*/m3)	9.7 (2.0)	31.3 (6.5)	0.08	23.3 (5.6)	1.2 – 1,200	10.5 (2.5)	2.2-83.0	0.1
Glucans (ng/m3)	1.1 (5.3)	1.8 (4.3)	0.28	1.6 (4,4)	0.33 – 45.5	0.91 (2.0)	0.40-3.3	0.3
Culturable fungi at 25°C (CFU/m3)**	3700 (9.1)	67,000 (10.1)	0.02		270 – >LOD***	4,700 (2.8)	1,300-34,000	
Culturable fungi at 37°C (CFU/m3)**	630 (3.1)	16,000 (10.5)	0.002		<LOD – 1,200,000	980 (3.7)	149-16,000	
Total spore counts (spores/m3)	60,000 (5.8)	460,000 (14.9)	0.10		8,200 – 67,000,000	43,000 (5.0)	8,400-2,500,000	

Table 2a: **Observed surface mold coverage for different types of material in the 20 homes where samples were taken**

	Material	N	Surface mold coverage* Mean ±SD	P-value
Wall	Drywall/wood	16	2.20 ± 1.7	
	Plaster/Tile	4	0.50 ± 0.6	0.07
Ceiling	Drywall/wood	16	0.90 ± 1.2	
	Plaster/Tile	4	0.03 ± 0.6	0.5

*Mold coverage values are based on the mean of the rank after arranging the mold coverage categorizes in rank order such that:
0= none; 1= <25%; 2=25-50%; 3=50-75%; & 4>75%.

Table 2b: **Endotoxin and glucan levels by type of interior wall material in the 20 homes where samples were taken**

	Material	N	GM (GSD)	P-value
Endotoxin	Drywall/wood	16	28.5 (6.4)	
	Plaster/Tile	4	10.4 (1.8)	0.3
Glucan	Drywall/wood	16	2.0 (4.6)	
	Plaster/Tile	4	0.7 (3.7)	0.2

Table 2c: **Endotoxin and glucan levels by type of floor material in the 20 homes where samples were taken**

	Material	N	GM (GSD)	P-value
Endotoxin	Hard Surface	8	23.3 (5.7)	
	Carpet/wood	12	16.8 (5.4)	0.3
Glucan	Hard Surface	8	2.3 (5.6)	
	Carpet/wood	12	1.2 (3.7)	0.4

Table 3: **Observed surface mold coverage for different types of material for all surveyed homes**

	Estimated Percent of Surface covered with mold			
	None	**Less than 50%**	**At least 50%**	**P-value**
Wall material				
Drywall/wood	42	23	14	
Plaster/Tile	18	8	4	0.5
Floor Material				
Tile/linoleum	21	9	9	
Carpet/wood	39	22	9	0.3

Technical Session 6

DAMS

Investigation into Crack Phenomena of Unreinforced Concrete Structures for Aseismic Evaluation of Concrete Dams

by

Tadahiko Sakamoto[1], Yoshikazu Yamaguchi[2], Takashi Sasaki[3], Kei Takafuji[4], Ken-ichi Kanenawa[5]

ABSTRACT

We have conducted research on non-linear analysis for concrete dams using the smeared crack model. Efforts to verify applicability and accuracy of such numerical analyses for concrete dams have been made through simulations for actual damages of existing concrete dams due to large earthquakes. But, a more quantitative evaluation of the cracking process of concrete dams using crack analysis is needed in order to use such analytical method to estimate the limit state of concrete dams against large earthquakes.

In the present study, we conducted shaking table tests on pillar-shaped unreinforced concrete specimens to investigate the effect of cracks on the dynamic behavior of concrete structures. The results showed that as tensile fracture progresses, the first resonant frequency of the specimen lowers and the damping increases. We simulated vibration tests by non-linear dynamic analysis based on the smeared crack model. Based on a comparison of the test results and numerical simulation, we discuss how to set parameters for numerical simulation such as the tension softening curve and damping ratio, to simulate the cracking behavior of unreinforced concrete structures such as concrete dams.

KEYWORDS: Non-linear FEM Analysis, Shaking Table Test, Smeared Crack Model, Tensile Fracture, Unreinforced Concrete Structure.

1. INTRODUCTION

As a consequence of frequent large earthquakes that have occurred in Japan in recent years, evaluating the seismic safety of various infrastructures has become an important and urgent issue. In this situation, the Ministry of Land, Infrastructure and Transport of the Japanese Government published the "*Guidelines for Seismic Performance Evaluation of Dams (Draft)*" [1] in March 2005.

According to the guidelines, numerical analysis considering the tensile fracture of concrete is needed to evaluate the seismic safety of concrete gravity dams in the event of a large earthquake. The authors have considered the seismic safety of concrete gravity dams by performing non-linear analysis using a smeared crack model [2]. However, the applicability of these kinds of analysis methods has only been confirmed in a qualitative manner based on a comparison with limited cases of cracking of existing dams [3]. Therefore, there is a need to quantitatively evaluate the occurrence and propagation phenomena of cracking caused by the dynamic load in order to accurately evaluate the seismic safety of dams. Examples of research conducted to develop this type of quantitative evaluation are studies by Tinawi et al. [4], Uruchida et al. [5] and Kashiwayanagi et al. [6], who performed vibration

---

[1] Chief Executive, Public Works Research Institute (PWRI), Tsukuba-shi, Ibaraki-ken 305-8516 Japan.

[2] Team Leader, Dam Structure Research Team, Hydraulic Engineering Research Group, ditto.

[3] Senior Researcher, ditto.

[4] Collaborating Researcher, ditto.

[5] Chief Official, River Planning Division, River Bureau, Ministry of Land, Infrastructure and Transport (MLIT), Chiyoda-ku Tokyo-to 100-8918 Japan.

testing of concrete gravity dam models.

This paper reports a study about vibration fracture of unreinforced concrete using pillar-shaped models made of low-strength concrete [7]. The results revealed the influence of tensile cracking of the concrete on the first resonant frequency and the damping ratio of the test model. A numerical analysis was attempted in order to simulate cracking in the test models by finite element analysis using the smeared crack model.

2. SHAKING TABLE TESTS

2.1 Experimental Method

2.1.1 Material Composition for Test Model

The test material used was low-strength concrete so that the vibration testing would cause tensile fractures. The concrete mix proportion conditions and the materials used are shown in Table 1. The maximum aggregate size was set at 20 mm so that the test materials would have a certain degree of fracture energy.

Table 1 Test model materials: Mix conditions and materials used

Water : cement ratio	330 %
Max. aggregate size	20 mm
Cement	Moderate heat Portland cement 67 kg/m^3
Admixture	Limestone powder 433 kg/m^3

2.1.2 Shape of Test Model

The shape of the test model was decided as shown in Fig. 1(a), taking into account the following conditions: (1) the first resonant frequency of the test model is within the range of the excitation capacity of the shaking table which is planned to be used and (2) it is possible to roughly specify the location where tensile cracking will occur. In order to control the first resonant frequency, a weight of 100 kg was applied to the top of the test model. Excitation was applied using a white noise waveform with maximum acceleration amplitude of about 30 gal, to calculate the resonance curve shown in Fig. 1(b). As a result, the first resonant frequency of the test model before fracturing was about 30 Hz.

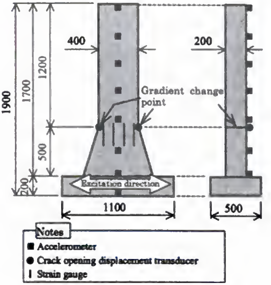

(a) Shape of the test model (unit: mm)

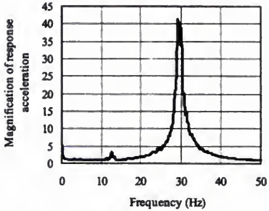

(b) Resonance curve

Fig. 1 Test model shape and resonance curve

2.1.3 Measurement Instruments

On the test model, accelerometers, crack opening displacement transducers and strain gauges were installed. The sampling interval was about 0.001 second (1,000 Hz). The layout of the major instruments is shown in Fig. 1(a). Visual observation was conducted using a high-speed video camera.

2.1.4 Input Acceleration Wave

The input wave was set as a sinusoidal wave of 22 Hz. In the case of excitation frequency of 22 Hz, the acceleration response multiplier at the top of the test model is expected to be about 2.5 times from Fig. 1(b). To make it possible to sufficiently observe the steady response of the test model in one excitation, the excitation time was set to 2 seconds. The amplitude was gradually increased at the beginning period of each excitation. The acceleration amplitude was set to be constant in one excitation, and it was increased step by step with the progress of excitation cases.

2.1.5 Material Properties of Test Model

Table 2 shows the material properties of the test model obtained by laboratory testing.

To obtain the tensile softening properties of the material, a wedge penetration type splitting test was performed in compliance with AAC13.1 of RILEM [8]. The specimen was a rectangular parallelepiped with width of 200 mm, height of 1700 mm and thickness of 100mm shown in Fig. 2. Fig. 3 shows the tensile softening curve estimated by a program provided by JCI [9] based on back analysis method by using the results of load – crack opening displacement results obtained by the wedge penetration type splitting test. And, approximated bilinear softening curve is shown in this Figure. This approximation was estimated so that it is possible to accurately reproduce the results of the wedge penetration type splitting test by FEM numerical analysis. The stress *ft* at the start of tensile softening of the bilinearly approximated tensile softening curve was 0.23 MPa and the fracture energy *Gf* was 10.5 N/m.

Table 2 Material properties

Property	Value
Compressive strength	1.85 MPa
Splitting tensile strength	0.17 MPa
Elastic modulus	5,260 MPa
Unit weight	2.3 t/m^3
Poisson's ratio	0.15

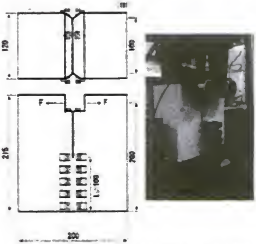

Fig. 2 Wedge penetration type splitting test

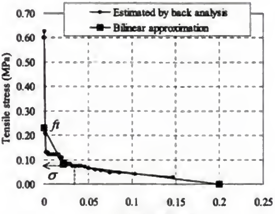

Fig. 3 Tensile softening curve obtained by the wedge penetration type splitting test

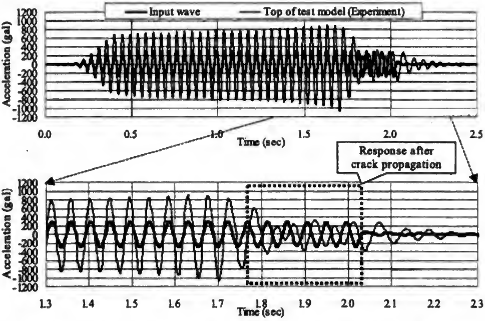

Fig. 4 Response acceleration at top of test model (Input acceleration 300 gal)

2.1.6 Response Acceleration of Top of Test Model

Fig. 4 shows the input acceleration and the response acceleration at the top of the test model in the case with input acceleration of 300 gal. The response at the top of the test model is shown to be steady-state vibration with identical phase to the input acceleration from 0.5 until about 1.5 seconds, but from about 1.7 seconds, the response acceleration amplitude falls sharply. This is presumed to be a result of a crack propagating in the test model and passing through it at the 1.7-second point. This was confirmed by the results of comparison analysis between crack width defined in 2.1.7 and picture data by high-speed video camera. A phase difference of about 160° was observed between the top response acceleration and the input acceleration after the crack passed through the test model.

2.1.7 Degree of Tensile Fracture

The degree of tensile fracture was defined by Eq. 1 in order to quantitatively evaluate the degree of tensile fracture of the test model. At the time when the degree of tensile fracture was 100%, the tensile softening state had ended and there was a completely opened tensile crack.

[Degree of tensile fracture (%)]

$$=(f_t-\sigma)\times 100/f_t \qquad (1)$$

where, f_t represents the stress at the start of tensile softening (0.23 MPa) and σ represents the tensile stress (tensile stress at crack surface) which corresponds to the crack opening displacement in Fig. 3. The crack width that was used here was calculated by subtracting the maximum elastic deformation from the measured crack opening displacement at the gradient change point shown in Fig. 1. The maximum elastic deformation Δx is obtained by the following equation.

$$\Delta x = f_t \times l/E = 0.0044 \text{ mm},$$

where, Δx: maximum displacement in the elastic range, f_t: stress at the start of tensile softening, E: elastic modulus, l: marked point interval between opening displacement gauges (100 mm).

Table 3 Degree of tensile fracture

Input acceleration amplitude (gal)	Crack opening displacement (mm)	Crack width (mm)	Tensile stress at crack surface (MPa)	Degree of tensile fracture (%)
30	0.0018	0.0000	–	0.0
150	0.0075	0.0031	0.209	9.3
300	0.0600	0.0556	0.065	72.0
900	0.1600	0.1556	0.020	91.3

In the test case with input acceleration amplitude of 30 gal, the crack opening displacement was set at 0.0 m because the measured crack displacement was not exceed the maximum displacement within the elastic range.

Table 3 shows the degree of tensile fracture in each test case calculated based on the crack width during steady state vibration. The crack width was calculated from the measured value by the crack opening displacement inducer, and the tensile stress at crack surface was evaluated the correspond value to the crack opening displacement on the bilinear approximation line in Fig. 2. In the test case with input acceleration amplitude of 30 gal, tensile cracking did not occur, and in the 150 gal case, tensile stress just over the tensile strength of material was produced and tensile fracturing occurred, although only to a small degree.

2.1.8 Relationship between First Resonant Frequency and Degree of Tensile Fracture

Fig. 5 shows the relationship of the degree of tensile fracture with the first resonant frequency calculated based on the response acceleration in the free vibration immediately after termination of the excitation. The open symbol plots in Fig. 5 and Fig. 6 show the analysis results discussed below. This reveals that as the fracture progresses, the first resonant frequency falls.

In the case with input acceleration amplitude of 150 gal, there is almost no decline of the first resonant frequency from 30 Hz prior to fracturing. On the other hand, in the 300 gal case, the first resonant frequency falls to about 20 Hz, which is lower than the frequency of the input waves (22Hz). This presumably caused the phase difference shown in Fig. 4.

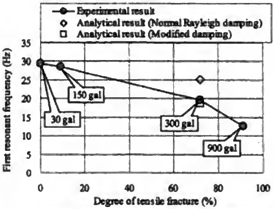

Note: numbers in the figure are the input acceleration amplitude.

Fig. 5 Relationship of the degree of tensile fracture with the first resonant frequency

2.1.9 Relationship between Damping Ratio and Degree of Tensile Fracture

Fig. 6 shows the relationship of the degree of tensile fracture with the apparent damping ratio obtained based on the response acceleration in the free vibration. The damping ratio was calculated as the average value when m = 1 to 4, and n = 3 based on Eq. 2.

$$\left| y_m / y_{m+n} \right| = \left(e^{2\pi h/\sqrt{1-h^2}} \right)^n \tag{2}$$

where, y_m and y_{m+n} represent the m and (m+n)th amplitude respectively, and h represents the damping ratio.

Fig. 6 reveals that as the degree of tensile fracture increases, the apparent damping ratio rises. In a vibration fracture test of a concrete gravity dam model performed by Tinawi et al., it was reported that the occurrence of a crack tended to increase the damping ratio [3]. It is hypothesized that on the fracture surface where the crack occurred, the impact of the re-closing of the crack induces a local fine fracture, which consumes energy. This would result in an increase in the apparent damping ratio accompanying the appearance of the crack.

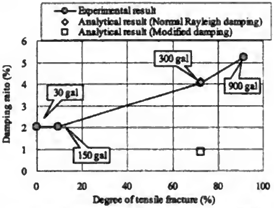

Note: numbers in the figure are the input acceleration amplitude.

Fig. 6 Relationship of the degree of tensile fracture with the damping ratio

3. NUMERICAL SIMULATION WITH NON-LINEAR FINITE ELEMENT METHOD

3.1 Numerical Analysis Method

Non-linear finite element analysis based on the smeared crack model was carried out to reproduce the results of the vibration testing.

The analysis was two-dimensional hypothesizing the plane stress state, and the concrete tensile softening phenomenon was represented by the bilinear tensile softening curve shown in Fig. 3. The damping matrix in the equation of motion was set by hypothesizing Rayleigh damping at a damping ratio of 2% based on the first and second resonant frequencies. The damping ratio was set so that it would be possible to simulate the behavior of the test model before fracturing. The bottom of the test model was considered to be a fixed boundary in FEM analyses.

3.2 Material Properties for Numerical Analysis

The material properties used for the analysis were set and based on the results of laboratory testing, excluding the elastic modulus *E*, as shown in Table 4. To make the first resonant frequency of the test model evaluated by the analysis correspond with the value observed in the test, the elastic modulus *E* was set at 6,500 MPa, which is a little higher than that evaluated by the material tests.

Table 4 Material properties for numerical analysis

Material property	Notation	Value
Elastic modulus	E	6,500 MPa
Poisson's ratio	ν	0.15
Unit weight	γ	2.3 t/m^3
Damping ratio	h	2%

3.3 Analytical Results

In the numerical analysis, the crack in the test model was almost passed through the test model in the case with input acceleration amplitude of 340 gal. On the other hand, in the vibration test, the crack passed through at 300 gal. This is presumably due to the fact that the stress at the start of tensile softening *ft* of the bilinearly approximated tensile softening curve in Fig.2 was about 35% larger than the splitting tensile strength of the test material. The analysis results conform closely to the test results in terms of the crack location.

Fig. 7 shows the response acceleration time history at the top of the test model obtained by analysis.

The following description focuses on the response after 1.0 second when the crack had almost passed through the test model. The phase difference of the top response acceleration to the input wave was calculated to be about only 80°. In the test, on the other hand, a phase difference of about 160° was caused, which is a very different value. Focusing on the reduction of the response acceleration amplitude after the crack passed through, the analysis found no rapid decline of the response acceleration amplitude after the crack passed through as observed by the test. One cause of this phenomenon was an over-evaluation of the viscous damping force in elements in which crack occurred. After a crack occurs, the damping force should not be transmitted passing the crack surface. The decline of the viscous damping force accompanying the occurrence of a crack is not considered by normal Rayleigh damping with smeared crack model.

In order to appropriately represent the reduction of the viscous damping force on the crack surface, reducing the damping force according to the state of the propagation of the crack was proposed by Bhattacharjee and Léger [10], and Kimata et al. [11]. In the present study, non-linear analysis with damping matrix which depends on the state of stiffness matrix with taking consideration of crack was performed. It is similar to methods which were used in abovementioned researches. The damping matrix was set to be consisted from only stiffness matrix, different from Rayleigh damping. In the following study, we call this damping "modified damping".

Fig. 8 shows the results of the analysis based on modified damping. Focusing on the response acceleration before cracking, from 0.5 second to about 1.0 second does not show a clear difference between the analysis using normal Rayleigh damping and the analysis with modified damping. This reveals that there are not so large differences between modified damping and Rayleigh damping on the response properties until the crack almost penetrate the test model. Next, focusing on the top response beginning at about 1.0 second when the cracking had propagated reveals large differences between the results in Fig. 7 and Fig. 8 . Using the method with modified damping, the phase difference between the input acceleration and the response acceleration at the top of the model was about 160°. This result conforms closely to the vibration test result. The analysis also represented the abrupt decline of the response acceleration amplitude after cracking. It can be seen that modified damping can more appropriately reproduce the response after propagation of the crack.

In Fig. 5 and Fig. 6, the first resonant frequency and the damping ratio obtained by numerical analyses in the case with input acceleration of 340 gal are also shown. Degree of tensile fracture of these data was equalized with result of vibration test in case of input acceleration of 300 gal. According to these figures, in the analysis with modified damping, although the first resonant frequency conformed closely to the test result, the damping ratio was lower than the test result. This is considered to be because the rise of the apparent damping accompanying the propagation of tensile fracture observed in the test was not considered in the numerical analysis.

There was also a little difference between the absolute values of the response acceleration amplitude after cracking obtained by analysis and by the vibration test. For these phenomena, it is necessary to study the damping ratio for the overall system according to the degree of progress of cracking (change of the resonant frequency of the overall structure by cracking).

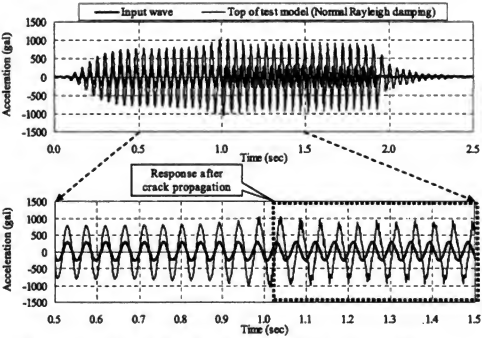

Fig. 7 Acceleration response at top of test model (Normal Rayleigh damping)

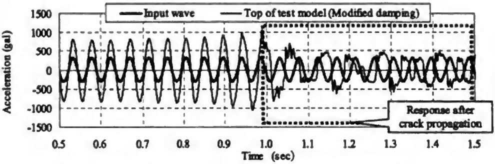

Fig. 8 Acceleration response at top of test model (Modified damping)

4. CONCLUSIONS

This research examined the performance of vibration fracture testing using a pillar-shaped test model made of low-strength concrete to investigate numerical analysis for aseismic evaluation of concrete dams. The following conclusions were drawn.

- This vibration test confirmed that the progress of tensile fracture was accompanied by a decline of the first resonant frequency and an increase in the apparent damping ratio.
- In the results of the analysis using the tensile softening curve, the location of the crack

conformed closely with that in the vibration test results.

- In the case of analysis using Rayleigh damping, the phase and amplitude of the response acceleration after the crack nearly penetrated were greatly different from those in the vibration test results.
- In the analysis with modified damping which damping matrix depend on state of stiffness matrix, the response acceleration at the top of the test model obtained by the analysis and that of the vibration test conformed closely.

A future challenge is to use the results of this research to propose a method of setting material properties including damping ratio for accurately evaluating the seismic safety of a concrete gravity dam. The authors have conducted a vibration fracture test using a large-scale model and simulation analyses for the vibration test, so we'd like to report those results in the near future.

5. REFERENCES

1. River Bureau, Ministry of Land, Infrastructure and Transport: *Guideline for Seismic Performance Evaluation of Dams (Draft)*, 2005.3. (in Japanese)
2. Sasaki, T., Kanenawa, K., Yamaguchi, Y. and Chiba, J.: Effect of ground motion level and dam shape on damage in concrete gravity dam during earthquakes, *Proceedings of 73rd Annual Meeting of ICOLD*, 2005.5.
3. for example, Zhang, H. and Ohmachi, T. 2 dimensional analysis of seismic cracking in concrete gravity dams, *Journal of Japan Society of Dam Engineers*, Vol.8, No.2, pp. 93-101, 1998.6
4. Tinawi, R., Léger, P., Leclerc. M. and Cipolla, G.: Seismic safety of gravity dams: From shake table experiments to numerical analyses, *Journal of Structural Engineering*, pp. 518-529, 2000.4.
5. Uruchida, S., Shimpo, T., Uchita, Y., Yagome, Y. and Saouma, V.: Dynamic centrifuge tests of concrete gravity dam, *Proceedings of 73rd Annual Meeting of ICOLD*, 2005.5.
6. Kashiwayanagi, M., Horii, H., Nakayama, Y. and Asaka, H.: Evaluation on crack propagation analysis for earthquake resistance assessment of gravity dams, *Proceedings of 73rd Annual Meeting of ICOLD*, 2005.5.
7. Sasaki, T., Takafuji, K., Yamaguchi, Y., Kanenawa, K. and Ishibashi, M.: Effect of Cracks on Dynamic Behavior Characteristics of Unreinforced Concrete Structures, *Proc. of 8th National Conference on Earthquake Engineering*, 2006.4.
8. RILEM AAC13.1: Determination of the specific fracture energy and strain softening of AAC, *RILEM Technical Recommendations for the Testing and Use of Construction Materials*, pp.156-158, 1994.
9. Japan Concrete Institute: Method of test for fracture energy of concrete by use of notched beam, *JCI-S-001-2003*, 2003. (in Japanese)
10. Bhattacharjee, S. S. and Léger, P.: Seismic cracking and energy dissipation in concrete gravity dams, *Earthquake Engineering and Structural Dynamics*, Vol.22, pp. 991-1007, 1993.
11. Kimata, H., Fujita, Y., Niimi, K., Hoshido, T., Kase, T., Hikawa, N. and Horii, H.: Seismic safety of concrete gravity dams based on dynamic crack propagation analysis during large-scale earthquakes, *Proceedings of 73rd Annual Meeting of ICOLD*, 2005.5.

Federal Initiatives for Security and Protection of Dams

Enrique E. Matheu, Ph.D.
Dams Sector Lead
Infrastructure Protection / Risk Management Division
Preparedness Directorate
US Department of Homeland Security

38th Meeting US-Japan Panel on Wind and Seismic Effects
15-17 May 2006 - Gaithersburg, MD
Technical Session 6 – DAMS

Homeland
Security

Department of Homeland Security

DHS Strategic Goals:

- **Awareness** - Identify and understand threats, assess vulnerabilities, determine potential impacts and disseminate timely information to homeland security partners and the American public.
- **Prevention** - Detect, deter and mitigate threats to our homeland.
- **Protection** - Safeguard our people and their freedoms, critical infrastructure, property and the economy of our Nation from acts of terrorism, natural disasters, or other emergencies.
- **Response** - Lead, manage and coordinate the national response to acts of terrorism, natural disasters, or other emergencies.
- **Recovery** - Lead national, state, local and private sector efforts to restore services and rebuild communities after acts of terrorism, natural disasters, or other emergencies.

Homeland
Security

National Infrastructure Protection Plan

Mandate: The Homeland Security Act of 2002 and the Homeland Security Presidential Directive 7 (HSPD-7) direct the development of a National Infrastructure Protection Plan (NIPP).

HSPD-7 specifies the following key content elements:

- A strategy to identify, prioritize, and coordinate the protection of critical infrastructure and key resources (CI/KR);
- Descriptions of activities which support each element of the strategy;
- A summary of initiatives for sharing CI/KR information and for providing CI/KR threat warning data; and
- Coordination and integration with other Federal emergency management and preparedness activities.

Homeland
Security

Critical Infrastructure / Key Resources

- **Critical Infrastructure**: Thirteen sectors that provide the production of essential goods and services, interconnectedness and operability, public safety and security that contribute to a strong national defense and thriving economy

- **Key Resources**: Facilities, sites and groups of organized people whose destruction could cause large-scale injury, death, or destruction of property and/or profoundly damage our national prestige and confidence.

Homeland
Security

National Infrastructure Protection Plan

Overarching Goal: Build a safer, more secure, and more resilient America by enhancing protection of the Nation's CI/KR to prevent, deter, neutralize, or mitigate the effects of deliberate efforts by terrorists to destroy, incapacitate, or exploit them; and to strengthen national preparedness, timely response, and rapid recovery in the event of an attack, natural disaster, or other emergency.

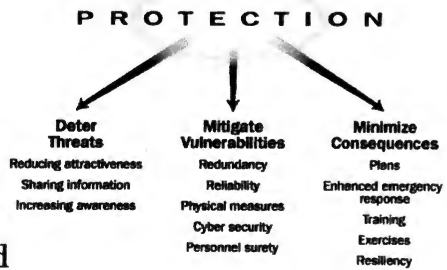

PROTECTION

Deter Threats
- Reducing attractiveness
- Sharing information
- Increasing awareness

Mitigate Vulnerabilities
- Redundancy
- Reliability
- Physical measures
- Cyber security
- Personnel surety

Minimize Consequences
- Plans
- Enhanced emergency response
- Training
- Exercises
- Resiliency

Homeland Security

NIPP Risk Management Framework

Managing Risk: The NIPP establishes the processes for combining consequence, vulnerability, and threat information to produce a comprehensive, systematic, and rational assessment of national or sector risk.

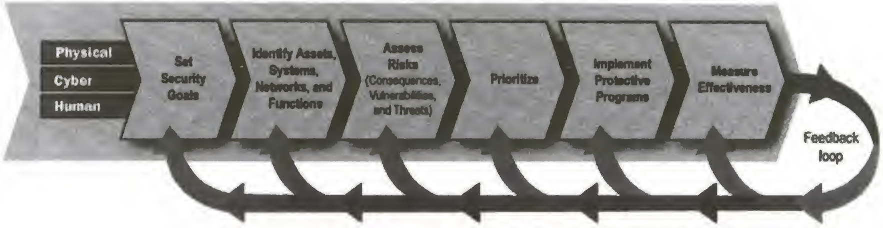
Physical
Cyber
Human
Set Security Goals
Identify Assets, Systems, Networks, and Functions
Assess Risks (Consequences, Vulnerabilities, and Threats)
Prioritize
Implement Protective Programs
Measure Effectiveness
Feedback loop

Continuous improvement to enhance protection of CI/KR

Homeland
Security

CI/KR Protection and Incident Management

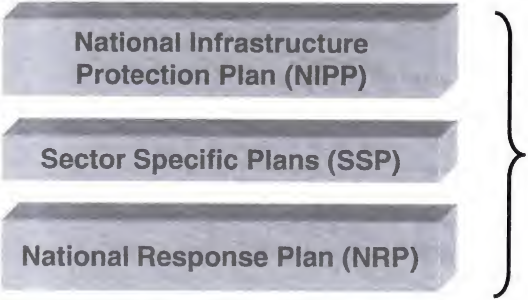

National Infrastructure Protection Plan (NIPP)

Sector Specific Plans (SSP)

National Response Plan (NRP)

Integrated approach addressing key elements of the Nation's homeland security mission in an all-hazards context.

Alert and warning systems for natural hazards, technological or industrial accidents, and terrorist incidents provide the bridge between the NIPP steady-state framework and the NRP incident management activities for actions related to both pre-incident prevention and post-incident response and recovery.

Homeland
Security

Sector Specific Agency

- HSPD-7 designates Federal Government SSAs for each of the CI/KR sectors. Their primary functions include:
  - *Implement the NIPP sector partnership model and risk management framework.*
  - *Develop the Sector Specific Plan and report sector-level performance to enable national cross-sector CI/KR protection program gap assessment. Develop protective programs and sector-specific protection guidance.*
  - *Coordinate and support comprehensive risk assessment & management programs for high-risk CI/KR, identify protection priorities, and incorporate them into the all-hazards approach to domestic incident management within the sector.*
  - *Provide an annual report to the Secretary of Homeland Security on efforts to identify, prioritize, and coordinate CI/KR protection.*

Homeland Security

CI/KR Sectors and Sector Specific Agencies

Agriculture and Food (meat, poultry, egg products)	Department of Agriculture
Public Health and Healthcare, Food (other than meat, poultry, egg products)	Department of Health and Human Services
Drinking Water, Wastewater, and Stormwater Treatment Systems	Environmental Protection Agency
Energy (production, refining, storage, and distribution of oil, gas, and electric power excepting commercial nuclear power facilities)	Department of Energy
Banking and Finance	Department of the Treasury
National Monuments and Icons	Department of the Interior
Defense Industrial Base	Department of Defense

Homeland
Security

CI/KR Sectors and Sector Specific Agencies

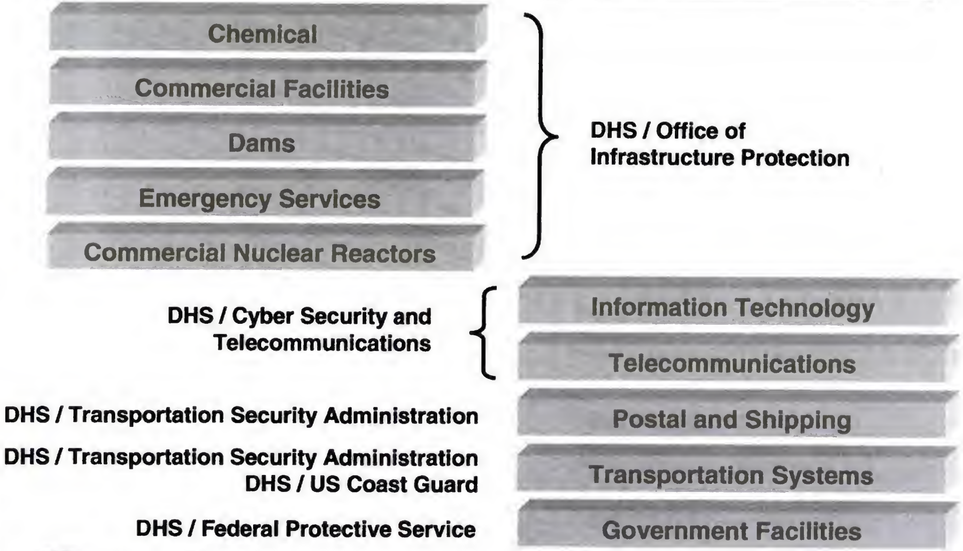

Chemical

Commercial Facilities

Dams

Emergency Services

Commercial Nuclear Reactors

DHS / Office of Infrastructure Protection

DHS / Cyber Security and Telecommunications

Information Technology

Telecommunications

DHS / Transportation Security Administration

Postal and Shipping

DHS / Transportation Security Administration
DHS / US Coast Guard

Transportation Systems

DHS / Federal Protective Service

Government Facilities

Homeland Security

Sector Partnership Model

Partnership Model: Provides the framework for security partners to work together in a robust public-private partnership.

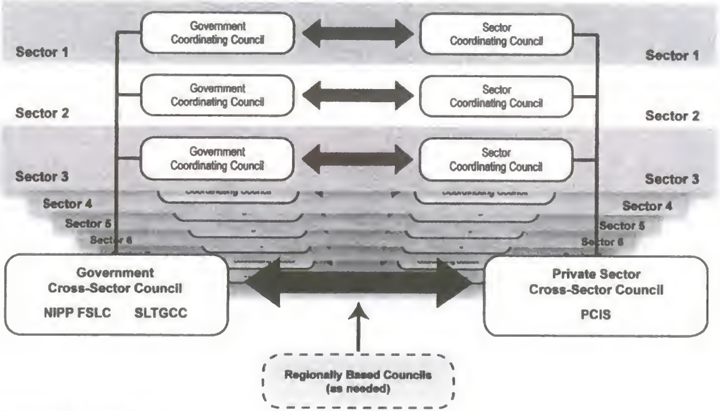

Sector 1

Government Coordinating Council

Sector Coordinating Council

Sector 1

Sector 2

Government Coordinating Council

Sector Coordinating Council

Sector 2

Sector 3

Government Coordinating Council

Sector Coordinating Council

Sector 3

Sector 4

Sector 4

Sector 5

Sector 5

Sector 6

Sector 6

Government Cross-Sector Council

NIPP FSLC SLTGCC

Private Sector Cross-Sector Council

PCIS

Regionally Based Councils (as needed)

Homeland Security

Sector Coordinating Council

- Representative of a broad base of CI/KR owners, operators, associations, and other entities – both large and small – within a sector. Primary functions include:
    - *Represent a primary point of entry for government into the sector;*
    - *Serves as a strategic communication mechanism between owners, operators and suppliers, and the government;*
    - *Identify, implement, and support the information sharing mechanisms that are most appropriate for the sector;*
    - *Facilitate organization and coordination of the sector's policy development regarding CI/KR protection planning and preparedness; exercises and training; and public awareness;*
    - *Advise on integration of Federal, State, regional, and local planning with private-sector initiatives;*

Homeland
Security

Government Coordinating Council

- Formed as the government counterpart for each SCC to enable interagency and cross-jurisdictional coordination.
- Comprised of representatives across various levels of government (Federal, State, local, or tribal). Functions include:
  - *Provide interagency strategic coordination and communication at the sector level.*
  - *Participate in planning efforts relating to the development, implementation, update, and revision of the NIPP and SSP.*
  - *Coordinate strategic communications, and issue management and resolution among government entities within the sector.*
  - *Coordinate with and support efforts of the SCC to plan, implement, and execute the Nation's CI/KR protection mission*

Homeland Security

Dams Sector – Ownership Distribution

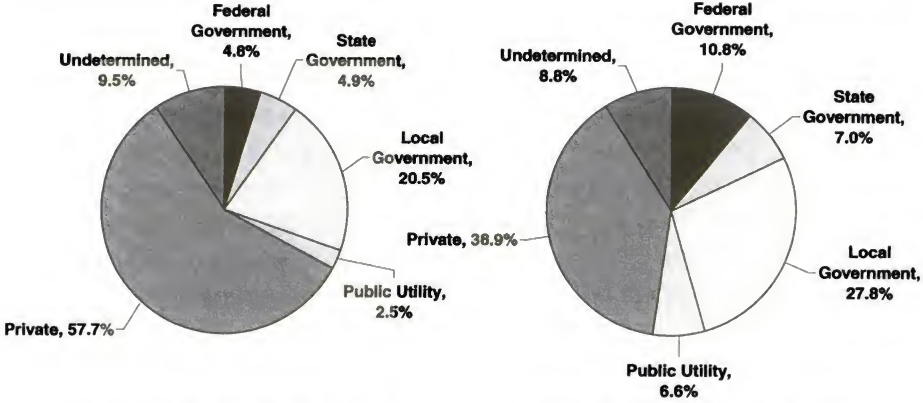

Total Number of Dams ≅ 79,000

High Hazard Dams ≅ 12,000

Homeland Security

Dams Sector GCC

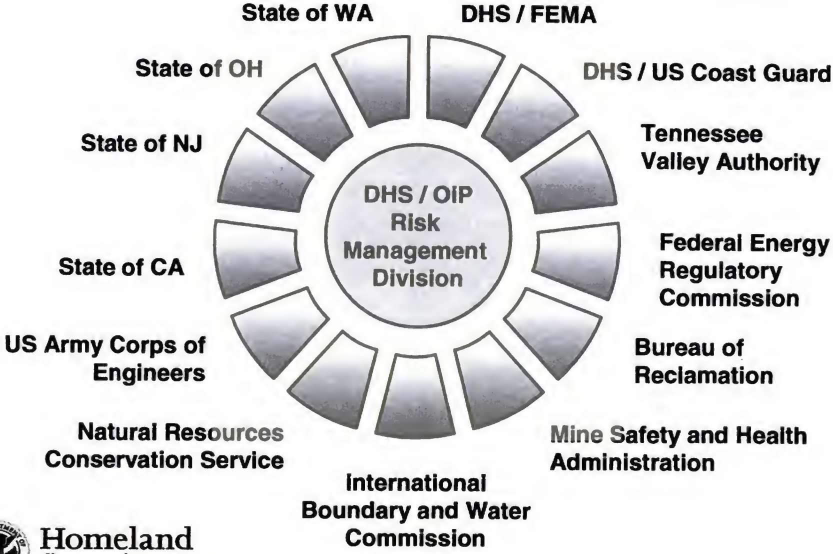

DHS / OIP Risk Management Division

State of WA

DHS / FEMA

DHS / US Coast Guard

Tennessee Valley Authority

Federal Energy Regulatory Commission

Bureau of Reclamation

Mine Safety and Health Administration

International Boundary and Water Commission

Natural Resources Conservation Service

US Army Corps of Engineers

State of CA

State of NJ

State of OH

Homeland Security

Risk Management Division

- **Mission**: Reduce the risk of the Nation's CI/KR to terrorism by developing, coordinating, integrating, and implementing efforts to identify, catalog, prioritize, and protect CI/KR, and facilitate the recovery of CI/KR from all hazards.
- **Objectives**:
  - *Identify and characterize CI/KR.*
  - *Implement NIPP and assess performance.*
  - *Develop and apply a risk-based prioritization process to build a comprehensive understanding of the nation's CI/KR.*
  - *Facilitate allocation of protective security expertise, equipment, facilities, and training.*
  - *Assist with training and exercise needs.*
  - *Establish local and regional protective security capacity.*

Homeland
Security

Dams Sector - RMD Programs

- RMD has SSA responsibilities for the Dams Sector.
- Several RMD programs have an important impact on the Dams Sector:
  - National Asset Database (NADB)
  - Risk Analysis and Management for Critical Asset Protection RAMCAP)
  - Protective Security Advisors (PSA)
  - Site Assistance Visits (SAV)
  - Buffer Zone Protection Program (BZPP)
  - International Outreach Programs

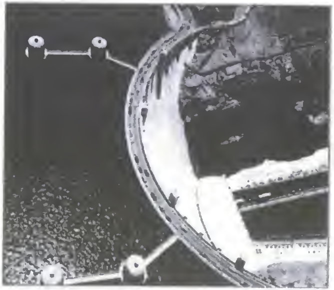

Homeland Security

National Asset Database

- The NADB is a repository and inventory for the universe of national infrastructure and resources.
- As such it will have as a subset, critical assets and key resources.
- Risk is dynamic, requiring an all-encompassing inventory.
- The NADB provides a foundation for strategic risk analysis and resource allocation, facilitates planning, and provides support to operational missions.
- Data is collected from Federal agencies, State and Local entities, commercial and private-sector databases as well as the NIPP process

Homeland
Security

National Asset Database

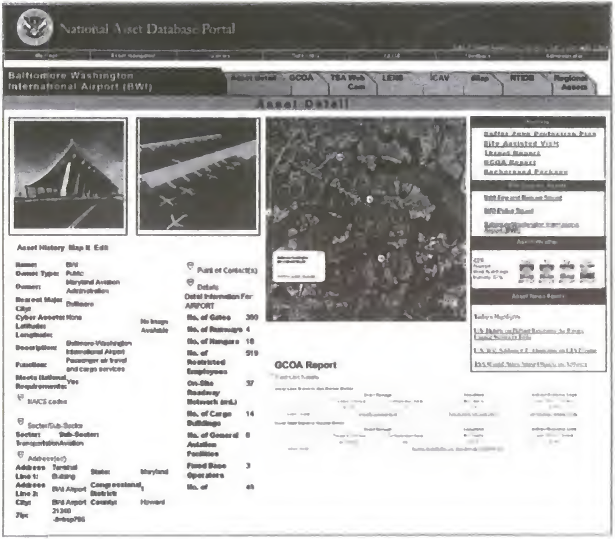

National Asset Database Portal

Baltimore Washington International Airport (BWI)

Asset Detail

Asset History Map It Edit

Name: BWI
Owner Type: Public
Owner: Maryland Aviation Administration
Nearest Major City: Baltimore
Cyber Assets: None
Latitude:
Longitude:
Description: Baltimore-Washington International Airport
Function: Passenger air travel and cargo services
Meets National Requirements: Yes

NAICS codes

Sector/Sub-Sector
Sector: Transportation
Sub-Sector: Aviation

Address(es)
Address Line 1: Terminal Building
State: Maryland
Address Line 2: BWI Airport
Congressional District: 1
City: BWI Airport
County: Howard
Zip: 21240

No Image Available

Point of Contact(s)

Details
Detail Information For AIRPORT

No. of Gates	300
No. of Runways	4
No. of Hangars	18
No. of Restricted Employees	519
On-Site Roadway Network (mi.)	37
No. of Cargo Buildings	14
No. of General Aviation Facilities	8
Fixed Base Operators	3
No. of	41

GCOA Report

GCOA Report

Homeland Security

Protective Security Advisor Program

- Protective Security Advisors (PSAs) are the DHS on-site critical infrastructure and vulnerability assessment specialists assigned to local communities throughout the United States.
- Serve as DHS liaisons between Federal agencies, state, territorial, local, and tribal governments, and the private sector.
- Serve as advisors regarding local infrastructure during activation of the National Response Plan

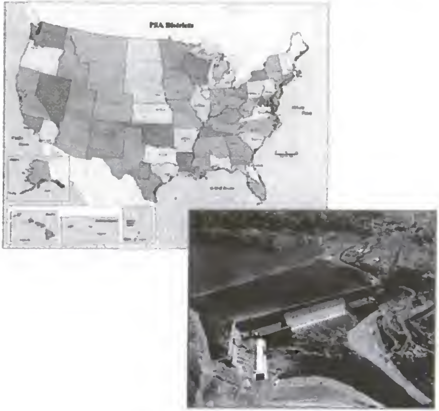

Homeland Security

Buffer Zone Protection Program

- The Buffer Zone is the area outside of a CI/KR facility that can be utilized to plan or launch an attack.
- Use site-specific Buffer Zone Plans to conduct a gap analysis of state and local first preventers' equipment, staffing, and training needs.

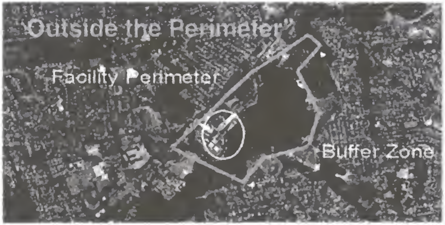

- Identify and/or enhance the existing procedures to prevent a terrorist incident at CI/KR facilities.
- Determine lines of communication and coordination among facilities, local, state, tribal, and Federal responders.

Homeland
Security

Site Assistance Visit Program

- Site Assistance Visits are designed to facilitate vulnerability identification and mitigation discussions between government and industry in the field.
- Facilitate identification of system connectivity and interdependencies
- Provide private sector with lessons learned and best practices.

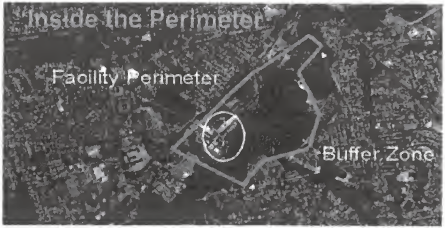

- Create a site-specific report from visit observations, expert inputs, and background data. Information is not made available to the public. Access is determined on a need-to-know basis.

Homeland
Security

International Collaboration

- Joint vulnerability assessments conducted on dams along the US-Mexico border, in collaboration with the International Boundary and Water Commission.

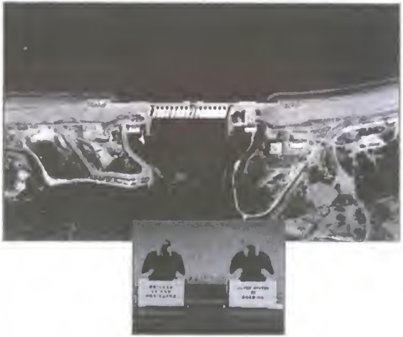

Homeland
Security

Homeland
Security

Establishment of Input Large-scale Earthquake Motions for Earthquake-proof Evaluation of Existing Dams

by

Nario Yasuda[1], Kazuhito Shimamoto[2], Takayuki Sano[3], Kohji Sujino[4]

ABSTRACT

In March 2005, the River Bureau of the Ministry of Land, Infrastructure and Transport issued the "Guidelines for Seismic Safety Evaluation of Dams (draft) and Explanation."

In establishing the earthquake motion for evaluating the seismic performance of dams against large-scale earthquakes, the earthquakes considered likely to have the greatest impact on the dam site (Scenario earthquakes) shall be selected based on information such as past earthquakes and relevant active faults, and then earthquake motions shall be estimated for the dam site.

There are several methods for establishing earthquake motion at a dam site, such as attenuation relationships for dams which are empirical and based on records of earthquake motions at the dam site, and statistical Green's function method which is semi-empirical.

This report describes the specific procedure for establishing large-scale earthquake motion at existing dam sites, and compares the earthquake motions predicted by several methods.

KEYWORDS: dam, large-scale earthquake, seismic performance, Level 2 earthquake motion, attenuation relationships, statistical Green's function method

1. INTRODUCTION

Large earthquake disasters have occurred since the 1995 Hyogoken-Nanbu Earthquake more than ten years ago, and a large earthquake is likely to occur in the near future. Thus, there is growing concern for the safety of infrastructures during a large earthquake.

In relation to dams, in March 2005, the River Bureau of the Ministry of Land, Infrastructure and Transport issued the "Guidelines for Seismic Safety Evaluation of Dams (draft) and Explanation" (hereafter, "Draft Guidelines") [1] which describe methods for evaluating the seismic performance of dams against large-scale earthquakes, assuming Level 2 earthquake motions.

In the Draft Guidelines, Level 2 earthquake motions are defined as "the strongest seismic ground motion potentially expected at a given dam site at present and in the foreseeable future," which follows the definition given in Phase 3 Recommendations [2] announced by the Japan Society of Civil Engineers immediately after the 1995 Hyogoken-Nanbu Earthquake.

This report describes the specific procedure for establishing large-scale earthquake motion (Level 2 earthquake motion) at N Dam, and compares the earthquake motions predicted by several methods. Figure 1 shows the outline of the method for establishing Level 2 earthquake motion. The process is explained below based on this figure.

---

1) Head, Water Management and Dam Division (WMDD), National Institute for Land and Infrastructure Management (NILIM), Ministry of Land, Infrastructure and Transport (MLIT), 1, Asahi, Tsukuba, Ibaraki, 305-0804, Japan

2) Senior Researcher, ditto

3) Researcher, ditto

4) Assistant section head, Electricity Infrastructure Division, Agency for Natural Resources and Energy Electricity and Gas Industry Department, Ministry of Economy, Trade and Industry, 1-3-1, Kasumigaseki, Chiyoda-ku, Tokyo, 100-8931, Japan (Former : Senior Researcher, WMDD, NILIM, MLIT)

2. CASE STUDY OF ESTABLISHING LEVEL 2 EARTHQUAKE MOTION

2.1 Selection of Scenario earthquakes

2.1.1 Literature review

First, data on active faults and seismic faults at plate boundaries that were likely to induce ground motions greatly affecting N Dam and on past earthquakes that had caused damages were compiled from literature including published results of existing studies. Documents included a revised edition of "Active faults in Japan", "Fault scarp parameter handbook for Japan", "Detailed digital map of active faults", "Metropolitan area active fault map", a revised edition of "Damage-inducing earthquakes of Japan", materials of the "Central Disaster Prevention Council" and materials of the "Headquarters for Earthquake Research Promotion". The results of surveys of Quaternary faults at and near dam sites were also used. Figure 2 shows the results of the investigation.

Secondly, data were extracted on faults that were generally within 50 km of the dam site. Even for faults that were more than 50 km away from the dam site, the fault was examined when a Scenario earthquake with a magnitude of 8 or higher is expected to occur at the fault. This work extracted various kinds of earthquakes and faults as shown in Table 1.

2.1.2 Selection of Scenario earthquakes

Among the various earthquakes listed in Table 1, the earthquakes that would likely have the greatest impact on N Dam were selected as the Scenario earthquakes.

The Scenario earthquakes were selected by presuming the intensity (acceleration response spectrum) of the seismic ground motion caused at the dam site by using attenuation relationships as described later.

Figure 3 shows the acceleration response spectra of the earthquake motion at the dam site due to various earthquakes, which were obtained by attenuation relationships. Figure 3 (a) is the result using the shortest distance equation, and Fig. 3 (b) is the result using the equivalent distance equation.

Based on Fig. 3, the earthquake caused by the Median tectonic line Akaishi-sanchi-seien fault zone, which is an inland type, and the anticipated Tokai Earthquake, which is an ocean type, were selected as the Scenario earthquakes at N Dam. When selecting the Scenario earthquakes, comparison was made by taking into account not only acceleration response spectra but also factors such as the type and duration of the earthquake.

2.2 Establishing Level 2 earthquake motion for evaluating the seismic performance of dams

2.2.1 Estimation of earthquake motions due to Scenario earthquakes

We estimated the earthquake motions at the N Dam site due to the Scenario earthquakes. In this study, we used empirical attenuation relationships based on earthquake motions recorded at the dam site, and the statistical Green's function method.

The processes of the estimations are explained below.

(1) Estimation of earthquake motions by empirical method

We estimated the acceleration response spectra of earthquake motion at the N Dam site due to the Scenario earthquakes using attenuation relationships.

Attenuation relationships for estimating earthquake motions have been developed based on numerous records of earthquake motions with respect to dam foundations in Japan. With these formulas, it is possible to estimate the intensity of earthquake motions at a particular dam site (acceleration response spectra) using distance from hypocenter, magnitude of earthquake and coefficients for individual types.

Acceleration response spectra of earthquake motions produced in ground (with an average shear wave velocity of approximately 0.7–1.5 km/s) that can serve as the dam foundation were estimated by attenuation relationships. Namely, these relationships were obtained as regression equations by performing statistical analysis as follows: Earthquake records were obtained from strong motion seismographs installed at locations such as in the bottom inspection galleries of dams. Statistical analysis was conducted with respect to acceleration response spectra values (mean values plus standard deviations) for parameters such as: shortest distance to fault plane, earthquake magnitude, and depth from ground surface to fault plane center.

There are two formulas depending on how the distance from the hypocenter is measured: the shortest distance formula (Eq. 1) in which the shortest distance between the fault plane and dam site is used, and the equivalent distance formula (Eq. 2) in which the distance between the dam site and virtual point source where seismic energy is equivalent to that from fault planes is used.[3][4]

$$\log S_A(T) = C_m(T)\,M + C(T)\,H_c - C_d(T)\log\{R + 0.334\exp(0.653M)\} + C_o(T) \quad (1)$$

$$\log S_A(T) = C_m(T)\,M + C_h(T)\,H_c - C_d(T)\,X_{eq} - \log X_{eq} + C_o(T) \quad (2)$$

where,

T : Characteristic period

$S_A(T)$: Average response spectra of two horizontal components

M: Magnitude (Japan Meteorological Agency magnitude) of earthquake occurring on a fault

H_c: Depth of fault plane center from ground surface, or 100 km, whichever is less

R: Shortest distance to fault plane

Xeq: Equivalent hypocentral distance

Cm (T), Ch (T), Cd (T), and Co (T): Regression coefficients obtained from numerous earthquake records.

In order to estimate earthquake motions by using attenuation relationships, it is necessary to establish specific distances between the dam site and faults (R or Xeq), magnitude of earthquakes occurring on faults (M), and depth of fault plane centers from ground surface (H_c).

Of these variables, the following values can be calculated based on the literature, provided that the locations of fault planes are known.

Regarding the magnitude (M) of earthquakes occurring on faults, in cases where relevant values are shown in the literature, then such values can be used. However, if only the lengths of faults are known, then the magnitudes of earthquakes that occur when pertinent faults are triggered can be estimated by using formulas such as relational equations empirically obtained between fault length and fault width or between fault area and earthquake magnitude.

① Earthquake caused by Median tectonic line Akaishi-sanchi-seien fault zone

The locations of the Median tectonic line Akaishi-sanchi-seien fault zone and N Dam site are shown in Fig. 4, and the fault parameters of the Akaishi-sanchi-seien fault zone are shown in Table 2. Figure 5 shows the acceleration response spectra at the N Dam site estimated by using attenuation relationships for dams based on the parameter. This figure shows that the spectrum which is estimated by the equivalent distance equation is covered by the spectrum which is estimated by the shortest distance equation.

② Anticipated Tokai Earthquake

As for earthquake motion due to the anticipated Tokai Earthquake, the Central Disaster Prevention Council has published acceleration time-history waveforms estimated by the statistical Green's function method.

(2) Estimation of earthquake motions by semi-empirical method

We estimated the acceleration time-history waveforms of earthquake motion at the N Dam site due to the Scenario earthquakes by using a semi-empirical method.

The semi-empirical method synthesizes the waveform of a large earthquake from the waveform of an existing small earthquake. There are two approaches: the empirical Green's function method and the statistical Green's function method.

The empirical Green's function method

synthesizes an element wave (Green's function) according to the destruction process of the assumed fault. An element wave is the waveform of a small and medium-sized earthquake that occurs in the hypocentral region of the assumed fault. The time-history of the waveform can be predicted, and the influence of the destruction process and the influence of asperity can be considered. However, it is necessary to have obtained an appropriate observation waveform beforehand at the evaluation point.

In the statistical Green's function method, the waveform with the average characteristic of many observed earthquake motions is used as an element wave, and so a suitable observed motion at the evaluation point is not needed. However, the vibration corresponding to a characteristic peculiar to the evaluation point is not reflected easily. The time-history of the waveform is calculated by a method similar to the empirical Green's function method.

① Earthquake caused by Median tectonic line Akaishi-sanchi-seien fault zone

Because there is no record of earthquake motion caused by the Akaishi-sanchi-seien fault zone, we used the statistical Green's function method.

The estimation procedure using this method is as follows.

Green's functions are created on the seismic base (shear wave velocity: approximately 3000 m/s) considering the characteristics of the epicenter and wave propagation path. The functions are converted to Green's functions on the engineering base (shear wave velocity: approximately 700 m/s) using one-dimensional multiple reflection theory. Strong ground motion is synthesized on the engineering base by convoluting Green's functions on the engineering base.

Causative fault parameters were basically established according to a "recipe" for predicting strong ground motion published by the Headquarters for Earthquake Research Promotion [5]. Table 3 lists the causative fault parameters established for calculation.

Establishing the locations of asperities and rupture starting points involves numerous uncertainties such as the quantities and locations of these parameters, and so predictions of seismic ground motions vary greatly. In this study, dozens of locations were assumed for asperities and rupture starting points (Fig. 6), and the acceleration time-history waveform and response spectra were calculated by applying the statistical Green's function method in 108 cases. A spectrum with a 90% probability of not exceeding the calculated spectra is shown in Fig. 7.

② Anticipated Tokai Earthquake

Figure 8 shows the position of the anticipated Tokai Earthquake and N Dam site.

It is difficult to predict the earthquake motion by the empirical Green's function method, because there is no observation record of motion at the N Dam site relating to earthquakes in the focal region of the Tokai Earthquake.

On the other hand, regarding the anticipated Tokai Earthquake, the Central Disaster Prevention Council [6] has published time-history waveforms of earthquake motions on the engineering base (shear wave velocity: approximately 700 m/s) calculated by the statistical Green's function method for each 1 square km.

As a dam foundation generally has a shear wave velocity of 0.7–1.5 km/s and is considered to be equivalent to the engineering base, we adopted the waveform at the N Dam site given by the Central Disaster Prevention Council as the estimated waveform for the foundation of N Dam.

Furthermore, due to the expression of stress reduction in two models (the S model) having different rupture starting points have been published: the S-1 model and S-2 model. The acceleration time-history waveform was estimated by using these fault models and the statistical Green's function method. Figure 9 shows the acceleration response spectra of those waveforms. This figure shows that the spectrum estimated by the S-1 model is almost covered by the spectrum estimated by the S-2 model.

2.2.2 Comparisons with earthquake motions observed in the past and those having lower-limit acceleration response spectrum for evaluation

(1) Comparison with earthquake motions observed in the past

The earthquake motions observed at and near the dam site were sufficiently small in comparison with earthquake motions with lower-limit acceleration response spectrum for evaluation. Therefore, the earthquake motions in the past would not have had the greatest impact on N Dam.

(2) Comparison with earthquake motions having lower-limit acceleration response spectrum for evaluation

(2)-1 Explanation of lower-limit acceleration response spectra for evaluation

The standard practice for establishing Level 2 earthquake motions is to use earthquake motions at dam sites based on Scenario earthquakes. However, in cases where active faults on which hypocenters may be located are not detected in surrounding areas, then the distances to the hypocenters of Scenario earthquakes turn out to be long, and so earthquake motions at the dam site are small.

On the other hand, there is intense seismic activity in Japan, so even if no active faults are detected on the ground surface, they may exist under the ground. The Draft Guidelines specify the following: Even if active faults on which earthquake hypocenters are located are not detected on the ground surface, it shall be assumed that there is a risk of occurrence of earthquakes of certain magnitudes. The acceleration response spectra shown in Fig. 10 shall be referred to as "lower-limit acceleration response spectra for evaluation." Even in cases where earthquake motions based on Scenario earthquakes are below these limit values, earthquake motions of these levels must be taken into account for evaluation as the lower limit.

As shown in the Recommendations of the Japan Society of Civil Engineers, earthquakes exceeding a magnitude of M6.5 often leave some sort of mark on the ground surface. Lower-limit acceleration response spectra for evaluation were set as follows: Earthquake motions that occur on ground surfaces during an earthquake with a magnitude of M6.5 directly under a dam site were calculated on a trial basis using tools such as attenuation relationships. To be on the safe side, standard deviations were added to averages. Acceleration response spectra were set such that the results thus calculated were safely covered and the effects of response characteristics (characteristic period bands) were taken into account.

In the 2000 Western Tottori Earthquake (M7.3), which occurred in October 2000, the active fault on which the hypocenter was located had not been known to exist. Views differ among experts as to whether or not this active fault would have been detected if detailed investigations had been made beforehand. However, this case actually occurred, and so the following was also performed: a trial calculation was made by taking into account an earthquake of the same magnitude (M7.3) located directly above the hypocenter, and the results confirmed that the lower-limit acceleration response spectra set as mentioned above safely enveloped the average levels of estimated earthquake motions caused by an earthquake of M7.3.

(2)-2 Comparison

The acceleration response spectra of the earthquake motion at the N Dam site calculated by the empirical and semi-empirical methods were compared with the lower-limit acceleration response spectrum for evaluation. The results are shown in Fig. 11.

As for the earthquake due to the Akaishi-sanchi-seien fault zone, the spectrum estimated by attenuation relationships (equivalent distance equation) and by statistical Green's function (specifically, a spectrum with a 90% probability of not exceeding the calculated spectrum) are almost covered by the lower-limit acceleration response spectrum for evaluation. Furthermore, a spectrum with a 90% probability of not exceeding the calculated spectrum is almost covered by the spectrum estimated by attenuation relationships (equivalent distance equation).

Comparing the spectra due to the anticipated Tokai Earthquake (S-2 model) and the lower-limit acceleration response spectrum for evaluation, it is not clear which is the larger.

In view of the above, the earthquake motion due to the anticipated Tokai Earthquake (S-2 model) and the earthquake motion with the lower-limit acceleration response spectrum for evaluation were selected as the earthquake motions that are likely to have the greatest impact on the N Dam.

2.2.3 Preparation of time-history waveform corresponding to acceleration response spectrum

We used the acceleration time-history waveform of earthquake motion selected in the previous section as the level 2 earthquake motion for evaluation.

(1) Earthquake motion due to the anticipated Tokai Earthquake (S-2 model)

For this earthquake, we adopted the waveform published by the Central Disaster Prevention Council. For dynamic analysis, we converted the horizontal components to the directions of the dam by linear transformation. Figure 12(a) shows the waveform after conversion.

(2) Earthquake motion with the lower-limit acceleration response spectrum for evaluation

We prepared the acceleration time-history waveform of earthquake motion with the lower-limit acceleration response spectrum for evaluation.

The phase characteristic was given by the recorded acceleration time-history waveform. In this study, we adopted the waveform observed at the foundation of Hitokura Dam and Gongen Dam in the 1995 Hyogoken-Nanbu Earthquake as the strong records. By adjusting the frequency characteristic of the waveform, we then derived the acceleration time-history waveforms (Fig. 12 (b) and (c)).

From the above, the acceleration time-history waveforms shown in Fig. 12(a)-(c) were established as the level 2 earthquake motions of N Dam.

3. CONCLUSIONS

This report described the specific procedure for establishing large-scale earthquake motion (Level 2 earthquake motion) at N Dam as follows:

1. Data on active faults and seismic faults at plate boundaries that were likely to induce ground motions greatly affecting N Dam and on past earthquakes that had caused damages were compiled from literature including published results of existing studies.
2. The Scenario earthquakes were selected by presuming the intensity (acceleration response spectrum) of the earthquake motion caused at the dam site by using attenuation relationships. As the Scenario earthquakes at N Dam, the earthquake caused by the Median tectonic line Akaishi-sanchi-seien fault zone, which is an inland type earthquake, and the anticipated Tokai Earthquake, which is an ocean type earthquake, were selected.
3. The earthquake motions at the N Dam site due to Scenario earthquakes were s estimated by empirical attenuation relationships and based on records of earthquake motions at the dam site, and the statistical Green's function method.
4. To select the earthquake motions that are likely to have the greatest impact on N Dam, the earthquake motions caused by the Scenario earthquakes were compared with the earthquake motions observed in the past, and earthquake motions with the lower-limit acceleration response spectrum for evaluation. As a result, the earthquake motion due to the anticipated Tokai Earthquake (S-2 model) and the earthquake motion with the lower-limit acceleration response spectrum for evaluation were selected as Level 2 earthquake motions.

4. REFERENCES

1) Flood Control Division, River Bureau, Ministry of Land, Infrastructure and Transport, "Draft Guidelines for Seismic Safety Evaluation of Dams Subjected to Large-Scale Earthquakes," March 2005 (in Japanese)
2) Japan Society of Civil Engineers (Ad Hoc Committee on Methods of Earthquake Resistant Design of Civil Engineering Structures), "Phase 3 Recommendations on Matters Including Seismic Performance and Methods of Earthquake Resistant Design of Civil Engineering Structures," 2000
3) Matsumoto, N., Yoshida, H., Sasaki, T., and Annaka, T., Response Spectra of Earthquake Motion at Dam Foundations, Proc. of Twenty-first International Congress on Large Dams (2003)
4) Matsumoto, N., Yoshida, H., Sasaki, T., and Annaka, T., "Response Spectra of Earthquake Motions at Dam Sites," Large Dams, No. 186, pp. 69–76, 2004
5) Earthquake Research Committee, Headquarters for Earthquake Research Promotion: Appendix: Methods for assessing strong seismic ground motion specifying the causative fault ("recipe"), Strong ground motion assessment on the assumption of the Hyuganada earthquake, http://www.jishin.go.jp/main/kyoshindo/05sep_hyuganada/furoku.pdf, September 2005 (in Japanese)
6) Central Disaster Prevention Council, Cabinet Office: Website of the Central Disaster Prevention Council, http://www.bousai.go.jp/jishin/chubou/index.html (in Japanese)

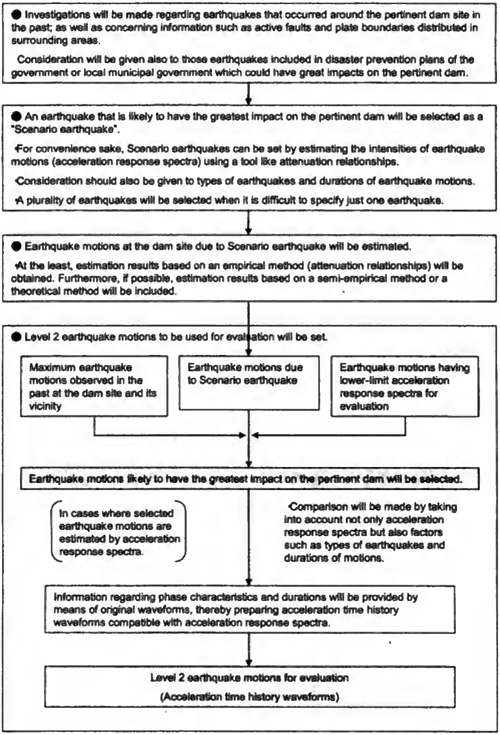

● Investigations will be made regarding earthquakes that occurred around the pertinent dam site in the past; as well as concerning information such as active faults and plate boundaries distributed in surrounding areas.

Consideration will be given also to those earthquakes included in disaster prevention plans of the government or local municipal government which could have great impacts on the pertinent dam.

● An earthquake that is likely to have the greatest impact on the pertinent dam will be selected as a "Scenario earthquake".

·For convenience sake, Scenario earthquakes can be set by estimating the intensities of earthquake motions (acceleration response spectra) using a tool like attenuation relationships.

·Consideration should also be given to types of earthquakes and durations of earthquake motions.

·A plurality of earthquakes will be selected when it is difficult to specify just one earthquake.

● Earthquake motions at the dam site due to Scenario earthquake will be estimated.

·At the least, estimation results based on an empirical method (attenuation relationships) will be obtained. Furthermore, if possible, estimation results based on a semi-empirical method or a theoretical method will be included.

● Level 2 earthquake motions to be used for evaluation will be set.

Maximum earthquake motions observed in the past at the dam site and its vicinity

Earthquake motions due to Scenario earthquake

Earthquake motions having lower-limit acceleration response spectra for evaluation

Earthquake motions likely to have the greatest impact on the pertinent dam will be selected.

(In cases where selected earthquake motions are estimated by acceleration response spectra.)

·Comparison will be made by taking into account not only acceleration response spectra but also factors such as types of earthquakes and durations of motions.

Information regarding phase characteristics and durations will be provided by means of original waveforms, thereby preparing acceleration time history waveforms compatible with acceleration response spectra.

Level 2 earthquake motions for evaluation

(Acceleration time history waveforms)

Fig. 1 Flowchart for establishing Level 2 earthquake motions to evaluate seismic performance

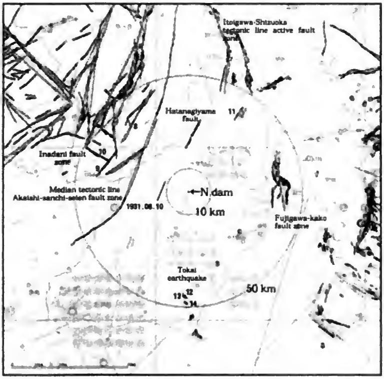

No.	Fault
1	Inadani fault zone (fault at the boundary)
2	Inadani fault zone (fault at the toe)
3	Inadani fault zone (throughout the fault zone)
4	Fujigawa-kako fault zone
5	Itoigawa-Shizuoka tectonic line active fault system
6	Median tectonic line Akaishi-sanchi-seien fault zone
7	Hatanagiyama fault
8	Shimoinadaki-higashi fault zone
9	Niino fault
10	Suzugesawa fault
11	Fujimisan fault
12	Niotsuji-higashi fault
13	Niotsuji-nishi fault
14	Maruohara fault
15	Anticipated Tokai earthquake
16	Earthquake of August 10, 1931

Fig. 2 Faults and past earthquakes around N Dam

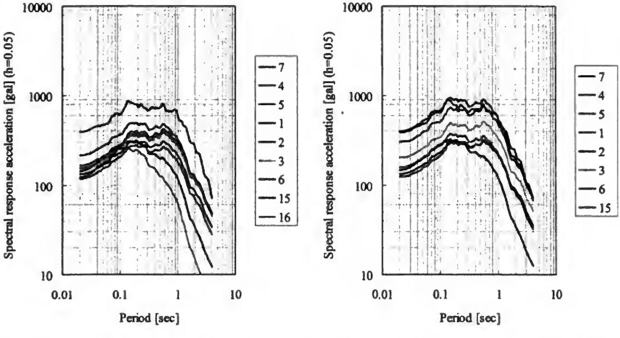

(a) shortest distance equation (mean + standard deviation) (b) equivalent distance equation (mean + standard deviation)

Fig. 3 Acceleration response spectra of earthquake motion at N Dam site caused by earthquakes considered in the selection of *Scenario earthquake* (calculated by attenuation relationships)

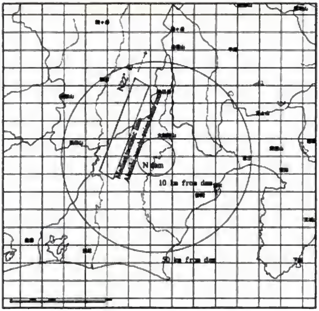

Fig. 4 Location of hypocenter fault model of Scenario earthquake
(① Earthquake caused by Akaishi-sanchi-seien fault zone)

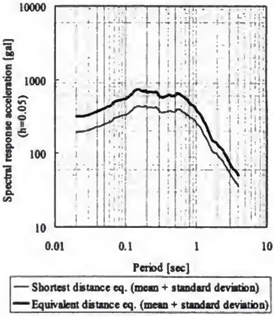

Fig. 5 Acceleration response spectra of earthquake motion at N dam site caused by Scenario earthquake
(① Earthquake caused by Akaishi-sanchi-seien fault zone, predicted by attenuation relationships)

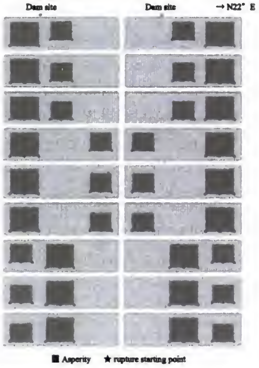

Asperity distribution 18 cases × rupture starting point 6 cases = total 108 cases

Fig. 6 Asperity distribution and rupture starting point in hypocenter fault model of Scenario earthquake (① Earthquake caused by *Akaishi-sanchi-seien fault zone*)

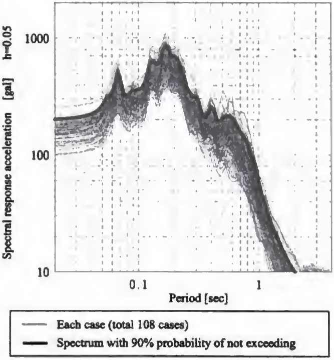

Fig. 7 Acceleration response spectrum of earthquake motion at N dam site caused by Scenario earthquake (① Earthquake caused by Akaishi-sanchi-seien fault zone, predicted by the statistical Green's function method)

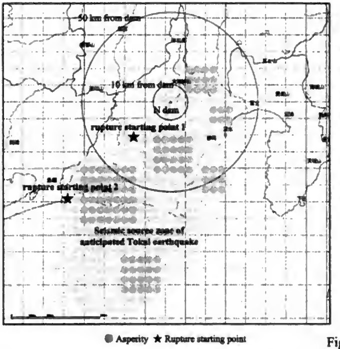
50 km from dam
10 km from dam
N dam
rupture starting point 1
rupture starting point 2
Seismic source zone of anticipated Tokai earthquake
● Asperity ★ Rupture starting point

Fig. 8 Location of the hypocenter fault model of Scenario earthquake (② Anticipated Tokai Earthquake by Central Disaster Prevention Council)

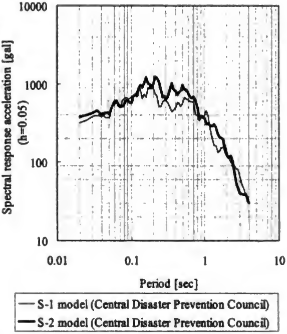

Fig. 9 Acceleration response spectra of earthquake motion at N Dam site caused by Scenario earthquake (② Anticipated Tokai Earthquake, predicted by the statistical Green's function method (Central Disaster Prevention Council))

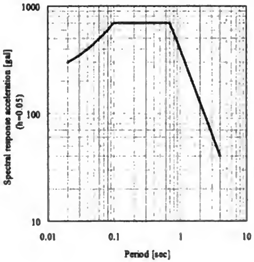

Fig. 10 Lower-limit acceleration response spectra for evaluation

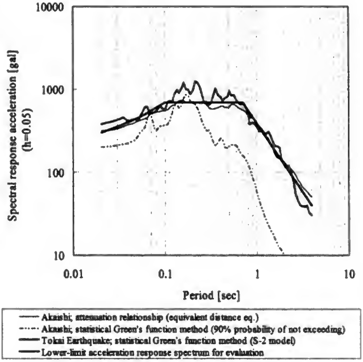

Fig. 11 Acceleration response spectra of earthquake motions at N Dam site caused by Scenario earthquake and lower-limit acceleration response spectra for evaluation

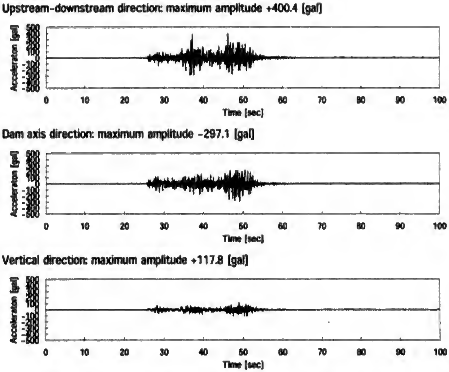
Upstream-downstream direction: maximum amplitude +400.4 [gal]

Dam axis direction: maximum amplitude -297.1 [gal]

Vertical direction: maximum amplitude +117.8 [gal]

(a) Anticipated Tokai Earthquake (Central Disaster Prevention Council, S-2 model)

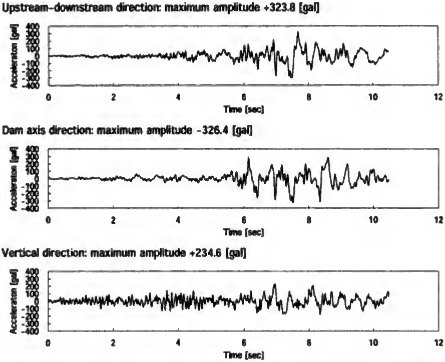
Upstream-downstream direction: maximum amplitude +323.8 [gal]

Dam axis direction: maximum amplitude -326.4 [gal]

Vertical direction: maximum amplitude +234.6 [gal]

(b) Earthquake motion with lower-limit acceleration response spectra for evaluation
(original waveform: waveform measured at Hitokura Dam during the 1995 Hyogoken-nanbu Earthquake)

Fig. 12 Level 2 earthquake motions used to evaluate seismic performance of N Dam

Upstream-downstream direction: maximum amplitude +309.5 [gal]

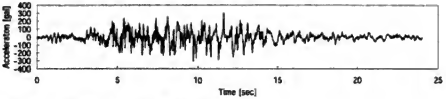

Dam axis direction: maximum amplitude -338.8 [gal]

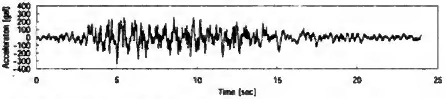

Vertical direction: maximum amplitude -280.0 [gal]

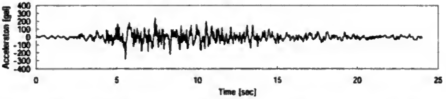

(c) Earthquake motion with lower-limit acceleration response spectra for evaluation
(original waveform: waveform measured at Gongen Dam during the 1995 Hyogoken-nanbu Earthquake)

Fig. 12 Level 2 earthquake motions used to evaluate seismic performance of N Dam

Table 1 Faults and past earthquakes which could affect N Dam

No.	Fault	Fault length	Magnitude	Focus depth	Fault dip	Certainty of existence of the active fault	Activeness	Probability of occurrence	Sources
1	Iradani fault zone (fault at the boundary)	49	7.7	-	NW, W	I	A	7.00%	Headquarters for Earthquake Research Promotion Data on fault dip are from Active Faults in Japan
2	Iradani fault zone (fault at the toe)	57	7.8	-	20 to 40 degrees west[*1]	I	A	6.00%	Headquarters for Earthquake Research Promotion
3	Iradani fault zone (throughout the fault zone)	78	8.0	-	NW, W	I	A	7.00%	Headquarters for Earthquake Research Promotion Data on fault dip are from Active Faults in Japan
4	Fujigawa-kako fault zone	80	8.0	-	W	I	A	11.00%	Headquarters for Earthquake Research Promotion Data on fault dip are from Active Faults in Japan
5	Itoigawa-Shizuoka tectonic line active fault system	150	8.0	-	Westward dip (in the south)	I	A	14.00%	Headquarters for Earthquake Research Promotion (No data available on turning points)
6	Median tectonic line Akaishi-sanchi-seien fault zone	52	7.8	-	S, E	I	B	-	Headquarters for Earthquake Research Promotion Data on fault dip are from Active Faults in Japan
7	Hatanagiyama fault	14	6.7	-	E	II	C	-	Matsuda (2000) Data on fault dip are from Active Faults in Japan
8	Shimoinadaki-higashi fault zone	27	7.2	-	E	II	B	-	Matsuda (2000) Data on fault dip are from Active Faults in Japan
9	Niino fault	14	6.7	-	E or W	II	B~C	-	Matsuda (2000) Data on fault dip are from Active Faults in Japan
10	Suzugasawa fault	10	6.5	-	S	I	B	-	Matsuda (2000) Data on fault dip are from Active Faults in Japan
11	Fujimisan fault	7	6.2	-	W	I	C	-	Active Faults in Japan Magnitude was calculated by Matsuda's equation
12	Niotsuji-higashi fault	3	5.6	-	SW or NE	I	B~C	-	Active Faults in Japan Magnitude was calculated by Matsuda's equation
13	Niotsuji-nishi fault	2	5.3	-	SW	I	C	-	Active Faults in Japan Magnitude was calculated by Matsuda's equation
14	Maruchara fault	2	5.3	-	S	I	C	-	Active Faults in Japan Magnitude was calculated by Matsuda's equation
15	Anticipated Tokai earthquake	-	7.7	-	NW	-	-	-	Central Disaster Prevention Council
16	Earthquake of August 10. 1931	-	5.9	0.0	-	-	-	-	Japan Meteorological Agency's annual seismic report (latest data are available)

(*1) shallower than 150 to 300 m below ground surface

Table 2 Parameters on fault of Scenario earthquake and attenuation relationships

(① Median tectonic line Akaishi-sanchi-seien fault zone, used in attenuation relationships)

(a) Parameters used in attenuation relationships

Dam site	Fault/earthquake	Type of focus	Japan Meteorological Agency magnitude	Shortest distance to fault (km)	Equivalent epicentral distance (km)	Depth of the center of fault plane (km)
N Dam	Median tectonic line Akaishi-sanchi-seien fault zone	Shallow crustal	7.6	23.9	28.5	10.5

(b) Parameters on the hypocenter fault

Japan Meteorological Agency magnitude	Fault length [km]	Fault width [km]	Fault area [km^2]	Dip [deg]	Depth of upper edge [km]	Depth of lower edge [km]
7.6	52	17	884	60	3	18

Table 3 Parameters on the hypocenter fault of Scenario earthquake

(① Median tectonic line Akaishi-sanchi-seien fault zone, used for the statistical Green's function method)

Characteristics of focus			Specified value	Source
Macro characteristics of focus		Latitude	137.82 [deg]	Report of the Headquarters for Earthquake Research Promotion
		Longitude	35.10 [deg]	Report of the Headquarters for Earthquake Research Promotion
		Strike θ	22 [deg]	Report of the Headquarters for Earthquake Research Promotion
		Dip δ	60 [deg]	
		Length L	52 [km]	Report of the Headquarters for Earthquake Research Promotion
		Width W	17 [km]	$W=(H_d-H_u)/sinq$
		Depth of the top edge of the fault below the ground surface d	3 [km]	Report of the Headquarters for Earthquake Research Promotion
		Fault area S	884 [km^2]	S=LW
		Reduction of static stress $\Delta\sigma$	4.03 [MPa]	Boatwrite (1988)
		Seismic moment M_0	4.35E+19 [Nm]	Wells and Coppersmith (1994) $S=4.24\times10^{-11}M_0^{1/2}$
		Moment magnitude M_w	7.03	Kanamori (1977) $\log M_0=1.5M_w+9.1$
		Secondary wave velocity V_s	3.46 [km/s]	
		Density ρ	2.70 [g/cm^3]	
		Rigidity μ	3.23E+10 [N/m^2]	$m=rV_s^2$
		Mean slippage D	1.5 [m]	$M_0=r\cdot D\cdot S$
		Short period level of entire fault A	1.86E+19 [Nm/s^2]	Dan et al. (2001) $A=2.46\times10^{17}M_0^{1/3}$
Micro characteristics of focus	Entire asperity	Area of entire asperity S_a	263 [km^2]	Boatwright (1988), Dan et al. (2001) $S_a=pr^2$ $r=(7p/4)\times M_0/(A\cdot R)\cdot V_s^2$
		Mean slippage of entire asperity D_a	3.0 [m]	Somerville et al. (1999) $D_a=D\times2$
		Seismic moment of entire asperity M_{0a}	2.59E+19 [Nm]	$M_{0a}=m\cdot D_a\cdot S_a$
		Reduction of static stress of asperity $\Delta\sigma a$	13.53 [MPa]	Madariaga (1979) $Ds_a=(S/S_a)\cdot Ds$
	First asperity	Area of asperity S_{a1}	175 [km^2]	
		Mean slippage of asperity D_{a1}	3.4 [m]	$D_{a1}=(g_1/Sg_i^3)\cdot D_a$
		Seismic moment of asperity M_{0a1}	1.91E+19 [Nm]	$M_{0a1}=m\cdot D_{a1}\cdot S_{a1}$
		Effective stress of asperity s_{a1}	13.53 [MPa]	$s_{a1}=Ds_a$
	Second asperity	Area of asperity S_{a2}	88 [km^2]	
		Mean slippage of asperity D_{a2}	2.4 [m]	$D_{a2}=(g_2/Sg_i^3)\cdot D_a$
		Seismic moment of asperity M_{0a2}	6.76E+18 [Nm]	$M_{0a2}=m\cdot D_{a2}\cdot S_{a2}$
		Effective stress of asperity s_{a2}	13.53 [MPa]	$s_{a2}=Ds_a$
	Background	Background area S_b	621 [km^2]	$S_b=S-S_a$
		Mean slippage in the background D_b	0.9 [m]	$M_{0b}=m\cdot D_b\cdot S_b$
		Seismic moment of the background M_{0b}	1.76E+19 [Nm]	$M_{0b}=M_0-M_{0a}$
		Effective stress of the background s_b	2.74 [MPa]	Dan et al. (2002) $s_b=(D_b/W_b)\cdot(p^{1/2}/D_a)\cdot r\cdot Sg_i^3\cdot s_a$
Other characteristics of focus		Rupture propagation velocity V_r	2.77 [km/s]	Kataoka et al. (2003) $V_r=0.8\cdot V_s$
		Rise time of first asperity tr_{a1}	1.20 [s]	Nakamura and Miyatake (2000), Kataoka et al. (2003) $tr=0.25\cdot W/Vr$
		Rise time of second asperity tr_{a2}	0.85 [s]	
		Rise time of the background tr_b	1.54 [s]	
		High frequency cutoff f_{max}	6.0 [Hz]	Tsurugi (1997)

Technical Session 7

TRANSPORTATION SYSTEMS

The FHWA Long-Term Bridge Performance Program

by

Hamid Ghasemi[1], Ian M. Friedland[2], Steven B. Chase[3], and Joey Hartmann[4]

ABSTRACT

The Federal Highway Administration is initiating a major program in early 2006 with the objective of improving knowledge regarding bridge performance over a long period of time. The FHWA Long-Term Bridge Performance (LTBP) program will instrument, monitor, and evaluate a large number of bridges throughout the United States in order to capture performance data over a 20-year period of time and, on the basis of the information collected from these structures, provide significantly improved life-cycle cost and performance and predictive models that can be used for bridge and asset-management decision-making. The LTBP program will also conduct forensic investigations on decommissioned bridges, as the opportunity arises.

KEYWORDS: structural health monitoring, damage detection, deterioration model, asset management

1.0 INTRODUCTION

Many transportation agencies in the United States and Japan, and throughout the world for that matter, have adopted systems, procedures, and tools that attempt to provide formal bridge and asset management. But, how many of these agencies actually manage their bridges and other highway assets in a fully rational and optimal manner?

The key components of rational and functional bridge or asset management systems include one or more databases that contain information on the characteristics of the assets being managed; databases and information on how structures and components deteriorate or result in reduced performance as a result of weather/climate, traffic, and other "environmental exposure" information; information and routines that quantify the effectiveness of various maintenance, repair, and rehabilitation strategies; information regarding the costs of various maintenance or repair strategies, and "user" costs related to the functionality of the asset; and decision-making models and algorithms that attempt to optimize the allocation of resources (e.g., funds, material, and labor) in order to achieve some performance goal for the network of assets and its individual components. Although many transportation agencies have adopted and employed bridge management tools like the AASHTOWare™ PONTIS program, there are still gaps in knowledge regarding how structures and materials perform and deteriorate over time (commonly referred to as life-cycle or life-cycle cost models), and how effective (and for how long) various maintenance, repair, or rehabilitation strategies really are for a given component or system. In addition, the materials being used for bridge construction today are changing rapidly and may be significantly different than conventional bridge materials (e.g., high performance steel, high performance concrete and self-consolidating concrete, fiber-reinforced polymer composites, and new alloys for rebar), and our long-term experience with the performance of these materials is quite limited.

---

[1] Senior Research Structural Engineer, Federal Highway Administration, McLean, Virginia

[2] Technical Director, Bridge and Structures R&D, Federal Highway Administration, McLean, Virginia

[3] Research Program Manager, Office of Infrastructure R&D, Federal Highway Administration, McLean, Virginia

[4] Senior Research Structural Engineer, Federal Highway Administration, McLean, Virginia

As a result, although many transportation agencies practice bridge management, there is still significant room for improvement in the information and data upon which the bridge management systems are based, and on the results and decision-making that occurs based on the output of these systems.

In order to address some of these gaps in knowledge, the Federal Highway Administration (FHWA) of the U.S. Department of Transportation will be initiating a Long-Term Bridge Performance (LTBP) program in 2006. This paper will discuss the initial vision and goals of the LTBP program, but it is likely that this will change somewhat over the planned 20-year lifetime of the LTBP program.

2.0 VISION

The FHWA's National Bridge Inspection Standards (NBIS) and associated National Bridge Inventory (NBI) database have facilitated the creation of one of the most comprehensive sources of bridge information in the world. However, the NBI is limited in the type of structural and performance data that it contains, and essentially provides no information on the individual elements or components of the bridges contained in it. Instead, the FHWA has developed a Bridge Management Information Systems (BMIS) Laboratory which supplements the standard NBI data with information regarding environmental exposure and, in some cases, element level data provided by selected State transportation agencies, in order to help facilitate data mining.

Both the NBI and element level data are typically collected using visual inspection techniques – hidden or inaccessible deterioration or damage, for example to prestressing strands or rebar within a concrete girder, is therefore not usually noted or collected as part of the regular biennial inspection that is required by the FHWA of all highway bridges open to the pubic. The qualitative, subjective, and possibly highly variable nature of this data is therefore inadequate for comprehensive long-term life-cycle decision-making. In addition, the operational performance of highway bridges (i.e., traffic congestion, accident data, overloads, freight movement across the structure) is not typically collected or reported on a statewide or national basis for highway bridges. An essential need, therefore, for support of effective bridge management is long-term bridge performance information.

In order to address this need, the FHWA is embarking on an ambitious multi-year research program known as the Long-Term Bridge Performance (LTBP) program. This program, which was authorized by the U.S. Congress in mid-summer 2005, is being modeled somewhat after the Long Term Pavement Performance (LTPP) Program, which has been conducted within the United States since 1989.

The LTBP program will include detailed inspections and periodic evaluations and testing on a representative sample of bridges throughout the United States in order to monitor and measure their performance over an extended period of time. At the current time, it is envisioned that as many as 2000 bridges will be included in the program, representing many structural types and materials, in a variety of conditions, exposures, and locations. As authorized by Congress, the program will run for 20 years. It is anticipated that the resulting LTBP database will provide high quality, quantitative performance data for highway bridges that will support improved designs, improved predictive models, and better bridge management systems.

A second component of the LTBP program will be a set of instrumented bridges that can provide continuous, long-term, structural bridge performance data. A third component of the program will include detailed forensic autopsies of a number of bridges each year, using some of the structures that are decommissioned by State transportation agencies each year. The intent is to collect actual performance data on deterioration, corrosion, or other types of degradation; structural impacts from overloads; and the effectiveness of various maintenance and improvement strategies typically used to repair or rehabilitate bridges. A preliminary description of the extent and intent of each of these components of the LTBP program is shown in Table 1.

3.0 IMPORTANT OF THE LTBP PROGRAM

The FHWA NBI contains information on more than 590,000 bridges, tunnels, and culverts – essentially, every highway structure which is open for public access, and is at least 20 feet (6.1 meters) in length. The average age of these structures is approximately 42 years. Figure 1 shows U.S. bridge distribution by material and deficiency. The number of structurally deficient and functionally obsolete bridges is approximately 83,000 and 133,000, respectively. In addition, there are about 10,000 bridges being constructed, replaced, or rehabilitated annually at a cost of over $7 billion, while total annual bridge costs, including maintenance and routine operation, are significantly higher. Although it may appear that we are keeping ahead of the current bridge deterioration rate of about 3,000 newly deficient bridges per year, most of the bridges being built today are using the same technologies, materials, and methods that were used to construct bridges 20 or more years ago.

This obviously creates a very difficult but important reason why effective bridge management tools are required in the United States, and why quality information on the actual condition, and effectiveness of maintenance and repair strategies, is critical.

4.0 SCOPING STUDY

In order to initiate the LTBP program, specifics regarding many aspects of LTBP criteria and program goals will need to be created and publicized throughout the United States. To assist in the development of this, the FHWA has employed the University of Delaware through its Center for Innovative Bridge Engineering (CIBrE) to prepare an overall proposed framework for the program. The specific objectives of the CIBrE scoping study include addressing issues and questions such as:

- What types of bridges and bridge components should be monitored?
- How should specific bridges be selected?
- What types of monitoring systems should be used?
- How should instrumentation plans be designed?
- What types of data should be collected?
- How will the data be used in the future?
- Based on how the data will be used, how should it be stored, organized, and made accessible to the bridge engineering user community?

To address these issues and questions, the CIBrE scoping study includes tasks that will address:

- A detailed identification of issues;
- The type of and process for selection of bridges;
- Development of performance monitoring plans;
- Selection of monitoring hardware and software;
- Identification of appropriate analytical tools and practical experimental testing protocols
- Management of data, meta-data, and data mining;
- Translating the results of data mining to practice (for both improved new design and construction, and overall bridge management); and
- Strategies for effective partnering with industry.

As one would imagine, there are many issues and parameters that will need to be addressed in the program. A short-list based on preliminary thinking associated with each of the tasks above includes those listed in Table 2.

5.0 EXPECTED OUTCOMES

The LTBP program will require and result in the investment of a significant amount of money, labor, and physical resources (hardware, software) over the life-time of the program. In order to justify these investments, there are major outcomes that we anticipate will be achieved. Among these are:

- Data/information and technology for effective

management, renewal, and protection of the existing highway infrastructure
- Advances in deterioration science and control to better understand:
  a) deterioration mechanisms that offer reliable scenario analyses at project, network and system levels; and
  b) deterioration models that can simulate interactions between pavement, bridges and traffic
- Reliable inspection/condition information thru non-destructive evaluation (NDE) tools and sensor data
- Optimum life-cycle cost models
- Maintenance and preservation/rehabilitation strategies
- Performance measures for operational, serviceability/durability, structural safety and rare extreme-event limit-states; and
- Rapid strengthening, repair, and retrofit schemes for emergency response following extreme events

In addition, it is likely that the LTBP will help foster the development and improvement of technologies related to effective bridge and asset management, including:

- New NDE tools for assessment of critical but typically inaccessible bridge elements and components such as pre-stressing tendons, suspension and cable stay bridge cables, bearings and dampers, component repairs (e.g., via fiber-wraps and shells), and seismic response control devices
- Wireless, multi-modal, wide-area sensing, imaging, networking, data acquisition, communication and computing technologies
- Data quality assessment measures, real-time data and image processing, wide area data warehousing and archival, data mining, data-based modeling, data visualization, data management, data optimization and control, and
- Technologies that may contribute to effective measures for homeland security, global warming, sound and vibration control

6.0 CONCLUSIONS

The FHWA Long-Term Bridge Performance program is an exciting opportunity that will provide significant advances in our knowledge of how highway structures perform over the long term. It will markedly improve our capabilities to design better, long-lasting structures and to more effectively manage the large number of structures already in service. Based on the information which will be collected and analyzed over the anticipated 20-year life of the program, we anticipate that the program will result in: (a) major improvements in materials and structures life-cycle models and cost analyses, (b) development of performance-based specifications; and (c) development of appropriate and quantifiable performance standards and measures.

The LTBP program is a highly ambitious program that will require creativity in field-based research, while ensuring far more stringent quality standards than that of a typical transportation research program. It would also entail a holistic system approach and considerable synergy between owners, bridge engineering community, academe, industry, and international community. It is a challenge which the FHWA believes can and will be met.

Table 1: Preliminary Plans for LTBP Program Components

Program Component	Sample Size	Purpose	Information Anticipated
Long-Term Performance (LTP) Sample Bridges	Large Numbers	Long-term periodic inspection and evaluation	High-quality, quantitative performance data to support improved designs, improved predictive models, and better bridge management systems
Instrumented Smart Bridges	< 100	Continuous monitoring of operational performance	Data about behavior under routine traffic conditions as well as rare, possibly extreme, events
Decommissioned Bridges	As available	Forensic autopsies	Information about capacity, reliability, and failure modes of bridges that have deteriorated from corrosion, overloads, alkali-silicate reaction, fatigue, fracture, etc.

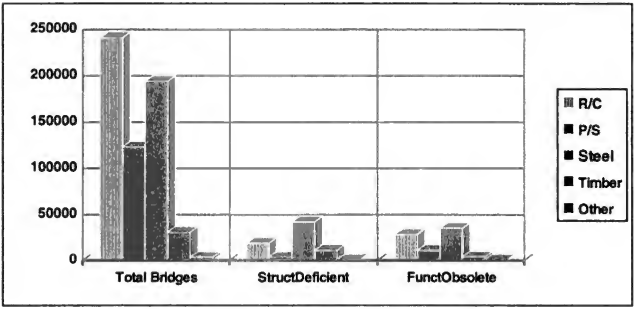

Figure 1: U.S. Bridge Distribution by Material and Deficiency

Table 2: Preliminary List of Parameters for Consideration

<table>
<tr>
<td>Identification of Issues
• Deterioration mechanisms
corrosion, spalling, cracking, fracture, fatigue, overloads, scour, settlement (soil conditions), explosion, chemical attack, collision, natural disasters (e.g., floods, earthquake), fire
• Bridge elements
piers/columns, deck, girders/beams, abutments, expansion joints, construction joints, wearing surface, cables, piles, footings, pylon/ tower, pier caps, bearings, backwall, embankments, pin and hangers, traffic barriers, handrails, connection hardware (welds, rivets, bolts), drainage system
• System for ranking and selecting
most common deterioration mechanisms; most detrimental deterioration mechanisms (capacity, serviceability, cost for repair, aesthetics), ability to inspect and monitor</td>
<td>Bridge Selection
• Types of bridges/structures
girder, truss, rigid frame, arch, cable stayed, suspension, slab, moveable, orthotropic, tunnels and other transportation systems, geotechnical structures, integral abutments
• Construction materials of bridges
steel, reinforced concrete, prestressed concrete, timber, advanced composites, high performance materials, specialty alloys, coatings
• Other criteria
geometric data (length, width, clearances), geographic location (climate and environmental conditions), traffic volume, what bridge crosses, maintenance practice
• Number of bridges/structures
LTBP sample bridges (periodic inspection), instrumented smart bridges, decommissioned bridges (autopsies)</td>
</tr>
<tr>
<td colspan="2">Performance Monitoring Plan
☐ Evaluation methods
visual and instrumented
☐ Data collected
short-term monitoring, long-term monitoring, periodic and continuous (structural health) monitoring, ambient data, controlled load test data, destructive test data
☐ How to minimize costs but maximize value?</td>
</tr>
</table>

Damage Investigation and the Preliminary Analyses of Bridge Damage caused by the 2004 Indian Ocean Tsunami

by

Shigeki Unjoh[1] and Kazuo Endoh[2]

ABSTRACT

At 08:07 a.m. local time on December 26, 2004, a large-scale earthquake with magnitude 9.0 occurred at the western coast of Northern Sumatra Island, Indonesia, which was the forth largest earthquake since 1900. The earthquake generated the tsunami with wave height exceeding 20 m. The tsunami affected the whole Indian Ocean area, and the damage became one of the heaviest natural disasters in human history with casualty more than 200,000 people as well as destructive damage to houses/buildings and infrastructures. The one of authors went to investigate the damage to the city of Banda Aceh, North Sumatra Island, as a member of the Japan Society of Civil Engineers (JSCE) Reconnaissance Team in March 2005, about two months later after the earthquake.

This paper presents the damage to the bridges caused by the earthquake. The significant damage including washout of bridge superstructures were caused by tsunami waves. Based on the investigation so far, the findings and lessons are summarized although more detailed investigation and careful review of the damage of bridges is still needed. Furthermore, preliminary analytical results to simulate the bridge wash-out damage mechanism is presented.

KEYWORDS: Indian Ocean Tsunami, Highway Bridges, Damage Investigation, Simulation Analysis

1. DAMAGE TO BRIDGES AND ROADWAYS

1.1 Area Investigated

Figure 1 shows the North Sumatra Island. City of Banda Aceh is located at the north of the island and Lhoknga is the west city and City of Meulaboh is located at about 250km south from Banda Aceh. The tsunami exceeding about 30m high maximum was estimated to affect the coast area from Lhoknga to Meaulaboh. In these areas, significant damage including complete washout of bridge superstructures and soil structures caused by tsunami waves were found. In the followings, the damages to bridges in cities of Banda Aceh and Lho'nga, and on the route between cities of Banda Ache and Meulaboh are briefly summarized.

1.2 City of Banda Aceh

The city of Banda Ache is located at the north of the Sumatra Island. 42 bridges in the affected area by tsunami at Banda Aceh were investigated. The height of the tsunami in the seaside area was estimated to be about 5-10m. The superstructures of 3 bridges were completely washed out and fallen down, and 5 bridges were remarkably affected with lateral displacement of 10cm–1m by the effect of Tsunami.

Photos 1 and 2 show one of the significantly damaged bridges. The simply-supported prestressed concrete girder bridge with span length of about 20m was washed out by the tsunami effect. The girder was just set on the top of abutments and there seemed to be no shear connection at the bearing supports. Tsunami height was just as the same height as the ceiling level of the 1st story of the houses. After the earthquake, a temporary bridge was provided to assure the traffic.

At the time of investigation when it was about two months later from the earthquake, the washed-out girder was reused and already settled on the original location as a permanent repair.

---

[1] Team Leader, Earthquake Engineering Research Team, Earthquake Disaster Prevention Research Group, Public Works Research Institute, Tsukuba-shi, Ibaraki-ken 305-8516 Japan

[2] Assistant Leader, Long-span Bridge Engineering Center, Honshu-Shikoku Express Highway Co. Ltd., Kobe-shi, 651-0088 Japan (Former Senior Research Engineer, PWRI)

Photos 3 and 4 show the other bridge where the superstructures were completely washed out. It was reported that the bridge had a relatively shallow superstructure made of wooden materials. Substructures were made of masonry materials filled with concrete mortar.

The photo is not shown here but the complete washout of superstructures was found at one more bridge. It was made of a prestressed concrete girder with shallow deck with 1 lane. The concrete members of substructures to support the girder laterally were failed by the lateral force effect of tsunami and then the girders were washed out.

Photos 5 to 8 show the typical damage to a bridge in which the significant lateral displacement was developed by the effect of tsunami wave. The superstructure of the bridge was 3 span simply-supported reinforced concrete girder and was supported by the wall type reinforced concrete piers. The rubber sheet type bearings were used and there was no shear key to laterally connect between girder and substructures. The decks were moved about 50cm laterally but the rotation was developed at the decks then the decks were wedged geometrically between the both abutments. The handrails were partly but heavily damaged and it was estimated that the handrails were broken down by the effect of the hit of boats or driftage. The washout effect at the backfill soils of abutments was also found.

Photos 9 and 10 show another bridge where the significant lateral displacement was developed. The bridge is a simply-supported reinforced concrete girder with span length of about 20m. The deck was moved in the transverse direction about 1m by the tsunami effect. The girder was supported by the rubber sheet type bearing and there was not any shear connection between girder and substructures.

Although several bridges were significantly damaged caused by the tsunami effect, on the other hand, there are several bridges without any significant damage even they seemed to be strongly affected by the tsunami. Photos 11 and 12 show a bridge without any significantly damage by tsunami. The height of tsunami was estimated about several meters over the bridge deck level. Heavy damage to houses and buildings was found around the bridge. The bridge was a long bridge with 10 span simply-supported concrete girders which were supported by circular reinforced concrete columns. The rubber bearings were used and the concrete block shear keys were provided between girders. Although the attached facilities beside the girders which were estimated as electricity or others were heavily failed but the main body of the bridge was not damaged. Slight damage to the shear keys as cracking was found. It is needed to investigate more including the tsunami height, but it is estimated from the bridge behavior that the shear keys seems to work well to resist against the lateral force caused by tsunami.

Photos 13 and 14 show another bridge to show the slight damage to shear keys. The bridge was 3 span simply-supported concrete girders and was supported by the rubber bearings and concrete block shear keys. The bridge was not affected by the tsunami. The shear keys were slightly damaged including the concrete cracking and failure. The damage was estimated to be caused by the earthquake ground motions.

As will be discussed later, many truss bridges with relatively longer spans were washed out in the west coast route from Banda Aceh to Meulaboh. The detailed investigation could not be made for all of the collapsed bridges but some collapsed bridges did not have the connection and shear keys between decks and substructures. Photos 15 and 16 show the behavior of the truss bridge with stiff bearing connections between deck and substructures. Since the bridge is located at the east of Banda Aceh, the tsunami height might not be so significant. But the tsunami height was clearly exceeded over the height of the upper truss member. There found no damage at the bridge. It is needed to investigate more in detail but the stiff bearing connection may be one of the reasons for no damage.

1.3 City of Lhoknga

The city of Lhoknga is located at the west of Banda Aceh. The area was significantly affected by the tsunami and the tsunami height is estimated to be over 30m at maximum. Photos 17 to 19 show the complete washout of 2 span simply-supported steel truss bridge, which was supported by the wall type reinforced concrete columns. The decks were supported by the bearings and a bolt was provided to connect deck and substructures. There was no stiff shear connection between deck and substructures except one bolt connection. Since the truss girders were washed out to the upstream side and the bolt to connect between deck and substructure were bended toward the upstream side, it was estimated that the decks were washed out by the tsunami wave in the direction of upstream side. This route is important route to connect between the north and the south, the temporary bridge was provided for emergency measures. It should be noted here that it is estimated the truss type bridge is employed for a relatively longer span bridge in the area.

Photos 20 and 21 show the behavior of the reinforced concrete box culvert bridges. The bridge is located in the cement factory which was significantly damaged by the Tsunami. Some damage was found at the sidewall but there was almost no damage at the main body of the bridge.

1.4 Route from Banda Aceh to Meulaboh

The city of Meulaboh is located at about 250km south from the city of Banda Aceh. There is a seaside route which is only roadway to connect between two cities. The tsunami was the most significantly affected on the route. According to the data investigated by the Katahira & Engineers International, total section of 56.6km of roads was unpassable and 126.7km was seriously damaged. Also, there were 186 bridges along the roads and 81 bridges were washed out or heavily damaged. JSCE team could not investigate the all of bridges by a land route but the investigation from the helicopter was made.

Photos 22 to 26 show the typical washout of the bridges in the route. All photos shown here were taken by UN. There are several steel truss bridges and the deck was completely washed out toward the upstream side. Since the most piers and abutments remained at the original location, it is estimated that the superstructures were washed out by the effect of tsunami. Photos 27 shows the washout of the roadways which were completely eroded by the tsunami effect. The settlement of land was also estimated along the coast and the erosion of the coastline was quite significant.

3. PRELIMINARY ANALYSIS

To simulate the dynamic behavior of bridges structures subjected to the Tsunami effect, the analytical study was made.

Figure 2 shows the section of the bridge superstructure analyzed. A steel I girder and the RC Slab with bridge length of 40m was assumed. The girder weight is assumed as about 5.4kN/m/girder. The deck is assumed to be supported by bearings. Deck height is assumed as 5m at the bearing level.

Figure 3 shows the assumed effect of Tsunami. Tsunami height is assumed as 30m considering the west coast at North Sumatra Island. And the velocity is assumed as 68km/h (about 20m/s) considering the observation and empirical equation. The analysis was made using the discrete element method assuming the particle of 10cm diameter. The flow was loaded from the right to left sides.

Figure 4 shows the time history behavior of the deck. It is found that the numerical analysis can roughly simulate that superstructure moves laterally by the effect of Tsunami. From this kind of analyses, forces which affect the bridge superstructures can be evaluated.

4. SUMMARY OF DAMAGE TO BRIDGES AND ROADS

More detailed investigation and careful review of the damage is still needed, but based on the above investigations, the following findings were so far obtained.

1) Tsunami Effect: Since tsunami is basically fast, strong and thick water flow with driftage, then lateral water pressure, floating effect and washout effect are the primary mechanical effect.

2) Concrete Bridges: If a bridge had a concrete deck with appropriate shear keys at bearing

supports, the bridge did not have a significant displacement or was not washed out during the tsunami effect. If there was no shear key, there were some bridges in which the deck was completely washed out or significantly displaced in the transverse direction.

3) Steel Bridges: The detailed investigation for all of the collapsed steel truss bridges could not be made. The washed-out truss bridge located in Lhoknga did not have any shear key, on the other hand, one truss bridge with stiff bearings at the east of Banda Aceh did not suffer any damage. Therefore, it is estimated that the shear keys may work well against the lateral tsunami force. The floating effect can be also controlled by the uplift stopper which connects between superstructures and substructures at bearing supports.

4) Foundations: It was found that some of the substructures as well as superstructures were completely washed out and missing. It is also important to protect the substructures from the washout. Wall-type piers, which are usually employed in this area, seemed to be survived well, and the foot protection work around foundations is effective if there is surrounding material which is easily washed out.

5) Abutment Backfill Soils: There found several damage to abutments where the backfill soils were washed out. To fill the soils as a temporary measure to assure the traffic is relatively easy. But if such damage should be prevented for abutments in which the longer repair work are needed after the earthquake, the bank protection at the abutment is effective.

6) Soil Structures: If the roads are constructed on the stiff ground (possibly, cutting ground, stiff clay layer/rock and so on), the roads seemed to be survived. On the other hand, the roads are on the soft or sandy soils (possibly, soil embankment with soft materials which is easy to be washed away), the roads seemed to be completely washed out. Such sandy soils sections are generally located closed to the seaside line, or the current or past river areas. Also, the erosion effect was very significant.

7) Ship Effect: The driftage of large ships seemed to influence the damage significantly. But the direct consideration of the effect of the hit of ships in the structural design does not generally become reasonable. Such ship control measures during tsunami are also important.

5. ACKNOWLEDGEMENTS

The author investigated the damage at the North Sumatra as a member of the Reconnaissance team of Japan Society of Civil Engineers. The investigation was made by Mr. Naoki Furukawa, Kajima Corporation, Mr. S. F. Wong, Penta-Ocean Construction Co. Ltd., and Prof. Thanthawi Jauhari of Syiah Kuala University-Indonesia. The authors thank all of the related agencies and people who supported the investigation. Regarding to the information on the bridge and road damage, the authors would like to express sincere appreciation to; Mr. Kazuo Yumita and Mr. Takashi Okumura of Katahira & Engineers International for their detailed information on the bridge damage from Banda Ache to Meulaboh, and Mr. Tim Randall of UN OCHA for his information on the air photos (Photos 22 to 27) on bridge damage from Banda Ache to Meulaboh.

6. REFERENCES

1. Japan Society of Civil Engineers, (2005), "The Damage induced by Sumatra Earthquake and Associated Tsunami of December 26, 2004, A report of the Reconnaissance team of Japan Society of Civil Engineers," *http://www.jsce.or.jp/committee/2004sumatra/report.htm*
2. Endoh, K. and Unjoh, S.: Analytical Study on the Response Characteristics of bridges against Tsunami, *2006 JSCE Annual Meeting*, Sep. 2006 (in Japanese).
3. Cundall,P.A. and O.D.L.Strack.: A discrete numerical model for granular assemblies, *Geotechnique*, pp.47-65, Vol. 29(1), 1979

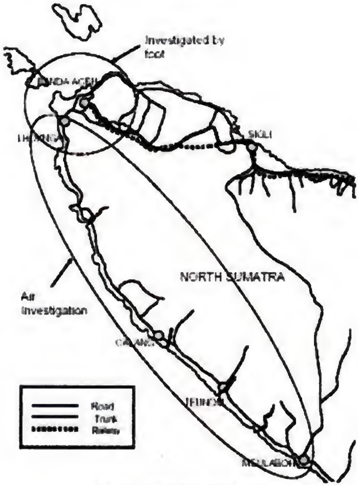

Figure 1 North Sumatra Island

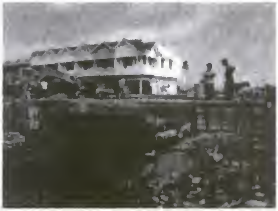

Photo 1 Repair of Washed-out Girder

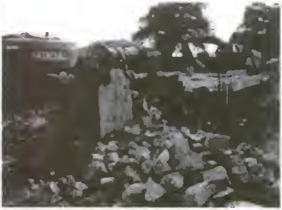

Photo 2 Collapse of Water Pipes Bridge

Photo 3 Complete Washout of Bridge
(reported as Wooden Superstructure)

Photo 4 Masonry Substructure and Washout Effect
of Surrounding Soils

Photo5 Damaged Bridge

Photo 6 Washout Effect of Backfill Soils

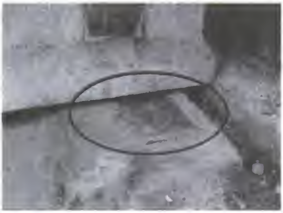

Photo 7 Lateral Displacement of Deck

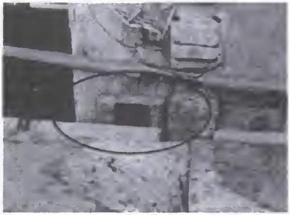

Photo 8 Rubber Sheet Type Bearing
and Lateral Displacement at Bearing

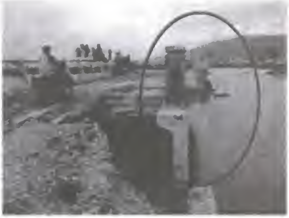
Photo 9 Lateral Displacement of Deck

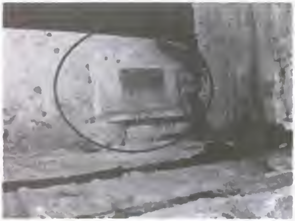
Photo 10 Displacement at Bearing

Photo 11 Undamaged Bridge by Tsunami

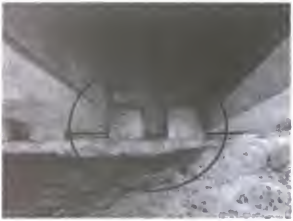
Photo 12 Concrete Block Shear Keys

Photo 13 Bridge affected by Shaking

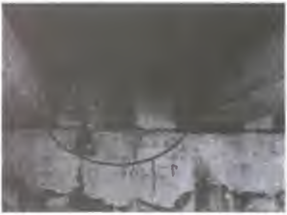
Photo 14 Slight Damage to Shear Keys by Shaking

Photo 15 Steel Truss Bridge without Damage

Photo 16 Steel Bearing Supports

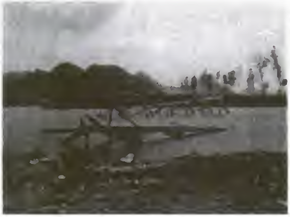

Photo 17 Washing out of Steel Truss

Photo 18 Temporary Bridge

Photo 19 Bearing Support and Bolt to connect between Deck and Substructures

Photo 20 Concrete Box Culvert Bridge

Photo 21 Concrete Box Culvert Bridge

Photo 22 Washout of Truss Bridge (1)

Photo 23 Washout of Truss Bridge (2)

Photo 24 Washout of Truss Bridge (3)

Photo 25 Washout of Truss Bridge (4)

Photo 26 Washout of Truss Bridge (5)

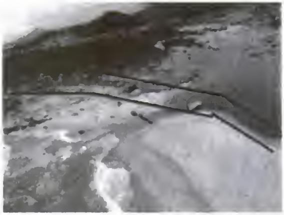
Photo 27 Erosion of Road and Coastline

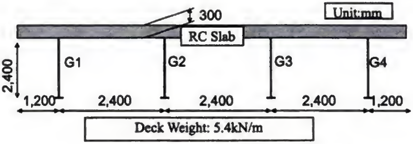

Figure 2 Assumed Deck Structure Analyzed

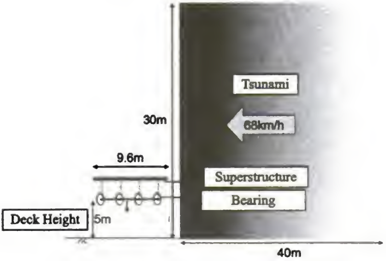

Figure 3 Assumed Effect of Tsunami

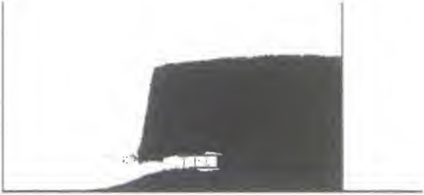

(a) 1.0 Second

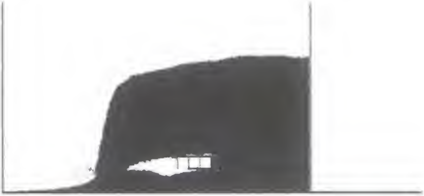

(b) 1.5 Second

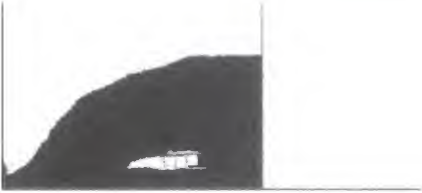

(c) 2.0 Second

Figure 4 Examples of Time History Behavior

Multi-hazards Design Criteria of Highway Bridge

by

George C. Lee[1], Mai Tong[2] and Phillip Yen[3]

ABSTRACT

Following the philosophy approach of the AASHTO LRFD, a study of commeasurable criteria for multiple hazard comparison is carried out as a research task of a FHWA contract to MCEER. This paper describes the general approach undertaken by the MCEER researchers to establish a platform for proper comparison of various hazard events and their expected impact to highway bridges.

1.0 INTRODUCTION

Multiple hazards (e.g. earthquake, wind gust, flood, vessel collision, traffic overload and accidents, and terrorist attacks etc.) must be properly considered in highway bridge design in addition to the normal functionality requirements. Current AASHTO bridge design specifications have provided detailed hazard loadings for each identified hazard. To further examine the bridge resistance to multiple hazards; it is necessary to compare hazard events and their expected impact to bridges for which consistent measurement criteria need to be established. For example, a simple criterion can be used to consider the occurrence of various hazards such as the return period or probability of exceedence in a given time period. However, it is not fully justifiable to apply such a criterion to calibrate the design hazard loadings of bridges since many other influential factors and uncertainties such as hazard duration, vulnerability of critical components, risk of hazard induced consequences, potential areas of impact and severities of hazard induced damage to a bridge may vary considerably from one hazard to another.

Indeed, in the current AASHTO specifications, the design hazard for earthquake is set at 475 year of return period, which has a 10% probability of exceedence in 50 years. Based on recent recommendation from NEHRP (NEHRP 2000), it is also intended to increase the return period to 2000~ 2500 years for significant bridges. And the proper return period of design earthquake is still under discussion in the research and professional community. Wind hazard is set at 50 year of return period according to ASCE 07-95. Scour is set at 100 year return period following FHWA HEC 18. In comparison, live load is set at the maximum of 75 years, which is the design life-span of the bridge (Ghosn, et al 2003). There is no uniform cross-the-board requirement for the hazard occurrence frequency set for design considerations.

2.0 FROM AASHTO LRFD TO IMPROVEMENT OF MULTIPLE HAZARD BRIDGE DESIGN

A main thrust of highway bridge design in the US is currently focused on the transition of AASHTO standard specifications to AASHTO LRFD specifications. Recognizing the advantage of LRFD design methodology, proper engineering comparison of multiple hazards for highway bridge design is important since the major uncertainty in design comes from the hazard loading demand.

From the point view of AASHTO LRFD design methodology, every bridge should be designed for the specified limit states. Both standard low intensity hazards a bridge experiences regularly and the extreme hazard events are represented by the design limit states. This means that the bridge structural system including its components and connections must be designed to reach the design failure mechanism first. Thus, unintended over-strength of a member or component is to be avoided, because it could result in damage (e.g. plastic hinge) at an undesirable location of the structure with adverse effects.

---

[1] Samuel P. Capen Professor of Engineering, University at Buffalo

[2] Senior Research Scientist, Multidisciplinary Center for Earthquake Engineering Research, University at Buffalo

[3] Senior Research Structural Engineer, FHWA

AASHTO LRFD differs from the AASHTO standard specifications in which the fundamental design methodology is founded on traditional allowable stress design, ASD, approach. A major weakness of ASD design is that all loads and load combinations are treated equally without considering the probability of both a higher-than-expected load and a lower-than-expected strength occurring at the same time and place. Therefore, it possesses little or no direct relationship between the assumed design standards and the actual resistance of many components in bridges, or the probability of events actually occurring (Kulicki 1999).

To overcome the weakness of the ASD approach, LRFD specifications are established on the basis of standard deviation or the coefficient of variation of a stochastic variable - failure index β, which is a measurement of a probability of failure for a given set of loads, or the nominal resistance of the components being designed.

The value of β directly corresponds to the probability of failure. The reliability indexes were evaluated for simulated and actual bridges designed according to the past specifications for both shear and moment. The range of reliability indexes cover a wide range from less than 2 to higher than 4. As the data prepared by (Nowak 1999) suggest that past practice is represented by $\beta = 3.5$, this value is selected as the target for the calibration of LRFD specifications. $\beta = 3.5$ corresponds a uniform probability of safety (1-probability of failure) which is equal to or greater than 99.98%.

The advantage of AASHTO LRFD is that it offers a uniform probability-based criterion to measure the safety level of a bridge design. Preferably, if a similar uniform standard could be established for comparison of the effects of multiple hazards on bridges, it would strengthen the AASHTO LRFD and provide a solid foundation for hazard load factor calibration. This, unfortunately, does not seem to be possible given the large uncertainties associated with hazard events and the reasons mentioned above. Following the fundamental methodology of LRFD and in view of lacking uniform criteria of hazard comparison in current multiple hazard bridge design, This FHWA research task is to explore and establish some possible and justifiable non-uniform commeasurable criteria.

3.0 COMMEASURABLE CRITERIA OF MULTIPLE HAZARDS FOR HIGHWAY BRIDGE DESIGN

The word "commeasurable" by definition means comparison on an "equal" basis. For comparisons of multiple hazard impacts or calibration of hazard loadings on bridges, the "equal" basis can be rather complicated to define. For example, a hazard classification based on a commeasurable return period is to set a reference for design loadings of individual hazards on the basis of hazard occurrences. In this regards, the commeasurable criterion has only considered the uncertainties of the hazard occurrence; but not the cause of hazards and the resistance of the structure. Vessel collision is a hazard which cannot be properly modeled by return period since the vessel size and weight in a particular river is physically restricted; therefore, the impact from collision will not significantly vary from one year to the next. It is measured as the rate of total collision incidents per year regardless of the location of the incidences.

The goal of a commeasurable criterion is not to judge the bridge design itself, but to offer an "equal" base to evaluate the possible impact of a potential hazard event on a bridge. As it is pointed out above, the "equal" base can be interpreted differently by "occurrence", "safety", "cost of repair", "interruption of services" etc.

There are several available commeasurable criteria other than the simple return period criterion. Based on reliability index β, different hazards may be compared by their load effect demand on major safety related individual components as described in API-LRFD (API-1992), or classified component groups (e.g. all steel members in bending, compression, or shear). Improving the simple component failure/ safety criteria, a comparison criterion may include a full range of system and component failure consequences (Moses, 2001). Additional factors to be considered include non-hazard caused bridge down time such as repair, serviceability, operability and life cycle cost.

For multiple hazard bridge design, some non-uniform commeasurable criteria are inevitably needed to justify the targeted design hazard level. Although the selection of such a criterion may not be directly visible to the design engineers as it may have been implied in the code specified load combination factors, a clearly established relationship between the design hazard level, desired bridge performances, and balance of resources will help bridge engineers to understand the various options and solutions to meet the requirements of future bridge design against multiple hazards.

4.0 NON-UNIFORM COMMEASURABLE CRITERIA AND BRIDGE PERFORMANCE UNDER HAZARD CONDITIONS

As pointed out in the above section, commeasurable criteria of multiple hazards for bridge design are most likely non-uniform, and thus they are not suitable to be applied uniformly to all bridge design. It often is associated with the performance requirements, level of acceptable uncertainty and prioritized importance factors. For example, the following is suggested as some basic desired performance levels for highway bridges.

1. Minimum (Basic) performance level
    - Life safety
    - System integrity (superstructure, foundation, pier, bearing, tower, cable, deck, etc.)
2. Serviceability performance level
    - Full traffic service
    - Restricted traffic service (weight, speed, volume, direction)
    - Temporary down time
    - Alternative route
3. Beyond normal functionality level
    - Evacuation
    - Rescue
    - Special transportation tasks (disaster relief)
    - Repair
    - Collapse control

Corresponding to the above performance levels, there may be potential critical issues of bridge performances under hazard conditions, in particular, under the extreme hazard events. For example the following list summarizes a few issues in each of the relevant performance levels.
In basic performance level:

- Possible scenarios of mass casualty on bridge and tunnels under severe hazard conditions
- Possible scenarios of bridge failure modes that may lead to a loss of system integrity

In service performance level:

- Rapid assessment and inspection methods to determine the bridge health condition after a severe event
- Restricted bridge service with identified damage
- Temporary repair and the bridge capability limit after the repair
- Cost benefit balance of hazard plans (strengthening, restricted traffic, temporary downtime, routing, etc.) for critical bridges

In beyond normal functionality level:

- Assessment of available technologies for improved resilience to terrorist attack
- Collapse of bridge
- Cost structure of possible scope of desired level performance and corresponding expenses

Despite the over simplification of this short list, it serves to illustrate that in order to compare hazard and hazard impacts for highway bridge, a more comprehensive basis of comparison should be established. In particular, these factors and considerations may vary from bridge to bridge.

5.0 FHWA SPONSORED RESEARCH AT MCEER

MCEER has successfully conducted several research projects resulted in seismic design guidelines of bridges in recent years. In the present FHWA project, earthquake hazard is expanded to multiple hazard resistant bridge design.

The goal of this current research task is to pave the way for developing multi-hazard design guidelines for future highway bridges. Under this long range goal, there are two levels of efforts and currently been explored by MCEER researchers.

- Development of a comprehensive scope of the multi-hazard design for highway bridges
- Establishment of commeasurable criteria for bridge design against multiple hazards

For the comprehensive integrated approach

In general, multi-hazard design for future highway bridges may face many challenges ranging from considering more frequent low to moderate intensity hazard loadings to combined multi-hazard extreme events; establishing proper design criteria for hazard resistance to balancing resources for maximized utility benefit; ensuring the public transportation safety to minimizing life cycle costs of bridge maintenance and services, developing mandated requirements for minimum safety concerns to owner discretionary options of hazard resilient design. The comprehensive evaluation is to explore the challenges of the multi-hazard bridge design and identify the key areas for the next phase major effort. In this task, the comprehensive scope of multi-hazard design for highway bridges is to be explored by

1. Evaluating each individual hazard design requirements in AASHTO LRFD.
2. Screening issues of concern for multiple hazard events (from low to high intensity).
3. Holding advisory panel discussions to explore possible approach to address these issues.

For Commeasurable Criteria Evaluation:

Within the short time duration of the project (two years), a focused effort is to be pursued to address the issue of developing consistent criteria to compare the effects of various hazards on bridges based on current AASHTO LRFD. This effort is to be limited to a few hazards at the beginning, which includes earthquake, wind, and flood. It will be extended to other hazards such as vessel collision, fire, traffic overload and potential man-made hazards in the future. Upon establishing some commeasurable criteria, a Monte Carlo simulations shall be carried out to check the various probability distributions between different loadings (load types and intensity) and the relevant critical failure modes. In particular, a safety based criterion will be compared to consequence-based criteria. The study is to be carried out following the path described in Figure 1.

6.0 SUMMARY

The above described research is the first step of a longer term R&D effort to improve bridge design guidelines against multiple hazards. The current research is to demonstrate in quantitative terms the benefits and limitations of some commeasurable criteria to be possibly employed for multiple hazards comparisons in bridge design. The effort is to extend the LRFD methodology and to explore a quantitative model for evaluation of multiple hazard load factor assumptions adopted in design code specifications.

7.0 ACKNOWLEDGEMENT

The research described in this paper, sponsored by the US Federal Highway Administration, is a research task being carried out at the Multidisciplinary Center for Earthquake Engineering Research at University of Buffalo under contract (DTFH61-98-6-00094)

8.0 REFERENCES

American Association of State Highway and Transportation Officials "AASHTO, LRFD Bridge Design Specifications" 2000

American Petroleum Institute, "Recommended Practice for Planning, Designing and Constructing Fixed Offshore Platforms-Load and Resistance Factor Design, 1992

Andrzej Nowak "Calibration of LRFD Bridge Design Code", NCHRP 368, 1999

Michel Ghosn, Fred Moses and Jian Wang, "Design of Highway Bridges for Extreme Events", NCHRP 489, 2003

Fred Moses, "Calibration of Load Factors for LRFD Bridge Evaluations" NCHRP 454, 2001

Kulicki, John M. "Design Philosophy of Highway Bridges", Bridge Engineering Handbook, 1999

Federal Emergency Management Agency, "NEHRP Recommended Provisions for Seismic Regulations for New Buildings and Other Structures 2000 edition", FEMA 368/369

Federal Highway Administration, "Evaluating Scour at Bridges," Hydraulic Engineering Circular No. 18 , 2001

In Figures 12 and 13 the soil stiffness and soil damping coefficients are plotted for two different amplitudes (ρ_{T1} = 0.002 m and (ρ_{T2} = 0.0015) vs. forcing frequencies. Both charts indicate a nearly linear decay in soil stiffness and soil damping with increasing forcing frequencies. This indicates that the soil softens with increasing the exiting frequency.

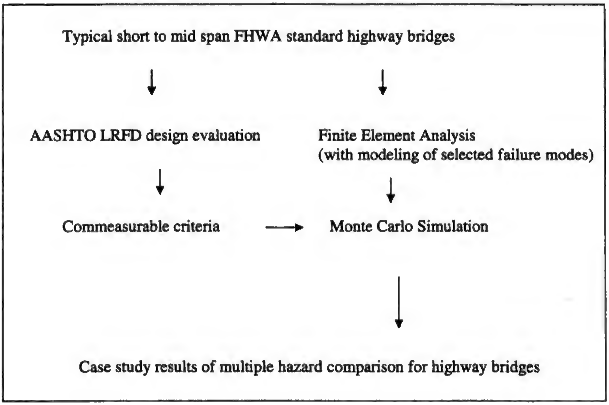
Typical short to mid span FHWA standard highway bridges
AASHTO LRFD design evaluation
Finite Element Analysis
(with modeling of selected failure modes)
Commeasurable criteria
Monte Carlo Simulation
Case study results of multiple hazard comparison for highway bridges

Figure 1. Project Study Path

Technical Session 8

FIRE PERFORMANCE OF STRUCTURES

Outline of the Fire Resistance Verification Method in the Building Standard Law of Japan

by

Mamoru Kohno[1]

ABSTRACT

Fire resistance of buildings is one of major issues in the building standard. In the Building Standard Law of Japan, fire provisions state the requirements for fire resistance and evacuation safety. The approach conventionally used for the compliance with the requirements for the fire resistance is use of fire-resistive constructions for principal building parts without taking the detailed fire conditions expected to occur inside the building.

The Fire Resistance Verification Method was introduced in May, 2000 as an alternative to the conventional fire-resistive construction approach. Duration and intensity of fires predicted to occur inside a building is evaluated and the fire performance of principal building parts against the fires is verified in the FRVM.

Fire resistance requirements in the Building Standard Law of Japan are briefly introduced and outline of the FRVM is explained through the verification process of protected steel columns.

KEYWORDS: Building Standard Law of Japan, Fire Provision, Fire Resistance, Performance Verification

1. INTRODUCTION

Most of building codes or building standards contains structural and fire safety provisions as its major components. In structural design process, the performance of a structure or portions of a structure is checked mostly based on calculation methods, e.g. the allowable stress design, the limit states design, etc. In the fire safety arena, however, fire resistance design has been such that a designer chose appropriate fire-rated constructions from catalogues or lists to comply with requirements specified in the regulation. Though fire resistance is linked to the behavior of structures, the approach used in ordinary design process has been quite different from those used for seismic or wind resistance design.

Technical bases for analysis of structural behavior under fire conditions have been developed by many researchers. Advanced designers have utilized the state-of-the-art method in the technical bases for the fire resistance design of building for quite long time. In Japan, however, only a designated technical committee could review such an advanced design and it took long time to get the required Ministerial approval for the building design till May, 2000.

In the 1998-2000 revision of the Building Standard Law of Japan (BSL), the fire resistance verification method (FRVM) was enacted. The FRVM contains prescriptive verification methods of fire performance of steel, reinforced concrete and wooden structural members taking parametric fires into account. This enabled ordinary engineers to evaluate the fire performance of structures under respective fire condition of the buildings. The process is similar to the cases of wind and seismic design of buildings.

2. REQUIREMENTS FOR FIRE RESISTANCE

The BSL requires a building to be fire-resistive according to its occupancy, size (i.e. number of story, height or floor area) and location. In the BSL the fire-resistive buildings are prescribed as the buildings that conform to the following criteria (*Article 2(9-2)*):

(a) Buildings whose principal parts come under either (1) or (2) below.

---

[1] Head, Fire Standards Division, Building Department, National Institute for Land and Infrastructure Management (NILIM), Tsukuba 305-0802, Japan

(1) Those which are of fire-resistive construction.

(2) Those which conform to technical criteria specified by Cabinet Order concerning the performances mentioned below (in the case of principal building parts other than exterior walls, only the performance mentioned in (i)): *Order Article 108-3.*

(i) Those which can withstand the heat of a fire predicted to occur inside the building according to the construction, building equipment, and use of the said building until the end of the said fire.

(ii) Those which can withstand the heat of a normal fire occurring in the area surrounding the said building until the end of the said fire.

(b) Building which have fire doors or other opening protective assembly specified by Cabinet Order at such openings in exterior walls liable to catch fire. *Order Articles 109 and 109-2.*

Conventional method to comply with the fire resistance requirements is of course (a)(1). In the BSL the fire-resistive construction is prescribed as follows (*Article 2(7)*):
Fire-resistive construction: The type of construction for walls, columns, floors and other parts of a building which conforms to technical criteria specified by Cabinet Order concerning fire-resistive performance* such as reinforced concrete structure and brick structure and which uses structural methods established by the Minister of Land, Infrastructure and Transport or which is proved by the Minister.
*(performance required for the said building parts to prevent a normal fire from causing both the collapse of the building and the spread of fire until the end of the said normal fire) *Order Article 107*

The performance required for each of the principal building parts are shown in Table 1. Required fire resistance time of each building part varies depending on the number of story where the part is used. Table 2 shows the details.

This approach for compliance with the fire resistance requirements is easy to apply and has been used for long time. Real fires occurring in buildings, however, are not identical with the nominal fire, e.g. fire defined in the ISO 834 or ASTM E 119. Generally, the fire-resistive constructions, or fire-rated constructions in more general term, are tested only against the standard fire temperature curve. Real performance of the fire-resistive constructions under general fire conditions is not clear though it is believed to be conservative.

The FRVM is an alternative approach to the conventional fire-resistive construction method.

3. THE FRVM FOR STEEL MEMBERS

The FRVM verify the performances pertaining to (a) (2) above and prescribe practical methods of calculation. The FRVM is provided in Article 108-3 of the Enforcement Order of the BSL and in Notification No. 1433 (2000) issued by the Ministry of Infrastructure, Land and Transport (MLIT).

Under the FRVM as they pertain to (a) (2) (i) above, the intensity and duration of fires occurring within enclosed spaces are predicted; On the other hand, pertaining to (a) (2) (ii) above, external fires are prescribed (in practical terms, 30 or 60 minutes of the ISO 834 standard fire temperature curve). It is verified that principal building parts, e.g. columns, beams, walls or other parts can resist (or can sustain to maintain the required performance) to the intensity and duration of enclosure or neighboring fires.

3.1 Flow of Verification Method

The FRVM prescribes verification methods of fire performance for steel, reinforced concrete and wooden structural members. All verification methods are structured so as to verify that "the retained fire resistance time" is longer than or equal to "the duration of the fire" at the final verification stage.

An outline of the FRVM for verifying the performance of columns and beams of steel-structure buildings pertaining to (a) (2) (i) above is introduced below. As shown in Fig. 1, the verification flow is divided into two parts—prediction of enclosure fires and calculation of the performance to be achieved by columns and beams in resisting the enclosure fires.

3.2 Duration and Temperature Rise Coefficient of Enclosure Fires

The first step in structural design is to make assumptions regarding actions that will affect the structural system (frames, members, etc.). In the case of fire resistance design, the first step is, of course, to make assumptions regarding the effect of fire-induced calorific heat on the structural system. Fires can in practice occur in a variety of building spaces and will be influenced by the indoor combustibles and ventilation, as well as the endoergic conditions and other factors of the walls, ceilings, floors and other structures. Even only with regard to combustibles, it is not easy to adopt a refined fire model that takes into account the size, location and material properties of combustibles in detail.

Therefore, fires are uniformly expressed by Equation (1) in the FRVM.

$$T_f(t) = \alpha t^{1/6} + 20 \quad (0 \le t \le t_f) \tag{1}$$

where

T_f : fire temperature (°C)

t : time lapse after fire outbreak (min.)

t_f : fire duration (min.)

α : fire temperature rise coefficient (°C/min.$^{1/6}$)

The fire duration, t_f (min.), is found by Equation (2) in which the calorific value of combustible materials in the room, Q_r (MJ), is divided by the heat release rate, q_b (MW).

$$t_f = Q_r / (60 q_b) \tag{2}$$

The calorific value of combustible materials in the room takes into account the effects of combustibles stored inside a room, interior finishes, fire spreading to adjoining rooms and other factors. The calorific value of combustibles stored inside a room is given in Table 3 by room category. Interior and other finishes are calculated according to the actual conditions of the rooms. The effects of adjoining rooms are valued at 0~15% of the total calorific value of these rooms (rate depends on the degree of fire resistance provided by the intervening walls); the resulting value is added to the calorific value of the room in question.

The heat release rate, q_b (MW), is calculated according to the surface area of combustibles and the ventilating conditions of the room. The fire temperature rise coefficient, α (°C/min.$^{1/6}$), on the other hand, is a parameter for expressing the intensity of a fire and is found by Equation (3). This equation calculates the balance between heat released by combustibles and heat losses resulting from perimeter wall areas (walls, floors and ceilings) and openings.

$$\alpha = 1280 \left(\frac{q_b}{\sqrt{\sum A_C I_h \sqrt{f_{op}}}} \right)^{2/3} \tag{3}$$

where

A_C : area of perimeter wall area (m^2)

I_h : thermal inertia (kW·s$^{1/2}$/m^2·K)

$f_{op} = \max\left\{ \sum A_{op} \sqrt{H_{op}}, A_r \sqrt{H_r} / 70 \right\}$

A_{op}, H_{op} : area (m^2) and height (m) of opening, respectively

A_r, H_r : floor area (m^2) and floor height (m), respectively

Meanwhile, the standard fire temperature curve of ISO834 conforms closely with the curve when the fire temperature rise coefficient is set at $\alpha = 460$ in Equation (1).

3.3 Retained Fire Resistance Time of Steel Members against Enclosure Fires

As shown in Table 1, load carrying capacity to enclosure fires is required for columns and beams—the principal structural parts of steel-structure buildings. Accordingly, the maximum fire duration—i.e. the period during which the principal structural parts of steel-structure buildings retain their load carrying capacity against heat produced by enclosure fires as expressed by Equation (1)—is defined as the retained fire-resistance time against enclosure fires.

In order to find the retained fire resistance time against enclosure fires, the first factor to be determined is the critical member temperature T_{cr} (°C), which is the critical temperature below which members retain their load carrying capacity. Following this, calculation is made of the fire duration, which is the time required for structural members to reach the critical member temperature in a fire having the fire temperature rise coefficient, α, determined in the previous section. The fire duration thus calculated becomes the retained fire-resistance time against enclosure fires.

For example, in the case of structural steel columns, the critical member temperature, T_{cr} (°C), is given by Equation (4).

$$T_{cr} = \min(T_B, T_{LB}, T_{DP}, 550) \qquad (4)$$

where

T_B: maximum temperature for overall buckling of the column (°C)

T_{LB}: maximum temperature for local buckling of the column (°C)

T_{DP} : maximum temperature for thermal deformation of the column (°C)

550: temperature to guarantee the soundness of joints (°C)

Under the FRVM, equations are given for calculating T_B and T_{LB} according to the geometrical and loading conditions of the columns. Further, because T_{DP} is a factor in guaranteeing that excess inter-story drift due to elongation of beams at elevated temperatures does not occur, the equation for calculating this factor in accordance with the geometrical conditions of the rooms is also given.

In cases where the structural steel columns are provided with fire-protective covering and possess the critical member temperature found by Equation (4), the retained fire-resistance time against enclosure fires is, basically, determined by Equation (5).

$$t_{fr} = \frac{9866}{\alpha^{3/2}}\left\{\frac{2}{h}\left\{\frac{1}{\ln\{h^{1/6}(T_{cr}-20)/1250\}}\right\}^2 + \frac{a_w}{(H_i/A_i)^2}\right\} \qquad (5)$$

where

h : member temperature rise coefficient

H_i: heated perimeter of the covering material (m)

A_i: cross-sectional area of the covering material (m^2)

a_w : temperature rise delay time coefficient stipulated in Table 4

The member temperature rise coefficient, h, is calculated by the following equation.

$$h = \frac{\phi K_0 (H_s/A_s)}{\left\{1+\frac{\phi R}{H_i/A_i}\right\}\left\{1+\frac{\phi C(H_s/A_s)}{2(H_i/A_i)}\right\}} \qquad (6)$$

where

ϕ : heated perimeter ratio calculated by $\phi = H_i/H_s$

H_s: heated perimeter of the member (m)

K_0: basic temperature rise rate stipulated in the following table (m/min.)

Steel category	Basic temperature rise rate
H-shaped steel	0.00089
Rectangular or cylindrical steel pipe	0.00116

A_s: cross-sectional area of the member (m^2)

R : coefficient of thermal resistance in Table 4

C : heat capacity ratio in the following table

Fire protective covering category	Heat capacity ratio
Sprayed rock wool	0.081
Fiber reinforced calcium silicate boards	0.136

Parameters a_w, K_0 and R are determined from a regression analyses based on a variety of heating tests for steel members with fire-protective coverings. The second term in Equation (5) expresses the delay in temperature rise due to the evaporation of water included in the fire-protective covering.

The FRVM also provides equations for structural steel beams that calculate the retained fire-resistance time against enclosure fires having systems similar to that mentioned above for structural steel columns.

3.4 Application of Fire-resistant Steel, Stainless Steel and other High-performance Steel Materials

Current FRVM provides calculation methods that take into account only reductions in the yield strength and elastic coefficient of ordinary steel at elevated temperatures. Accordingly, even when fire-resistant steel and stainless steel having superior properties at elevated temperature than ordinary steel are to be applied, their correspondingly higher performance properties cannot be assessed. To remedy this situation, examinations to improve the current FRVM are underway.

4. CONCLUSIONS

Outline of the FRVM in the BSL is explained through the verification process of protected steel columns. The FRVM is an alternative to the conventional fire-rated construction approach. The verification process is similar to that of wind or seismic design in that the actions and response of structures are evaluated according to particular conditions of the buildings.

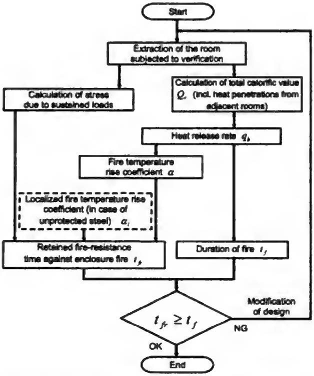
Start
Extraction of the room subjected to verification
Calculation of stress due to sustained loads
Calculation of total calorific value Q_r (incl. heat penetrations from adjacent rooms)
Heat release rate q_b
Fire temperature rise coefficient α
Localized fire temperature rise coefficient (in case of unprotected steel) α_l
Retained fire-resistance time against enclosure fire t_{fr}
Duration of fire t_f
$t_{fr} \geq t_f$
Modification of design
NG
OK
End

Fig.1 Verification Flow of Steel Members for Enclosure Fire under the FRVM

Table 1 Fire Resistance Required for Principal Structural Parts

Required performance	Principal structural parts						
	Exterior wall	Partition wall	Column	Beam	Floor	Stair	Roof
Enclosure fire:							
Load-carrying capacity	R*	R*	R	R	R	R	R
Insulation	--	R	--	--	R	--	--
Integrity	R	--	--	--	--	--	R
Exterior fire:							
Load-carrying capacity	R*	--	--	--	--	--	--
Insulation	R	--	--	--	--	--	--

R: Required, R*: Required in the case of bearing wall, --: Not required

Table 2 Required Fire Resistance Time for Fire-resistive Constructions

Load-carrying capacity:

Parts of buildings		Stories of buildings		
		Uppermost story, and second to fourth stories from the uppermost story	Fifth to fourteenth stories from the uppermost story	Fifteenth story or more from the uppermost story
Walls	Partition walls (limited to bearing walls)	1 hour	2 hours	2 hours
	External walls (limited to bearing walls)	1 hour	2 hours	2 hours
Columns		1 hour	2 hours	3 hours
Floors		1 hour	2 hours	2 hours
Beams		1 hour	2 hours	3 hours
Roofs		30 minutes		
Stairs		30 minutes		

Insulation:

Walls and Floors	1 hour
Parts other than parts liable to catch fire of external walls that are non-bearing walls	30 minutes

Integrity:

External walls	1 hour
Roofs and parts other than parts liable to catch fire of external walls that are non-bearing walls	30 minutes

Table 3 Calorific Value per Unit Floor Area of Combustibles Stored inside a Room

	Room category			Calorific value (MJ/ m^2)
(1)	Habitable room of a dwelling			720
	Bedroom or sickroom in a building other than a dwelling			240
(2)	Office or other room similar thereto			560
	Conference room or other room similar thereto			160
(3)	Classroom			400
	Arena or other room similar thereto in a gymnasium			80
	Exhibition room or other room similar thereto in a museum or art gallery			240
(4)	Salesroom in a department store, store engaged in commodity sales, or other similar thereto	Salesroom selling books or furniture or other room similar thereto		960
		Other parts		480
	Dining facility or other dining rooms	Simple dining room		240
		Other dining room		480
(5)	Theater, movie theater, entertainment hall, grand-stand, public hall, assembly hall, or other room provided for use similar thereto	Seating space	Immovable seating	400
			Other seating	480
		Stage area		240
(6)	Parking garage or automobile repair shop	Parking space or other part similar thereto		240
		Automobile passageway or other part similar thereto		32
(7)	Corridor, stairway, or other passageway			32
	Vestibule, lobby, or other part similar thereto	Those in a building provided for use as a theater, movie theater, entertainment hall, grand-stand, public hall, assembly hall, or other use similar thereto, or as department store, store engaged in commodity sales, or other use similar thereto		160
		Others		80
(8)	Machine rooms of elevators or other equipment			160
(9)	Rooftop plaza or balcony			80
(10)	Storage or other room used to store objects			2,000

Table 4 Temperature Rise Delay Time and Thermal Resistance Coefficients

Fire protective covering category	Steel category	Temperature rise delay time coefficient	Thermal resistance coefficient
Sprayed rock wool (excluding the spray-applied to metal lath method for H-shaped steel)	H-shaped steel	22,000	310
	Square steel pipe or cylindrical steel pipe	19,600	390
Fiber reinforced calcium silicate boards (limited to this made by membrane enclosure)	H-shaped steel	28,300	815
	Square steel pipe or cylindrical steel pipe	32,000	700

Fire Endurance Testing of Floor Systems – Effects of Scale and Restraint

by

John L. Gross[1]

ABSTRACT

Three standard fire resistance tests (ASTM E 119) were conducted on a composite floor system to study the effects of 1) test restraint conditions, and 2) scale of the test. Two full-scale tests, 35 ft[2] (10.7 m) span, and one half-scale test, 17 ft (5.2 m) span, were conducted. Two tests were conducted under restrained conditions and one under unrestrained conditions. Results showed that the full-scale restrained floor system obtained a fire resistance rating of 1½ h, while the full-scale unrestrained floor system achieved a 2 h rating. Past experience with the ASTM E119 test method would lead one to expect that the unrestrained floor assembly would not perform as well as the restrained assembly, and therefore, would receive a lower fire rating. For the full- and half-scale floor systems tested in the restrained condition, the full-scale specimen obtained a fire resistance rating of 1½ h, while the half-scale specimen achieved a 2 h rating. Both tests would be expected to produce the same fire resistance rating.

KEYWORDS: ASTM E119, fire; fire resistance; fire testing; floor systems; standard fire resistance tests; testing

1.0 INTRODUCTION

NIST's World Trade Center (WTC) investigation (NIST, 2005) allowed the opportunity to conduct full- and reduced-scale tests of the floor system used in the WTC towers. These tests duplicated, as closely as practical, the steel truss-supported composite concrete floor system. In practice, a floor assembly such as that used in the WTC towers is neither restrained nor unrestrained but is likely somewhere in between. Testing under both restraint conditions, then, bounds expected performance under the standard fire exposure, and provides a comparison of unrestrained ratings developed from both restrained and unrestrained test conditions. Also, the spans of the WTC floor system were up to 60 ft (18.3m) while furnaces used in establishing fire resistance ratings in the US allow spans of approximately 18 ft (5.5 m). Thus the extrapolation of results of a reduced-scale test may be an issue.

Full-scale tests were conducted in both the restrained and unrestrained support conditions. Further, a roughly one-half scale test of the restrained floor system was also conducted. A description of the WTC floor system, scaling and conduct of the tests, and results (fire resistance ratings) are presented here.

2.0 FIRE RESISTANCE TESTING

The fire rating of structural materials and assemblies is generally determined through testing, and in the values for customary units as the primary units of measure.

---

[1] National Institute of Standards and Technology, Building and Fire Research Laboratory, 100 Bureau Drive, Gaithersburg, MD 20899 USA

[2] The policy of the National Institute of Standards and Technology is to use the International System of Units (metric units) in all its publications. However, in North America in the construction industry, certain non-SI units are so widely used instead of SI units that it is more practical and less confusing to include measurement

United States, such testing is frequently conducted in accordance with ASTM E 119, "Standard Test Methods for Fire Tests of Building Construction and Materials" (ASTM, 2000). This standard was first published in 1917 as a tentative standard ASTM C 19 and was first adopted as ASTM E 119 in 1933. Since its introduction, the test method has been modified and updated, although its essential character has remained unchanged. The test methods described in ASTM E 119 prescribe a standard fire exposure for comparing the test results of building construction assemblies. For the tests of floors and roofs, a test assembly is structurally loaded and the standard fire exposure is applied to the underside of the specimen. The assembly is evaluated for its ability to contain the fire by limiting flame spread and heating of the unexposed surface while maintaining the applied load. The assembly is given a rating, expressed in hours, based on these conditions of acceptance.

Since 1971, versions of the ASTM E 119 Standard differentiate between testing and classifying thermally restrained and unrestrained floor assemblies. According to Appendix A4 of ASTM E 119-73 (ASTM, 1973), a restrained condition is "one in which expansion at the support of a load carrying element resulting from the effects of fire is resisted by forces external to the element." In an unrestrained condition, the element is free to expand and rotate at its supports. It is customary in the United States to conduct standard fire tests of floor assemblies in the restrained condition.

The current standard describes a means to establish restrained and unrestrained ratings for floor assemblies from restrained test samples. For restrained ratings from restrained test samples, the conditions of acceptance are based on limiting flame spread, limiting temperatures on the unexposed surface of the slab, and failure of the assembly to sustain the applied load. For an unrestrained rating determined from a restrained test sample, the conditions of acceptance are based on the same criteria and, in addition, temperature limitations are placed on the main structural members.

In addition, since 1971, the ASTM E 119 Standard describes a means to establish unrestrained ratings from unrestrained test samples. For unrestrained samples, the fire resistance rating is again based on limiting flame spread, exceeding temperatures on the unexposed surface of the slab, and failure to sustain the applied load; there are no limiting temperatures on the steel structural members when the test sample is installed in an unrestrained condition.

3.0 CONDUCT OF TESTS

The floor system design consisted of a lightweight concrete floor slab supported by steel trusses. The main composite trusses were spaced at 6 ft - 8 in. (2.0 m) on center (o.c.) and had a nominal clear span of either 35 ft (10.7 m) or 60 ft (18.3 m). The steel trusses were fabricated using double-angles for the top and bottom chords, and round bars for the webs. The web members protruded above the top chord in the form of a "knuckle" which was embedded in the concrete slab to develop composite action. Additionally, the floor system included bridging trusses (perpendicular to main trusses) spaced 13 ft - 4 in. (4.0 m) o.c. Figure 1 is a cutaway of the composite floor system showing the main and bridging trusses, metal deck and concrete slab.

3.1 Test variables

NIST studied two factors, the effect of (1) scale of the test, and (2) test restraint conditions. To this end, three tests were designed and conducted as follows:

Test #1: Full-scale, restrained test condition
Test #2: Full-scale, unrestrained test condition
Test #3: Reduced-scale, restrained conditions

3.2 Preparation of Test Assemblies

Original shop drawings by Laclede Steel[3] (manufacturer of the steel trusses) were used for the design of the 35 ft (10.7 m) span and 17 ft (5.3 m) span test assemblies. The steel trusses faithfully duplicated the geometry of the original design. Since equipment for making the resistance welds is not available in the United States, metal inert gas (MIG) welding was used and the welds were designed per American Institute of Steel Construction (AISC) Specification (AISC, 2001) to develop the web diagonal capacities in tension or compression. This requirement was based on available test data indicating that weld capacities exceeded proof loads by a factor in excess of 2.0. In addition, the steel angles and round bars, reinforcing steel, welded wire fabric, metal deck, lightweight concrete, and primer paint were all matched as closely as practical. Sprayed Fire Resistant Material (SFRM) was applied to the steel trusses at a specified thickness of 0.75 in (19 mm).

3.3 Description of Tests and Loading

3.3.1 Full-scale Tests - 35 ft (10.7 m) span

The full-scale tests were conducted at the Underwriters Laboratories (UL) furnace facility in Toronto, Canada. Loading of the floor slab with an applied load to "simulate a maximum load condition" as required by ASTM E 119, was accomplished through a combination concrete block and water-filled containers which were tied off to prevent them from damaging the fire brick and instrumentation in the event of a catastrophic failure of the floor system.

3.3.2 Reduced-scale Test - 17 ft (5.2 m) span

For the reduced-scale test specimens, the size of the truss members and thickness of concrete slab were selected to allow the most information to be extracted as practicably possible considering the Standard Fire Resistance Test is a test of the assembly's ability to contain a fire and is based on both thermal response (flame spread and heating of the unexposed surface) and structural response (support the applied load) to the standard fire. The sizes of the steel members, thickness of concrete slab, and truss spacing were selected to be the same as in the full-scale tests. Otherwise, the geometry was scaled by roughly half. This scaling required that the loading be increased by a factor of 2.

The reduced-scale tests were conducted at the UL furnace facility in Northbrook, Illinois. The superimposed uniform load was applied through a combination of concrete blocks, water-filled containers and hydraulic actuators located along the trusses.

4.0 TEST RESULTS

As noted above, prior to 1971, the ASTM E 119 Standard did not differentiate between testing and classifying thermally restrained and unrestrained floor assemblies. The 1961 revision of ASTM E 119, the revision referenced in the 1968 New York City Building Code, is used here for reporting the Standard Fire Test ratings. Using this revision, a single rating is developed. The year 2000 revision of the Standard is used here for reporting restrained and unrestrained ratings.

A photograph of the underside of the full-scale, restrained test specimen after almost 2 h of exposure is shown in Figure 2. Buckling of the compression diagonals can be seen as well as bowing of the metal deck between supports. Upon cooling, the test specimen recovered at least half of the deflection achieved during the test. Sectioning of the slab revealed that the bowing resulted from spalling of the concrete.

---

[3] Certain trade names and company products are mentioned in the text or identified in an illustration in order to adequately specify the experimental procedure and equipment used. In no case does such an identification imply recommendation or endorsement by the National Institute of Standards and Technology, nor does it imply that the products are necessarily the best available for the purpose.

Table 1 shows results for all three tests giving the times (in minutes) to reach the conditions of acceptance, and the Standard Fire Test rating (in hours) for both the 1961 and 2000 revisions of ASTM E119[4]. Note that in none of the tests did the floor assembly fail to support the applied load. Several observations can be made from the results (ratings) shown in Table 1 as follows:

- The restrained full-scale floor system obtained a fire resistance rating of 1½ h while the unrestrained floor system achieved a 2 h rating. Past experience with the ASTM E119 test method would lead one to expect that the unrestrained floor assembly would receive a lower fire rating.
- A fire rating of 2 h was determined from the reduced-scale test while a fire rating of 1½ h was determined from the full-scale test.
- The above result raises the question of whether or not a fire rating based on the ASTM E119 performance of a 17 ft (5.2 m) span floor assembly is scalable to a larger floor system of, say, up to 60 ft (18.3 m).

5. OBSERVATIONS AND CONCLUSIONS

The tested floor assemblies are similar, though not identical, to steel joist and concrete floor systems that are widely used in low rise construction. The test results provide valuable insight into the behavior of these widely used assemblies and also identify issues regarding scaling and restraint that require further study for floor systems and possibly other types of structural component.

The tests show temperature damage to the bridging trusses and buckling (in the full scale tests) of compression diagonals and the vertical strut near the supports. No evidence of knuckle failures was seen in the tests.

The ASTM E 119 standard test method has been used for several decades and has, for the most part, served its intended purpose well when taken together with the fire rating requirements. This is supported by historical fire loss data for more than half a century for different high-rise building occupancies. In addition, there are extensive data and experience that have been developed using the test method.

The NIST tests have identified areas where further study related to the standard test method may be warranted. The issues related to the test method that NIST will consider in formulating its recommendations include:

- the scale of the test for prototype assemblies that are much larger than the tested assemblies,
- the effect of restraint conditions on test results,
- the repeatability of test results (e.g., do multiple fire resistance tests conducted under the same conditions yield the same results?),
- the acceptance criteria to evaluate the load carrying capacity of the tested assemblies (currently tests are stopped before the load carrying capacity of the assembly is reached because other acceptance criteria are met or because the deflection becomes excessive and assembly failure could damage the furnace).

---

[4] ASTM E 119 contains the following statement regarding precision and bias: No comprehensive test program has been conducted to develop data on which to derive statistical measures of repeatability (within-laboratory variability) and reproducibility (among-laboratory variability). The limited data indicate that there is a degree of repeatability and reproducibility for some types of assemblies. Results depend on factors such as the type of assembly and materials being tested, the characteristics of the furnace, the type and level of applied load, the nature of the boundary conditions (restraint and end fixity), and details of workmanship during assembly.

REFERENCES

American Institute of Steel Construction (AISC) (2001). Manual of Steel Construction: Load and Resistance Factor Design, 3rd Edition, Chicago, Il.

ASTM (2000). "Standard Test Methods for Fire Tests of Building Construction and Materials," ASTM E 119-00, ASTM International, Conshohocken, Pa.

ASTM (1973). "Standard Test Methods for Fire Tests of Building Construction and Materials," ASTM E 119-73, ASTM International, Conshohocken, Pa.

Beitel, J, and Iwankiw, N. (2002). "Analysis of Needs and Existing Capabilities for Full-Scale Fire Resistance Testing," NIST GCR 02-843, National Institute of Standards and Technology, Gaithersburg, Md.

NIST (2005). *Federal Building and Fire Safety Investigation of the World Trade Center Disaster: Final Report on the Collapse of the World Trade Center Towers*. NIST NCSTAR 1. Gaithersburg, MD, September

Table 1. Results of ASTM E119 Standard Fire Tests

Test	Description	Times to Reach Conditions of Acceptance (min)				Failure to Sup-port Load	Test Termin-ated (min)	Standard Fire Test Rating (h)		
		Temperature on Unexposed Surface		Steel Temperatures				ASTM E 119-61	ASTM E119-00	
		Average Temp Ambient+ 250 °F (121°C)	Maximum Temp Ambient+ 325 °F (163 °C)	Average Temp 1100 °F (593 °C)	Maximum Temp 1300 °F (704 °C)			Rating	Restr-ained Rating	Unrestr-ained Rating
1	35 ft (10.7 m), restrained	—	111	66	62	(3)	116(1)	1 ½	1 ½	1
2	35 ft (10.7 m), unrestrained	—	—	76	62	(3)	146(2)	2	—	2
3	17 ft (5.3 m), restrained	180	157	86	76	(3)	210(2)	2	2	1

(1) Imminent collapse
(2) Vertical displacement exceeded capability to measure accurately
(3) Did not occur

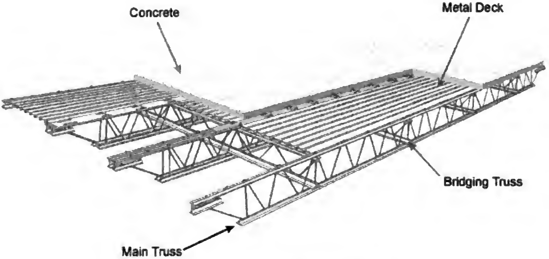

Figure 1. Floor system tested

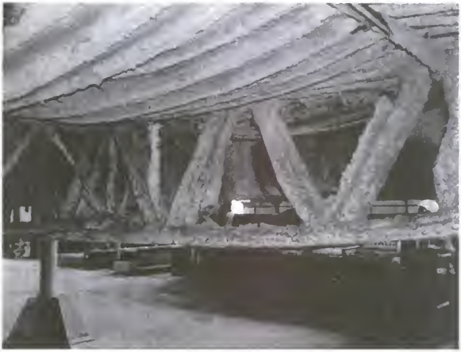

Figure 2. Buckled truss webs and bowed metal deck

A Study on the Collapse Control Design Method for High-rise Steel Buildings

by

Akira Wada [1], Kenichi Ohi [2], Hiroyuki Suzuki [3],
Mamoru Kohno [4] and Yoshifumi Sakumoto [5]

ABSTRACT

Two direct causes led to the collapse on September 11, 2001 of the World Trade Center towers: column damage caused by aircraft crash and the resulting large-scale fires. In spite of this damage, the towers remained standing after the crashes for 102 and 56 minutes, respectively, during which many lives were saved. The collapse of the WTC towers, however, may be taken as an alert that local failures can trigger a progressive collapse. It was also a landmark event in that it alerted construction engineers to the importance of preventing progressive collapse in similar structures.

Prevention of progressive collapse requires the development of design technologies for frames that have high redundancy. The Japan Iron and Steel Federation together with the Japanese Society of Steel Construction established the committee on "The Study on Redundancy of High-Rise Steel Buildings" in June 2002 in an attempt to study and provide a better understanding on progressive collapse by collaboration with Council on Tall Buildings & Urban Habitat. This paper presents a new collapse control design method for high-rise steel building structures. The basic concept of the present collapse control design methods is to save human lives. Therefore, the method presented here to prevent progressive collapse until the completion of evacuation makes assumptions about which structural members are likely to be lost and proposes the idea of 'key elements' that are linked with a building's core section to serve as the evacuation route and consist of structural members indispensable for supporting redistributed vertical loads.

KEYWORDS: Collapse Control Design, Key Element, Progressive Collapse

1. INTRODUCTION

The collapse of the World Trade Center towers (WTC1 and WTC2) was the direct result of column damage and large-scale fires caused by airplane crashes. In spite of this, WTC1 and WTC2 remained standing for 102 minutes and 56 minutes respectively, during which many lives were saved. The fact that so many lives were saved is reportedly due to the large deformation capacity or load redistribution capacity inherent in steel structures [1]. From this, it can be understood that the tower structures of the World Trade Center (hereinafter referred to as "WTC") had a certain degree of redundancy. Nevertheless, the WTC collapse serves as a warning about progressive collapse triggered by a local collapse that causes an entire building collapse. It was a landmark event that alerted construction engineers to the importance of preventing progressive collapse in other similar buildings.

The British Standards and Building Standards [2] were the first to incorporate the prevention of progressive collapse in design standards. The incorporation of measures against progressive collapse was based on proving through experience and was made to prevent the kind of progressive collapse attributed to a gas explosion in 1968 in a 22-story high-rise residential building in Ronan Point, United Kingdom. Further, in the Building Standards of

---

[1] Professor, Tokyo Institute of Technology, Ookayama 2-12-1, Meguro, Tokyo 152-8550, Japan

[2] Professor, Kobe University, Rokkodai-machi 2-1, Nada, Kobe 657-8501, Japan

[3] Professor, University of Tsukuba, Tenodai 1-1-1, Tsukuba 305-8573, Japan

[4] Head, Fire Standards Division, Building Department, National Institute for Land and Infrastructure Management (NILIM), Tsukuba 305-0802, Japan

[5] General Manager, Nippon Steel Corporation, Otemachi 2-6-3, Chiyoda, Tokyo 100-8071, Japan

New York City (NYC Standards) established in February 2003, the following recommendation was made regarding the prevention of progressive collapse such as that seen in the WTC collapse.

"Recommendation 1: Publish structural design guidelines for optional application to ensure robustness and resistance to progressive collapse."

Meanwhile, studies are now underway along with extensive discussions in a variety of related fields regarding the development of a simple, practical design method. In order to suppress progressive collapse, it is necessary to develop a technology for designing frames with high redundancy. With this in mind, the Japan Iron and Steel Federation established the Committee to Study the Redundancy of High-Rise Steel Buildings within the Japanese Society of Steel Construction; this committee has carried out the following studies aimed at improving the safety of high-rise buildings:

- A study of collapse control design methods based on seismic- and fire-resistant technologies used in Japan, and
- A study to quantify the redundancy of high-rise steel buildings in Japan aimed at producing a frame with high redundancy.

In this paper, findings obtained from the collapse of the WTC are described and a method to prevent progressive collapse is examined. Further, a collapse control design method that can prevent the occurrence of progressive collapse is outlined.

2. FINDINGS FROM WTC COLLAPSE

In order to structure a progressive collapse control design method for high-rise buildings with higher redundancy, the Committee to Study the Redundancy of High-Rise Steel Buildings organized the causes of the WTC collapse with reference to the available literature [1] and then outlined its findings. Fig. 1 shows the study results for the cause of the WTC collapse. From this figure, it is understood that in cases where vertical load supporting members are lost due to unexpected loads or to accident and where vertical load supporting members lose functionality due to large-scale fire, it is important to provide measures whereby local collapse does not lead to entire collapse. To achieve this goal, it is necessary to increase vertical load redistribution capacity by providing back-up systems for multiplying the number of loading routes, as shown in Table 1. Further, it is necessary to secure the plastic deformation capacity and fire resistance of individual steel members and joints between them.

High-rise steel buildings constructed in Japan using seismic-resistant design have surplus capacity vis-à-vis stationary vertical loads and employ connections with appropriate load-bearing capacity for the joints. Because of this, it is believed that vertical load redistribution capacity can be increased with minimal added cost. Further, as stated in the following, the application of SN steel (low yield-point high performance steel), fire-resistant (FR) steel and concrete-filled steel tube (CFT) structures facilitates improved plastic deformation capacity in remaining members when some columns are lost and during fire.

3. ASSESSMENT METHOD

3.1 Setting Targets

Fig. 2 shows the difference between the concepts employed in the present collapse control design (right) and those found in conventional structural and fire-resistant designs (left).

Generally, it is difficult and uneconomical to conduct structural design by assuming accidental loads due to extreme events. Accordingly, in contrast to conventional methods, the present design method assesses and improves the redundancy of buildings by assuming the loss of structural members such as columns and beams due to accidents and assessing how many members might be lost and the probability of entire collapse occurring.

Because it is fair to expect that fire separations will break and that fire will spread not only horizontally but also vertically, it is necessary when estimating member loss to pay attention to the effect (increasing the degree of loss) that fire will have.

Based on the above, designers discuss whether or not a structure is designed both in terms of structure and fire resistance to compensate for the loss of members and whether or not collapse control design is to be applied. When collapse control design is used, the key-element members are specified in the frame design according to an assessment flow as described in the next section. Priority is given to protecting the key-element members so as to improve building redundancy.

3.2 Assessment Flow

Fig. 3 shows an outline of assessment flow. In the following, the present collapse control design method is explained in terms of assessment flow.

3.2.1 Assessing Risk and Judging Whether or Not to Use Collapse Control Design

When considering the probability of explosions and airplane crashes caused by terrorist attack, it is not always reasonable to incorporate the effects of such unexpected loads into an original design. Further, such a design approach offers the possibility of exceeding the allowable economic limits. It is also difficult to forecast the behavior of structural members and frames to accidental loads and to reflect the structural response in the design work commonly being undertaken.

In the present design method, the effect of unexpected loads caused by terrorist explosions and aircraft crashes is not assessed directly. Rather, losses or declines in the yield strength of vertical load supporting members that are brought about by the application of unexpected loads are assessed and are reflected in the design work.

Based on the concept that improving the redundancy of buildings minimizes the risk of a progressive collapse, the present design method aims to compensate for loss or decline in the yield strength of members that support vertical loads. In the initial design stage, structural designers judge whether or not to apply the collapse control design method, taking into account the risk of explosions and airplane crashes in the building under consideration. Buildings exposed to limited risks may not require a collapse control design method; only a conventional design method will be selected in these cases.

Further at this stage of design, the potential scale of column member loss is assumed by taking into account the degree of risk involved and the importance of the building, i.e. the effect it would have in the case of collapse. The British Standards and Building Standards [2] prescribe the prevention of progressive collapse even in the case of one column being lost. In cases when the design of a building requires more appropriate redundancy, it is desirable to determine the number of columns to be lost in the design. More practical determination of the members to be lost can be made after fixing the sectional dimensions of the members by means of conventional structural and fire-resistant design methods.

3.2.2 Basic Design

The basic design work takes into account the scale of the members to be lost. At this stage, it is important to proceed with the design work in collaboration with structural engineers and architects, as well as fire-resistant design engineers. Although conventional design work assumes cooperation between structural engineers and architects and between architects and fire-resistant design engineers, adequate cooperation between structural engineers and fire-resistant design engineers has been lacking. More practically, because the arrangement of the core by architects and the selection of the frame system and the arrangement of columns by structural engineers are deeply related to the arrangement of fire separations and the selection of fire protection, the present design method requires that the design work be carried forward by accepting suggestions offered by fire-resistant design engineers.

In order to enhance the redundancy of high-rise buildings, it is important to secure vertical evacuation routes or to arrange the core and safeguard the core inside. Fig. 4 shows a typical core arrangement. It is desirable to distribute and symmetrically arrange stairway locations so as to raise the probability of being able to secure evacuation routes. It is understandable that well arranged cores offer higher redundancy. Further, it is desirable to construct the fire separation with materials having excellent impact resistance and fire resistance in order to prevent fire from spreading into the core section.

During basic design, the selection of the frame system parallels the arrangement of the core. Fig. 5 shows frame deformation after the loss of three columns on the 1st floor in various frame systems (identical cross sections for all columns and beams) [3]. In the analysis, the vertical load is applied so that the axial force ratio becomes 0.35. As shown in the figure, in cases with the functional loss of three columns (except for the moment resistant frame structure), the frame does not suffer entire collapse although it does experience local collapse on certain floors. This shows that braces installed to provide resistance against wind and seismic loads are effective in redistributing vertical loads. To this end, it is desirable to select a frame system that will have a high load redistribution capacity after the functional loss of vertical load supporting members.

3.2.3 Selection of Members to Be Lost and Key Elements

After completion of the basic design, the cross section of the members is decided in conformity with conventional structural and fire-resistant design. In the present design method, the concept of key elements is adopted as a means to improve cost-effective redundancy in a manner that conforms to British Standards and Building Standards [2].

When the cross section of the members is decided in conformity with conventional structural design, the members to be lost are determined and the key elements are selected. The members to be lost are determined taking into account the scale of a potential explosion and the risks involved. At this stage, the key elements can be excluded from the members to be lost on the premise that they will be reasonably safe because they are protected with every available measure. In the present collapse control design method, the determination of key elements is cited as an important requirement. The key elements are those members whose loss directly affects the risk of a chain-reaction collapse; the specifications of fire protection etc. of the key element are to be determined so as to secure the greatest possible safety against extreme actions.

According to the analytical results in Fig. 6 [3] and the analyses in References [3] and [4], it is known that the loss of corner columns is the greatest cause of reducing vertical load supporting capacity. Accordingly, it is desirable to set the corner columns as key elements and to adopt for them methods and materials conducive to improving redundancy, such as FR steel, CFTs and the blanket-type fire protection introduced below. In selecting the key elements, they are to be arranged in a concentrated manner—such as selecting only corner columns, providing the chosen columns with sufficient excess strength (lower axial force ratio of columns) so that they alone could support the loads on all floors, or possibly selecting every third column as a key element.

In setting the key elements, it may be effective to use the sensitivity analysis in Reference [6]. However, this method of analysis has not reached the point where it is always applied in conventional design work. Advances in simple analysis programs and other developments are expected in this field.

3.2.4 Prevention of Chain-reaction Collapse

After setting the key elements, an assessment regarding the prevention of chain-reaction collapse is made. There are three assessment methods: assessment using only the axial force ratio of columns, simple assessment and detailed assessment.

1) Assessment using only the axial force ratio of columns

When conducting an assessment that uses only the axial force ratio of columns, a check is made of axial force ratio of columns at the earliest stage when the loss of vertical load supporting members is not taken into account; this is done to improve qualitative safety. It is known from the analyses in References [4] and [5] that the use of the axial force ratio of columns during stationary vertical loading is effective as a simple assessment method for preventing chain-reaction collapse. When vertical load supporting members are lost, the vertical load is redistributed to other vertical load supporting members via beams, outrigger trusses and hat braces. Generally, these members are arranged in designs as wind- and seismic-resistant members, but when vertical load supporting members are lost, they function as vertical load redistribution members. In cases where a certain surplus exists in the working axial force ratio of columns, these members have a surplus capacity for supporting redistributed vertical loads. Accordingly, improvements in redundancy are enhanced by setting a critical value for the axial force ratio and suppressing the maximum value of the axial force ratio of columns, n_{max}, to a level below the limiting value.

$$n_{max} < n_{limit} \tag{1}$$

In this paper, the limiting value $n_{limit} = 0.25$ is proposed, based on the analytical results in [3] and [4].

2) Simple assessment

Simple assessment is a method to check the load redistribution capacity of columns and beams at the moment when vertical load supporting members are lost.

First, a simple check is made of the vertical load redistribution capacity of the beam shown in Fig. 7; when needed, vertical load redistribution members are arranged. The vertical load redistribution capacity is checked with the following equation [4].

$$\sum_{j=1}^{n} P_j < \sum_{i=1}^{N} \frac{{}_{b}M_{pi}}{L} \tag{2}$$

The left-hand side indicates the total sum of axial forces supported by the lost columns and the right-hand side the total sum of share capacity of the adjoining beams. In cases when the above equation is not satisfied, vertical load redistribution members such as outrigger braces and hat braces are provided to compensate for the shortage of the beam capacity.

Next, the total axial force borne by the columns assumed to be lost is redistributed evenly to the adjoining two columns as shown in Fig. 8; the axial force ratio thus obtained is checked by the following equation.

$$n_r \le n_{r\text{-}limit} = 1.0 \tag{3}$$

3) Detailed assessment

Further, in cases when a detailed assessment is to be conducted, members such as columns are removed and a static incremental analysis of planar or three-dimensional frames is carried out following the simple assessment. In cases involving more complex frames etc., a detailed analysis is conducted depending on the judgment of the designers. For more detail, the readers should refer to [4] and [5].

3.2.5. Protection and the Detail Design of Key Elements

Due care is paid to protect the key elements so that they are not lost even in extreme events. Further, it is desirable to adopt materials and methods (such as FR steel, CFTs and blanket-type fire protection) for the key elements that enhance redundancy in the sections where they are located.

The detail design stage includes the design of beam-column connections, the design of floor systems, the design of fire separations and connection details, and the determination of fire protection specifications. As stated above, in order to meet emergency conditions that arise because of the loss of structural members, adopting connections with sufficient load-carrying capacity for joining beams to columns and columns to columns is important element in securing the deformation capacity of members, realizing the integration of floor systems and ensuring the fire resistance of key elements.

4. MATERIALS AND METHODS EFFECTIVE IN PROTECTING KEY ELEMENTS

Finally, brief descriptions are given of FR steel and unprotected CFT structures—representative materials and methods effective in protecting key elements—and of fire protection that offers excellent impact resistance.

Fig. 9 shows the temperature-induced transition in yield strength of FR steel and general steel. FR steel retains more than 2/3 of its specified yield strength at room temperatures until 600 °C is exceeded; therefore, its application is effective in retaining the load supporting capacity of beams and columns during large-scale fires. Fig. 10 shows the results of loaded fire-resistance tests for unprotected CFT (Fig. 11). The figure clearly indicates that in cases of axial force ratios at 0.25 or under, unprotected CFT structures can withstand loading for more than 3 hours. A blanket-type fire protection, as is in Photo 1, generally has higher impact resistance than spray-type or dry board-type fire protections and also provides effective protection against explosions.

5. CONCLUSIONS

Findings obtained from the WTC collapse and measures to prevent progressive collapse were examined and a collapse control design method was proposed. The present design method aims at increasing the redundancy of buildings by making assumptions regarding the loss of structural members and assessing the possibility of an entire collapse occurring.

"Guidelines for Collapse Control Design" (Japanese and English versions) were published in two volumes [7, 8] and supplementary volume (English version only) [9] by the collaborative effort of The Japan Iron and Steel Federation and Council on Tall Buildings & Urban Habitat.

6. REFERENCES

1. FEMA: *World Trade Center Building Performance Study*, FEMA 403, 2002.
2. British Standards and Building Standards; BS5950: Part 1, 1990.
3. Suzuki, I., Wada, A., Ohi, K., Sakumoto, Y., Fusimi, M. and Kamura, H.; Study on High-rise Steel Building Structure That Excels in Redundancy, Part II Evaluation of Redundancy Considering Heat Induced by Fire and Loss of Vertical Load Resistant Members, *Proc. CIB-CTBUH International Conf. on Tall Buildings*, pp. 251-259, 2003.
4. Murakami, Y., Fushimi, M. and Suzuki, H.; Thermal Deformation Analysis of High-rise Steel Buildings, *Proc. of the CTBUH Seoul International Conf. on Tall Buildings*, 2004.
5. Sasaki, M., Keii, M., Yoshikai, S. and Kamura, H.; Analytical Study of High-rise Steel Buildings in Case of Loss of Columns, *Proc. of the CTBUH Seoul International Conf. on Tall Buildings*, 2004.
6. Ohi, K., Ito, T. and Li, Z.; Sensitivity on Load Carrying Capacity of Frames to Member Disappearance, *Proc. of the CTBUH Seoul International Conf. on Tall Buildings*, 2004.
7. Japanese Society of Steel Construction & Council on Tall Building and Urban Habitat: *Guidelines for Collapse Control Design –Construction of Steel Buildings with High Redundancy–, Vol. 1 Design*, 2005.
8. Japanese Society of Steel Construction & Council on Tall Building and Urban Habitat: *Guidelines for Collapse Control Design –Construction of Steel Buildings with High Redundancy–, Vol. 2 Research*, 2005.
9. Japanese Society of Steel Construction & Council on Tall Building and Urban Habitat: *Guidelines for Collapse Control Design, Supplement Volume –Materials and Methods Effective in Enhancing Redundancy–, High-performance Steel Products for Building Construction*, 2005.

Table 1 Measures to Prevent Progressive Collapse

- Increase of load transfer (and evacuation) routes·
- Increase of load redistribution capacity·
- Securement of plastic deformation capacity (members and materials)·
- Increase of connection strength (connection with load-carrying capacity)·
- Selection of fire protection materials·
- Securement of fire resistance of structural members proper (members and materials)

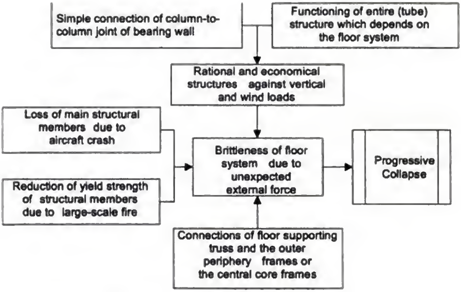
Simple connection of column-to-column joint of bearing wall
Functioning of entire (tube) structure which depends on the floor system
Rational and economical structures against vertical and wind loads
Loss of main structural members due to aircraft crash
Reduction of yield strength of structural members due to large-scale fire
Brittleness of floor system due to unexpected external force
Progressive Collapse
Connections of floor supporting truss and the outer periphery frames or the central core frames

Fig. 1 Analysis of Causes of WTC Collapse

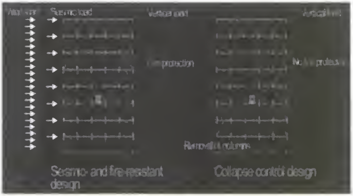

Fig. 2 Image of Collapse Control Design

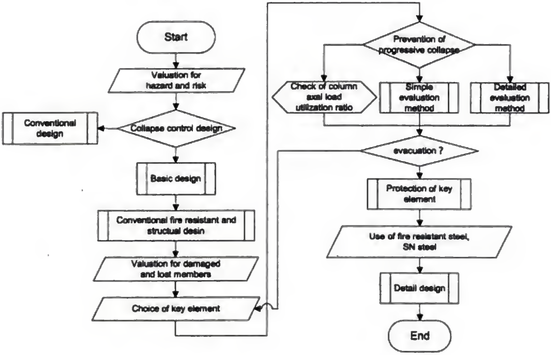
Start
Valuation for hazard and risk
Conventional design
Collapse control design
Basic design
Conventional fire resistant and structual desin
Valuation for damaged and lost members
Choice of key element
Prevention of progressive collapse
Check of column axial load utilization ratio
Simple evaluation method
Detailed evaluation method
evacuation ?
Protection of key element
Use of fire resistant steel, SN steel
Detail design
End

Fig. 3 Outline of Recommended Flow of Collapse Control Design

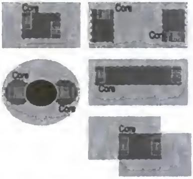

Fig. 4 Typical Core Arrangement

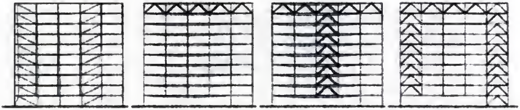

(a) MRF (b) MRF with hat-bracing (c) MRF with hat -and-core bracing (d) Super frame

Fig. 5 Analysis Results for Various Frame Systems at Time of Column Loss

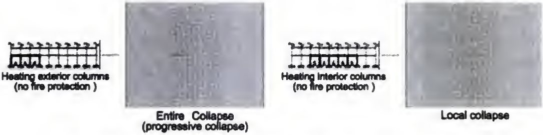

Fig. 6 Analysis Results for Thermal Elasto-Plasticity and Buckling during Fire

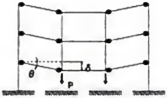

Fig. 7 Simple Assessment of the Vertical Load Supporting Capacity of Beams

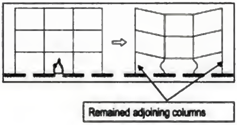

Fig. 8 Assessment of the Loading Capacity of Remaining Adjacent Columns

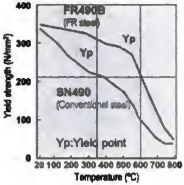

Fig. 9 Transition in Yield Strength of FR Steel and General Steel due to Temperature

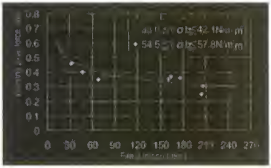

Fig. 10 Heated Loading Test Results for Unprotected CFT Column

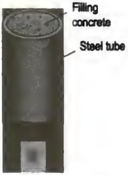

Fig. 11. Unprotected CFT Column

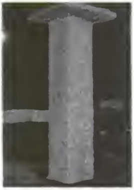

Photo 1. Blanket-type Fire Protection

Committee to Study the Redundancy of High-rise Steel Buildings

- Chairman
  - Akira Wada, Tokyo Institute of Technology
- Leader (Structure WG)
  - Kenichi Ooi, The University of Tokyo (currently Kobe University)
- Leader (Fire Resistance WG)
  - Hiroyuki Suzuki, The University of Tsukuba
- Members
  - Mitsumasa Fushimi, Nippon Steel Corporation
  - Kazunari Fujiwara, Kobe Steel, Ltd.
  - Takashi Hasegawa, National Institute for Land and Infrastructure Management (currently Building Research Institute)
  - Kenichi Ikeda, Shimizu Corporation
  - Hisaya Kamura, JFE R&D Corporation
  - Hiroki Kawai, ABS Consulting
  - Michio Keii, NIKKEN SEKKEI Ltd.
  - Isao Kimura, Nippon Steel Corporation
  - Mamoru Kohno, Building Research Institute (currently National Institute for Land and Infrastructure Management)
  - Yukio Murakami, JFE Steel Corporation
  - Tadao Nakagome, Shinshu University
  - Isao Nishiyama, Building Research Institute (currently National Institute for Land and Infrastructure Management)
  - Taro Nishigaki, Taisei Corporation
  - Masamichi Sasaki, Sumitomo Metal Industries, Ltd.
  - Mutsuo Sasaki, Nagoya University
  - Takeshi Takada, Kobe Steel, Ltd.
  - Shigeru Yoshikai, Kajima Corporation

CTBUH Task Group for Guidelines

- Members
  - Ron Klemencic, President, Magnusson Klemencic Associates
  - Hal Iyengar, (Retired) Partner Skidmore, Owings & Merrill
  - Robert Solomon, Assistant Vice President for Building and Life Safety Codes, National Fire Protection Association
  - Richard Bukowski, Senior Engineer, Building and Fire Research Laboratory, National Institute of Science and Technology
  - Dr. John M. Hanson, President, Hanson Consulting Associates
  - Dr. John W. Fisher, Professor, Emeritus of Civil Engineering, Lehigh University
  - Dr. Edward (Xiaoxuan) Qi, Associate Principal

Coordinators

Yoshifumi Sakumoto, Nippon Steel Corporation
Roger Wildt, P.E., RW Consulting Group

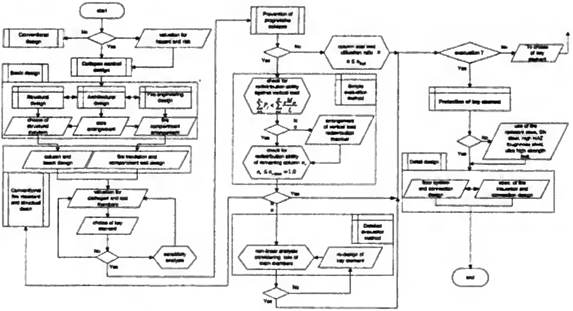
start
No
Yes
Conventional design
valuation for hazard and risk
Collapse control design
Basic design
Structural design
Architectural design
Fire engineering design
choice of structural system
core arrangement
fire compartment arrangement
column and beam design
fire insulation and compartment wall design
Conventional fire resistant and structural design
valuation for damaged and lost members
choice of key element
sensitivity analysis
Prevention of progressive collapse
Simple evaluation method
Detailed evaluation method
re-design of key element
evacuation ?
Protection of key element
Detail design
end

Fig. 12 Flow of Collapse Control Design (Detail)

The Need for International Collaboration on Structural Fire Endurance Research

by

William L. Grosshandler and Kuldeep Prasad[1]

ABSTRACT

A concerted effort is required to accelerate the development of the engineering tools needed to support the ambitious goal of scientifically-based performance predictions of building materials, products, structural elements, and systems up to the point of imminent fire-caused collapse. This paper reviews the general state of fire/structure test methods and models, identifies the research needed to move building fire codes and standards to a performance basis, and makes the case for the establishment of an international structural fire endurance laboratory as an essential component of this effort.

KEYWORDS: structural fire endurance, testing, fire resistance, research

1.0 INTRODUCTION

Societies dictate that buildings and other structures used routinely by civilian populations need to withstand severe, but anticipated, natural and manmade hazardous events, including earthquakes, wind storms, floods, heavy snows, and fires. The degree of severity anticipated is a choice made at the local, regional or federal government level, depending upon the country. A reliable data base has been established in the U.S. and Japan on the occurrence and severity of natural hazards; however, setting the severity level for manmade fires (accidental or intentional) is complicated by three factors: the historical data base on structural fires is sparsely populated and/or unreliable, extrapolation of historical data to future events is highly uncertain due to changes in human activities, and almost all fires have the potential of being severe given the right set of circumstances that may be out of the control of the building designer.

This article provides a glimpse into how society approaches structural fire safety, its reliance on prescriptive approaches to fire resistance design, the current level of understanding of how structures behave in fires, and the identification of research needed to move building fire codes and standards to a performance basis. Progress hinges on our ability to establish an international structural fire endurance research facility.

2.0 PERSPECTIVE

The enormity of the loss of life and the economic impact caused by the destruction at the World Trade Center (WTC) in New York on September 11, 2001, has caused many jurisdictions to reconsider the degree of severity of a fire that might be anticipated, and has highlighted for the engineering community the need to better understand the technical issues associated with the buildings that collapsed that day, as well as the likely performance of other buildings under severe fire conditions.

Assuming that a level of severity can be established by the appropriate authority having jurisdiction, the challenge for the engineer is to translate a specified fire scenario into heat fluxes onto the boundaries of the structure, into heat fluxes through building lining materials and structural insulation, into temperatures and temperature gradients within the structural elements, into thermal degradation (including phase changes and chemical reactions) and breaching of building partitions, into thermally-induced strain of the load bearing elements (including thermal expansion, and elastic, plastic, and creep strains), into redistribution of the loads, into mechanical failure of individual components, and eventually into local or global collapse.

---

[1] Fire Research Division, Building and Fire Research Laboratory, National Institute of Standards and Technology, Gaithersburg, Maryland, 20899-8660, USA

Significant progress has been made in understanding many of the above phenomena, but the time scales and length scales associated with the different processes span a range so large that we are restricted in our ability to model with any certainty the true performance of the whole structure to the imposed fire. To circumvent the difficulty of predicting the performance of the structure under fire conditions, engineers and building code officials have relied upon furnace tests of individual structural elements or structural assemblies to rate one design against another, based upon the amount of time the element or assembly can survive the furnace environment before failing.

3.0 STANDARD TEST METHOD

The predecessor to the current standard fire resistance test for loaded and unloaded structural elements, ASTM E119 (ASTM 200a), was originally released in the U.S. in 1918. While a number of revisions were made to the standard throughout the twentieth century (refer to Grosshandler (2006) for a more complete review of the development of these furnace tests over the past 100 years), the prescriptive nature for the test method remains unaltered, in spite of changing fire loads and significant advances in our knowledge of fire and structural behavior. As early as the 1950s the engineering community was beginning to understand a number of situations that caused the standard fire exposure time-temperature curve, originally established by Ingberg (1928), to vary significantly from reality, including post-flashover fires, ventilation controlled fires, and different insulation properties of wall linings. More was understood about the thermal response of columns and beams to changes in temperature, with new analytical, numerical, and experimental methods being developed to predict column buckling, beam deflection and truss deflection.

In the standard test, full size structural elements, or portions of structural systems, are evaluated by mounting them in a fixture, exposing them to a flame in a furnace whose temperature rises as shown in Figure 1, and by noting the time at which failure occurs. The failure criteria, summarized in Table 1, depend upon the element's function and material, whether the article is load-bearing, and whether it is restrained. The rating of the test article is equal to the time (to the next lowest half-hour increment for times up to two hours, and to the next lowest hour for longer times) when any of the criteria indicated are exceeded.

It is expected that a 2-hour (h) rated article would resist failure in a real fire for a longer period of time than a similarly functioning 1-h rated article, and this is invariably the case. What can not be expected, however, is that a structure composed of elements that are 2-h rated would necessarily withstand an actual fire for two hours, or that that the structure would necessarily fail after two hours. The inability of the fire resistance rating to act as an absolute predictor of performance in an actual fire was recognized from the beginning when the forerunner of ASTM E119 was published in 1918. Over the years, however, the reference to fire resistance ratings in common time units has become interpreted to relate closely (or at least conservatively) to the actual expected time that a structure or element would be expected to resist a fire.

The fire resistance rating of a structural element or assembly can be greatly enhanced by applying a thermal insulation to the surfaces exposed to the high temperatures of the furnace. Sprayed fire resistive materials (SFRM) were introduced over 40 years ago as a lower labor cost, lighter weight alternative to concrete and lath/plaster. The SFRM derived its fire resistive properties from water of hydration contained in the gypsum or portland cement used to bind various fibers and other fillers. In addition to SFRM, intumescent materials, suspended ceilings and drywall assemblies, concrete encasements, tiles, and plaster/lath are used today to increase the ability of a structure to endure a fire. It is not uncommon for some of these materials, when applied in accordance with the manufacturer's instructions, to increase the fire resistance rating of a structural element by factors of four or more, a result of great consequence for steel construction, but also important for aluminum, timber and composite materials.

The shortcomings of the current methods for rating the fire resistance of structural elements and systems are numerous; some are obvious and have been recognized for years. The obvious shortcomings include:

- The size of the test article is limited to the size of the furnace (on the order of 5 m x 5 m x 2 m).
- The support conditions for the test article do not adequately mimic field use.
- The load conditions for the test article do not adequately mimic field use.
- The thermal environment of the furnace does not mimic a real fire.
- There is no universally accepted definition of the failure-to-meet-load criteria.
- The tests reveal no fundamental information about the performance of the specimen and provide little guidance on how to improve performance.
- The tests require specialized facilities and can be expensive to run.
- The furnaces themselves are not standardized; hence, the same specimen could receive different ratings if tested in two different facilities.
- Ratings are based upon a single test, with no way to quantify the uncertainty or safety factor.

In spite of severe shortcomings, these test methods continue to be used throughout the world. The reasons are based upon the following arguments:

- A massive data base using the standard fire resistance test method has been established and is in continual use.
- The historical record suggests that the test methods are conservative, since the number of losses due to the collapse of commercial buildings in fires is relatively small.
- Alternative methods have not been developed yet that are acceptable to the major parties who have widely divergent interests.

4.0 RECENT RESEARCH

4.1 Real-scale Test Programs

In addition to the standard furnace tests on individual building elements described above, many experiments have been conducted with different assemblies of various sizes and materials for different purposes. One of the largest under a controlled environment was on an eight story steel frame structure constructed within a dirigible hangar in Cardington, UK. Organized through a collaboration of universities, industries and European governments, one of the major objectives was to investigate how load is redistributed from a column or floor weakened by a localized fire to stronger elements that may be adjacent or more distant. A general conclusion from the study was that redistribution improves the robustness of the structure, which suggests that if this phenomena were well understood and predictable in general, that the fire proofing requirements could be lessened. Some representative articles and reports that describe different aspects of the Cardington test program include Kirby (1997), Sanad, et al. (1999), Gillie, et al. (2001), Lamont, et al. (2001), and Lennon and Moore (2003). Moss and Clifton (2004) reported on an effort to model the entire structure during the fire tests.

The literature is filled with tests and experimental measurements of individual structural members at elevated temperatures. Table 2 provides references that represent the kinds of experimental investigations that have been reported recently.

4.2 Material Properties

The response of a structure to fire differs greatly with the selection of materials for construction. While mechanical properties of most structural materials at ambient conditions are well documented, the properties of these same materials at temperatures that they might reach in a fire are sparse at best, and often non-existent. During the conduct of the investigation into the collapse of the WTC towers (NIST 2005), an extensive database was developed of the physical, thermal and mechanical properties of structural steels at elevated temperatures (Luecke, et al., 2005; Banovic, et al., 2005). Outinen and Makelainen (2004) also compiled the mechanical properties of structural steel at elevated temperatures. The mechanical properties at elevated temperatures of high strength concrete have been reviewed by Phan and Carino (1998), and the thermal properties of reinforced concrete at high temperatures have been examined by Lie and Kodur (1996) and by Kodur and Sultan (2003). A heat flux gauge was developed by Jansson (2004) specifically for determining the thermal conductivity, thermal diffusivity and heat capacity of structural materials, including wood, concrete, gypsum, and SFRM at temperatures up 725 °C. Extensive measurements of the thermophysical properties of gypsum panels and SFRM were also conducted in connection with the WTC investigation (Carino, et al., 2005).

4.3 Fire Modeling

Within the discipline of structural engineering it has been customary to treat fire as a quasi-steady, homogeneous bath that increases the temperature of a structural member or assembly in a uniform manner. Hence, structure temperature becomes an independent variable against which force, stress, strain and deflection are plotted. Neither time nor thermal gradients are considered as first-order parameters. The key to design, then, is to keep the temperature below a limit such that the demand-to-capacity ratio does not exceed unity. For such an approach, the details of fire growth and spread are irrelevant.

In many cases time is a primary factor that can act either to increase or decrease the performance of a structure in a fire. The temperatures in a real fire builds up more quickly than the temperature in a standard furnace test; however, the fire cannot sustain these high temperatures at any one location because the fuel is consumed (unless the fire is being fed by a continuous fuel source such as a broken natural gas line). A uniform bath and homogeneous temperature model cannot capture either of these phenomena. In addition to the transitory nature of the fire, creep, which is irreversible and time dependent, can play a significant role in the response of the structure.

Zone fire models have been developed that allow one to account for a growing fire in a room and the transport of hot gases and smoke to other locations in a building. Olenick and Carpenter (2003) identified almost 50 different zone models in their survey of the field. These include, for example, BRANZFIRE (Building Research Association of New Zealand, 2000), MAGIC (Gautier, et al., 1999), and CFAST (Peacock, et al., 2005). Because these models lead to algebraic and ordinary differential equations, they can rather quickly solve for the time varying temperature within a particular volume (usually divided into an upper and lower zone) in a multi-room building. Many of the zone models will also predict the heat flux to the boundaries of the compartment, although the heat transfer into the walls and structure is not computed in any detail.

The complexity of problems that can be solved using computational fluid dynamics models has increased in direct proportion to the speed of computers, which is now to the point that meaningful engineering calculations of room fires can be done on a personal computer. McGrattan (2005) elegantly described where we are and where we are going with CFD fire modeling in general. The Fire Dynamic Simulator (FDS) (McGrattan, 2004) has been developed specifically for doing realistic fire calculations and currently is used throughout the world for fire protection engineering design purposes.

4.4 Structural Modeling

The development of finite element modeling techniques provided engineers a tool that could begin to deal with complex solid mechanics problems. While mechanical engineers applied finite element analysis (FEA) techniques to heat transfer and thermo-mechanical designs associated with power systems and manufacturing processes, civil and structural engineers were mostly concerned with buildings and large civil structures that could be treated as fixed at the environmental temperature.

Models have been developed over the past 20 years to predict the fire endurance of specific structural elements or materials, and these are briefly reviewed by Olenick and Carpenter (2003). Examples of more general codes include TASEF (Sterner and Wickstrom, 1990), THELMA (Spearpoint, 2001), and SAFIR (Franssen, 2003).

The Proceedings of the International Association of Fire Safety Science (IAFSS) archive many of the significant advances in the analysis and numerical prediction of how structures behave in fire. The IAFSS symposium held in Beijing in 2005 was particularly rich in this area, and an examination of the proceedings of this symposium greatly simplifies anyone's effort to review the topic. An excellent assessment of our capability to numerically model the behavior of structures, and a look into the future, was provided by Franssen (2005). Baum (2005) assessed the current state of our ability to predict the response of a complex structure to a fire. The algorithm called the Fire Structure Interface (Prasad and Baum, 2005a; Prasad and Baum, 2005b), or FSI, allows coupling of the FDS finite volume model output to an ANSYS (2003) finite element model, an exercise made difficult by the shear magnitude of the degrees of freedom and the discontinuity of the element structures at the interface. Additional references on structural/fire models and experiments are provided in the review article by Grosshandler (2006).

5.0 RESEARCH NEEDS

A workshop held at NIST (Grosshandler, 2002) identified areas where efforts should be focused that would lead to the goal of scientifically-based performance predictions of building materials, products, structural elements, and systems up to the point of imminent fire-caused collapse. These included the need for more data on the properties of building materials, more measurements on the behavior of connections and assemblies, improved computational models, and standard test methods that supported performance-based codes.

5.1. Properties of Materials

Scientifically-based performance predictions require detailed knowledge of the thermal and mechanical properties of materials. Specifically, the workshop recommended research to:

- identify experimental techniques for measuring the thermal and mechanical properties of structural materials (normal and high strength concrete, normal and fire resistant steel, steel/concrete composite, aluminum, fiber-reinforced composite, timber) at temperatures up to their failure point;
- standardize measurement methods and use them to accumulate a consistent,

reliable high temperature data base on the thermal and mechanical properties that dominate the response of a structure to a severe fire , to the failure point; and

- develop experimental protocols for measuring, at elevated temperature, the thermal and mechanical properties of non-structural building materials (gypsum partitions, glazing, fire stops, intumescent coatings, structural fireproofing) that impact structural integrity during a fire, and accumulating a consistent, reliable high temperature data base. .

5.2 Real-scale Laboratory Facilities

Facilities exist nowhere in the world for measuring the response to load of real-scale structural connections and assemblies in closely controlled, realistic fire environments (Beitel and Iwankiw, 2002). These measurements are essential to support the development of models and predictive tools for demonstrating the benefit of new materials and designs, and to assist understanding how a structure might fail in a severe case of arson or terrorist attack that exceeds the design threshold.

Current practice in the construction industry is to test structural components and assemblies at full-scale. However, this is most often not possible because of the size of a full-scale specimen and the high temperatures of the fire. In addition, one needs to account for the structural frame surrounding the element. As a result, insufficient data exist to properly extrapolate the response of a reduced-scale specimen in a test to the performance of that component full-size in a building system subjected to real fires. A structural fire endurance research facility is needed to develop a comprehensive understanding of the effects of length-scale on performance.

A real-scale structural fire endurance facility that permits, and promotes, international research would, for example, lead to:

- experimental methods and protocols for measuring the thermal and mechanical behavior of fireproofing as installed and when degraded by time, temperature, and stress;
- experimental methods and protocols for measuring the response of structural connections (including welds, bolts, rivets and adhesives) when exposed to severe fire conditions and loads, including during the cool-down period;
- fully instrumented experimental facilities for exposing floor and wall composite assemblies to controlled fires under measured loads, to failure;
- larger-scale test facilities to the extent necessary to extrapolate the behavior of connections and assemblies to the behavior of whole building frames;
- development of more efficient non-linear structural and CFD algorithms to expand the number of significant physical phenomena (e.g., creep, concrete cracking and spalling, fireproofing damage) and the range of length scales that can be practically accommodated; and
- development of efficient and verified subgrid models to better resolve the heat transfer from the fire environment to the structural elements, and for failure of structural connections and interfaces at elevated temperatures, eventually leading to full collapse analysis.

6.0 CONCLUDING REMARKS

A concerted effort is required to accelerate the development of the engineering tools needed to support the ambitious goal of scientifically-based performance predictions of building materials, products, structural elements, and systems up to the point of imminent fire-caused collapse. New experimental facilities are needed that will provide tight control over the thermal and mechanical loading of structural assemblies at real scale to support the development of the new measurement and predictive methods that will enable the development of these tools. Increased international collaboration in this area would permit leveraging of scarce resources.

A properly designed and equipped structural fire endurance laboratory will provide the following benefits:

- a scientific basis for assessing the response of buildings to extreme threats, the integrity of buildings that have experienced an extreme fire, and performance of alternative remediation approaches;
- acceleration of the development of cost effective materials and technologies into building practices and of engineering tools that support performance-based design alternatives;
- harmonization of best practices in testing laboratories and mitigation of the erection of technically unfounded international trade barriers for building products and materials; and
- safer, more flexible, and possibly less expensive buildings.

7.0 REFERENCES

Alfawakhiri, F., Sultan, M., 2001, *Interflam 2001, Proceedings, 9th International Fire Science and Engineering Conference*, pp. 431-442, Interscience Communications Limited, London.

Ali, F., Nadjai, A., Glackin, P., Silcock, G., 2003, *Fire Safety Science, Proc. of the 7th Int'l Symp.* pp. 1001-1012, Int'l Assoc. for Fire Safety Science, London.

ANSYS Corp., 2003, *ANSYS Release 8.0 Documentation.*

ASTM, 2000a, "ASTM E 119-00: Standard Test Methods for Fire Tests of Building Construction Materials," ASTM International, West Conshohocken, PA.

ASTM, 2000b, "ASTM E 1529-00: Std. Test Meth. for Determining Effects of Large Hydrocarbon Pool Fires on Struct. Members and Assemblies," ASTM Int'l, West Conshohocken, PA.

Banovic, S., McCowan, C., Luecke, W., 2005, *Fed. Build'g & Fire Safety Invest. of the WTC Disaster: Physical Properties of Structural Steels,* NCSTAR 1-3E, Gaithersburg, Sept.

Baum, H., 2005, *Fire Safety Science, Proceedings of the Eighth International Symposium*, pp. 3-20, Int'l Association for Fire Safety Science, London.

Beitel, J., Iwankiw, N., 2002, "Analysis of Needs and Existing Capabilities for Full-scale Fire Resistance Testing of Structural Connections," Hughes Associates, NIST GCR 02-834, Dec.

Bernhart, D., Buchanan, A., Dhakal, R., Moss, P., 2005, *Fire Safety Science, Proc. of the 8th Int'l Symp.*, Int'l Assoc. for Fire Safety Science, London.

Building Research Association of New Zealand, 2000, "A User's Guide to BRANZFIRE Software."

Carino, N., Starnes, M., Gross, J., Yang, J., Kukuck, S., Prasad, K., Bukowski, R., 2005, *Fed. Build'g & Fire Safety Investigation of the WTC Disaster: Passive Fire Protection,* NIST NCSTAR 1-6A, Nat. Inst. of Standards and Technology, Gaithersburg, Sept.

Chang, J., Buchanan, A., Moss, P., 2005, *Fire and Materials 29*, 181-194.

Delin, M., Walmerdahl, P., 2001, *Interflam 2001, Proc., 9th Int'l Fire Science and Engrg. Conf.*, pp. 567-580, Interscience Communications Ltd, London.

Frangi, A., Fontana, M., 2005, *Fire Safety Science, Proc. of the 8th Int'l Symp.*, pp. 279-290, International Association for Fire Safety Science, London.

Frangi, A., Fontana, M., 2003, *Fire Safety Science, Proc. of the 7th Int'l Symp.*, pp. 1111-1122, International Association for Fire Safety Science, London.

Franssen, J-M., 2005, *Fire Safety Science, Proceedings of the Eighth International Symposium*, pp. 21-36, Int'l Association for Fire Safety Science, London.

Franssen, J-M., 2003, "SAFIR. A Thermal/Structural Program Modelling Structures under Fire," Proc. NASCC 2003, AISC, Inc., Baltimore, April.

Gautier, B., Pages, O., Thibert, E., 1999, *Interflam 1999, Proceedings, 8th Int'l Fire Science and Engineering Conf.*, pp.

1217-1222, Interscience Commun. Ltd, London.

Gillie, M., Usmani, A., Rotter, M., O'Connor, M., 2001, *Fire Safety Journal 36*, 745-767.

Grosshandler, W. (ed.), 2002, "Fire Resist. Determination and Perf. Prediction Research Needs Workshop: Proc.," NISTIR 6890, Nat. Inst. of Stds. and Technology, Gaithersburg, Sept.

Grosshandler, W., 2006, "The Response of Structures to Fire -- Advances and Challenges in Predicting Behavior," *Proceedings of the 13th International Heat Transfer Conference*, Sydney.

Harada, K., Enomoto, A., Uede, K., Wakamatsu, T., 2000, *Fire Safety Science, Proc. of the 6th Int'l Symp.*, pp. 1063-1074, Int'l Assoc. of Fire Safety Science, Bethesda.

Hirashima, T., Uesugi, H., 2005, *Fire Safety Science, Proceedings of the 8th International Symposium*, Int'l Assoc. for Fire Safety Science, London.

Ingberg, S.H., 1928, *Quarterly of NFPA 22*, 43-61.

Janssens, M., 2004, *Fire and Materials 28*, 199-207.

Jansson, R., 2004, *Interflam 2004, Proceedings, 10th Int'l Fire Science and Engineering Conf.*, pp. 181-188, Interscience Commun. Ltd, London.

Jong, F., Clancy, P., 2004, *Fire and Materials 28*, 209-225.

Kamikawa, D., Hasemi, Y., Wakamatsu, T., Kagiya, K., 2003, *Fire Safety Science, Proceed. of the Seventh International Symposium*, pp. 989-1000, Int'l Assoc. for Fire Safety Science, London.

Kirby, B., 1997, *Fire Safety Science, Proc. of the Fifth International Symposium*, pp. 1129-1140, International Association of Fire Safety Science, Boston.

Kodur, V., Cheng, F., Wang, T., Sultan, M., 2003, *Journal of Structural Engineering 129*, 253-249.

Kodur, V., Sultan, M., 2003, *J. of Materials in Civil Engineering 15*, 101-107.

Kodur, V., Sultan, M., 2000, *Fire and Materials 24*, 9-16.

Kodur, V, Sultan, M., Wang, T., Cheng, F., 2003, *Fire Safety Science, Proceedings of the Seventh International Symposium*, pp. 1013-1024, International Assoc. for Fire Safety Science, London.

Korzen, M., Magonette, G., Buchet, P., 1999, *Interflam 1999, Proceedings, 8th Int'l Fire Science and Engineering Conference.*, pp. 897-910, Interscience Communications Limited, London.

Lamont, S., Lane, B., Usmani, A., 2005, *Fire Safety Science, Proceedings of the Eighth International Symposium*, pp. 177-188, International Assoc. for Fire Safety Science, London.

Lamont, S., Usmani, A., Drysdale, D., 2001, *Fire Safety Journal 36*, 815-839.

Laverty, D., 2001, *Journal of Applied Fire Science 10*, 127-148.

Leghazouli, A., Izzuddin, B., 2001, *Fire Safety Journal 36*, 769-794.

Lennon, T., Moore, D., 2003, *Fire Safety Journal 38*, 623-643.

Lie, T., Kodur, V., 1996, *Canadian Journal of Civil Engineering 23*, 511-517.

Lim, L., Buchanan, A., Moss, P., 2004, *Fire and Materials 28*, 95-125.

Liu, T., Liew, K., 2004, *Interflam 2004, Proceedings, 10th International Fire Science and Engineering Conf.*, pp. 157-168, Interscience Communications Limited, London.

Luecke, W., McColskey, J., McCowan, C., Banovic, S., Fields, R., Foecke, T., Stewart, T., Gayle, F., 2005, *Federal Build'g & Fire Safety Investigation of the WTC Disaster: Mechanical Properties of Structural Steels,* NIST NCSTAR 1-3D, Gaithersburg, Sept.

Manzello, S., Gann, R., Kukcuk, S., Prasad, K., Jones, W., 2004, *Interflam 2004, Proceed., 10th Intern'l Fire Science & Engrg. Conf.*, pp. 245-256, Interscience Communications Ltd., London.

McGrattan, K. (ed), 2004, "Fire Dynamics Simulator (V. 4), Technical Reference Guide," NIST Special Publication 1018, Nat'l Inst. of Standards and Technology, Gaithersburg, July.

McGrattan, K, 2005, *Fire Safety Science, Proceedings of the 8th Int'l Symposium,* pp. 53-68, Int'l Assoc. for Fire Safety Science, London.

Moss, P., and Clifton, G., 2004, *Fire and Materials 28*, 178-198.

NIST, 2005, *Federal Building and Fire Safety Investigation of the WTC Disaster: Final Report of the Nat'l Construction Safety Team on the Collapses of the WTC Towers,* NIST NCSTAR 1, Gaithersburg, Sept.

Olenick, S., Carpenter, D., 2003, *Journal of Fire Protection Engineering 13*, 87-110.

Outinen, J., Makelainen, P., 2004, *Fire and Materials 28*, 237-251.

Pagni, P., 2003, *Fire Safety Science, Proceedings of the Seventh International Symposium*, pp. 3-22, Int'l Assoc. for Fire Safety Science, London.

Peacock, R., Jones, W., Reneke, P., Forney, G., 2005, *CFAST: Consolidated Model of Fire Growth and Smoke Transport (V. 6). User's Guide*, NIST SP 1042; Nat'l Institute of Standards and Technology, Gaithersburg, MD, August.

Phan, L., Carino, N., 1998, *J. of Materials in Civil Engineering 10*, 58-64.

Prasad, K., Baum, H., 2005a, *Federal Building and Fire Safety Investigation of the WTC Disaster: Fire Structure Interface and Thermal Response of the WTC Towers,* NCSTAR 1-5G, Nat. Institute of Standards and Technology, Gaithersburg, Sept.

Prasad, K., Baum, H., 2005b, *Proc. of the Combustion Institute*, 30:2255-2262.

Sanad, A., Rotter, J., Usmani, A., O'Connor, M., 1999, *Interflam 1999, Proceed., 8th Int'l Fire Science and Engineering Conf.*, pp. 1045-1056, Interscience Communications Ltd., London.

Spearpoint, M., 2001, *Fire Technology 37*, 109-128.

Spyrou, S., Davison, B., Burgess, I., and Plank, R., 2004, *Fire and Materials 28*, 83-94.

Sterner, E., Wickstrom, U., 1990, "TASEF - Temperature Analysis of Structures Exposed to Fire - User's Manual," Swedish National Testing and Research Institute, SP Report 1990:05, Boras.

Takeda, H., 2005, *Fire Safety Science, Proceedings of the 8th Int'l Symposium*, pp. 291-302, Int'l Assoc. for Fire Safety Science, London.

Williams, B., Bisby, L., Kodur, V., Su, J., Green, M., 2005, *Fire Safety Science, Proceedings of the 8th Int'l Symposium*, pp. 247-258, International Association for Fire Safety Science, London.

Wu, C-W., Lin, T-H., Lei, M-Y., Chung, T-H., Huang, C-C., Chiang, W-T., 2005, *Fire Safety Science, Proceed. of the 8th Intt'l Symp.*, pp. 327-338, Int'l Assoc. for Fire Safety Science, London.

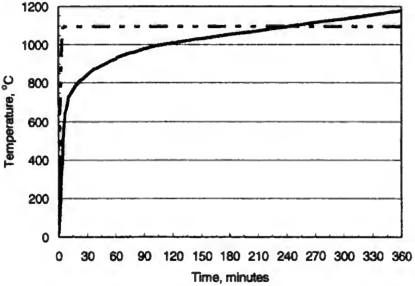

Figure 1: Standard furnace heating curves (ASTM, 2000a; 2000b)

Table 1: Example Failure Criteria for Various Structural Elements (ASTM, 2000a)

Element	Load Criteria	Temperature Criteria	Breach Criteria
floor systems*	Unable to maintain max design load	• Ave. temp. increase on unexposed side > 139 °C. • Max temp. increase on unexposed side > 181 °C. steel structural support • Ave. temperature of steel > 593 °C • Max temperature measured on steel > 704 °C concrete structural support • Ave. temperature of tension steel > 427 °C • Ave. temperature of reinforcing steel > 593 °C	Hot gases able to ignite cotton target on unexposed side
beam*	Unable to maintain max design load	• Average temperature > 593 °C • Max temperature measured > 704 °C	na
column	Unable to maintain max design load	none	na
steel col. or beam	none	• Ave. temperature of column > 538 °C • Max temperature measured on column > 649 °C	na
bearing wall	Unable to maintain max design load	• Ave. temperature increase on unexposed side > 139 °C. • Max temperature increase on unexposed side > 181 °C.	Hot gases able to ignite cotton target on unexposed side
non-bearing partition	na	• Ave. temperature increase on unexposed side > 139 °C. • Max temperature increase on unexposed side > 181 °C.	Hot gases able to ignite cotton target on unexposed side
*The rating of an element tested in a frame that restrains it from bending or expanding may be reduced by a factor of 2 over the same element tested in an unrestrained fashion.			

Table 2: Representative recent experimental investigations of heated structural elements

Materials	Element	Citation
steel	joists	Alfawakhiri, F., and Sultan, M., 2001
steel + insulation	floor trusses	Chang, et al., 2005
steel	H-columns	Hirashima, and Uesugi, 2005
steel	columns	Kamikawa, et al., 2003
steel	cellular beams	Liu and Liew, 2004
steel	columns	Korzen, et al., 1999
steel	joints	Spyrou, et al., 2004
concrete	columns	Ali, et al., 2003
reinforced concrete	beams	Bernhart, et al., 2005
high strength concrete	columns	Kodur, et al., 2003
precast concrete	walls	Lim and Buchanan, 2003
reinforced concrete	beams	Williams, et al., 2005
timber	structures	Frangi and Fontana, 2005
wood	structural members	Janssens, M., 2004
wood	structural members	Jong and Clancy, 2004
wood studs	shear walls	Kodur and Sultan, 2000
wood frame	exterior walls	Takeda, 2005
timber-concrete	slabs	Frangi and Fontana, 2003
gypsum-metal studs	partitions	Manzello, et al., 2004
glass	partitions	Wu et al., 2005
glass	facade	Delin and Walmerdahl. 2001
glass	windows	Harada, et al., 2000
glass	windows	Pagni, 2003

MANUSCRIPTS AUTHORED BUT NOT PRESENTED ORALLY

Interpretation of Slope Failure Distribution Triggered by the Northern Pakistan Earthquake on 8 October 2005 using SPOT5 Stereo-imageries

by

Hiroshi P. Sato[1], Mamoru Koarai[1], Hiroshi Une[1], Hiroyuki Hasegawa[1],
Junko Iwahashi[1] and Izumi Kamiya[1]

ABSTRACT

This paper presents distribution of slope failures triggered by the northern Pakistan earthquake using 2.5m resolution SPOT5 (System pour l'Observation de la Terre 5) images. The stereo-images taken on October 20 and 27, 2005 were interpreted, as a result, 2,424 slope failures were detected. According to field survey, most of the slope failures were shallow slides. Over the one-third of the detected slope failures occurred within one kilometer of the active faults. Form this study, it was found that remote sensing is effective tool to estimate the damages in wide area, and it is important to know the existence and location of active fault to prevent earthquake disasters in advance.

KEYWORDS: SPOT5, Pakistan, earthquake, interpretation, active fault

1. INTRODUCTION

Northern Pakistan earthquake (Mw7.6) of October 8, 2005 occurred in the Kashmir region in the northwestern part of the Himalayas. The epicenter is north-northeast direction and 105 km away from Islamabad.

The crustal deformation was spatially mapped with Synthetic Aperture Radar (SAR) data from the European Space Agency's ENVISAT [1], and it was found that the newly deformed area occupies a 90-kilometer-long northwest-southeast trending strip. Heavily damaged area north of Muzaffarabad has the maximum deformation up to six-meter uplift as observed by the satellite.

There are known active faults (Muzaffarabad and Tanda faults) stretching to the northwest and southeast near the epicenter [2], which reveal some uplift (on the northern side) and dextral (right-lateral) strike-slip activities. The detected crustal deformation was along these active faults and all observations were consistent with previously known directions of past fault movements.

According to Pakistan Government, 87,350 were dead as of November 8, 2005. The earthquake occurred in mountain and in distant area from the capital city, it was difficult to know the earthquake disaster immediately. It is important to collect the slope failures location for restoration activities and taking measures against secondary disaster.

2. METHODS

2.1 SPOT5 image interpretation

After the earthquake, SPOT5 (System pour l'Observation de la Terre 5) panchromatic images were taken on October 20 and 27, 2005. The incident angle of October 20 and 27 images is at the left side of 26.4 degree and at the right side of 30.4 degree, respectively.

As shown in Fig. 2, these images make stereoscopic vision, and through the stereo-images slope failures were interpreted and delineated on the images. Fig. 2 shows north area of Muzaffarabad. In the figure the circle #5 shows not slope failures but the flexure cliff along the surface rupture of the earthquake fault. Slope failures were interpreted as white-bright slope, especially the right side of the river. In delineating such the slope failure, each slope failure was divided as considering unit slope. However, the interpreted area contains high mountain areas covered with snow, and it was difficult to interpret slope failures in

---

[1] Geography and Crustal Dynamics Research Center, Geographical Survey Institute, Tsukuba-shi, Ibaraki-ken 305-0811 Japan

such the area. In the case the slope failures were not interpreted.

2.2 Methods of slope failures delineation

2.2.1 Preparation of ortho-images

To delineate the interpreted slope failures, in advance, orthographic (ortho-) images were prepared, namely, to overlay the map, SPOT5 images were geometrically corrected using ground control points (GCPs). The 34 mountain summits' location and elevation, whose data were gathered from 90m-resolution SRTM (Shuttle Radar Topography Mission), were used as the GCPs.

After the geometric correction calculation, root mean square errors at the 34 GCPs showed c.a. 72m at east-west direction, c.a. 62.3m at north-south direction, respectively. This error indicates the location of ortho-image randomly shifts not more than one grid of SRTM data.

2.2.2 Comparison of interpreted slope failures with pre-earthquake SPOT5 image

The interpreted slope failures may contain the slope failures occurred before the earthquake. To remove such the slope failures, the interpreted slope failures were superimposed on the orthography of SPOT5 image taken on March 2, 2004. Finally, the interpreted area is the overlap between before and after earthquake images, 55km by 51 km in area except high mountain area covered with snow.

3. RESULTS AND DISCUSSION

The interpreted slope failures were overlaid on the SRTM data, and shown in Fig. 3. The total count of the slope failures was 2,424. Comparing Fig. 3 with Fig. 1, most of them occurred on the hanging wall side. Furthermore, many slope failures occurred along Muzaffarabad fault and Tanda fault. Fig. 4 shows relation between slope failures and distance from these active faults. It was found that over the one-third of them occurred within one kilometer from the active fault.

To fit area size of the slope failures for SRTM resolution, the large-scale slope failures at the size of 100m by 100m (1 ha in area) and more, namely, 207 counts, were selected. Furthermore, the relation between large-scale slope failures and slope calculated from SRTM was investigated. The result is shown in Fig. 5. The minimum and maximum slope was 8.4 degree and 52.3 degree, respectively. The most failures, 44 counts, occurred at the slope of 30-35 degree, 87 counts failures occurred at the slope of 35 degree and more, and 76 counts occurred at the slope of less than 30 degree. There is a slight tendency that more large-scale slope failures occurred at steeper slope than at gentler slope.

Fig. 6 shows relation of 207 counts failures between slope (degree) and distance from the active faults. It infers that large-scale failures occurred not only at steep slope but also at gentle slope in the near area from the active faults, slope failures of 10-15km from the faults occurred at steeper slope (43.4 - 46.3 degree). However, at the distance of c.a. 18km or further, large-scale slope failures also occurred at the gentler slope (less than 30 degree). It is not concluded that large-scale slope failures occurred at steeper slope when they located at further distance from the active faults.

Fig. 7 shows vertical curvature frequency distribution of 207 counts failures. The vertical curvature [3] was calculated from SRTM. It is the index which shows plus and higher values when cross section of topography is more convex, minus and lower values when more concave. Vertical curvature is zero, it means linear slope. The most failures occurred at the curvature of +0.1 - +0.2, 37 counts, 128 counts occurred at the curvature of more than zero (at convex slope), and 79 counts occurred at the curvature of less than zero (at concave slope). Form Fig. 7, there is the tendency that more large-scale slope failures occurred at the convex slope than at the concave slope.

4. CONCLUSIONS

By interpreting slope failures using SPOT5 stereo-images, characteristics of slope failures were revealed as mentioned before. In the monsoon season heavily rain may cause secondary slope failures, and many residents who live on the slope may suffer from the secondary damage of slope failure. To prevent and mitigate such the damage, further monitoring may be important. The interpreted slope failures data will help such disaster prevention measures.

5. REFERENCES

1. Fujiwara, S., Tobita, M., Sato, H.P., Ozawa, S., Une, H., Koarai, M., Nakai, H., Fujiwara, M., Yarai, H., Nishimura, T. and Hayashi, F.: Satellite data gives snapshot of the 2005 Pakistan earthquake, *EOS, Transaction of American Geophysical Union*, 87, 73-77, 2006.
2. Nakata, T., Tsutsumi, H., Khan, S.H. and Lawrence, R.D., Active Faults of Pakistan, Research Center for Regional Geography, Hiroshima University, Japan, 141pp., 1991.
3. Zevenbergen, L.W. and Thorne, C.R.: Quantitative analysis of land surface topography, *Earth Surface Processes and Landforms*, 12, 47-56, 1987.

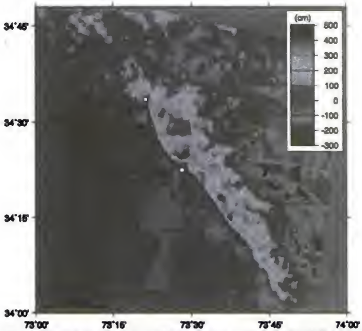

Fig.1 Detected crustal deformation using ENVISAT/SAR data (wavelength of 5.6 cm, C-Band) [1]. Positive values indicate the movement toward the SAR satellite in the line-of-sight direction (upward and/or E-SE displacement). Solid black lines show Muzaffarabad and Tanda faults [2] and star mark is the epicenter.

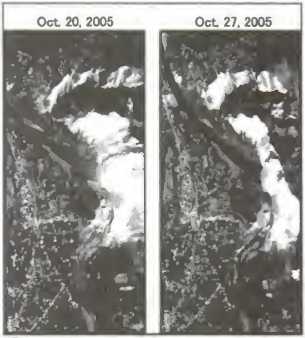

Fig.2 SPOT5 stereo-imagery in the damaged area of north Muzaffarabad

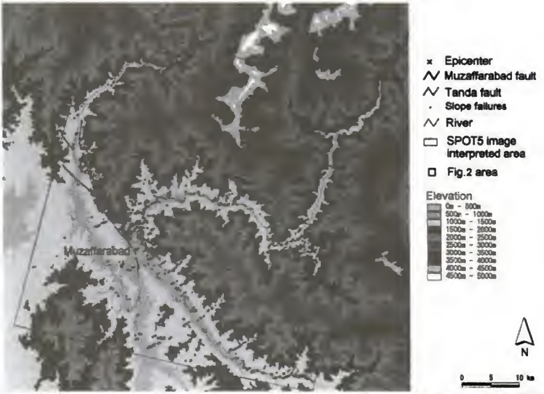

Fig. 3 Distribution of slope failures triggered by the earthquake. Elevation data are based on SRTM.

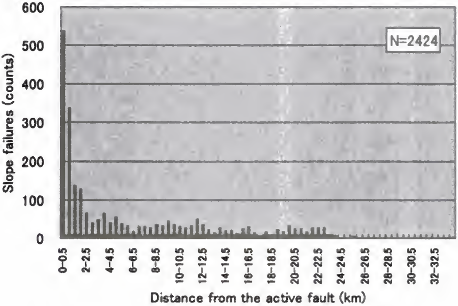

Fig. 4 Slope failures frequency distribution on distance from the active fault

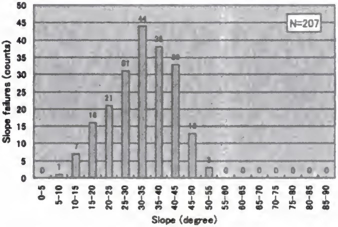

Fig. 5 Large-scale slope failure frequency distribution on slope (degree)

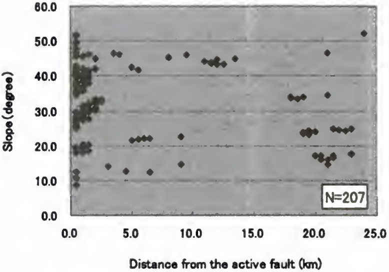

Fig. 6 Relation between distance from the active fault and slope (degree)

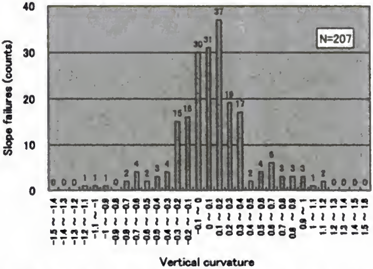

Fig. 7 Large-scale slope failures frequency distribution on vertical curvature

APPENDIX

REPORT OF TASK COMMITTEE A
GEOTECHNICAL ENGINEERING AND GROUND MOTION

Date: 15 May 2006

Place: National Institute of Standards and Technology, Gaithersburg, MD, USA

Attendees:	U.S. Side --	Mehmet Celebi (Chair)	USGS
	Japan Side --	Keiichi Tamura (Chair)	NILIM
		Eiji Kohama	PARI

1. Objective and Scope of Work

The objectives of work include:
(1) To promote sharing of strong motion earthquake data among researchers and practicing engineers, and enhance the availability of technology for evaluating the destructive effects of earthquake motion, and
(2) To promote research on the dynamic behavior of soils, foundations and earth structures during earthquakes.

The scope of work includes:
(1) Exchange strong motion data regularly and identify significant issues.
(2) Exchange information on technological developments, state-of-the-art and practice related to strong motion recording, hazard mapping, soil-structure interaction, soil behavior and stability during earthquakes,
(3) Exchange field data related to geotechnical engineering, and
(4) Plan and conduct programs of cooperative research and/or workshops in coordination with the proposed or ongoing programs.
(5) Plan and form a cooperative post-earthquake survey team after a major event.
(6) Exchange information and conduct studies related to correlation of damage with ground motion.

2. Accomplishments

(1) The proceedings of the Third Workshop on Soil-Structure Interaction, which was held in Menlo Park, CA on 29-30 March 2004, have been uploaded to the following Panel's website:
http://www.pwri.go.jp/eng/ujnr/tc/a/ssi_w3/index.html
(2) The Task Committee contributed to the planning and execution of a large-scale experiment on soil-foundation system using the NIED's E-Defense.
(3) In cooperation with FHWA, MoDAT (Missouri Department of Transportation), MCEER and USGS (Mehmet Celebi), the seismic monitoring network at the new cable-stayed bridge, Cape Girardeau (Missouri) Bridge, with structural and site arrays, has been completed. Real-time continuous data from this network can be viewed or obtained from IRIS (Incorporated Research Institutions for Seismology) web site: www.iris.edu.

3. Future Plans

The future plans include:
(1) Plan a workshop on Real-Time Instrumentation of Densely Urbanized Areas and Instrumentation of Civil Engineered Structures including health monitoring. Temporary committee will include Dr. Fujiwara of NIED, Dr. Okawa of BRI, Mr. Shoji of NILIM, Dr. Borcherdt, Dr. Wald and Dr. Celebi of USGS. The committee will explore cooperation with other Task Committees.
(2) The efforts for holding the Fourth Workshop on Soil-Structure Interaction in Japan will be

continued within about three years from the previous one. The responsible members will be Dr. Celebi (USGS), Dr. Todorovska (USC), Dr. Okawa (BRI) and Dr. Iiba (NILIM).

(3) Explore the possibility of joint research and/or workshop on damage detection techniques. The responsible members will be Dr. Sugano (PARI), Dr. Todorovska and Dr. Celebi. Cooperation with Task Committee B to have joint workshops will be explored.

4. Related Activities

(1) Dr. Eiji Kohama, Senior Research Engineer of the Port and Airport Research Institute (PARI) continues the research activities as a visiting researcher at the University of California, Berkeley (UCB).

(2) During the period 30 January - 3 February 2006 Dr. Michael K. Sharp, at the request of the Japanese Government, traveled with a group to Japan to engage in a technical exchange related to levees and levee performance, specifically as a result of hurricane Katrina. This technical exchange was arranged by the Ministry of Land, Infrastructure and Transport (MLIT). Technical presentations were made to several components of MLIT including River Bureau, National Institute for Land and Infrastructure Management, Regional Development Bureaus and Public Works Research Institute, in addition to the Japan Dam Engineering Center and the Japan Institute of Construction Engineering.

REPORT OF TASK COMMITTEE B
NEXT-GENERATION BUILDING AND INFRASTRUCTURE SYSTEMS

Date: 15 May 2006

Place: National Institute of Standards and Technology, Gaithersburg, MD USA

Attendees:	U.S. Side -	George C. Lee (Co-Chair)	University at Buffalo
		Douglas Foutch (Co-Chair)	NSF
		Vilas Mujumdar	NSF
		Josephine Malilay	CDC
		William Roper	George Mason University
		Hamid Ghasemi	FHWA
		Noël Raufaste	NIST
	Japan-side -	Taiki Saito (Acting Co-Chair)	BRI
		Chikahiro Minowa	NIED
		Koichi Morita	BRI
		Yoshihiro Iwata	BRI
		Taichiro Okazaki	Univ. of Minnesota (BRI Guest Researcher)

1. Objective and Scope of Work

(1) Objective

The objectives of the Task Committee are to enhance the development and implementation of innovative and new 1) structural and non-structural materials; 2) enabling technologies such as structural health monitoring and multi-hazard performance based engineering; 3) evaluation, analysis, design, construction, and maintenance methods through cooperative individual and organized and networked analytical and experimental approaches for the next-generation building and infrastructure systems.

Opportunities during the next five years include topics on multi-hazard resilient buildings, embedded systems for the health and productivity of occupants, and collaborations with other researchers and practitioners.

(2) Scope-of-Work

a) Conduct joint workshops and joint meetings to identify research opportunities, new projects including multi-hazard risk reduction strategies and measures, and make recommendations for the UJNR Panel.
b) Encourage the development and application of new technologies, smart sensors, and intelligent materials to improve the health, safety, and productivity of construction workers and building occupants.
c) Develop new materials and technologies for condition assessment, retrofit of existing buildings, and design of new buildings.
d) Coordinate development of databases, test procedures, and guidelines for interpretation of test results and their applications.
e) Coordinate joint research including the utilization of experimental facilities.
f) Enhance the exchange of information and personnel.

2. Accomplishments

During 2005-2006, the Task Committee developed a concept to foster collaborative efforts involving several Panel Task Committees to pursue collaborations as recommended in the Panel's Strategic Plan. A planning workshop to develop the details was unavoidably cancelled from its planned spring 2006 date. Initial planning to reschedule this workshop was conducted during the 38th Joint Panel Meeting involving representatives from Task Committees G (Transportation Systems), Task Committee I (Fire Performance of Structures), and the former Task Committee F (Advanced Information and Communication Technology for Disaster Prevention and Public Health Evaluation). These discussions resulted in an agreement to conduct the T/C Workshop in January or February 2007, Hawaii.

3. Future Plans

(1) Plan and conduct a two-part Task Committee workshop in January or February 2007, in Hawaii to formulate the foci of cooperative objectives of T/C B and a strategic plan to realize the targeted T/C objectives. Emphasis will be given to realize a five-year plan and to encourage collaborations with other T/Cs, UJNR Panels, and the construction community.

One of the workshop foci will be on "Multi-Hazard Risk Reduction for Building Systems. Its principal thrusts address:

- High Performance Materials and Advanced Technologies
- Performance Based Design Methodologies
- Multi-Hazards e.g., Earthquakes, Wind, Storm Surge and Tsunamis, Fires, Environmental Health Hazards, System Integrity and Functionality.

The other foci will be on "Multi-hazard Risk Reduction for Highway Bridges". Discussions will be held with Task Committee G to identify cooperative bridge related infrastructure research projects and action plans.

(2) Accelerate communication on performance-based engineering and identify cross-Panel joint research on topics such as:
   a) Performance-based engineering approaches that will serve as a technical base for improving codes and standards,
   b) Embedded systems for human health, safety, and productivity that lead to better understanding of the performance of buildings and structures.
   c) Develop a database on building state and function relationships and a design system for business and/or serviceability continuity plan, and
   d) Refine seismic response evaluation and multi-hazard response prediction.

(3) Realize effective communication among its T/C members through using a ListServe or Task Committee Web Site that will stimulate discussions among its membership for identifying candidate joint research opportunities, topics for information, and serve as a coordinating center.

(4) Encourage performing cooperative research on infrastructure systems by partnering with T/C G, Transportation Systems. Opportunities will be discussed during the January or February 2007 T/C Workshop.

REPORT OF TASK COMMITTEE C
DAMS

Date: 15 May 2006

Place: National Institute of Standards and Technology, Gaithersburg, MD, USA

Attendees:	U.S. Side --	Robert Hall (Co-Chair)	USACE
		Enrique Matheu (Co-Chair)	USACE/DHS
	Japan Side --	Yoshikazu Yamaguchi (Co-Chair)	PWRI

1. Objective and Scope of Work

To develop technical insights into better understanding the response of dams to seismic effects, the T/C will plan, promote, and develop research initiatives to assist in assuring seismic safety and economical protective countermeasures against earthquake loading for these critical structures.

The scope of work includes:

(1) Develop methods of analysis for seismic design of dams including outlet works.
  - a) Comparative analysis of design methods and evaluation criteria used by U.S. and Japan.
  - b) Development of "Design Earthquake Ground Motions" for analysis and evaluation of dams.
  - c) Assessment of models and numerical procedures used for seismic dynamic analysis.

(2) Perform research to better understand the dynamic characteristics of dam construction materials and site conditions.
  - a) Strength and deformation characteristics of concrete, soil and rock materials during earthquakes.

(3) Evaluate observed performance of dams and outlet works during earthquakes.
  - a) Develop a database that contains measured ground accelerations and dynamic response of dams and outlet works during earthquakes, and other related information necessary to evaluate their seismic behavior, such as experimental and/or analytical data with description of test and analysis procedures used.
  - b) Investigation of damage mechanisms due to earthquake loading.
  - c) Application of the analysis of the observed dynamic behavior to the improvement of design criteria.

2. Accomplishments

(1) Technical exchange and collaborative research on "***Non-linear stress analysis of concrete dams***" has been conducted between the U.S. (U.S. Army Engineer Research and Development Center & Louisiana State University) and Japan (Public Works Research Institute). The shaking table experiments for concrete dam models were conducted at PWRI in 2005. Both the U.S. Army Corps of Engineers and the U.S. Bureau of Reclamation have recently conducted similar tests at different scales and the joint comparison and evaluation of tests results will be beneficial to advance the state of the art in constitutive modeling of mass concrete structures.

(2) Technical exchange and collaborative research on "***Experimental characterization of non-linear tensile behavior of mass concrete***" has been conducted between the U.S. (U.S. Army Engineer Research and Development Center & U.S. Bureau of Reclamation) and Japan (Public Works Research Institute).

3. Future Plans

(1) The Task Committee will hold the ***"4th U.S.-Japan Workshop on Advanced Research for Dams"*** during the fall of 2006 in Tsukuba, Japan. The agenda for the Workshop will be determined through correspondence between the Chairs of the Task Committee on Dams of the UJNR Panel on Wind and Seismic Effects.

(2) The Task Committee will continue the current efforts focused on the development of improved mechanisms to facilitate the continuous exchange of results of research activities and general technical information related to dam earthquake engineering.

(3) The Task Committee will coordinate exchange visits of scientists and engineers from the U.S. and Japan. A series of case histories of mutual interest will be identified and prioritized and they will serve as the focus for this exchange program.

(4) The Task Committee will promote the development of joint research programs. The following topics have been identified as areas for future collaborative research:

    a) ***Non-linear stress analysis of concrete dams:***
    The Task Committee will continue their collaboration in this research to include both analytical and experimental data. This problem will be one of the themes for the upcoming Workshop in Japan.

    b) ***Global stability analysis of concrete dams:***
    The Task Committee will conduct a review of the minimum requirements for sliding and overturning stability currently in use in the U.S. and Japan. The Task Committee recognizes the importance of this collaborative effort, as the corresponding guidelines are currently subject to revision and update both in the U.S. and Japan.

    c) ***Criteria for seismic analysis progression:***
    The Task Committee will review and compare the state of practice in the U.S. and Japan regarding current recommendations for progression of seismic analysis based on stages of increasing complexity.

    d) ***Seismic evaluation of embankment dams:***
    The Task Committee will review criteria and guidelines for post-earthquake stability and deformation analysis of embankment dams.

    e) ***Dam-foundation interaction:***
    The Task Committee will develop collaborating research efforts to review and develop improved numerical models for dam-foundation interaction.

    The activities corresponding to the four areas indicated above will be addressed sequentially and the corresponding schedule will depend on the progress of the corresponding guidance documents, some of which are currently under discussion, development and/or review in the U.S. and Japan.

(5) Following large earthquakes in the U.S. or Japan, the Task Committee will assemble a joint reconnaissance team to investigate the performance of concrete dams, earth and rockfill dams, and outlet works.

4. Related Activities

(1) The Ministry of Land, Infrastructure and Transport, Japanese Government completed the *Guidelines for Seismic Safety Evaluation of Dams (Draft)* in March 2005. This document was applied to four existing dams during the fiscal year of 2005 in order to verify and revise it. This procedure will be continued for other existing dams during the fiscal year of 2006.

(2) The U.S. Army Corps of Engineers has completed the *Engineering Circular No. 1110-2-6058: Stability Analysis of Concrete Structures*. This document contains new criteria for stability analysis of concrete gravity structures, and it is still under review.

REPORT OF TASK COMMITTEE D
WIND ENGINEERING

Date: 15 May 2006

Place: National Institute of Standards and Technology, Gaithersburg, Maryland, USA

Attendees:	U.S. Side --	John Gaynor	(Co-Chair)	NOAA
		Nicholas Jones	(Co-Chair)	Johns Hopkins University
		Harold Bosch		FHWA
		William Fritz		NIST
		Joseph Main		NIST
		Partha Sarkar		Iowa State University
	Japan Side --	Hiroshi Sato	(Acting Co-Chair)	PWRI
		Yoshihiro Iwata		BRI

1. Objective and Scope of Work

To exchange technical information and to jointly plan, promote, and foster research and dissemination, in order to improve understanding of wind and its effects on structures, to establish more rational wind-resistant design procedures for structures, and to contribute collaboratively and synergistically to wind hazard mitigation. Specific objectives for the Task Committee include:

(1) Strategically and collaboratively, identify research needs in wind hazard mitigation in the areas of new technology, basic and applied research in meteorology, wind and structural engineering, and in social and economic impacts of wind events.
(2) Facilitate cooperation and collaborative research between U.S. and Japanese researchers in wind hazard mitigation.
(3) Identify and exchange successful advances in wind engineering and wind hazard mitigation.

The scope of the US-Japan collaboration includes:

(1) Characterization of strong wind, especially extreme winds in the atmospheric boundary layer.
(2) The study of wind effects including wind loading on and wind-induced response of structures.
(3) Conduct of experimental and analytical research to predict wind effects.
(4) Joint participation in damage surveys, and wind hazard and risk assessments.
(5) Development of new technologies for wind hazard mitigation.

2. Accomplishments

(1) International collaborative studies on wind tunnel estimates of wind effects on low-rise buildings have been conducted. BRI continues a survey on wind pressure measurements on a low rise building, having been offered the wind tunnel model by NIST. In these studies, a series of wind tunnel tests are almost completed, and the wind tunnel measurement results obtained in various wind tunnel facilities in the US (Clemson University and Texas Tech), Canada (Univ. of Western Ontario), France (CSTB), and Japan are being compared. These results were synthesized into joint papers presented in June 2005 at the ICOSSAR Conference in Rome and in September 2005 at APCWE6 in Seoul.

(2) The measured flutter derivatives for several bridge decks were compared and discussed between Partha Sarkar (Iowa State University) and Hiroshi Sato (PWRI). This comparison was part of the "Benchmark Study on Flutter Derivatives" that was originally conceived and initiated in October 2002 during the Third Wind Engineering Workshop. While the flutter derivatives for the streamlined bridge decks matched very well between the two wind tunnel measurements, there were some discrepancies for the rectangular bridge sections. This latter mismatch is assumed to be due to displacement amplitude dependency of the flutter derivatives that is currently being investigated.

3. Future Plans

(1) As a follow-up to the workshop on "Reducing Losses from Wind: Collaborative Opportunities for the 21st Century" (third U.S.-Japan Workshop held in Seattle, U.S. in October 2002) a Fourth Workshop, "New Challenges for Reduction of High-Wind Disasters" will be hosted by the Japanese members in Tsukuba on July 20-22, 2006.

(2) Seek additional opportunities to pursue collaborative research on the following topics:
  a) Wind characteristics and wind hazard mitigation.
    i) Wind characteristics in complex terrains.
    ii) Validation of wind models with full-scale data (opportunities for joint field studies).
    iii) Arrange for the hosting of colleagues interested in participating in quick-response post-storm damage assessments.
    iv) Downscale meteorological wind models for input to structural response wind models.
  b) Wind effects on buildings.
    i) Development of reliable and consistent aerodynamic loads and probabilistic methodologies for performance-based structural design.
    ii) Comparison of wind tunnel data sets and CFD results to full-scale measurements.
  c) Wind effects on bridges
    i) Prediction and mitigation of wind-induced vibration of stay cables.
    ii) Establish guidelines, criteria, and formats for sharing data from full-scale measurements, and identify potential collaborative instrumentation opportunities.
  d) Evolving Technologies
    i) Next-generation wind tunnels for the simulation of non-stationary winds (straight-line, tornado and microburst).
    ii) Applications of structural control
    iii) New field observation capabilities in high winds at small spatial scales and at high time frequency resolution

(3) Exchange technical information on the following topics
  a) Wind characteristics and wind hazards
  b) Wind pressures, loadings and performance of buildings
  c) Wind-induced response of flexible, cable-suspended bridges and their components
  d) New prediction and mitigation techniques for wind effects

(4) Investigate opportunities for technical collaboration with other UJNR task committees on the following topics
  a) Collaboration with fire engineering researchers by making use of unique facilities: Fire Research Wind Tunnel and Wind and Rain Test Laboratory
  b) Consider development of a compendium listing of relevant resources and facilities for wind engineering research
  c) Storm surge and shallow wave effects on structures

(5) Engage in more regular interaction and communication among Task Committee members. Use email (e.g., quarterly updates on activities) and exchange visits between full Panel meetings was

suggested as a means of facilitating and coordinating collaborative activities.

(6) Continue to improve process, mechanisms, and funding for interaction on reconnaissance teams after future hurricane/typhoon impacts.

(7) Strategically and collaboratively construct a vision and plan for wind engineering research needs for the next decade, and formulate collaborative activities around those plans. Draft a strategic plan to meet the task committee's objectives.

4. Related Activities

(1) In 2005 typhoons and hurricanes made landfalls in the U.S. and Japan sequentially in 2004. A record number of Atlantic and Gulf hurricanes were recorded. Of note in the U.S, Hurricane Katrina and Hurricane Rita made landfall in the southern states in late August and September 2005. Hurricane Katrina developed into a Category 5 in the Gulf of Mexico and impacted the city of New Orleans, Louisiana on 29th August. As of the end of 2005, 1,313 people were known dead and 2.5 million families had been affected. Economic impact was estimated at about $200 billion. Twenty three typhoons occurred in the northwest Pacific in 2005. Three of those typhoons made landfall in Japan and damaged houses and buildings. A rollover accident of a limited express train by a wind gust occurred on the Uetsu line in Yamagata Prefecture at the end of 2005 resulting in five fatalities. Damage surveys were conducted by wind engineers in both countries, and information exchange occurred between the two countries.

(2) The Missouri DOT, along with FHWA, hosted the second national workshop on the effect of Wind Induced Vibration on Cable Stay Bridges in St. Louis from April 25-27, 2006. The workshop had over 100 attendees, mostly from state DOTs and consulting engineering firms. Presentations were made by experts from the U.S., Canada, and Japan. As part of this workshop, results from the collaborative work between Masaru Matsumoto (Kyoto University), Nick Jones (Johns Hopkins University), and Joe Main (NIST) were presented.

(3) Published the report, *Disaster Reduction interagency Windstorm Impact Reduction Implementation Plan,* U.S. President's Office of Science and Technology (OSTP)/National Science and Technology Council (NSTC) Subcommittee for Disaster Reduction.

REPORT OF TASK COMMITTEE G
TRANSPORTATION SYSTEMS

Date: 15 May 2006

Place: National Institute of Standards and Technology, Gaithersburg, MD USA

Attendees:	U.S. Side --	W. Phillip Yen (Chair)	FHWA
		Hamid Ghasemi	FHWA
		William Roper	GMU
	Japan Side --	Shigeki Unjoh (Acting Chair)	PWRI

1. Objective and Scope of Work

The objectives of work include:

(1) To plan, promote and foster research on the behavior of transportation facilities when subjected to wind and seismic forces, and

(2) To disseminate research results and provide specifications and guidelines based on the Task Committee's findings.

The scope of work includes investigation of existing and new bridges design, the behavior of whole bridge systems and/or single component of a bridge without limitation on their size and function.

2. Accomplishments

(1) The 21st US-Japan Bridge Engineering Workshop was held during 3-5 October, 2005 at PWRI in Tsukuba, Ibaraki, Japan. 20 U.S. and 70 Japanese Participants attended the workshop. 45 Technical papers were presented and discussed on the following main topics: a) Foundation Engineering and b) Bridge Management

(2) The proceedings of the 21st US-Japan Bridge Engineering Workshop were printed and distributed in April 2006. The program and papers of the workshop will be copied to the Panel's web-site at the PWRI (http://www.pwri.go.jp/eng/ujnr/tc/g/tc_g.htm)

3. Future Plans

(1) The 22nd US-Japan Bridge Engineering Workshop will be held in the fall of 2006 in the U.S. Specific program and itinerary will be proposed by the U.S.-side Task Committee G with the concurrence of the Japan-side Task Committee.

(2) Both sides agreed to study Post Earthquake Damage Evaluation.

(3) Both sides agreed to propose a focus area on "Multi-hazard Risk Reduction for Highway Bridges". Discussions will be held with Task Committee B to identify cooperative bridge related infrastructure research projects and action plans.

(4) Following a devastating earthquake or hurricane (typhoon) in the US or Japan, the Task Committee will form a joint reconnaissance team to investigate the performance of transportation systems.

(5) Exchange technical information on the following topics:

  a) Seismic design and retrofit of highway bridges including the development of seismic response modification devices, smart materials, seismic retrofit for long-span bridges, and the development of damage evaluation methods using sensor systems.

  b) Seismic and aerodynamic response of long-span bridges including suspension and cable stayed bridges, with emphasis on behavior of composite materials, cable inspection, vibration control, and corrosion protection.

c) Recommendation of additional Task Committee be added that will focus on Health Monitoring

(6) Both sides agreed to pursue the following two research topics as cooperative studies.

a) Performance Criteria – Limit States
  - Relationship between performance criteria and structural response
  - Relationship between damage and loss of function
  - Realistic performance criteria
  - Philosophical framework for performance-based design and assessment

b) Three Dimensional Effects
  - Effect of multi-dimensional input on superstructure and substructure
  - Simplified, effective 3D modeling
  - Total failure analytical modeling

And the Task Committee encourages the following research themes and information sharing activities:

a) High-performance materials
b) Input ground motion
c) Foundation – soil –structure systems
d) Assessment of component and system uncertainty
e) Seismic intervention
f) Size effects testing
g) Sequential failure of bridge systems
h) Performance and risk sensor data management and analysis systems.

REPORT OF TASK COMMITTEE H
STORM SURGE AND TSUNAMI

Date: 15 May 2006

Place: National Institute of Standards and Technology, Gaithersburg, MD. USA

Attendees:	U.S. Side --	Solomon Yim (Co-Chair)	OSU
	Japan Side --	Takashi Tomita (Co-Chair)	PARI
		Katsuya Oda	NILIM

1. Objective and Scope of Work

The objectives of work include:

(1) To exchange scientific and technical information
(2) To jointly plan, promote and foster research and dissemination of knowledge
(3) To develop measures to prevent and mitigate damages from storm surges and tsunamis

The scope of work includes:

(1) Perform joint research on storm surge and tsunami occurrences, generation, propagation, and coastal effects. Develop database on storm surge, tsunami and wave measurements.
(2) Improve coordination of strategies and systems for observations of tsunamis and storm surges by field surveys, satellites, and in-situ measurements.
(3) Exchange results and status of storm surge and tsunami mitigation activities including analysis of the problem, planning, warning, and engineering approaches.
(4) Exchange information on development of technologies such as numerical models to predict propagation processes, land-fall locations, inundation and run-up heights, and wave characteristics, improved instrumentation, and use of satellite communication for detection and warning.
(5) Facilitate research result and technology development disseminations through exchange of literature, technical reports at joint meetings, special workshops, joint projects, and direct interaction among participants.
(6) Develop planning, design and construction guidelines in storm surge and tsunami flooding zones to serve as a model for international standards.
(7) Provide technical support to develop storm surge and tsunami mitigation programs worldwide.
(8) Encourage conduct of joint investigation following storm surge and tsunami events.

2. Accomplishments

(1) The 2nd International Workshop on Coastal Disaster Prevention was held on January 18-20, 2006 in Tokyo, Japan with the support of Panel on Wind and Seismic Effects of UJNR. Researchers and practitioners attended the workshop including the following:

Nobuhisa Kobayashi, UD, USA
Harley S. Winer, USACE, USA
Solomon Yim, OSU, USA
Taro Arikawa, PARI, Japan
Koji Fujima, National Defense Academy, Japan
Noriaki Hashimoto, Kyushu U, Japan
Haruo Hayashi, Kyoto U, Japan
Masakazu Higaki, JMA, Japan
Tetsuya Hiraishi, PARI, Japan
Fumihiko Imamura, Tohoku U, Japan

Yasuyuki Kajiwara, MLIT, Japan
Fuminori Kato, NILIM, Japan
Hiroyasu Kawai, PARI, Japan
Yoshiaki Kawata, Kyoto U, Japan
Norimi Mizutani, Nagoya U, Japan
Toshihiko Nagai, PARI, Japan
Tatsuyuki Shishido, CDIT, Japan
Shigeo Takahashi, PARI, Japan
Tomoyuki Takahashi, Akita U, Japan
Tomotsuka Takayama, Kyoto U, Japan
Takashi Tomita, PARI, Japan
Shin'ya Tsukada, JMA, Japan
Jun Yoshimura, MRI, Japan
Subandono Diposaptono, Ministry of Marine Affairs and Fisheries, Indonesia
Saman P. Samarawickrama, U Moratuwa, Sri Lanka
Panitan Lukkunaprasit, Chulalongkorn U, Thailand
Ahmet C. Yalciner, Middle East Technical U, Turkey

(2) Dr. Yim participated in a Task Committee G related Workshop on Bridges hosted by FHWA (Philip Yen) at Tsukuba, Japan in October 2005.
(3) Dr. Yim, Mr. Oda and Mr. Kawai participated in survey of storm surge damages of Hurricane Katrina in 2005.
(4) In February 2006, Dr. Tomita participated in survey of recovery progress from the 2004 Indian Ocean Tsunami in Thailand.

3. Future Plans

(1) Create joint research between the US and Japan to develop and improve numerical models of storm surge and tsunami dynamics and to exchange experimental and field data. The following topics have been identified as areas of future research collaboration on storm surges and tsunamis:
    (a) field observation
    (b) characterization
    (c) physical experiment models
    (d) numerical simulation models
    (e) effects on coastal structures and damage estimations
    (f) design of protective structures for different levels
    (g) hazard maps development and warning system design
    (h) risk assessment including hazard beyond designed levels
(2) Each side will develop database for existing and planned experiments including description and parameters of experiments to maximize overall available experimental data for understanding of physical behavior, numerical model validation and structural design.
(3) Hold the next workshop in the US in July 2006.
(4) The US Side Co-Chair, Dr. Yim will contact Dr. Bernard US Side Co-chair, Mr. Gaynor (Co-Chair T/C D) regarding the study of storm surge, and Dr. Philip Yen (Chair T/C G) regarding storm surge and tsunami effects on bridges.

4. Related Activities

(1) US side T/C members worked on a research project predicting tsunami effects on Oregon coastal bridges due to potential Cascadia Subduction Zone earthquake.
(2) US side T/C members worked on a research projects reconstructing storm surge damage on a levee in New Orleans due to Katrina Hurricane.

(3) Drs. Tomita and Yim jointed the PIANC (International Navigation Association), MarCom Working Group 53 on "Recommendations with regard to the design and construction of maritime structures in tsunami prone areas", which held their kicked off meeting in January 2006.

(4) Japan Side T/C members have cooperative research activities in Technical Committee on Technologies to Estimate and Reduce Tsunami Damages, Japan Society of Civil Engineers.

(5) Ministry of Land, Infrastructure and Transport, Japan and PARI held a Workshop on Tsunami Disaster Mitigation on August 16-25, 2005. Researchers and practitioners participated including those from India, Indonesia, Maldives, Sri Lanka and Thailand, countries that suffered major damages from the 2004 Indian Ocean Tsunami.

REPORT OF TASK COMMITTEE I
FIRE PERFORMANCE OF STRUCTURES

Date: 15 May 2006

Place: National Institute of Standards and Technology, USA

Attendees:	U.S. Side --	John Gross (Co-Chair)	NIST
		Alexander Maranghides	NIST
	Japan Side --	Mamoru Kohno (Co-Chair)	NILIM

1. Objective and Scope of Work

The objectives of work include:

(1) Increase the availability of technology for evaluating the methods of fire/structural interaction that will be used to improve the performance of structures under fire loads.

(2) Promote post disaster investigations of fires following natural and technological disasters that enhance the Panel's core competencies in structural fire technologies.

(3) Encourage the development and sharing of research findings among the world's researchers and practitioners on the behavior of structural systems to fires.

The scope of work includes:

(1) Plan and conduct workshops and cooperative research on topics that improve the understanding of fire growth and service life predictions of the performance of structural components to fire loading.

(2) Exchange data on the performance of structural systems and components to fires and related modeling and simulation analyses.

(3) Exchange information on technological developments, state-of-art and practice related to the control of fire spread in buildings.

(4) Exchange information on technological developments related to the performance of structures exposed to fires.

(5) Exchange data on large fire analysis from natural and technological disasters to accurately simulate fire initiation and growth in urban environments.

(6) Develop the technical bases to revise structural-fire related codes, standards, and practice.

2. Accomplishments

(1) Added new members to the U.S. side: Dr. Kuldeep Prasad (replacing Dr. Anthony Hamins) of NIST, Prof. Jay Gore of Purdue University, and (tentatively) Prof. Greg Deierlein of Stanford University.

(2) Workshop planning continuing on gap identification between theory and practice and research needs for fire/structural interactions such as steel connections in fires, to be held in November 2006 in connection with the ISO TC92 meeting in Japan.

(3) Held initial meeting to explore collaborations with Panel Task Committees with complementary interest in structural-fire performance such as: Task Committee G – Transportation Systems and Task Committee B – Next Generation Building and Infrastructure Systems, and with the professional societies, trade associations, and academia.

3. Future Plans

The future plans include:

(1) Explore the feasibility of creating a bi-lateral survey team to investigate fire-structure damage after major natural/technological disaster.

(2) Share Task Committee findings with the international research community.
(3) Plan a Task Committee I, Workshop on Fire Performance of Structures, November 2006, Japan.

NIST Technical Publications

Periodical

Journal of Research of the National Institute of Standards and Technology—Reports NIST research and development in metrology and related fields of physical science, engineering, applied mathematics, statistics, biotechnology, and information technology. Papers cover a broad range of subjects, with major emphasis on measurement methodology and the basic technology underlying standardization. Also included from time to time are survey articles on topics closely related to the Institute's technical and scientific programs. Issued six times a year.

Nonperiodicals

Monographs—Major contributions to the technical literature on various subjects related to the Institute's scientific and technical activities.

Handbooks—Recommended codes of engineering and industrial practice (including safety codes) developed in cooperation with interested industries, professional organizations, and regulatory bodies.

Special Publications—Include proceedings of conferences sponsored by NIST, NIST annual reports, and other special publications appropriate to this grouping such as wall charts, pocket cards, and bibliographies.

National Standard Reference Data Series—Provides quantitative data on the physical and chemical properties of materials, compiled from the world's literature and critically evaluated. Developed under a worldwide program coordinated by NIST under the authority of the National Standard Data Act (Public Law 90-396). NOTE:The Journal of Physical and Chemical Reference Data (JPCRD) is published bimonthly for NIST by the American Institute of Physics (AIP). Subscription orders and renewals are available from AIP, P.O. Box 503284, St. Louis, MO63150-3284.

National Construction Safety Team Act Reports—This series comprises the reports of investigations carried out under Public Law 107-231, the technical cause(s) of the building failure investigated; any technical recommendations for changes to or the establishment of evacuation and emergency response procedures; any recommended specific improvements to building standards, codes, and practices; and recomendations for research and other appropriate actions to help prevent future building failures.

Building Science Series—Disseminates technical information developed at the Institute on building materials, components, systems, and whole structures. The series presents research results, test methods, and performance criteria related to the structural and environmental functions and the durability and safety characteristics of building elements and systems.

Technical Notes—Studies or reports which are complete in themselves but restrictive in their treatment of a subject. Analogous to monographs but not so comprehensive in scope or definitive in treatment of the subject area. Often serve as a vehicle for final reports of work performed at NIST under the sponsorship of other government agencies.

Voluntary Product Standards—Developed under procedures published by the Department of Commerce in Part 10, Title 15, of the Code of Federal Regulations. The standards establish nationally recognized requirements for products, and provide all concerned interests with a basis for common understanding of the characteristics of the products. NIST administers this program in support of the efforts of private-sector standardizing organizations.

*Order the **following** NIST publications—FIPS and NISTIRs—from the National Technical Information Service, Springfield, VA 22161.*

Federal Information Processing Standards Publications (FIPS PUB)—Publications in this series collectively constitute the Federal Information Processing Standards Register. The Register serves as the official source of information in the Federal Government regarding standards issued by NIST pursuant to the Federal Property and Administrative Services Act of 1949 as amended, Public Law 89-306 (79 Stat. 1127), and as implemented by Executive Order 11717 (38 FR 12315, dated May 11, 1973) and Part 6 of Title 15 CFR (Code of Federal Regulations).

NIST Interagency or Internal Reports (NISTIR)—The series includes interim or final reports on work performed by NIST for outside sponsors (both government and nongovernment). In general, initial distribution is handled by the sponsor; public distribution is handled by sales through the National Technical Information Service, Springfield, VA 22161, in hard copy, electronic media, or microfiche form. NISTIR's may also report results of NIST projects of transitory or limited interest, including those that will be published subsequently in more comprehensive form.

UNIVERSITY OF ILLINOIS-URBANA
3 0112 078756191

U.S. Department of Commerce
National Institute of Standards
and Technology
Gaithersburg, MD 20899-0001

Official Business
Penalty for Private Use $300